UNIVERSITY OF TULSA
THE GRADUATE SCHOOL

Conditioning Geostatistical Model to Three-Dimensional, Three-Phase Flow Production Data by Automatic History Matching

by
Ruijian Li

A dissertation submitted in partial fulfillment of
the requirements for the degree of Doctor of Philosophy
in the Department of Petroleum Engineering
2001

UNIVERSITY OF TULSA

THE GRADUATE SCHOOL

Conditioning Geostatistical Model to Three-Dimensional, Three-Phase Flow Production Data by Automatic History Matching

by

Ruijian Li

A DISSERTATION

APPROVED FOR THE DISCIPLINE OF

PETROLEUM ENGINEERING

By Dissertation Committee

_____ Co-Chairperson

_____ Co-Chairperson

_____

_____

ABSTRACT

Ruijian Li (Doctor of Philosophy in Petroleum Engineering)
Conditioning Geostatistical Model to Three-Dimensional, Three-Phase Flow Production Data by Automatic History Matching
(126 pp.-Chapter V)
Co-Directed by Drs. Albert C. Reynolds and Dean S. Oliver

(337 words)

In this work, I describe the development of a general automatic history matching procedure to generate maximum a posteriori (MAP) estimates and realizations of reservoir model parameters by conditioning to three-dimensional three-phase production data. The algorithm is based on fully implicit, three-dimensional, three-phase, variable bubble point black oil flow equations. We are able to estimate gridblock permeability (both horizontal and vertical) and porosity, well skin factor, and three-phase relative permeability curves. Several types of model parameters can be estimated simultaneously. The observed data can be pressure, gas-oil ratio, water-oil ratio, and any combination of these three types of data. An adjoint system of equations for computing the sensitivity coefficients of three-dimensional, three-phase flow production data has been developed and implemented. Using the adjoint solution, we are able to compute the sensitivity of pressure, gas-oil ratio, water-oil ratio to the gridblock permeability and porosity, well skin factor and parameters used in the relative permeability curves. I illustrate comparison of results with an alternate method that the sensitivity coefficients generated by the adjoint method are highly accurate. The advantage of the adjoint method is that the number of linear system solutions is independent of the number of model parameters so this method can be used for large

simulation models. We show that the adjoint equation can be directly constructed from the Jacobian matrices computed in fully implicit simulator. This approach can hand the problems with large number of data and highly compressible reservoirs. The Levenberg-Marquardt method is applied to minimize the objective functions. The Levenberg-Marquardt method is more robust than regular Gauss-Newton method. Our results indicate that conditioning to more types of data improve the estimate results of model parameters and has greater reduction in uncertainty. Gas-oil ratio data tend more useful than water-oil ratio data in resolve reservoir model parameters. We can estimate three-phase relative by conditioning to production data. It is possible to estimate the absolute and relative permeability simultaneously.

TABLE OF CONTENTS

LIST OF FIGURES

LIST OF TABLES

ACKNOWLEDGMENTS

This work was supported by the TUPREP member companies and a grant from Schlumberger Foundation, Inc. The reservoir simulator used in this study was provided by Chevron Petroleum Technology Company.

CHAPTER I

INTRODUCTION

To optimize oil or gas field development and predict reservoir future performance, one first needs to determine the rock property fields of the petroleum reservoir. Because the reservoir is thousands of feet underground, it is usually impossible to directly measure the reservoir parameters except at well locations. However, the rock property fields can be constructed by applying inverse or parameter estimation algorithms using indirect measurements, such as production data. In this research work, a general procedure, known as automatic history matching, has been developed and implemented to generate estimates or multiple realizations of model parameters conditioned to three-dimensional, three-phase production data and prior information. The types of production data that can be used in this procedure include wellbore pressure, gas-oil ratio and water-oil ratio. In a petroleum reservoir, the gridblock permeabilities and porosities, skin factors, and relative permeability are the most important model parameters for determining the performance of the reservoir. This work focuses on generating estimates and multiple realizations of these reservoir model parameters. The ultimate objective of this work is to evaluate uncertainty in predicted reservoir performance under three-phase flow conditions. This uncertainty can be quantified by generating multiple realizations conditioned to production data (e.g., pressure, GOR and WOR) and predicting reservoir performance with each realization.

Automatic history matching is an inverse procedure. Usually, inverse problems are underdetermined and the solutions are non-unique. So generating estimates or multiple realizations of the model parameters is a difficult problems. The inverse

problems of interest reservoir engineers are even more challenging for several reasons. First, there are a large number of model parameters to be estimated in a reservoir model. A reservoir simulation model may use tens of thousands or even a million gridblocks. The reservoirs are usually heterogeneous and the model parameters are spatial variables. Each gridblock at least has one model parameter (for example, permeability) and often more. Second, the number of data is insufficient. We only can measure data at the wellbore or on the surface. Today, one can use permanent downhole sensors to obtain high frequency data in the time domain. However, the data in the spatial domain is still very sparse and much of the observed data is redundant. The third reason is that the solution of the problem is non-unique. There are many models that give an acceptable match of the data. In our approach, we either find the most probable model or generate multiple realizations by sampling the a posteriori probability density function to evaluate the uncertainty. The fourth reason is that the relationship between model parameters and production data is highly nonlinear for multi-phase flow problems, especially when a gas phase is present in the model. This makes estimation and sampling more difficult. If the initial guess is far away from the true model, the estimated model may never converge to the neighborhood of the true model.

The inverse procedure presented here is under the framework of Bayesian inference. The solution of the inverse problem is an a posteriori probability density function (a posteriori pdf) on the space of the reservoir model. The posteriori pdf includes two parts. The first part is the priori distribution, which comes from the static data, such as geologic, core, well logs, and seismic data. The second part is a likelihood function, which involves the difference between the predicted data from a given model and the observed data. In this work, the observed data are production data, also referred to as dynamic data. Through the posteriori pdf, one can construct a most probable model (maximum a posteriori estimate) or generate a set of realizations of reservoir parameters by sampling the posteriori pdf. In this

way, the uncertainties in the observed data and model parameters can be integrated in the inverse procedure.

Typically, automatic history matching utilizes gradient information and thus requires a procedure for generating sensitivity coefficients and a procedure for optimizing an objective function which includes a sum of squares of production data mismatch terms. We use either the Gauss-Newton method with restricted-step or the Levenberg-Marquardt method for optimization. The experiments that we have done to date indicate that the Levenberg-Marquardt algorthm is more robust. To apply the optimization procedures, one needs to calculate sensitivity coefficients. An efficient adjoint algorithm to calculate sensitivity of three-dimensional three-phase flow production data to model parameters has been derived and implemented. As we show in Chapter 3, our implementation of the adjoint method gives highly accurate sensitivity coefficients.

1.1 Literature Review

Automatic history matching has its origins in the work of Jacquard (1964) who presented an analytical formula for the sensitivity of pressure to a small perturbation in a uniform permeability field and Jacquard and Jain (1965) who derived and implemented the first numerical procedure to compute sensitivity coefficients. Using their procedure for computing sensitivity coefficients, Jacquard and Jain constructed estimates of two-dimensional permeability fields by history-matching single-phase flow pressure data by minimizing an objective function equal to the sum of squared pressure data mismatch terms. They used a combination of zonation (fewer than twenty zones of different permeability) and a procedure similar in spirit to the Levenberg-Marquardt algorithm to avoid the numerical instabilities that can arise when solving an ill-conditioned inverse problem. Jahns (1966) adapted the basic ideas of Jacquard and Jain (1965) to estimate both permeability and porosity fields

by matching single-phase flow pressure data. Interestingly, Jahns did not use the method of Jacquard and Jain (1965) to compute sensitivity coefficients, using instead a finite difference method. To compute the sensitivity of data to an individual model parameter with this method requires one simulation run, i.e., one additional simulation run per model parameter for each iteration of the Gauss-Newton procedure which Jahns applied to minimize the objective function. However, Jahns only considered on the order of twenty parameters and as noted by him, the finite-difference method is actually faster than the procedure of Jacquard and Jain (1965) if the number of model parameters is small. Jahns used a zonation procedure to limit the number of parameters but applied a sequence of minimization procedures. At each minimization step, the number of zones was increased.

On the order of ten years after the fundamental work discussed in the preceding paragraph, a series of interesting papers related to automatic history matching appeared. The procedure of Jacquard and Jain (1965) was derived using an electric circuit analogue, but motivated directly by this work, Carter et al. (1974) published an elegant mathematical derivation of an efficient procedure to calculate sensitivity coefficients. Carter et al. (1974) considered single-phase flow problems, or more precisely, assumes the underlying partial differential equation is linear, i.e., rock and fluid properties must be considered to be independent of pressure. His procedure technically gives the sensitivity of reservoir simulator gridblock pressures to gridblock permeabilities and porosities. In finite-difference simulators, well gridblock pressures are typically related to wellbore pressure by some variation of Peaceman's method (Peaceman, 1983). For three-dimensional single-phase flow problems, one could compute the sensitivity of wellbore pressure to model parameters by first computing the sensitivity of each gridblock pressure penetrated by a well to model parameters using a straightforward three-dimensional version of the Carter et al method; however, this would require one simulation run for each such gridblock. He et al. (1997) developed an approximate procedure to compute directly the sensitivity of wellbore pressures to

the rock property fields avoiding the necessity to compute the sensitivity coefficients related to all well gridblock pressures. The He et al. procedure requires one reservoir simulation run per well to calculate the information needed for all sensitivities. However, sensitivity coefficients computed by this procedure are only approximate when significant vertical flow occurs through wells or in gridblocks penetrated by wells.

The methods for computation of sensitivity discussed to this point are rather specialized; they are only applicable to single-phase flow problems. For multiphase flow, there are several viable method for computing the sensitivity of data to the model parameters. The simplest (but least efficient) approach is to perturb the value of each model parameter, then compute the change due to the perturbation. Beck and Arnold (1977) used this method to calibrate friction parameters in open channel flow. This is the method that Jahns (1966) used for single-phase flow. Because it is so simple, it is used as a basis for comparison with the results from other methods for multi-phase flow (see Wu (1999)). It is extremely inefficient for a large number of model parameters, however, as it requires $M + 1$ simulation runs to compute the sensitivity of data to M model parameters.

A more efficient method for computation of sensitivity coefficients is based on the repeated solution of a differential equation for the sensitivity coefficients. A sensitivity equation is derived by differentiating the flow equations with respect to a single model parameter. The resulting equations must be solved as many times as there are model parameters. Because the only difference is in the right hand side, it is possible to improve the efficiency by use of a solver especially designed for problems with multiple right hand sides (Killough et al., 1995). Although we are not sure who originally proposed this method, it is discussed in Yeh's (1986) review of parameter identification methods where it is referred to as the sensitivity coefficient method. It was introduced to the petroleum engineering literature by Anterion et al. (1989), where it was referred as the gradient simulator method.

Although the gradient simulator method (Anterion et al., 1989) can be used

to generate sensitivity coefficients for automatic history matching of multiphase flow data, this is not feasible if the number of model parameters is large. The gradient simulator method still requires that we solve a matrix problem with multiple right hand sides at the end of each reservoir simulator time step. The number of right hand sides is equal to the number of model parameters. If, however, one can justify describing the reservoir using only a few model parameters, e.g., some form of zonation makes sense, then the gradient simulator is feasible. In every case for which the gradient simulator method has been used (Jacquard and Jain, 1965; Tan and Kalogerakis, 1992; Bissell et al., 1994; Bissell, 1994), the number of parameters was artificially reduced. However, if the set of model parameters include the porosities and permeabilities for every grid cell, computation of sensitivity coefficients with the gradient simulator method is not feasible. If the number of model parameters is large, the model can often be reparameterized using the subspace method (Reynolds et al., 1996) and then we can directly compute the sensitivity of the each subspace vector to the model parameters (Abacioglu et al., 2000).

The only other general method for computation of sensitivity of data to model parameters is the adjoint method, which was proposed independently by Chen et al. (1974) and Chavent et al. (1975). The adjoint method can be and has been applied to multiphase flow problems, see for example Lee and Seinfeld (1987a), Yang et al. (1988), Makhlouf et al. (1993) and Wu et al. (1999). The adjoint procedure developed in this disertation allows us to calculate the sensitivity of any individual production data to the model parameters or simply to compute the objective function that is to be minimized. (For the examples considered here, the model parameters are all gridblock permeabilities (x, y and z- directions), porosities, skin factors, and parameters defined relative permeabilities.) The generation of individual sensitivity coefficients requires the solution of the adjoint system with N_d right-hand sides (see Wu et al., 1999), where N_d is the number of observed production data we wish to history match. Thus, if N_d is large, it may be more efficient to use a method that only

requires the gradient of the objective function but does not require the calculation of individual sensitivity coefficients. To calculate the gradient of the objective function, we need only solve a single adjoint system. For this reason early researchers relied exclusively on optimization techniques that required no derivative information except for the gradient of the objective function. See, for example, the papers by Wasserman et al. (1975), Lee and Seinfeld (1987a), Yang et al. (1988), and Makhlouf et al. (1993) When N_d is large, it is possible that a preconditioned conjugate gradient method with an appropriate preconditioning matrix may prove to be more efficient than the Levenberg-Marquardt method, but we have not investigated this possibility.

Although several others have previously used the adjoint method for multiphase flow history matching, the computation of the sensitivity of individual data to model parameters has only been done for oil-water system (Sun, 1994; Wu et al., 1999). The computation of data sensitivity coefficients (as opposed to only the gradient of the total objective function) has several advantages. First, a great deal of insight into the information content of various data can be gained from an examination of sensitivities. The sensitivities of three-phase flow data to model parameters can be extremely complicated and non-intuitive. This is especially true for gas-oil ratio data. Second, the computation of individual sensitivities allow us to use the rapidly convergent Newton-like methods for history matching. Previous researchers have been limited to the more slowly convergent conjugate gradient (Makhlouf et al., 1993) or variable metric (Yang et al., 1988) approaches. Third, it is possible to compute the Hessian when individual sensitivities are available. The inverse of the Hessian sometimes provides a useful measure of uncertainty in model parameters. In particular, we often find it useful to examine the normalized a posteriori variance for model parameters. While this is only an approximation of the actual variance, and the variance is sometimes a poor measure of uncertainty in problems with highly correlated parameters, comparison of variance from various types of data can provide additional insight into the value of data for reducing uncertainty.

Relative permeability curves have a great impact on reservoir behavior in reservoir simulation and history matching. However, little work has been done to improve estimate of relative permeability curves by conditioning to production data. (Kulkarni and Datta-Gupta, 2000), (Yang and Watson, 1991), (Lee and Seinfeld, 1987a) and (Lee and Seinfeld, 1987b) presented some results for estimating relative permeability from production data in the water-oil two-phase flow problems. (Lee and Seinfeld, 1987b) estimated the absolute permeability and the exponents in the relative permeability expressing for water-oil two-phase reservoir. (Kulkarni and Datta-Gupta, 2000) presented a streamline approach by using water-oil cut data to estimate relative permeability curves. To the best of our knowledge, all previous works estimating relative permeability by conditioning to production data are limited to water-oil two-phase flow problems. In this work, we present an approach to estimate relative permeability curves for three-phase flow problems by conditioning to production data. We can estimate three-phase relative permeability curves only or estimate three-phase relative and absolute permeability simultaneously. Our approach also can be applied to water-oil or gas-oil two phase cases. The relative permeability models can be conditioned to pressure, gas-oil ratio, water-oil ratio and any combinations of these three types of data. The results indicate that integrating more types of data improve estimate results.

1.2 Data Integration and History Matching

Automatic history matching is an inverse procedure for which a numerical reservoir simulator is required as a forward model. In this work, we use an existing reservoir simulator, the Chevron Limited Applications Simulation System (CLASS), as the forward model. CLASS is a three-dimensional, three-phase black-oil reservoir simulator using a variable bubble-point fluid characterization. As CLASS uses a fully implicit numerical scheme, our adjoint approach is based on implicit reservoir

simulation equations.

As we pointed out previously, there is insufficient information for the accurate estimation of gridblock properties from data available in petroleum reservoir engineering. By using all available non redundant data to estimate the rock property fields, however, the estimate can be made as accurate as possible. The procedure presented here can integrate various types of data, including both static data and dynamic data, to improve the MAP estimate results and reduce the uncertainties of model parameters. The results will show that integrating more independent data improves the estimated results, but some types of data are more useful than others in reducing uncertainty.

If the number of model parameters is very large, there are not sufficient independent data to resolve all the model parameters. In this case, application of the Gauss-Newton method to maximum likelihood estimation would fail because the Hessian would be ill-conditioned unless some form of regularization is applied. In this work, we use a prior geostatistical model to provide regularization. With this approach, the history matching problem is equivalent to a Bayesian estimation problem (Gavalas et al., 1976; Tarantola, 1987; Oliver, 1994; He et al., 1997; Wu et al., 1999). We calculate sensitivity coefficients with the adjoint method. The availability of sensitivity coefficients allows the application of the Gauss-Newton and Levenberg-Marquardt algorithms which exhibit approximate quadratic convergence in a neighborhood of a minimum. Since sensitivity coefficients are calculated, the a posteriori covariance matrix can be generated; this matrix provides a measure of uncertainty in the estimates of reservoir model parameters. The adjoint solution and history matching procedure presented here are based on a finite-difference formulation of the flow equations. As such, the method can be applied to single-phase oil or gas flow, or to multiphase flow problems; it is not restricted to physical problems where streamline simulators can used to generate accurate results efficiently.

There are 5 chapters and 3 appendices in this dissertation. Chapter 2 briefly

describes the theory of automatic history matching. It includes discussions of Baysesian inversion, the construction of the MAP estimate and multiple realizations, data measurement errors, and the Gauss-Newton and Levenberg-Marquardt algorithms. Chapter 3 discusses the computation of sensitivity coefficients using the adjoint method. In Chapter 3, we compare the procedures of two popular methods for computing sensitivity coefficients, the adjoint method and gradient simulator method. We also show some examples of sensitivity coefficients and comparison of sensitivity coefficients from the adjoint method and from the finite difference method. Chapter 4 presents applications of our history matching procedure. It includes both 2D and 3D examples of three-phase flow problem. Examples include the computation of maximum a posteriori estimates or realizations of permeability and porosity fields, skin factors, and relative permeability by conditioning to the pressure, gas-oil ratio, and water-oil ratio. In Chapter 5, the conclusions and the research contributions of this work are summarized. In Appendices A, B, and C, the detailed formulations for the application of history matching to 3D, 3-phase flow problems are presented. Appendix A discusses the general 3D, 3-phase flow simulation equations and well constraint equations. Appendix B describes how to calculate the derivatives in the adjoint system equations. Appendix C discusses how to calculate sensitivity coefficients for various cases once the adjoint variables are obtained.

CHAPTER II

THE THEORY OF AUTOMATIC HISTORY MATCHING

2.1 Bayesian Inversion

The inverse procedure used in this work is based on Bayesian inversion theory. In a petroleum reservoir, m denotes the vector of reservoir model parameters that we want to estimate. The ultimate goal is to predict future performance of the reservoir and assess the uncertainty in the prediction. For that reason, we focus on the problem of estimating reservoir properties that affect fluid flow, and more precisely, the parameters that are required as input to the reservoir simulator. The model parameters that are estimated include horizontal permeability, vertical permeability and porosity at each gridblock, a skin factor at each well and parameters which define the two sets of two phase relative permeability curves. If the model parameters are horizontal permeability, vertical permeability, and skin, we write m as

$$m = \begin{bmatrix} m_k \\ m_{k_z} \\ m_s \end{bmatrix}, \tag{2.1}$$

where m_k is the vector of horizontal log-permeability of every gridblock; m_{k_z} is the vector of vertical log-permeability and m_s is the vector of skin factor. These reservoir parameters are modeled as random variables, so m is a random vector. From a purely history matching point of view, we wish to construct an estimate of m from production data (dynamic data) and static data (well logging data, geology data, and seismic data). However, there are an infinite number of models which will give equally reasonable matches of the data, and it is desirable to define a procedure

for generating a particular estimate or to characterize the uncertainty in reservoir descriptions. From both the philosophical and practical points of view (see Tarantola (1987) and Omre et al. (1993)), the most challenging part of the inverse problem is the determination of a representative pdf for reservoir parameters. Similar to the recent work on automatic history matching by He et al. (1997) and Wu et al. (1999), we follow ideas that can be found in Tarantola (1987) and simply assume that a prior geostatistical model can be adequately represented by a multivariate Gaussian distribution for m.

The prior pdf for m is then given by

$$\pi_p(m) = c \exp\Big\{ -\frac{1}{2}(m - m_{\text{prior}})^T C_M^{-1}(m - m_{\text{prior}})\Big\}, \tag{2.2}$$

where c is the normalizing constant. Note the model which has the highest probability based on Eq. 2.2 is $m = m_{\text{prior}}$, thus it is convenient to think of m_{prior} as the best estimate of the model based on static data.

2.2 Prior Model

The inverse procedure developed in this work is quite general. We can estimate gridblock permeabilities (including horizontal and vertical permeabilities), gridblock porosities, well skin factors, and relative permeabilities. We also can estimate several types of model parameters simultaneously. For example, we can estimate horizontal permeability, vertical permeability, and well skin factors simultaneously. If semivariograms are available for each type of model parameters, the prior covariance matrix for each type of model parameters can be constructed for a stationary random field. If one wishes to estimate several model parameters simultaneously, one can apply the Xu et al. (1992) screening hypothesis to generate cross covariance matrices.

Here, we show how to generate prior covariance matrix for a reservoir model where the horizontal log permeability, vertical log permeability, and skin factor in each

well are estimated simultaneously. For simplicity, we assume an isotropic reservoir so that $k = k_x = k_y$. In this case, the horizontal log-permeability field (gridblock $\ln(k)$'s) and the vertical log-permeability field (gridblock $\ln(k_z)$'s) are modeled as correlated stationary Gaussian random fields with specified means and covariance matrices C_k and C_{k_z}, respectively. In the prior model, each well skin factor is treated as an independent Gaussian variable with specified mean and variance. If the skin factor was estimated by fitting pressure data with a classical well testing model solution using nonlinear regression, then the estimate of the skin factor would be its prior mean and its variance can be constructed directly from the same information used to construct confidence intervals.

The vector of prior means is given by

$$m_{\text{prior}} = \begin{bmatrix} m_{k,\text{prior}} \\ m_{k_z,\text{prior}} \\ m_{s,\text{prior}} \end{bmatrix}. \tag{2.3}$$

We let C_k denote the prior covariance matrix for m_k, C_{k_z} denote the prior covariance for k_z, C_{k,k_z} denote the cross covariance matrix between k and k_z and let C_s denote the $N_w \times N_w$ model covariance matrix for the vector of well skin factors. Then, the prior model covariance matrix is given by

$$C_M = \begin{bmatrix} C_k & C_{k,k_z} & O \\ C_{k,k_z} & C_{k_z} & O \\ O & O & C_s \end{bmatrix}, \tag{2.4}$$

where the O's denote null submatrices of the appropriate size. If horizontal and vertical permeability are not correlated, then C_{k,k_z} is also a null matrix.

As mentioned above, the cross covariance matrix C_{k,k_z} is evaluated using the screening hypothesis of Xu et al. (1992)

$$C_{k,k_z} = C_{k_z,k} = \frac{\rho_{k,k_z}\sigma_k}{\sigma_{k_z}} C_{k_z}, \tag{2.5}$$

where ρ_{k,k_z} is the correlation coefficient between the horizontal log-permeability k and vertical permeability k_z; σ_k and σ_{k_z} are the standard deviation of the horizontal and vertical log-permeability, respectively.

2.3 Construction of Maximum A Posteriori Estimate

For a given model m, d denotes the predicted, true or calculated data corresponding to d_{obs}. If m is the true reservoir from which d_{obs} was obtained and there are no measurement errors, then $d = d_{\text{obs}}$. As d depends on the model, we write

$$d = g(m), \tag{2.6}$$

to represent the operation of calculating d given m. In our work, Eq. 2.6 represents the operation of running the reservoir simulator to calculate d.

Bayes' theorem (see Tarantola (1987)) indicates that the a posteriori pdf (conditional to observed data) for the model variables is proportional to the product of the prior pdf and the likelihood function for the model and is given by

$$\pi(m) = c \exp\{-O(m)\}, \tag{2.7}$$

where

$$O(m) = \frac{1}{2}\Big[\big(m - m_{\text{prior}}\big)^T C_M^{-1}\big(m - m_{\text{prior}}\big) + \big(g(m) - d_{\text{obs}}\big)^T C_D^{-1}\big(g(m) - d_{\text{obs}}\big)\Big]. \tag{2.8}$$

In the Eq. 2.8, C_M is the model covariance matrix and C_D is the data covariance matrix. C_M defines the relationship among the model parameters. The model covariance matrix C_M can be constructed from the prior information, the knowledge about the model parameters from the static data. In the Newton-like optimization algorithm, the first part of objective function Eq. 2.8, $1/2[(m - m_{\text{prior}})^T C_M^{-1}(m - m_{\text{prior}})$, also serves as a regularization term. The data covariance matrix C_D is based on the

confidence about the data. If the measurement errors are big, one should use a big variance. Otherwise, one should choose a small variance. Usually, we assume that there is no correlation among the data, so the matrix C_D is a diagonal matrix.

The maximum a posterior (MAP) estimate is the most probable model of the posterior pdf, Eq. 2.7, so the MAP estimate is obtained by maximizing the posterior pdf, Eq. 2.7, or minimizing the objective function, Eq. 2.8. For the three-phase flow examples considered in this work, we condition the geostatistical model to three types of production data, pressure, gas-oil ratio, water-oil ratio and to combinations of these three kinds of data. The set of model parameters refers to reservoir simulator gridblock permeabilities and gridblock porosities. The objective function to be minimized depends on the data used as conditioning data. Let $d_{\text{obs},p}$ denote the vector of conditioning pressure data, $d_p = g_p(m)$ denote corresponding predicted pressure data for a given model m and let $C_{D,p}$ denote the associated data covariance matrix. We assume that all measurement errors are Gaussian with means equaled to zero. We also assume all measurement errors are independent so all data covariance matrices are diagonal. The corresponding notation for gas-oil ratio data are $d_{\text{obs},g}$, $d_g = g_g(m)$ and $C_{D,g}$. For water-oil ratio data, we use $d_{\text{obs},w}$, $d_w = g_w(m)$ and $C_{D,w}$.

In matching only pressure data, the objective function to be minimized is

$$O_p = O_p(m) = \frac{1}{2}\big(m-m_{prior}\big)^T C_M^{-1}\big(m-m_{prior}\big)+\frac{1}{2}\big(g_p(m)-d_{\text{obs},p}\big)^T C_{D,p}^{-1}\big(g_p(m)-d_{\text{obs},p}\big). \tag{2.9}$$

In matching only producing GOR data, the objective function to be minimized is

$$O_g = O_g(m) = \frac{1}{2}\big(m-m_{prior}\big)^T C_M^{-1}\big(m-m_{prior}\big)+\frac{1}{2}\big(g_g(m)-d_{\text{obs},g}\big)^T C_{D,g}^{-1}\big(g_g(m)-d_{\text{obs},g}\big). \tag{2.10}$$

In matching only WOR data, the objective function to be minimized is

$$O_w = O_w(m) = \frac{1}{2}\big(m-m_{prior}\big)^T C_M^{-1}\big(m-m_{prior}\big)+\frac{1}{2}\big(g_w(m)-d_{\text{obs},w}\big)^T C_{D,w}^{-1}\big(g_w(m)-d_{\text{obs},w}\big). \tag{2.11}$$

We can generate a MAP estimate by matching any combinations of types of data. For example, if we wish to condition the model to both pressure and gas-oil ratio, the objective function to be minimized is given by

$$O_{pg} = O_{pg}(m) = \frac{1}{2}\big(m - m_{prior}\big)^T C_M^{-1}\big(m - m_{prior}\big) + \frac{1}{2}\big(g_p(m) - d_{\text{obs},p}\big)^T C_{D,p}^{-1}\big(g_p(m) - d_{\text{obs},p}\big) + \frac{1}{2}\big(g_g(m) - d_{\text{obs},g}\big)^T C_{D,g}^{-1}\big(g_g(m) - d_{\text{obs},g}\big). \tag{2.12}$$

If we wish to condition the reservoir model to all three types of data, pressure, gas-oil ratio and water-oil ratio, the objective function to be minimized is given by

$$O_{pgw} = O_{pgw}(m) = \frac{1}{2}\big(m - m_{prior}\big)^T C_M^{-1}\big(m - m_{prior}\big) + \frac{1}{2}\big(g_p(m) - d_{\text{obs},p}\big)^T C_{D,p}^{-1}\big(g_p(m) - d_{\text{obs},p}\big) + \frac{1}{2}\big(g_g(m) - d_{\text{obs},g}\big)^T C_{D,g}^{-1}\big(g_g(m) - d_{\text{obs},g}\big) + \frac{1}{2}\big(g_w(m) - d_{\text{obs},w}\big)^T C_{D,w}^{-1}\big(g_w(m) - d_{\text{obs},w}\big). \tag{2.13}$$

Note that there are no arbitrary weighting terms for the pieces of the objective function. Relative weighting is determined by the magnitude of the measurement errors for each type of data.

Eqs. 2.9 to 2.13 can all be written in the form of Eq. 2.8. For example, in the Eq. 2.13, let

$$g(m) = \begin{bmatrix} g_p(m) \\ g_g(m) \\ g_w(m) \end{bmatrix}, \tag{2.14}$$

$$d_{\text{obs}} = \begin{bmatrix} d_{\text{obs},p} \\ d_{\text{obs},g} \\ d_{\text{obs},w} \end{bmatrix}, \tag{2.15}$$

and

$$C_M = \begin{bmatrix} C_{D,p} & O & O \\ O & C_{D,g} & O \\ O & O & C_{D,w} \end{bmatrix}, \tag{2.16}$$

so the Eq. 2.13 can be written as the form of Eq. 2.8.

2.4 Gauss-Newton and Levenberg-Marquardt Algorithms

In this work, the MAP estimate is obtained by minimizing the objective function of Eq. 2.8 using either the Gauss-Newton method or the Levenberg-Marquardt method. For cases where the initial production data mismatch is large, the Levenberg-Marquardt algorithm is more robust and converges faster than the standard Gauss-Newton method with restricted-step. However, it is likely that this advantage accrues mainly from choosing a large initial value of the parameter λ and the fact that at future iterations the Levernberg-Marquardt incorporates an automatic procedure to control the change in model parameters over an iteration. If a method to damp model changes at early iterations were introduced into the Gauss-Newton method, it is likely that its convergence properties would improve; see Wu et al. (1999).

In the Gauss-Newton procedure, the model parameters at iteration $l+1$ are updated by

$$m^{l+1} = m^l + \mu_l \delta m^{l+1}, \tag{2.17}$$

and where μ_l is calculated by the restricted step procedure and δm^{l+1} is given by

$$\delta m^{l+1} = m_{prior} - m^l - C_M G_l^T (C_D + G_l C_M G_l^T)^{-1}[(g(m^l) - d_{\text{obs}}) - G_l(m^l - m_{prior})], \tag{2.18}$$

where the matrix G_l denotes the $N_d \times N_m$ sensitivity coefficient matrix evaluated at m^l. N_d is the number of data and N_m is the number of model parameters. The entry in the ith row and jth column of G_l represents the sensitivity of the ith calculated data

g_i to the jth model parameter evaluated at m^l, i.e., this entry is $\partial g_i(m^l)/\partial m_j$, where m_j is the jth entry of m. Physically, the sensitivity coefficient $\partial g_i(m^l)/\partial m_j$ gives a measurement of how much the computed data $g_i(m^l)$ will change when the model parameter m_j is changed. So given the mismatch between observed and computed data, sensitivity coefficients provide an indication of how we should modify the model parameters in order to match the observed data.

In the Levenberg-Marquardt method, the model parameters are updated by

$$m^{l+1} = m^l + \frac{m_{prior} - m^l}{1+\alpha} - C_M G_l^T((1+\alpha)C_D + G_l C_M G_l^T)^{-1} \\ [(g(m^l) - d_{\text{obs}}) - \frac{1}{1+\alpha} G_l(m^l - m_{prior})]. \tag{2.19}$$

In the preceding equation, α is the damping factor. Note that this is not the standard LM algorithm but follows the formulation introduced by Bi et al. (1999). When α is large, the change in the model from iteration l to iteration $l+1$ is small. In all applications we have done to date, we have set the initial value of α equal to 10^4 or 10^5. Normally, either 10^4 or 10^5 works fine for different cases. If m^{l+1} computed from Eq. 2.19 results in a reduction in the objective function, we decrease α by a factor of ten for the next iteration; if m^{l+1} computed from Eq. 2.19 results in an increase in the objective function, we multiply α by ten for the next iteration.

The convergence criteria for the Gauss-Newton and Levenberg-Marquardt methods are given by

$$\frac{O(m^{l+1}) - O(m^l)}{O(m^{l+1}) + 10^{-14}} \leq \epsilon_1, \tag{2.20}$$

and

$$\frac{\parallel \delta m^{l+1} \parallel}{\parallel \delta m^l \parallel + 10^{-14}} \leq \epsilon_2, \tag{2.21}$$

where ϵ_1 and ϵ_2 are set equal to 10^{-3}. For convergence, we require that both criteria are satisfied.

2.5 Data Measurement Errors

As in previous TUPREP research (see, for example, Wu (1999)), the production data measurement errors are modeled as independent Gaussian random variables. Specifically, we assume that pressure measurement errors are independent identically distributed Gaussian random variables with mean zero and constant variance σ_{pd}^2. We assume that gas-oil ratio (GOR) measurement errors are independent identically distributed Gaussian random variables with mean zero and constant variance σ_{gd}^2. For water-oil ratio, we use the method presented by Wu et al. (1999). With this model, variance of the water-oil ratio (WOR) is calculated as

$$Var[e_{WOR}] = WOR_{obs}^2 \epsilon_o^2 + \frac{1}{q_{o,obs}^2} \sigma_{q_{w,obs}}^2, \tag{2.22}$$

where

$$\epsilon_m^2 = \frac{Var[q_{m,obs} - q_m]}{q_{m,obs}^2}, \tag{2.23}$$

and

$$\sigma_{q_w,obs} = \max[\epsilon_w q_{w,obs}, \sigma_{q_w,obs}^{\min}]. \tag{2.24}$$

Here, $q_{m,obs}$, $m = o, w$ denotes the observed rate. In the examples shown in this work, we choose $\sigma_{q_w,obs}^{\min} = 2STB/D$, $\epsilon_o = 0.01$ and $\epsilon_w = 0.02$. The data measurement error of WOR is related to the magnitude of the water-oil ratio. When the q_w is large, $\sigma_{q_w,obs}$ increases as q_w increases; when the q_w is small or very close to zero, the water rate data variance $\sigma_{q_w,obs}$ is considered to be a constant, $\sigma_{q_w,obs}^{\min}$.

2.6 Evaluation of Uncertainty

The best way to evaluate uncertainty in reservoir properties would be to construct a large suite of realizations by sampling the pdf of Eq. 2.7; see, for example, Hegstad and Omre (1997), Omre et al. (1996), He (1997) or Wu (1999). Although sampling the pdf is preferable, to do so rigorously may be difficult and the computational expense of generating a large set of realizations can be significant. For the

case where we simply construct the MAP estimate of the model, the a posteriori covariance matrix can be used to provide an approximate evaluation of uncertainty in individual model parameters.

2.6.1 Posterior Covariance

According to Tarantola (1987), the linearized approximation to the posteriori covariance matrix, C_{MP}, is given by

$$C_{MP} = C_M - C_M G_\infty^T (G_\infty C_M G_\infty^T + C_D)^{-1} G_\infty C_M. \tag{2.25}$$

Here, G_∞ denotes the sensitivity coefficients matrix evaluated at the MAP estimate obtained by conditioning to production data. The covariance matrix C_M provides a measurement of the prior uncertainty in the model parameters and the a posterioiri covariance matrix provides an approximation to the uncertainty after conditioning to production data. C_{MP} would give an exact representation of the posterior uncertainty if data were linearly related to the model. Note if the data were completely insensitive to the model parameters then G_∞ would be a null matrix. In this case, Eq. 2.25 reduces to $C_{MP} = C_M$, i.e., as expected, conditioning the model to insensitive data does not reduce the uncertainty in model parameters. The diagonal entries of C_M and C_{MP}, respectively, represent the prior and a posteriori variances of model parameters. Here, we simply estimate the reduction in the uncertainty by comparing the ratio of the a posteriori variance of each model parameter to its prior variance. If the ratio is unity, the uncertainty in the model parameter is not reduced by conditioning to production data, if the standard deviation is reduced by a factor of 10, we say the uncertainty has been reduced by 90 per cent or a factor of 10 and so on.

2.6.2 Multiple Realizations

Except in the case where data are linearly related to the model, the preceding method is only approximate and for a highly nonlinear problem with a multi-modal

a posteriori probability density function, the analysis is tenuous. In such cases, it is possible to evaluate the uncertainty by generating a suite of conditional realizations which represent a correct sampling of the a posteriori pdf. Unfortunately, sampling correctly is not computationally efficient for the problems of interest to us; see, Oliver et al. (1997) and Cunha (1996). Currently, realizations are generated by the randomized maximum likelihood method, Kitanidis (1995) and Oliver et al. (1996). In this procedure, a realization is generated by minimizing the following objective function:

$$O_r(m) = \frac{1}{2}(m - m_{uc})^T C_M^{-1}(m - m_{uc}) + \frac{1}{2}(g(m) - d_{uc})^T C_D^{-1}(g(m) - d_{uc}), \quad (2.26)$$

where m_{uc} is an unconditional simulation of m from prior model and d_{uc} is an unconditional simulation of conditioning production data.

Because we have assumed that the prior pdf for model parameters is multi-Gaussian, the unconditional realization of m can be generated from

$$m_{uc} = m_{\text{prior}} + C_M^{1/2} Z_M, \quad (2.27)$$

where Z_M is a vector of independent normal deviates with zero mean and unit variance, and $C_M^{1/2}$ is a square root of the model covariance matrix. $C_M^{1/2}$ can be generated by using Cholesky decomposition of prior covariance matrix.

Similarly, the unconditional realization of d_{obs} is generated by,

$$d_{uc} = d_{\text{obs}} + C_D^{1/2} Z_D, \quad (2.28)$$

where Z_D is a vector of independent normal deviates with zero mean and unit variance, and $C_D^{1/2}$ is a square root of the data covariance matrix.

Using Cholesky decomposition of the prior covariance matrix to generate unconditional realization is only plausible for small problems. For large problems, we could use sequential Gaussian cosimulation to generate unconditional realizations.

CHAPTER III

COMPUTATION OF SENSITIVITY COEFFICIENTS FOR 3D, 3-PHASE FLUID PROBLEMS BY THE ADJOINT METHOD

3.1 Sensitivity Coefficients

In this work, we develop a general adjoint procedure for computing sensitivity coefficients for three-dimensional, three-phase flow problems. This procedure is based on the general three-dimensional, three-phase, fully-implicit, black-oil flow simulation equations. The sensitivity coefficients which can be generated by this procedure include the sensitivity of wellbore pressure, GOR, WOR or objective function to simulator gridblock permeabilities, porosities, skin factors, and the parameters used in relative permeability correlations. We use a Cartesian coordinate system and the reservoir boundaries are assumed to be no-flow boundaries. The permeability and porosity fields are heterogeneous. The wellbore constraint conditions could be rate specified or bottom hole pressure specified.

The adjoint procedure presented in this chapter has been implemented in Fortran 90 and is fully functional. We have coupled the codes with an existing fully implicit, black-oil simulator (CLASS) from Chevron. By using an existing simulator, we were able to focus on the calculation of sensitivity coefficients and history matching, instead of focusing on the development of another simulator. The adjoint procedure codes we have developed are totally separate from the simulator. It would not be difficult to modify the adjoint codes to work with other commercial simulators.

Before using the CLASS simulator, we attempted to use BOAST 3, an IMPES simulator from DOE, as the forward model. Our adjoint procedure is based on fully implicit simulation equations. On the other hand, the BOAST 3 is an IM-

PES simulator. After extensive experimentation, we realized that the inconsistency between the fully implicit simulation equation and the IMPES simulator was causing significant inaccuracy in sensitivity coefficients for three-phase, three-dimensional flow problems, even when we used very small time steps for the IMPES simulator. Only in the water-oil, two-dimensional flow case was the fully implicit adjoint procedure capable of generating accurate sensitivity coefficients by working with an IMPES simulator. In general, one should use the same formulation in the adjoint equations to compute sensitivity coefficients as are used in the reservoir simulator.

In this work, individual sensitivity coefficients are evaluated by the adjoint procedure. We show that the system of adjoint equations can be written in a very compact form.

3.2 The Reservoir Simulator

For simplicity, the reservoir is assumed to be a rectangular parallelepiped which occupies the region

$$\Omega = \{(x, y, z) \mid 0 < x < L_x, 0 < y < L_y, 0 < z < L_z\}. \tag{3.1}$$

The simulator used is based on a fully-implicit, finite-difference formulation of the three-phase flow, black-oil equations expressed in an x–y–z coordinate system which apply on Ω; see Eq. 3.1. At each of the N gridblocks, three finite difference equations apply. These $3N$ equations represent the mass balances for each of the three components. In addition, a constraint is applied at each of the N_w wells to yield N_w additional equations. At each well at each time step, either an individual phase flow rate, the total flow rate or the wellbore pressure may be specified as a well constraint. In the results considered here, capillary pressures are assumed to be negligible.

For gridblock i, the primary variables in our formulation are $p_i, S_{w,i}$ and $S_{g,i}$. In addition, the flowing wellbore pressure, $p_{wf,j}$ at the jth well is a primary variable.

We let y^n denote a column vector which contains the set of primary variables at time step n. At gridblock i, the finite difference equation for component u can be written as

$$f_{u,i}(y^{n+1}, y^n, m) = f_{u,i}^{n+1} = 0, \tag{3.2}$$

for $u = o, w, g$ and $i = 1, \ldots, N$. The well constraints are represented by

$$f_{wf,j}(y^{n+1}, y^n, m) = f_{wf,j}^{n+1} = 0, \tag{3.3}$$

for $j = 1, 2, \ldots, N_w$. If the flowing wellbore pressure at well j at time t^{n+1} is specified to be equal to $p_{wf,j,0}^{n+1}$, then Eq. 3.3 is given by

$$f_{wf,j}(y^{n+1}, y^n, m) = p_{wf,j}^{n+1} - p_{wf,j,0}^{n+1} = 0. \tag{3.4}$$

Eqs. 3.2 and 3.3 represent the system of $3N + N_w$ equations that are solved to obtain the values of the primary variables at time $t^{n+1} = t^n + \Delta t^n$. For wells at which the flowing bottom hole pressure is specified, phase flow rates at each well are computed by Peaceman's equation (Peaceman, 1983). The complete system of equations can formally be written as

$$f^{n+1} = f(y^{n+1}, y^n, m) = \begin{bmatrix} f_{o,1}^{n+1} \\ f_{w,1}^{n+1} \\ f_{g,1}^{n+1} \\ f_{o,2}^{n+1} \\ \vdots \\ f_{g,N}^{n+1} \\ f_{wf,1}^{n+1} \\ \vdots \\ f_{wf,N_w}^{n+1} \end{bmatrix} = 0, \tag{3.5}$$

where

$$y^{n+1} = \begin{bmatrix} p_1^{n+1} \\ S_{w,1}^{n+1} \\ S_{g,1}^{n+1} \\ p_2^{n+1} \\ \vdots \\ S_{g,N}^{n+1} \\ p_{wf,1}^{n+1} \\ \vdots \\ p_{wf,N_w}^{n+1} \end{bmatrix}, \tag{3.6}$$

and

$$m = \begin{bmatrix} m_1 \\ m_2 \\ \vdots \\ m_{N_m} \end{bmatrix}. \tag{3.7}$$

and where N_m is the number of model parameters.

Eq. 3.5 is solved by the Newton-Raphson method (Aziz and Settaari, 1979) which can be written as

$$J^{\nu}\delta y^{\nu+1} = -f^{\nu} \tag{3.8}$$

$$y^{\nu+1} = y^{\nu} + \delta y^{\nu+1}, \tag{3.9}$$

where ν is the iteration index and

$$J^{\nu} = [\nabla_{y^{\nu}} f^T]^T, \tag{3.10}$$

is the Jacobian matrix evaluated at y^{ν}, which represents the νth approximation for y^{n+1}.

3.3 Adjoint Equations

We define a general scalar function by

$$\beta = \beta(y^1, ..., y^L, m), \tag{3.11}$$

where L corresponds to the last time t^L at which one wishes to compute sensitivity coefficients. The objective is to compute the sensitivity of β to changes in the model parameters m. We obtain an adjoint functional J by adjoining Eq. 3.5 to the function β:

$$J = \beta + \sum_{n=0}^{L} (\lambda^{n+1})^T f^{n+1}, \tag{3.12}$$

where λ^{n+1} is the vector of adjoint variables at time step $n+1$, and is given by

$$\lambda^{n+1} = \left[\lambda_1^{n+1}, \quad \lambda_2^{n+1}, \quad \ldots, \quad \lambda_{3N+N_w}^{n+1}\right]^T. \tag{3.13}$$

Taking the total differential of Eq. 3.12, and doing some simple rearranging gives

$$\begin{aligned} dJ &= d\beta + \sum_{n=0}^{L} \left\{ (\lambda^{n+1})^T [\nabla_{y^{n+1}} (f^{n+1})^T]^T dy^{n+1} + [\nabla_m (f^{n+1})^T]^T dm \right\} \\ &\quad + \sum_{n=0}^{L} (\lambda^{n+1})^T [\nabla_{y^n} (f^{n+1})^T]^T dy^n \\ &= d\beta + BT + \sum_{n=1}^{L} \{ [(\lambda^n)^T [\nabla_{y^n} (f^n)^T]^T \\ &\quad + (\lambda^{n+1})^T [\nabla_{y^n} (f^{n+1})^T]^T] dy^n + (\lambda^n)^T [\nabla_m (f^n)^T]^T dm \}, \end{aligned} \tag{3.14}$$

where

$$\begin{aligned} BT = (\lambda^{L+1})^T \{ &[\nabla_{y^{L+1}} (f^{L+1})^T]^T dy^{L+1} \\ &+ [\nabla_m (f^{L+1})^T]^T dm \} + (\lambda^1)^T [\nabla_{y^0} (f^1)^T]^T dy^0. \end{aligned} \tag{3.15}$$

The total differential of β can be written as

$$d\beta = \sum_{n=1}^{L} [\nabla_{y^n} \beta]^T dy^n + [\nabla_m \beta]^T dm. \tag{3.16}$$

The initial conditions are fixed, so

$$dy^0 = 0. \tag{3.17}$$

Choosing

$$\lambda^{L+1} = 0, \tag{3.18}$$

it follows that $BT = 0$. Using this result and Eq. 3.16 in Eq. 3.14 and rearranging the resulting equation gives

$$dJ = \sum_{n=1}^{L} \Big[\Big\{ (\lambda^n)^T [\nabla_{y^n} (f^n)^T]^T + (\lambda^{n+1})^T [\nabla_{y^n} (f^{n+1})^T]^T + [\nabla_{y^n} \beta]^T \Big\} dy^n \Big] + \{ [\nabla_m \beta]^T + \sum_{n=1}^{N} (\lambda^n)^T [\nabla_m (f^n)^T]^T \} dm. \tag{3.19}$$

To obtain the adjoint system, the coefficients multiplying dy^n in Eq. 3.19 are set equal to zero, i.e., we require that the adjoint variables satisfy

$$(\lambda^n)^T [\nabla_{y^n} (f^n)^T]^T + (\lambda^{n+1})^T [\nabla_{y^n} (f^{n+1})^T]^T + [\nabla_{y^n} \beta]^T = 0. \tag{3.20}$$

Taking the transpose of Eq. 3.20, gives the adjoint system

$$[\nabla_{y^n} (f^n)^T] \lambda^n = -[\nabla_{y^n} (f^{n+1})^T] \lambda^{n+1} - \nabla_{y^n} \beta. \tag{3.21}$$

where

$$\nabla_{y^n} [f^n]^T = \begin{bmatrix} \frac{\partial f^n_{o,1}}{\partial p^n_1} & \frac{\partial f^n_{w,1}}{\partial p^n_1} & \cdots & \frac{\partial f^n_{g,N}}{\partial p^n_1} & \frac{\partial f^n_{wf,1}}{\partial p^n_1} & \cdots & \frac{\partial f^n_{wf,N_w}}{\partial p^n_1} \\ \frac{\partial f^n_{o,1}}{\partial S^n_{w,1}} & \frac{\partial f^n_{w,1}}{\partial S^n_{w,1}} & \cdots & \frac{\partial f^n_{g,N}}{\partial S^n_{w,1}} & \frac{\partial f^n_{wf,1}}{\partial S^n_{w,1}} & \cdots & \frac{\partial f^n_{wf,N_w}}{\partial S^n_{w,1}} \\ \frac{\partial f^n_{o,1}}{\partial S^n_{g,1}} & \frac{\partial f^n_{w,1}}{\partial S^n_{g,1}} & \cdots & \frac{\partial f^n_{g,N}}{\partial S^n_{g,N}} & \frac{\partial f^n_{wf,1}}{\partial S^n_{g,1}} & \cdots & \frac{\partial f^n_{wf,N_w}}{\partial S^n_{g,1}} \\ \frac{\partial f^n_{o,1}}{\partial p^n_2} & \frac{\partial f^n_{w,1}}{\partial p^n_2} & \cdots & \frac{\partial f^n_{g,N}}{\partial p^n_2} & \frac{\partial f^n_{wf,1}}{\partial p^n_2} & \cdots & \frac{\partial f^n_{wf,N_w}}{\partial p^n_2} \\ \vdots & \vdots & \cdots & \vdots & \vdots & \cdots & \vdots \\ \frac{\partial f^n_{o,1}}{\partial S^n_{g,N}} & \frac{\partial f^n_{w,1}}{\partial S^n_{g,N}} & \cdots & \frac{\partial f^n_{g,N}}{\partial S^n_{g,N}} & \frac{\partial f^n_{wf,1}}{\partial S^n_{g,N}} & \cdots & \frac{\partial f^n_{wf,N_w}}{\partial S^n_{g,N}} \\ \frac{\partial f^n_{o,1}}{\partial p^n_{wf,1}} & \frac{\partial f^n_{w,1}}{\partial p^n_{wf,1}} & \cdots & \frac{\partial f^n_{g,N}}{\partial p^n_{wf,1}} & \frac{\partial f^n_{wf,1}}{\partial p^n_{wf,1}} & \cdots & \frac{\partial f^n_{wf,N_w}}{\partial p^n_{wf,1}} \\ \vdots & \vdots & \cdots & \vdots & \vdots & \cdots & \vdots \\ \frac{\partial f^n_{o,1}}{\partial p^n_{wf,N_w}} & \frac{\partial f^n_{w,1}}{\partial p^n_{wf,N_w}} & \cdots & \frac{\partial f^n_{g,N}}{\partial p^n_{wf,N_w}} & \frac{\partial f^n_{wf,1}}{\partial p^n_{wf,N_w}} & \cdots & \frac{\partial f^n_{wf,N_w}}{\partial p^n_{wf,N_w}} \end{bmatrix}, \tag{3.22}$$

$$\nabla_{y^n}[f^{n+1}]^T = \begin{bmatrix} \frac{\partial f_{o,1}^{n+1}}{\partial p_1^n} & \frac{\partial f_{w,1}^{n+1}}{\partial p_1^n} & \cdots & \frac{\partial f_{g,N}^{n+1}}{\partial p_1^n} & \frac{\partial f_{wf,1}^{n+1}}{\partial p_1^n} & \cdots & \frac{\partial f_{wf,N_w}^{n+1}}{\partial p_1^n} \\ \frac{\partial f_{o,1}^{n+1}}{\partial S_{w,1}^n} & \frac{\partial f_{w,1}^{n+1}}{\partial S_{w,1}^n} & \cdots & \frac{\partial f_{g,N}^{n+1}}{\partial S_{w,1}^n} & \frac{\partial f_{wf,1}^{n+1}}{\partial S_{w,1}^n} & \cdots & \frac{\partial f_{wf,N_w}^{n+1}}{\partial S_{w,1}^n} \\ \frac{\partial f_{o,1}^{n+1}}{\partial S_{g,1}^n} & \frac{\partial f_{w,1}^{n+1}}{\partial S_{g,1}^n} & \cdots & \frac{\partial f_{g,N}^{n+1}}{\partial S_{g,N}^n} & \frac{\partial f_{wf,1}^{n+1}}{\partial S_{g,1}^n} & \cdots & \frac{\partial f_{wf,N_w}^{n+1}}{\partial S_{g,1}^n} \\ \frac{\partial f_{o,1}^{n+1}}{\partial p_2^n} & \frac{\partial f_{w,1}^{n+1}}{\partial p_2^n} & \cdots & \frac{\partial f_{g,N}^{n+1}}{\partial p_2^n} & \frac{\partial f_{wf,1}^{n+1}}{\partial p_2^n} & \cdots & \frac{\partial f_{wf,N_w}^{n+1}}{\partial p_2^n} \\ \vdots & \vdots & \cdots & \vdots & \vdots & \cdots & \vdots \\ \frac{\partial f_{o,1}^{n+1}}{\partial S_{g,N}^n} & \frac{\partial f_{w,1}^{n+1}}{\partial S_{g,N}^n} & \cdots & \frac{\partial f_{g,N}^{n+1}}{\partial S_{g,N}^n} & \frac{\partial f_{wf,1}^{n+1}}{\partial S_{g,N}^n} & \cdots & \frac{\partial f_{wf,N_w}^{n+1}}{\partial S_{g,N}^n} \\ \frac{\partial f_{o,1}^{n+1}}{\partial p_{wf,1}^n} & \frac{\partial f_{w,1}^{n+1}}{\partial p_{wf,1}^n} & \cdots & \frac{\partial f_{g,N}^{n+1}}{\partial p_{wf,1}^n} & \frac{\partial f_{wf,1}^{n+1}}{\partial p_{wf,1}^n} & \cdots & \frac{\partial f_{wf,N_w}^{n+1}}{\partial p_{wf,1}^n} \\ \vdots & \vdots & \cdots & \vdots & \vdots & \cdots & \vdots \\ \frac{\partial f_{o,1}^{n+1}}{\partial p_{wf,N_w}^n} & \frac{\partial f_{w,1}^{n+1}}{\partial p_{wf,N_w}^n} & \cdots & \frac{\partial f_{g,N}^{n+1}}{\partial p_{wf,N_w}^n} & \frac{\partial f_{wf,1}^{n+1}}{\partial p_{wf,N_w}^n} & \cdots & \frac{\partial f_{wf,N_w}^{n+1}}{\partial p_{wf,N_w}^n} \end{bmatrix}, \quad (3.23)$$

and

$$\nabla_{y^n}\beta = \begin{bmatrix} \frac{\partial \beta}{\partial p_1^n} \\ \frac{\partial \beta}{\partial S_{w,1}^n} \\ \frac{\partial \beta}{\partial S_{g,1}^n} \\ \frac{\partial \beta}{\partial p_2^n} \\ \vdots \\ \frac{\partial \beta}{\partial S_{g,N}^n} \\ \frac{\partial \beta}{\partial p_{wf,1}^n} \\ \vdots \\ \frac{\partial \beta}{\partial p_{wf,N_w}^n} \end{bmatrix}. \quad (3.24)$$

Eq. 3.21 with initial condition 3.18 is solved backwards in time for $n = L, L-1, \ldots, 1$. In the above equations, $\nabla_{y^n}(f^n)^T$ and $\nabla_{y^n}(f^{n+1})^T$ are $3N+N_w$ by $3N+N_w$ matrices, and $\nabla_{y^n}\beta$ is a $3N + N_w$ dimensional column vector.

The matrix multiplying λ^{n+1} in Eq. 3.21 is a diagonal band matrix which is only related to the accumulation terms in the reservoir simulation equations. Note that the coefficient matrix $(\nabla_{y^n}(f^n)^T)$ in the adjoint system is simply the transpose of the Jacobian matrix of Eq. 3.10 evaluated at y^n. This is an important result as it means that one can extract the matrices involved in the adjoint equations directly

from the Jacobian matrices used in the simulator. This avoids the tedious process of directly deriving the individual adjoint equations. In this sense, our derivation shows that the adjoint method is somewhat similar to the gradient simulator method Anterion et al. (1989) in that the coefficient matrices that appear in both problems can be formed directly from Jacobian matrices used in solving the finite-difference equations by the Newton-Raphson method. As the adjoint system is solved backwards in time, information needed to compute the transpose of the Jacobian matrices must be saved from the simulation run, whereas, in the gradient simulator method, the desired sensitivity coefficients are computed at each time step during the simulation run.

The detailed equations for computing the derivatives $\nabla_{y^n}(f^n)^T$, $\nabla_{y^n}(f^{n+1})^T$, and $\nabla_{y^n}\beta$ in the adjoint equation Eq. 3.21 are given in the appendix A.

Considering J as a function of m , we can write its total differential as

$$dJ = (\nabla_m J)^T dm. \tag{3.25}$$

By comparing Eq. 3.19 and Eq. 3.25, it follows that the desired sensitivity coefficients for J, or equivalently, β, are given by

$$\nabla_m J = \nabla_m \beta + \sum_{n=1}^{L} [\nabla_m (f^n)^T](\lambda^n) \tag{3.26}$$

where

$$\nabla_m [f^n]^T = \begin{bmatrix} \frac{\partial f^n_{o,1}}{\partial m_1} & \frac{\partial f^n_{w,1}}{\partial m_1} & \frac{\partial f^n_{g,1}}{\partial m_1} & \frac{\partial f^n_{o,2}}{\partial m_1} & \cdots & \frac{\partial f^n_{g,N}}{\partial m_1} & \frac{\partial f^n_{wf,1}}{\partial m_1} & \cdots & \frac{\partial f^n_{wf,N_w}}{\partial m_1} \\ \frac{\partial f^n_{o,1}}{\partial m_2} & \frac{\partial f^n_{w,1}}{\partial m_2} & \frac{\partial f^n_{o,1}}{\partial m_2} & \frac{\partial f^n_{o,2}}{\partial m_2} & \cdots & \frac{\partial f^n_{g,N}}{\partial m_2} & \frac{\partial f^n_{wf,1}}{\partial m_2} & \cdots & \frac{\partial f^n_{wf,N_w}}{\partial m_2} \\ \vdots & \vdots & \vdots & \vdots & \vdots & \vdots & \vdots & \vdots & \vdots \\ \frac{\partial f^n_{o,1}}{\partial m_{N_m}} & \frac{\partial f^n_{w,1}}{\partial m_{N_m}} & \frac{\partial f^n_{o,1}}{\partial m_{N_m}} & \frac{\partial f^n_{o,2}}{\partial m_{N_m}} & \cdots & \frac{\partial f^n_{g,N}}{\partial m_{N_m}} & \frac{\partial f^n_{wf,1}}{\partial m_{N_m}} & \cdots & \frac{\partial f^n_{wf,N_w}}{\partial m_{N_m}} \end{bmatrix}, \tag{3.27}$$

and

$$\nabla_m \beta = \begin{bmatrix} \frac{\partial \beta}{\partial m_1} \\ \frac{\partial \beta}{\partial m_2} \\ \vdots \\ \frac{\partial \beta}{\partial m_{N_m}} \end{bmatrix}. \tag{3.28}$$

The matrix $\nabla_m [f^n]^T$ is a N_m by $3N + N_w$ sparse matrix and $\nabla_m \beta$ is a N_m dimensional column vector.

In Eq. 3.26, the gradient $\nabla_m \beta$ involves the partial derivatives of β with respect to the model parameters. If the jth model parameter does not explicitly appear in the expression for β, then $\partial \beta / \partial m_j = 0$. For example, if $\beta = p^n_{wf}$, then we set $\nabla_m \beta = 0$ in Eq. 3.26.

For the results considered here, the choices of β are restricted to the wellbore pressure, GOR and WOR at time steps where observed data for these variables are used as conditioning data. If one wishes to use a conjugate gradient (Makhlouf et al., 1993) or variable metric method (Yang and Watson, 1988), then one need only compute the gradient of the objective function and this can be done by setting $\beta = O(m)$ in the adjoint procedure. In this case, one only need solve the adjoint system Eq. 3.21 once to obtain the gradient.

From the formula given in Eq. 3.26, it is easy to write down the equations to calculate the sensitivity coefficients for various cases. For example, to calculate sensitivity of p_{wf}, GOR and WOR to permeabilities (k_x, k_y and k_z) and porosity (ϕ), define vectors of model parameters k_x, k_y, k_z and ϕ are defined by

$$m_{k_x} = k_x = [\ k_{x,1} \quad k_{x,2} \quad \cdots \quad k_{x,M}\ ]^T, \tag{3.29}$$

$$m_{k_y} = k_y = [\ k_{y,1} \quad k_{y,2} \quad \cdots \quad k_{y,M}\ ]^T, \tag{3.30}$$

$$m_{k_z} = k_z = [\ k_{z,1} \quad k_{z,2} \quad \cdots \quad k_{z,M}\ ]^T, \tag{3.31}$$

and

$$m_\phi = \phi = [\ \phi_1 \quad \phi_2 \quad \cdots \quad \phi_M\ ]^T. \tag{3.32}$$

From Eq. 3.21, we obtain the equation to calculate sensitivity to k_x, k_y, k_z and ϕ,

$$\nabla_{k_x} J = \nabla_{k_x}\beta + \sum_{n=1}^{L}[\nabla_{k_x}(f^n)^T](\lambda^n), \tag{3.33}$$

$$\nabla_{k_y} J = \nabla_{k_y}\beta + \sum_{n=1}^{L}[\nabla_{k_y}(f^n)^T](\lambda^n), \tag{3.34}$$

$$\nabla_{k_z} J = \nabla_{k_z}\beta + \sum_{n=1}^{L}[\nabla_{k_z}(f^n)^T](\lambda^n), \tag{3.35}$$

and

$$\nabla_{\phi} J = \nabla_{\phi}\beta + \sum_{n=1}^{L}[\nabla_{\phi}(f^n)^T](\lambda^n), \tag{3.36}$$

where J is p_{wf}, GOR or WOR at some specified time step L.

3.4 Comparison of Adjoint Method and Gradient Simulator Method

In the gradient simulator method, one takes the derivative of Eq. 3.5 with respect to a component of m, say m_i. This gives

$$\begin{aligned} 0 &= \frac{df(y^{n+1}, y^n, m)}{dm_i} \\ &= \frac{df^{n+1}}{dm_i} \\ &= [\nabla_{y^{n+1}}[f^{n+1}]^T]^T \frac{\partial y^{n+1}}{\partial m_i} + [\nabla_{y^n}[f^{n+1}]^T]^T \frac{\partial y^n}{\partial m_i} + \frac{\partial f^{n+1}}{\partial m_i}. \end{aligned} \tag{3.37}$$

It follows that the equation for sensitivity coefficients can be written as

$$[\nabla_{y^{n+1}}[f^{n+1}]^T]^T \frac{\partial y^{n+1}}{\partial m_i} = -[\nabla_{y^n}[f^{n+1}]^T]^T \frac{\partial y^n}{\partial m_i} - \frac{\partial f^{n+1}}{\partial m_i}. \tag{3.38}$$

Eq. 3.38 is the formulation used to calculate the sensitivity coefficients in the gradient simulator method.

The coefficient matrix ($[\nabla_{y^{n+1}}[f^{n+1}]^T]^T$) on the left hand side in Eq. 3.38 is the Jacobian matrix. It is the same as the one used to solve flow equations in

the simulator. This matrix can be directly extracted from the last Newton iteration at each time step provided a fully implicit simulator is used. In the adjoint system, Eq. 3.21, the coefficient matrix ($[\nabla_{y^n}(f^n)^T]$) on the left hand side is the transpose of Jacobian matrix. The right hand side of Eq. 3.21 and Eq. 3.38 are very similar. One can expect that it takes about the same amount of CPU time to solve Eq. 3.21 and Eq. 3.38 once. Consider an inverse problem with N_m model parameters and N_d data for which sensitivities are desired. Using the adjoint method, one needs to solve the adjoint system of Eq. 3.21 N_d times. Using the gradient simulator method, one needs to solve Eq. 3.38 N_m times. If the number of observed data is far fewer than the number of model parameters ($N_d << N_m$), the adjoint method is much more efficient than the gradient simulator method.

If a conjugate gradient method is used instead of a Newton-like method to minimize the objective function, one only needs the gradient of the objective function and does not need the sensitivity of the data to the model parameters. In this case, the adjoint system Eq. 3.21 only needs to be solved once. However, the conjugate gradient method usually takes many more iterations to converge comparing with Newton-like method (Makhlouf et al. (1993)). If one can find good preconditioner to improve the convergence of the conjugate gradient method, an automatic history procedure using the conjugate gradient method to minimize the objective function and the adjoint method to calculate the gradient could be efficient.

3.5 Examples of Sensitivity Coefficients

Several examples are chosen to illustrate that our implementation of the adjoint method yields accurate compute sensitivity coefficients for three-phase, three-dimensional flow problems. In some cases, comparison with the finite difference method is conducted to check the accuracy.

The particular examples presented here would be a challenge for some methods that rely on assumptions of small compressibility and unchanging flow directions. The first example is a 3-D, three-phase flow problem with water injection. This example provides insight into the complexity offered by a three dimensional problem under three-phase flow conditions. In this example, the sensitivity coefficients computed from the adjoint method are compared with the sensitivity coefficients computed from the finite difference method. The results show that the agreement of sensitivity coefficients between the two methods is nearly perfect. Second presents a 2-D solution-gas drive example that illustrates the complex behavior of the sensitivity of GOR, even when gravity can be ignored. The third example is a two-dimensional vertical cross-section for which gravity segregation is important. In this case, we are able to obtain insight on whether one can estimate vertical permeability from production data from a restricted entry well in a solution-gas drive reservoir.

3.5.1 A 3D, Three-Phase Example to Compare Sensitivity from Adjoint Method and Finite Difference Method

We created a synthetic, three-dimensional, three-phase reservoir model to compare the sensitivity coefficients generated from the adjoint method with those generated from the finite difference method. The reservoir is homogeneous with uniform horizontal permeability ($k_x = k_y = 40$ mD) and uniform vertical permeability ($k_z = 4$ mD). The porosity is 0.22 throughout the reservoir. The simulation grid is 11 by 11 by 3. An injection well is located at areal gridblock (8,8) with water

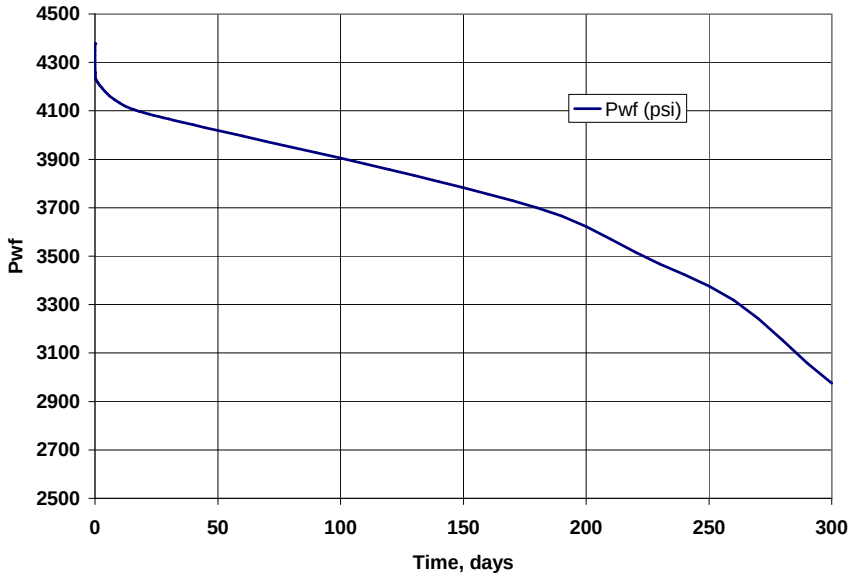

Figure 3.1: Bottom-hole pressure at producing well.

injection at rate 900 STB/d only into the bottom layer (layer 3). A well at areal gridblock (3,3) produces a total flow rate of 1000 RB/d from the top two layers, layer 1 and 2. This results in strong cross flow in the reservoir, allowing us to explore the possibility of estimating vertical permeability from production data. The reservoir is a oil reservoir with initial reservoir pressure 4511 psi at the center layer and the initial bubble point pressure 4417 psi. The production rate is greater than the injection rate under reservoir conditions, so the reservoir pressure and bottom hole pressure (Fig. 3.1) decrease with time. The reservoir pressure drops below the bubble point soon after the begining of simulation. There is water break through in the producing well at about 180 days (Fig. 3.2) and the simulation continues to 300 days.

The equation for computing the sensitivity of predicted data $g(m)$ to the jth model parameter m_j ($\frac{\partial g(m)}{\partial m_j}$) using the finite difference method is

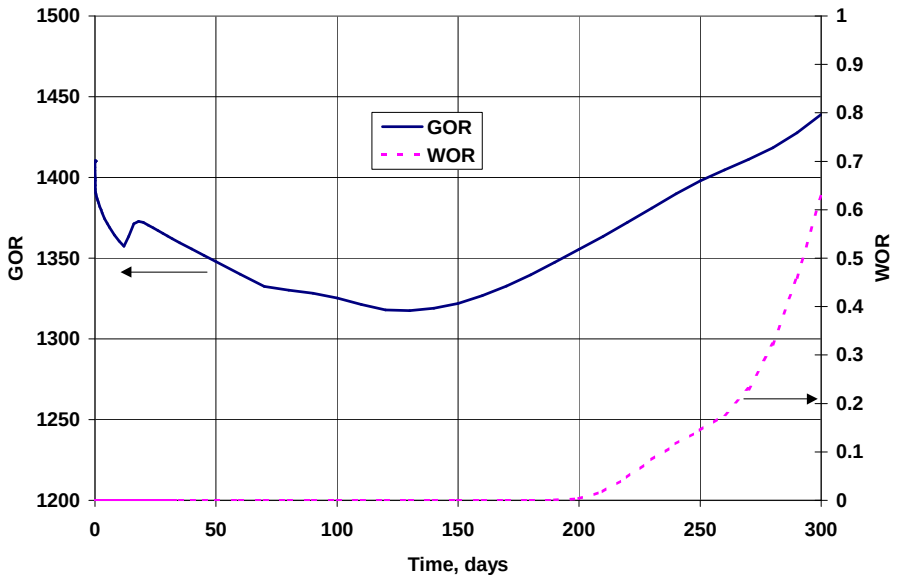

Figure 3.2: Gas-oil ratio and water-oil ratio at producing well.

$$\frac{\partial g(m)}{\partial m_j} = \frac{g(m + \delta m_j e_j) - g(m)}{\delta m_j}, \tag{3.39}$$

where e_j is a unit column vector with its jth entry equal to unity and all other entries equal to zero, δm_j is the perturbation of m_j. Here, g(m) may be any data, e.g., p_{wf}m GOR or WOR.

In the finite-difference method for calculating sensitivity coefficients, we perturb the permeability or porosity in each gridblock and compute the changes in pressure, gas-oil ratio and water-oil ratio. The magnitude of the perturbation in properties would seem to be critical for the accuracy of the finite difference method. If the perturbation is too small, the results will be effected by roundoff errors. If the perturbation is too large, the quadratic term which has been neglected in the Taylor expansion may become important. Extensive experimentation with the magnitude of

the perturbation showed that the calculated sensitivity coefficients are fairly stable, i.e., the same sensitivity results were obtained for a certain range of the perturbation. Based on our experiment, we chose the magnitude of the perturbation to be around 0.01% of the values of the parameters to be perturbed. This choice always resulted in accurate sensitivity coefficients as long as each simulator run in the finite-difference method used the exactly same time step sequence, i.e., the time step sequences in the simulator run for computing $g(m + \delta m_j e_j)$ and $g(m)$ in Eq. 3.39 should be identical. Otherwise, it some inaccuracy mat be introduced.

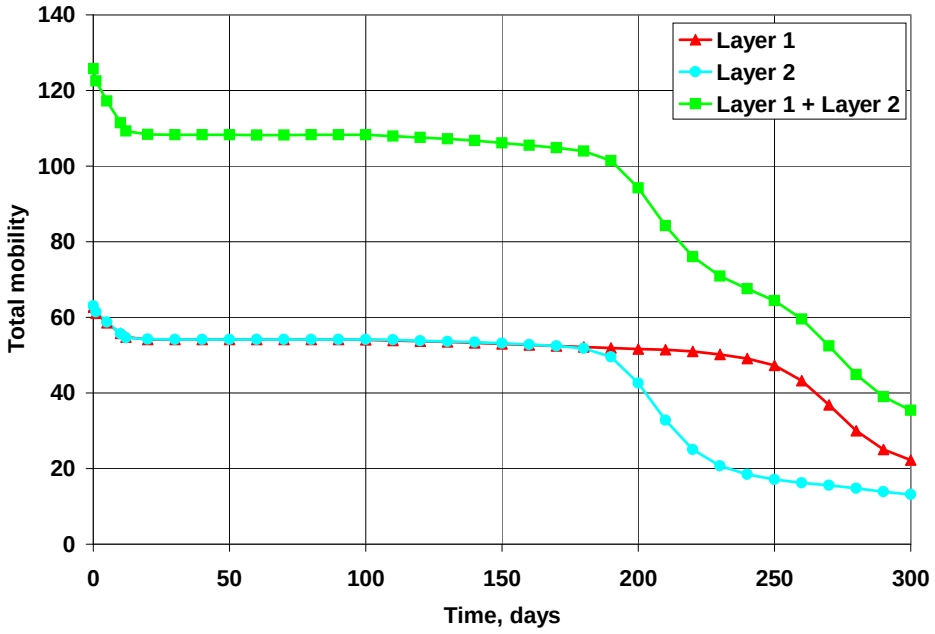

Figure 3.3: The total mobility in the producing well gridblocks as a function of time.

Fig. 3.3 shows the total mobility in the producing well gridblocks changes as a function of time. It is easy to see that the total mobilities, in both layer 1 and layer 2, decrease with time.

Fig. 3.4, 3.5, and 3.6 present, respectively, the water, oil, and gas saturation

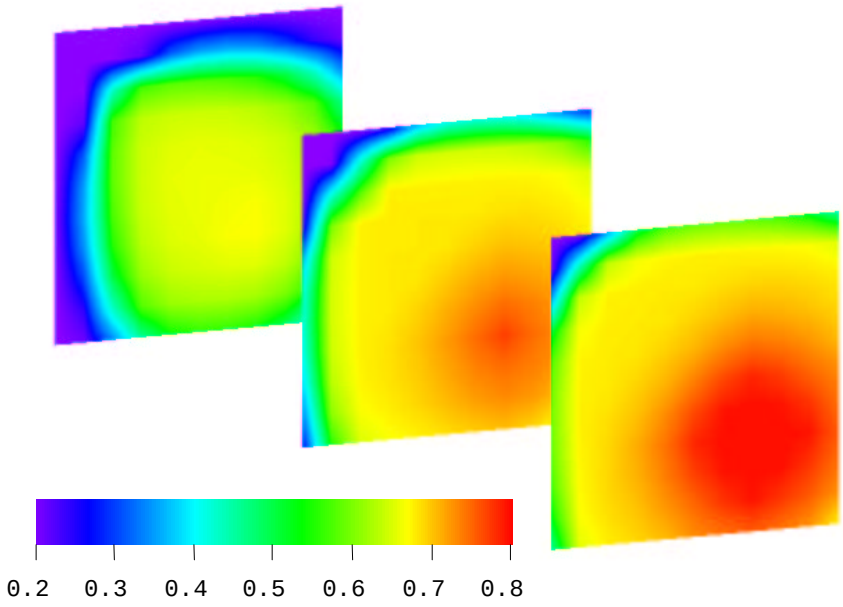

Figure 3.4: The water saturation distribution at 300 days.

distribution at 300 days. From these figures, we can see the saturation distributions in each layer. We also can see the gravity segregation effect.

Because the convergence rate in history matching depends on the accuracy of the gradients, we have extensively tested the accuracy of the sensitivity coefficients computed from the adjoint method. The comparison of sensitivity coefficients from the adjoint method and from the finite difference method has been done for various cases, including 2D and 3D solution-gas drive, water-oil two phase flow, and three-phase flow reservoirs. In all cases, the agreement between sensitivity coefficients from the adjoint method and from the finite different method is nearly perfect (see, for example, Figs. 3.7-3.15). In most cases, the results from the two methods agree to 3 or 4 significant digits. In all cases, the mismatch is less than 1%.

Fig. 3.7 shows the sensitivity of p_{wf} to horizontal permeability at 300 days. Just as expected, the bottom hole pressure is extremely sensitive to the horizontal

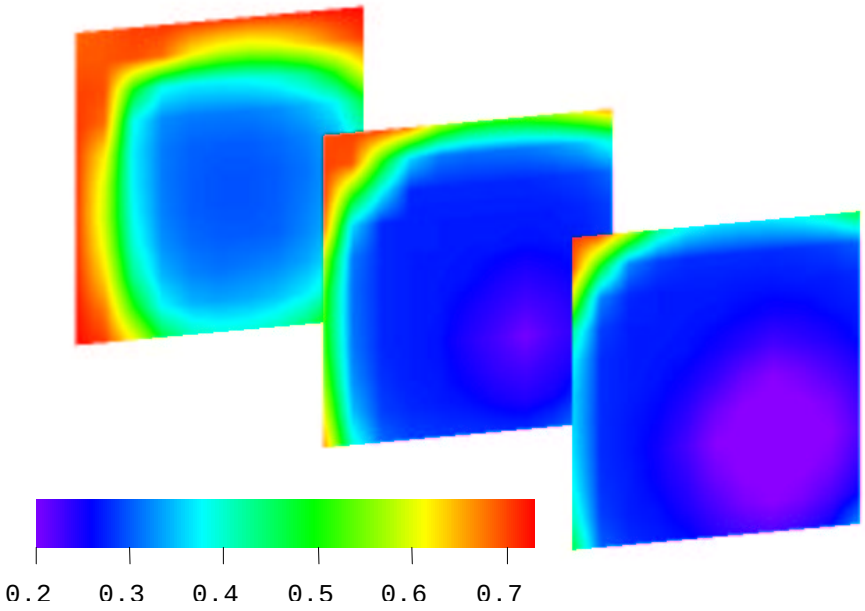

Figure 3.5: The oil saturation distribution at 300 days.

permeability of wellbore gridblocks. The producing well is only completed in the top two layers, so the magnitude of sensitivity is high only for the top two layers. Fig. 3.8 shows the sensitivity of p_{wf} to vertical permeability k_z at 300 days. Unlike horizontal permeability, the vertical permeability is not involved in the wellbore model (Peaceman equation), so $\partial p_{wf}/\partial k_z$ is not extremely high at the wellbore gridblock. Actually, it could be even lower than the sensitivity to vertical permeability at a gridblock without a well. Because water is injected into the bottom layer, increasing k_z will result in more water flow to the top layers and decrease total mobility, resulting in a larger pressure drop and lower pressure. This is why in the area between wells the sensitivity of p_{wf} to vertical permeability is negative. Fig. 3.9 presents the sensitivity of p_{wf} to porosity at 300 days of production. Increasing the porosity in a gridblock delays the water advance. So the total mobility will be higher and the pressure drop smaller. This results in a higher pressure and thus the sensitivity of p_{wf} to porosity

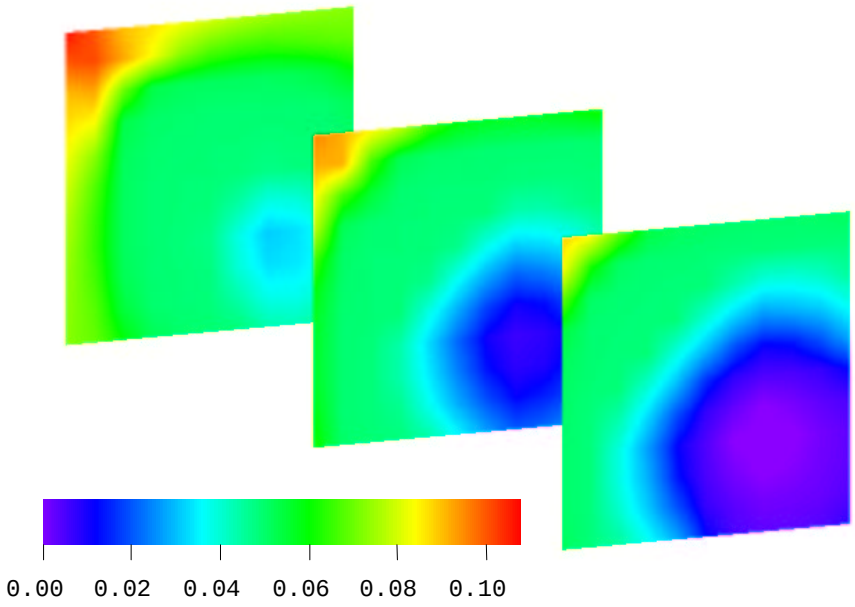

Figure 3.6: The gas saturation distribution at 300 days.

is positive. The p_{wf} is very sensitive to the porosity at the water front.

Fig. 3.10, 3.11, and 3.12 show the sensitivity of WOR to horizontal permeability, vertical permeability and porosity at 300 days respectively. An increase in horizontal permeability causes the water to move faster from the injection well to the producing well, and the WOR to be higher. This is the reason that $\partial \mathrm{WOR}/\partial k$ is positive in the region between wells (Fig. 3.10). Similarly, more water moves from the bottom layer to top layers as vertical permeability increases, so $\partial \mathrm{WOR}/\partial k_z$ is also positive between wells (Fig. 3.11). On the other hand, an increase in porosity will delay water moving to producing well. Sensitivity of WOR to porosity is negative in the swept region (Fig. 3.12).

Sensitivity of the gas-oil ratio is more complicated and very difficult to understand. The GOR includes two sources. One source is dissolved gas, which is increased as pressure increases. The other part is free gas, and the amount of free gas

production decreases as pressure increases. If dissolved gas dominates in the GOR, we expect GOR to increase as pressure increases. If free gas dominates in the GOR, the GOR will decrease as pressure increases. The critical gas saturation (S_{gc}) for this reservoir is about 0.05. Fig. 3.14 shows the sensitivity of GOR to vertical permeability k_z. In this example, we know that the pressure decreases as k_z increases. At 300 days (Fig. 3.14), free gas is the primary contributor to gas production at the well, so $\partial \text{GOR}/\partial k_z$ is positive between the wells. Fig. 3.15 shows the sensitivity of GOR to the porosity. As we discussed in the previous section, an increase in porosity, ϕ, causes the pressure to increase in the reservoir. At 300 days (Fig. 3.15), free gas is dominant in most areas, so the $\partial \text{GOR}/\partial \phi$ is negative.

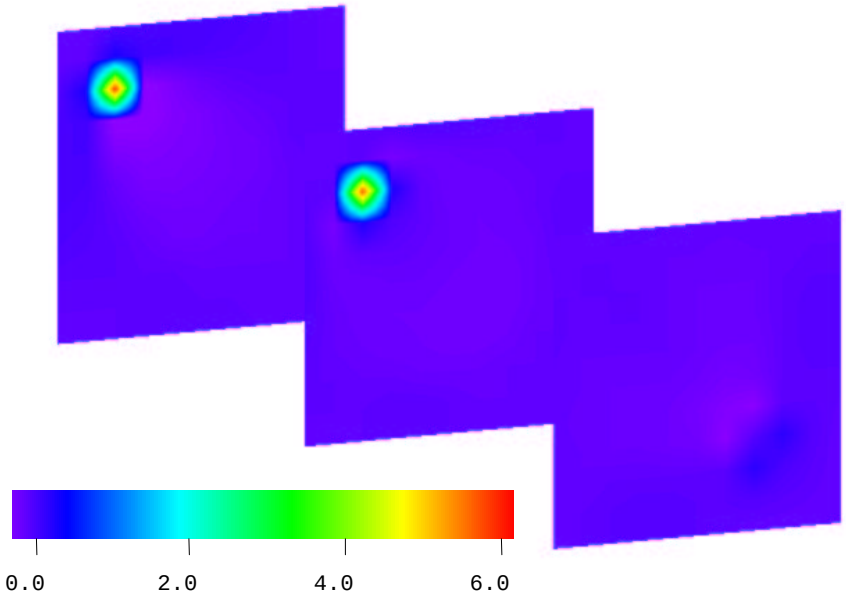

(a) Adjoint method.

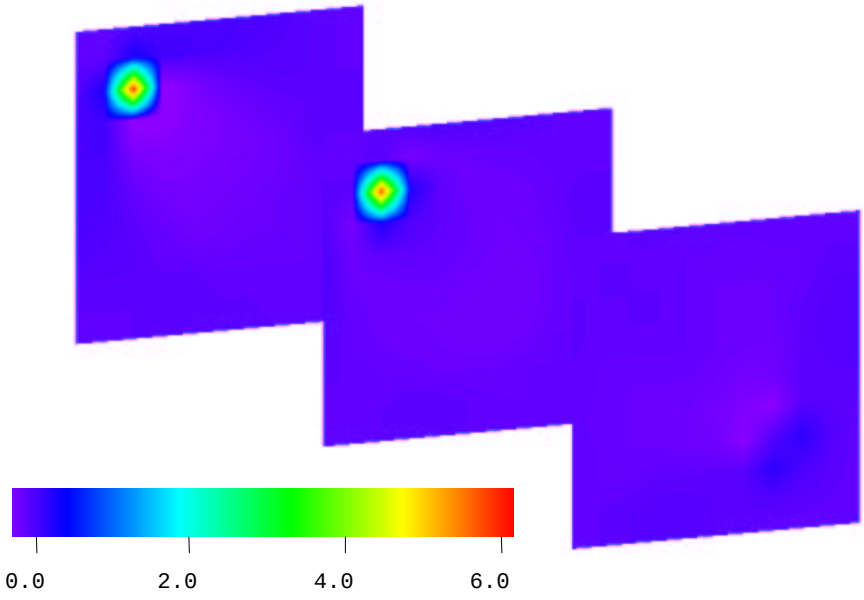

(b) Finite difference method.

Figure 3.7: Sensitivity of bottom-hole pressure at producing well to horizontal permeability at 300 days.

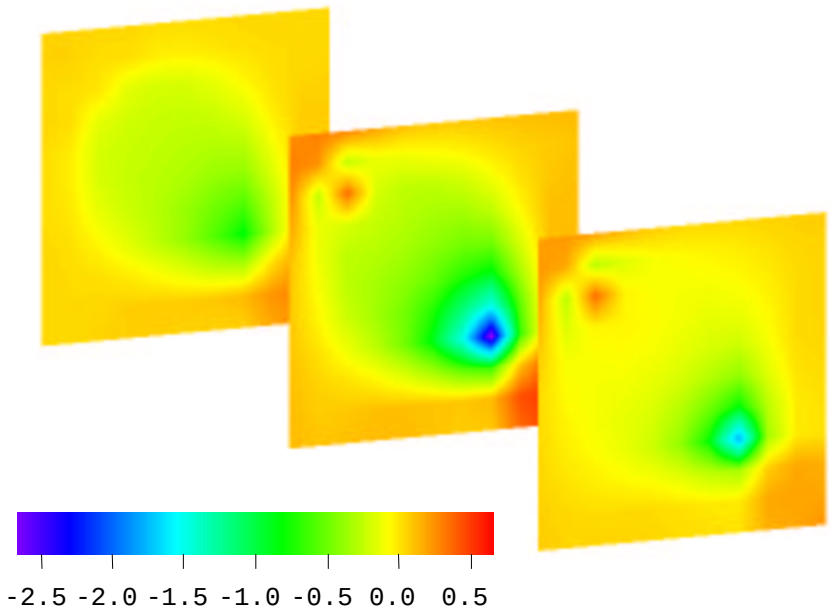

(a) Adjoint method.

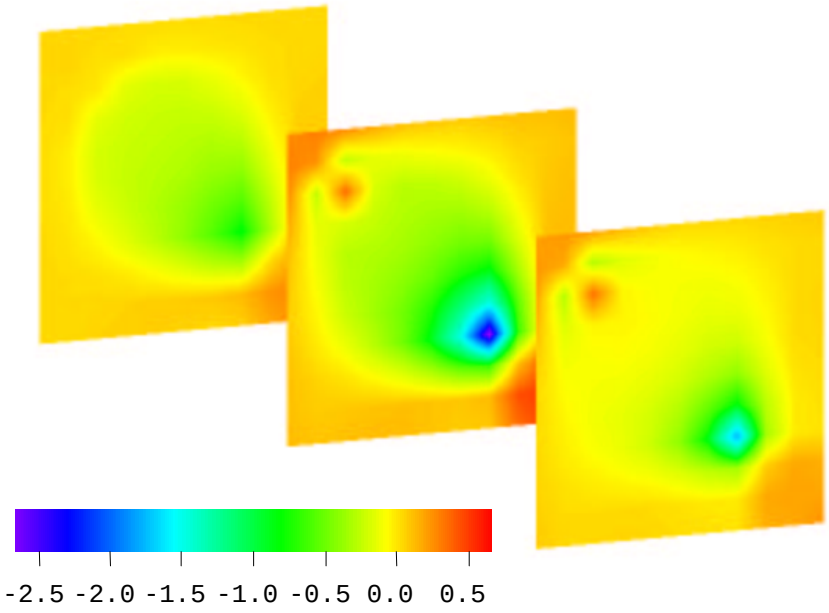

(b) Finite difference method.

Figure 3.8: Sensitivity of bottom-hole pressure at producing well to vertical permeability at 300 days.

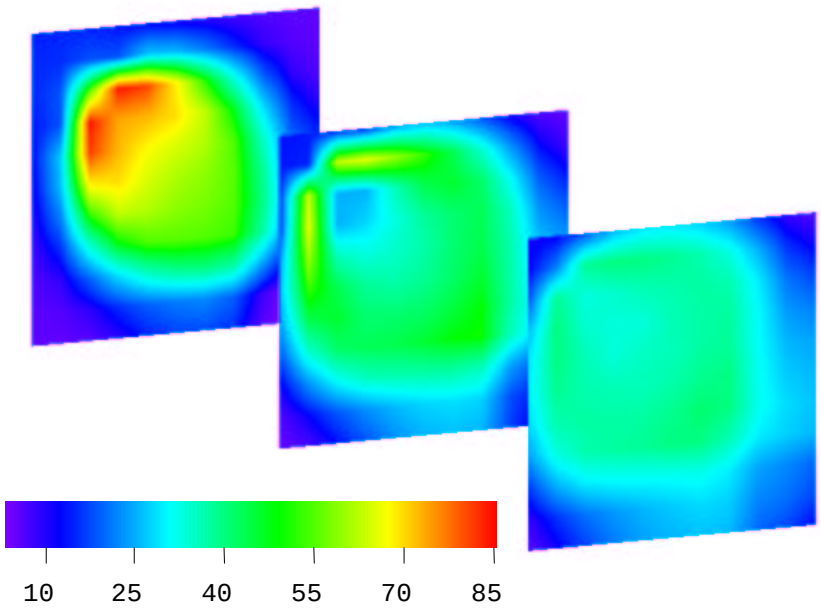

(a) Adjoint method.

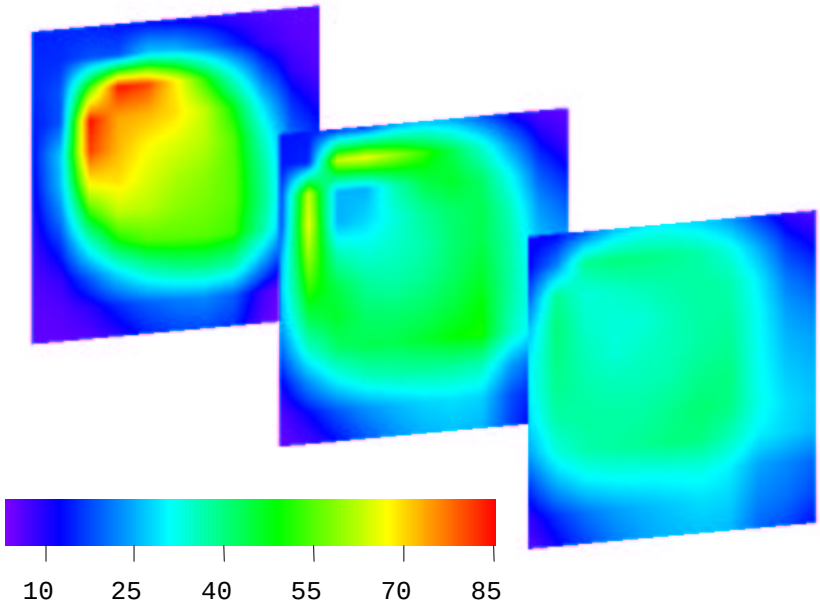

(b) Finite difference method.

Figure 3.9: Sensitivity of bottom-hole pressure at producing well to porosity at 300 days.

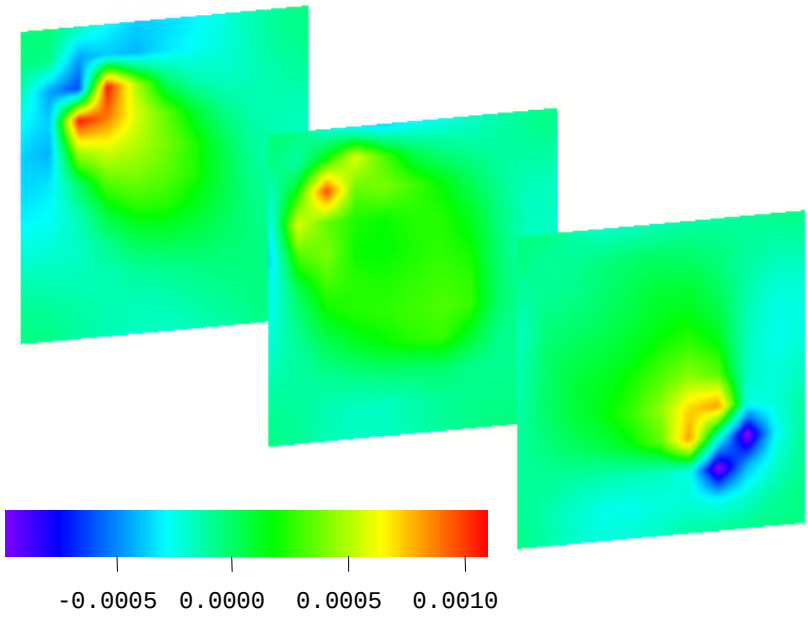

(a) Adjoint method.

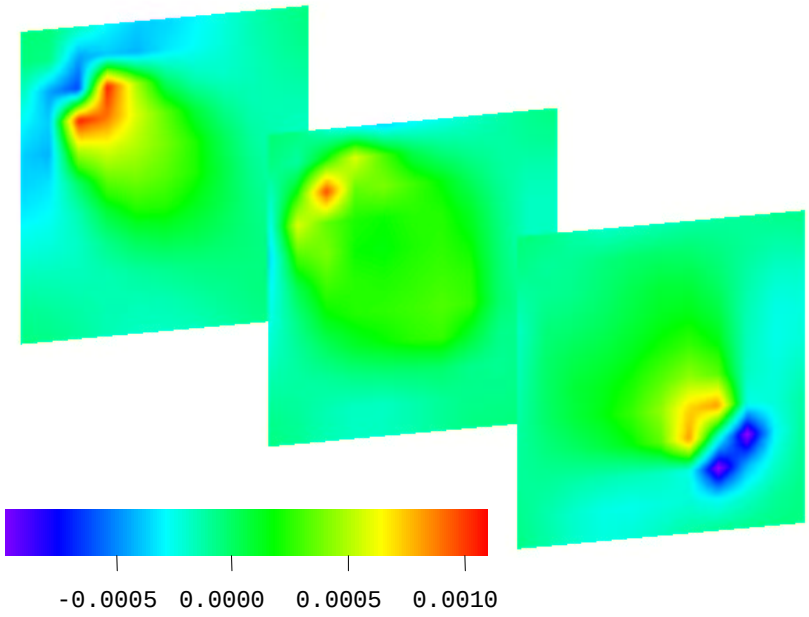

(b) Finite difference method.

Figure 3.10: Sensitivity of water-oil ratio at producing well to horizontal permeability at 300 days.

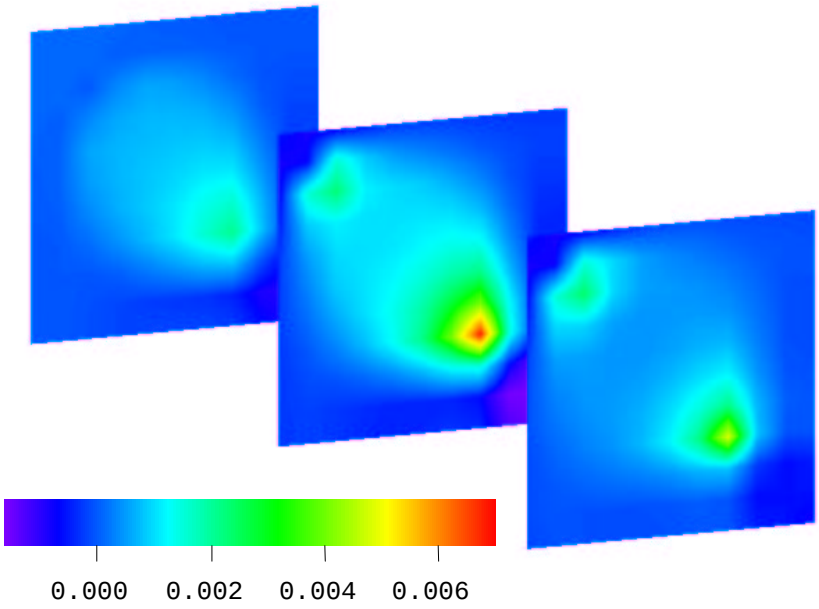

(a) Adjoint method.

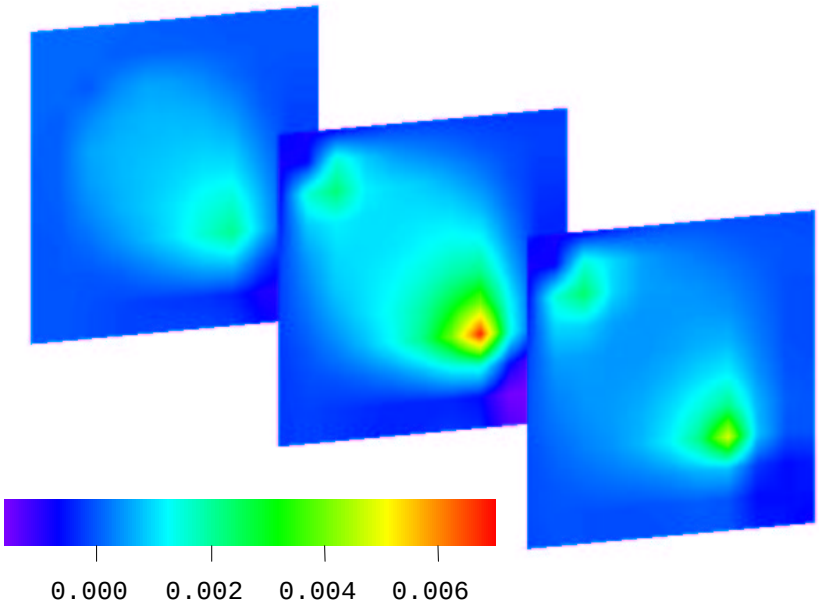

(b) Finite difference method.

Figure 3.11: Sensitivity of water-oil ratio at producing well to vertical permeability at 300 days.

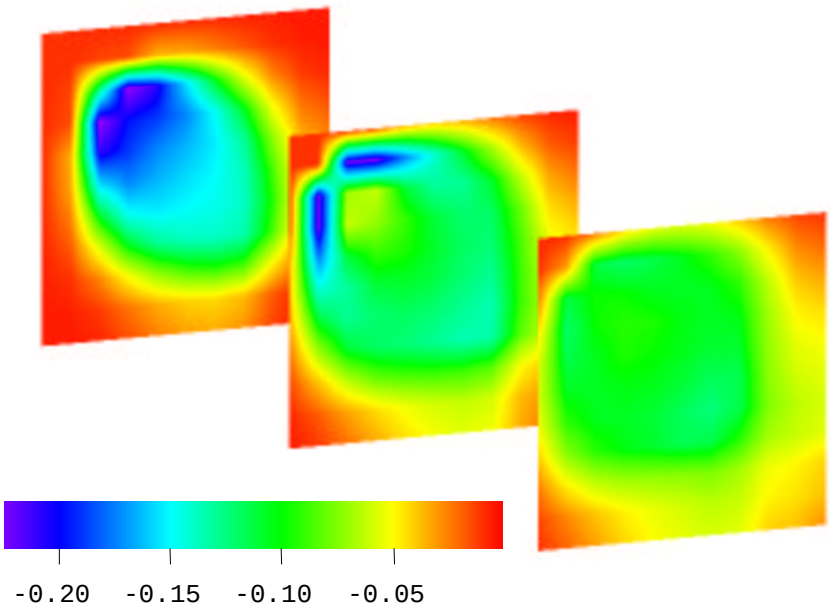

(a) Adjoint method.

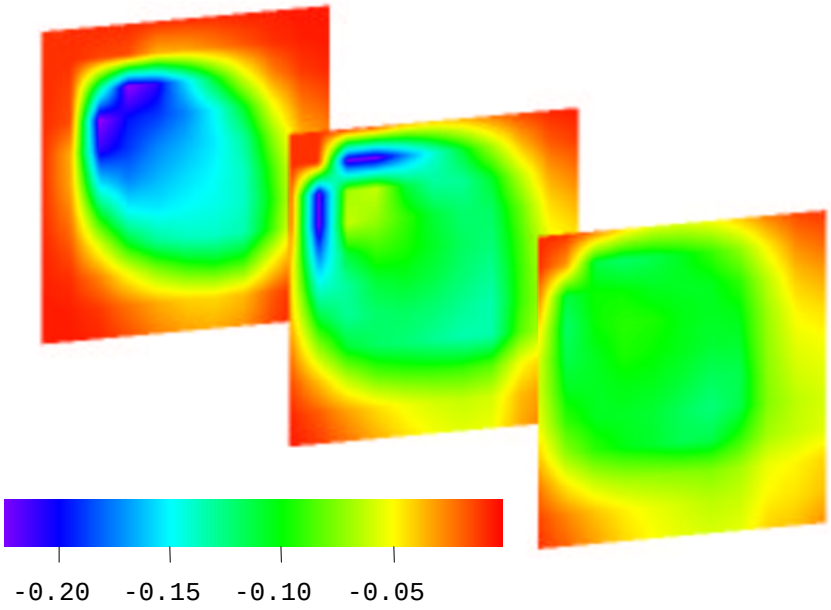

(b) Finite difference method.

Figure 3.12: Sensitivity of water-oil ratio at producing well to porosity at 300 days.

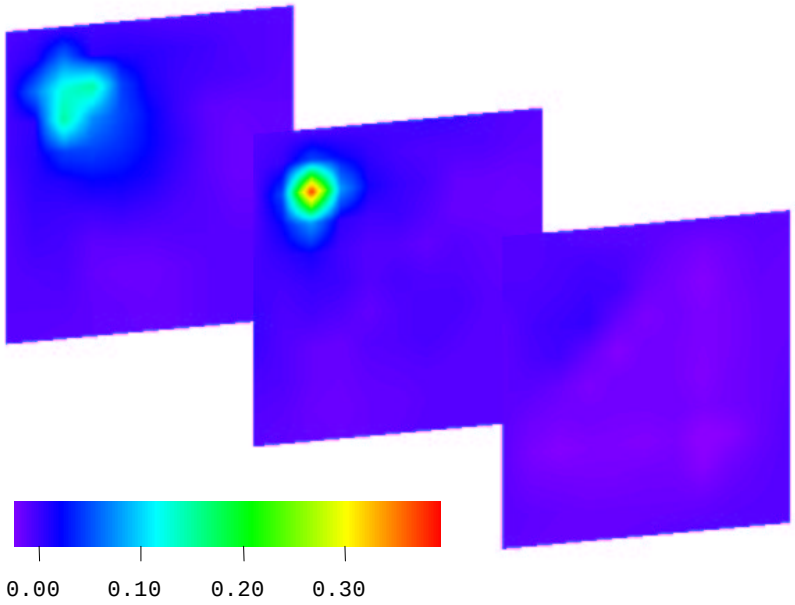

(a) Adjoint method.

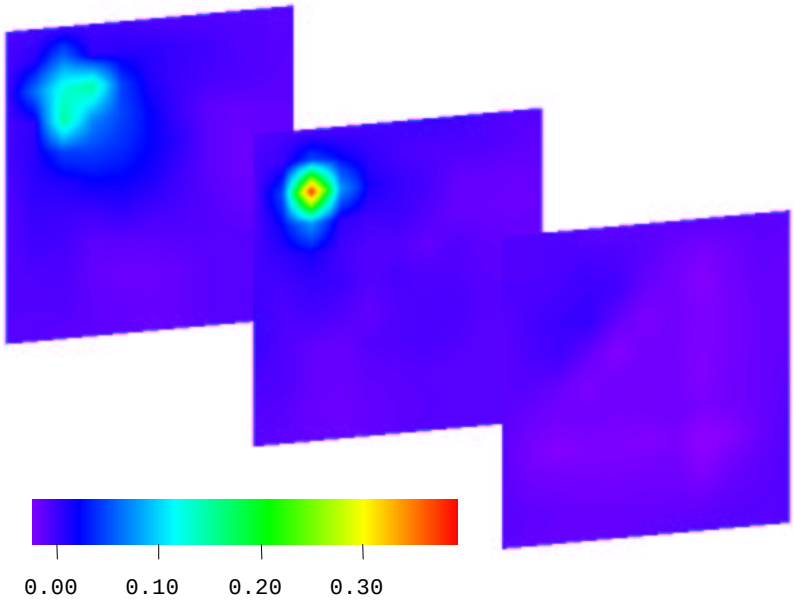

(b) Finite difference method.

Figure 3.13: Sensitivity of gas-oil ratio at producing well to horizontal permeability at 300 days.

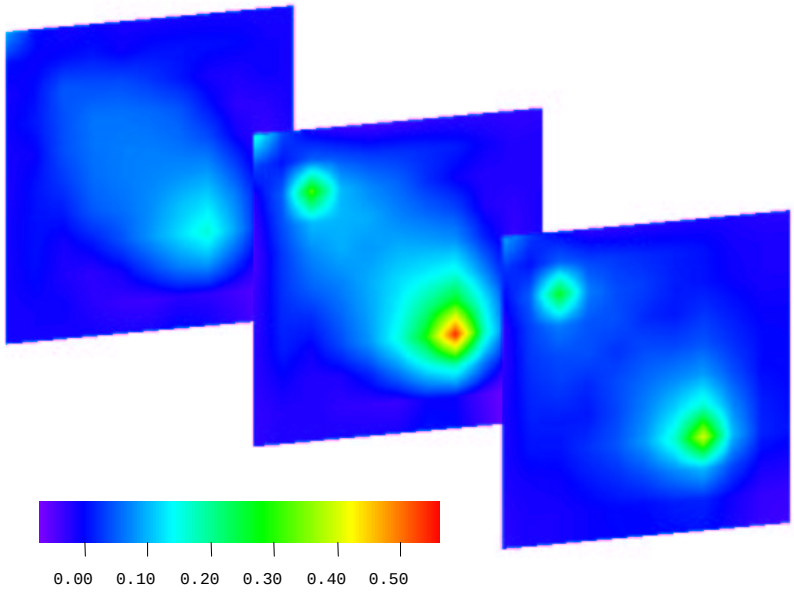

(a) Adjoint method.

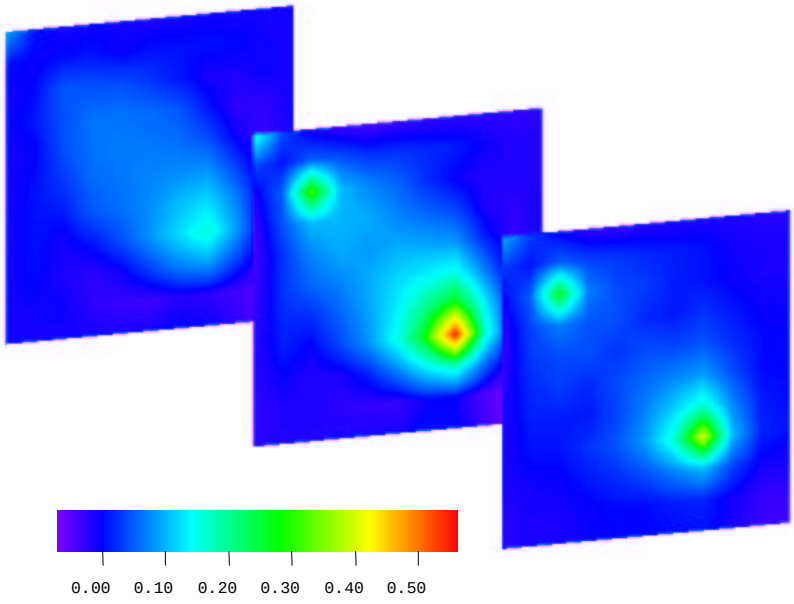

(b) Finite difference method.

Figure 3.14: Sensitivity of gas-oil ratio at producing well to vertical permeability at 300 days.

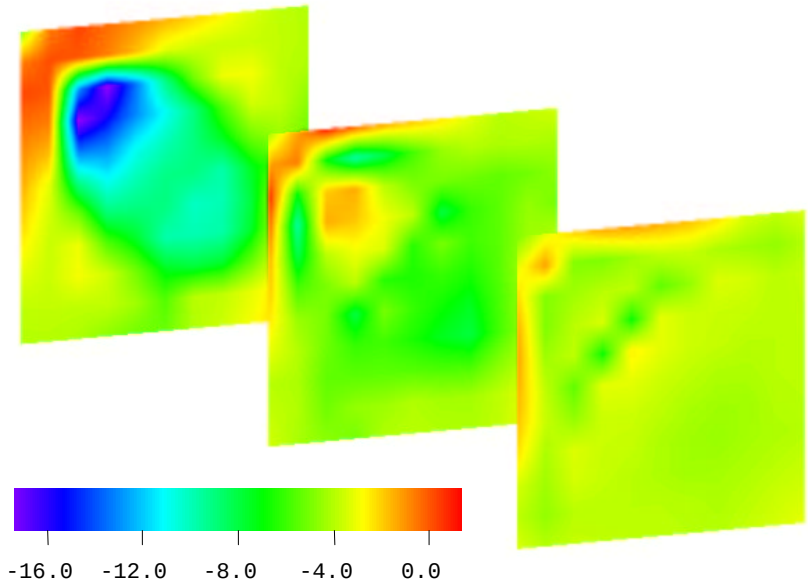

(a) Adjoint method.

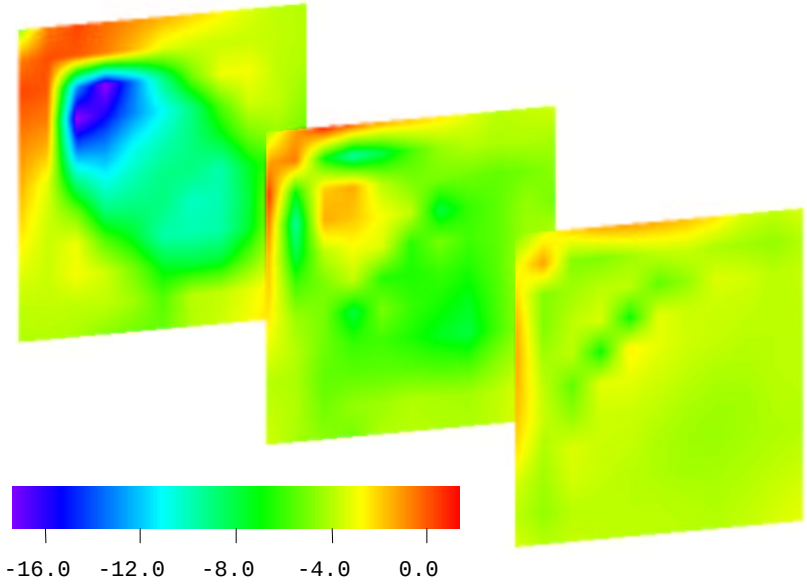

(b) Finite difference method.

Figure 3.15: Sensitivity of gas-oil ratio at producing well to porosity at 300 days.

3.5.2 A 2D Solution Gas Drive Example

The grid of the reservoir model is 21 by 21 with 40 feet by 40 feet gridblocks. The reservoir is a homogeneous reservoir. The permeability and porosity are 40 mD and 0.22, respectively, in each gridblock. The initial reservoir pressure is 4500 psi and the bubble point pressure is 4417 psi. There is a single producing well at gridblock (1,1) which is produced at a constant oil rate of 200 STB/d. The reservoir pressure drops below the bubble point pressure very soon after the reservoir starts producing oil.

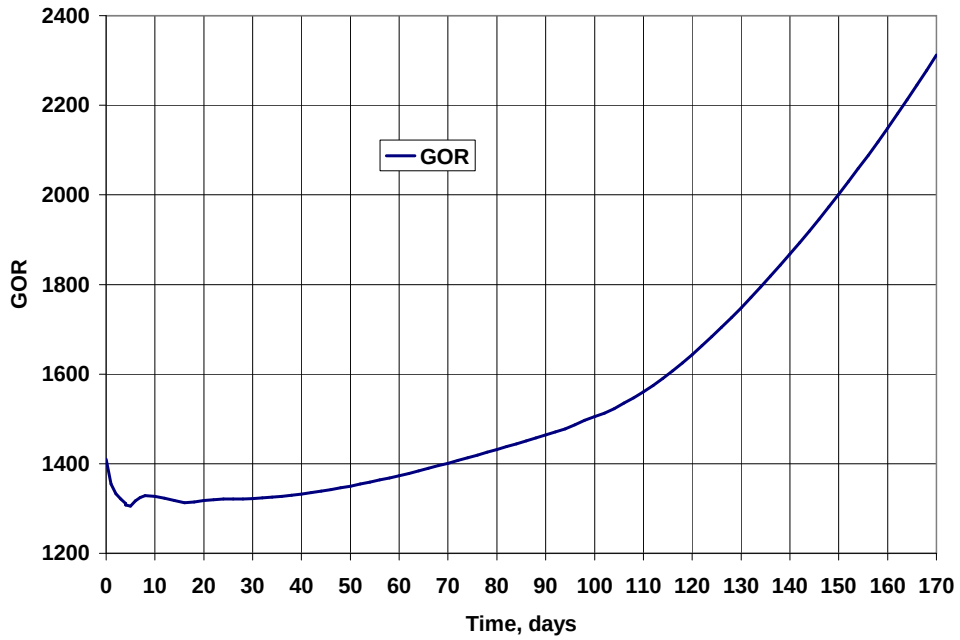

Figure 3.16: Producing gas-oil ratio.

Fig. 3.16 shows the producing gas-oil ratio as a function of time. From 1 to 5 days, the GOR decreases with the time. The reservoir pressure also drops with time. Lower pressure will result in a lower solution gas-oil ratio as gas comes out of solution. During this period, the gas saturation in all gridblocks is below the

critical gas saturation (S_{gc}=0.05) and no free gas is produced, so the GOR decreases with time. From about 5 days, free gas begins to flow in the reservoir, so the GOR increases with time.

In this example, we investigate the behavior of sensitivity coefficients at 4 days, 80 days, and 170 days. At 4 days, all gridblock pressures are just below the bubble point pressure. However, the gas saturation in all gridblocks is less than critical gas saturation 0.05. There is therefore no free gas flowing in the reservoir at 4 days. At 80 days, the gas saturation ranges from about 0.055 to 0.09. All gridblocks have mobile free gas. At 170 days, the gas saturation is between 0.119 to 0.137, and the relative permeability to gas is moderately high.

Figs. 3.17 to 3.20 show the sensitivity coefficients for flowing well bore pressure and producing GOR with respect to permeability and porosity along a row of gridblocks in the x-direction. A distance equal to zero pertains to the well bore gridblock (1,1). The distance 800 feet pertains to the gridblock (1,21).

Sensitivity of p_{wf} to Permeability

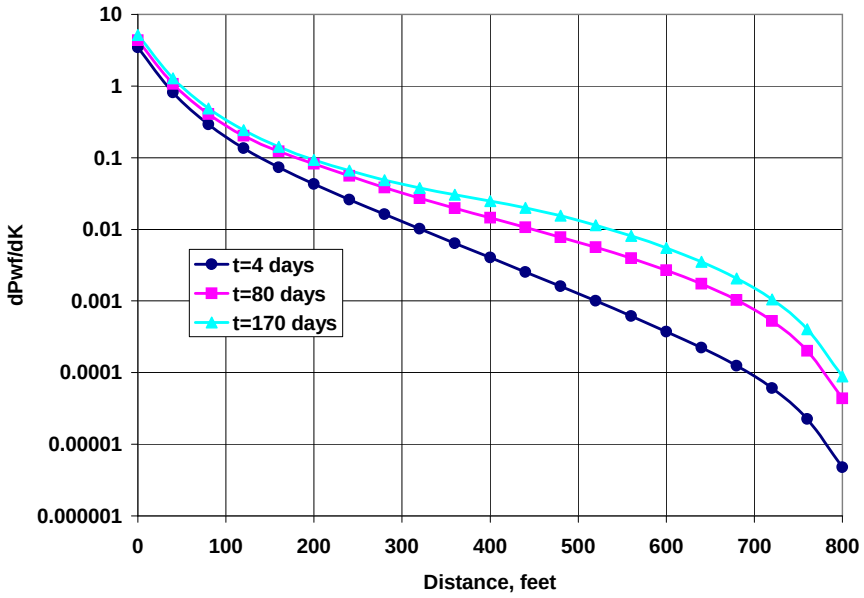

Figure 3.17: Sensitivity of bottom hole pressure to permeability.

Fig. 3.17 shows the sensitivity of p_{wf} to permeability at three different times. Just as expected, the bottom hole pressure is extremely sensitive to the permeability of the well bore gridblock. Note that a log scale is used for the ordinate axis. As the distance away from the well increases, the sensitivities decrease very fast. Comparing the sensitivities at 4 days, 80 days, and 170 days, we can see that at the later time, pressures are more sensitive to outside gridblocks. All the values of the sensitivities to permeability are positive. This makes sense. As the permeability increases, the pressure drop will decrease. So the pressure will be higher and the sensitivity coefficient is positive.

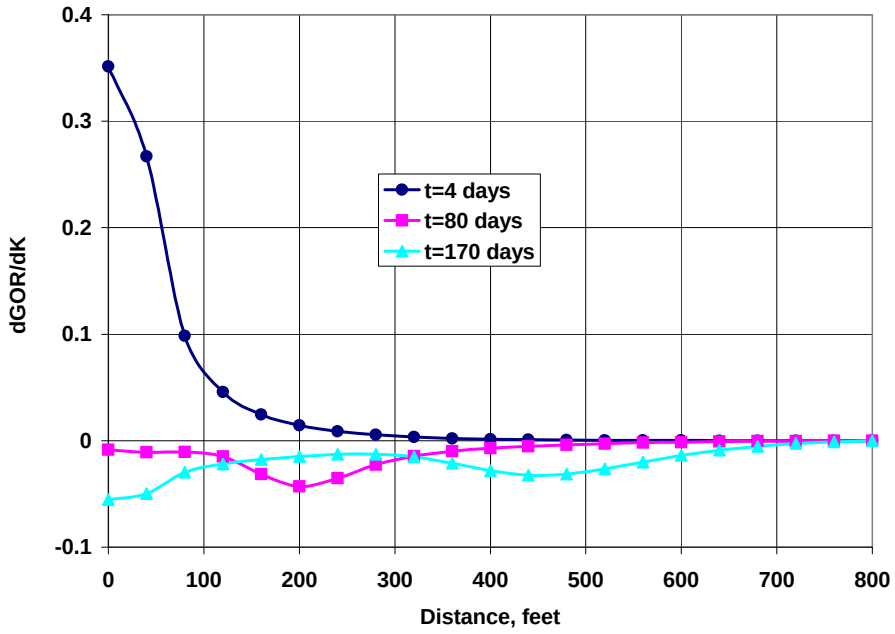

Figure 3.18: Sensitivity of GOR to permeability.

Sensitivity of GOR to Permeability

Unlike the sensitivity of pressure, the GOR is not always highly sensitive to the wellbore gridblock (Fig 3.18). At the early time (4 days), GOR is more sensitive to permeability around well bore. However, at the later times (for example, at 80 days), the GOR could be more sensitive to the permeabilities of the gridblock far from the wellbore than to these near the well-bore. At 4 days, there is no free gas flowing in the reservoir. As we discussed previously, the pressure increases with the permeability. The increase in pressure will result in more dissolved gas, and the GOR will increase. So the sensitivity of GOR to permeability is positive. At 80 days and 170 days, there is a lot of mobile free gas in the reservoir. As the pressure increases due to an increase in permeability, more free gas will be dissolved, and the gas saturation will decrease. At this stage, free gas dominates the reservoir production and the gas production rate

will decrease with increasing permeability, so the sensitivity coefficients are negative.

Sensitivity of p_{wf} to Porosity

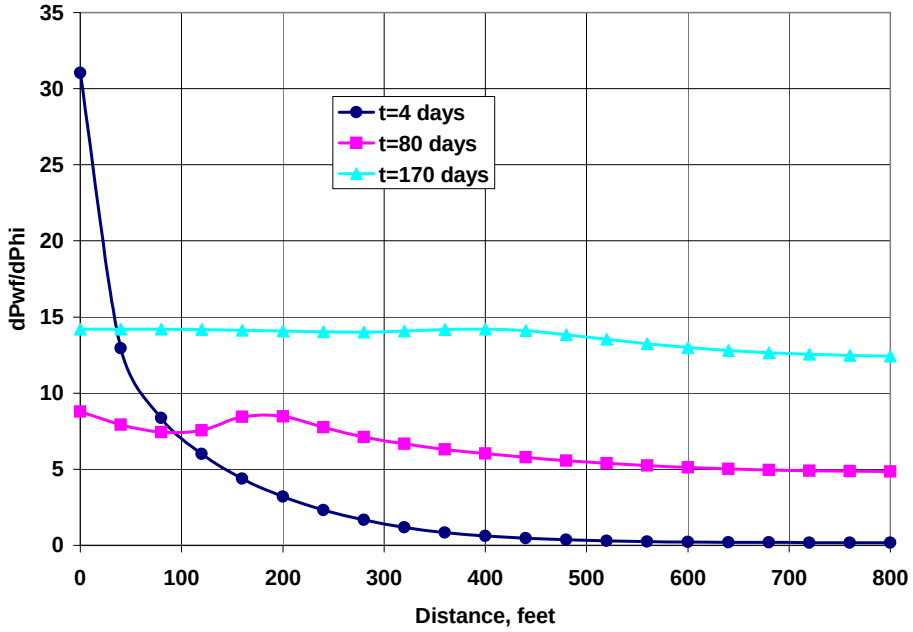

Figure 3.19: Sensitivity of bottom hole pressure to porosity.

Fig 3.19 shows the sensitivity of p_{wf} to the porosity along the same row of gridblocks introduced in the previous two figures. The values of these sensitivity coefficients are always positive. This is because an increase in the porosity provides pressure support and results in higher pressure. It is very clear that p_{wf} becomes more sensitive to the porosity of gridblocks far from the well at the later times.

Sensitivity of GOR to Porosity

Fig 3.20 presents the sensitivity of GOR to porosity. An increase in the porosity will result in an increase in pressure. At 4 days, there is no free gas flowing

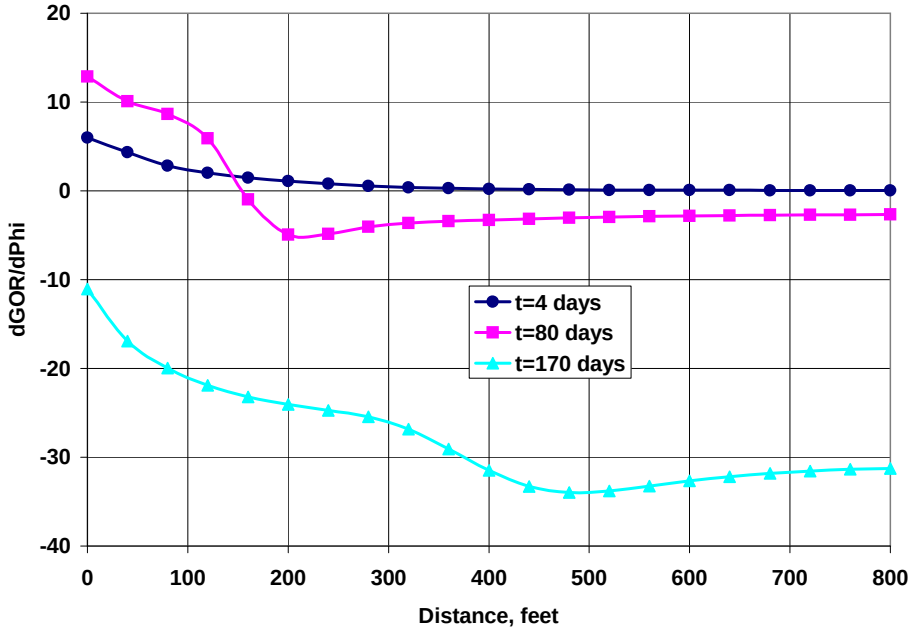

Figure 3.20: Sensitivity of GOR to porosity.

in the reservoir, an increase in the pressure will increase the gas production rate. So the sensitivity is positive. At the 170 days, the free gas is dominant, so the sensitivity is negative.

3.5.3 A Cross Section Example

In this section, we consider a vertical cross section solution gas drive reservoir. The number of gridblocks is 15 in the x-direction, 8 in the z-direction (vertical direction) and 1 in the y-direction. The size of gridblocks is 40 feet in the x and y-direction, and 30 feet in the z-direction. The horizontal and vertical permeabilities are 40 mD and 4 mD in each gridblock, respectively. The porosity field is uniformly distributed with a value of 0.22. The single producing well is located at the bottom center (gridblock (8,1,8)) of the reservoir and produced at a constant oil rate of 50 STB/d. This reservoir is an oil reservoir and the initial oil saturation is 0.8. The initial water saturation is 0.2, which is equal to the irreducible water saturation S_{wc}. The initial reservoir pressure is 4500 psi at the bottom layer of the reservoir and the bubble point pressure is 4417 psi. The reservoir pressure drops below bubble point very soon after the beginning of simulation run. The simulation is run from 0 to 400 days. The average reservoir pressure drops to about 1650 psi at 400 days.

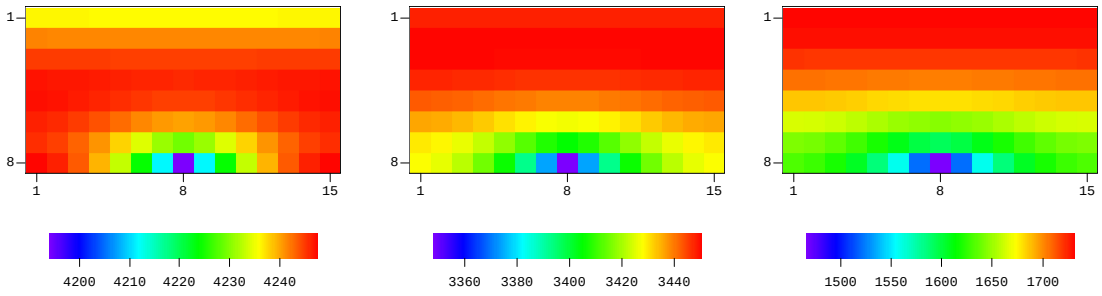

(a) 30 days . (b) 200 days. (c) 400 days.

Figure 3.21: Pressure distribution.

Fig. 3.21 shows the pressure distribution in the reservoir at 30 days, 200 days, and 400 days. At 30 days, we still can see the gravity effect on the pressure

distribution. From the top layer to the next 3 layers, the gridblock pressures increase gradually with depth. The reservoir pressure clearly decreases with time. The lowest pressure is always in the well bore gridblock.

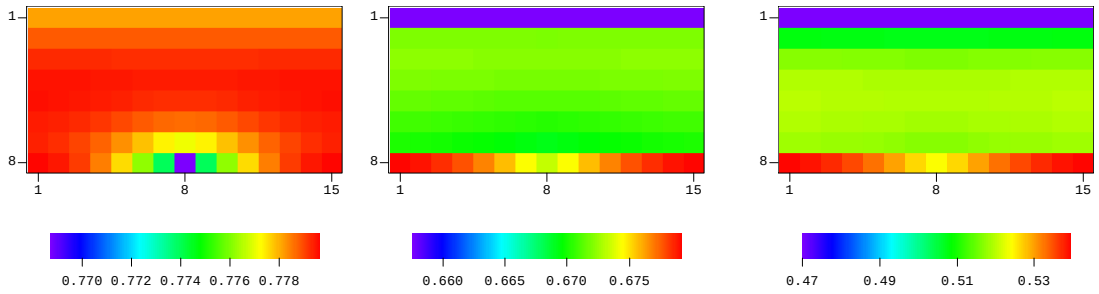

(a) 30 days . (b) 200 days. (c) 400 days.

Figure 3.22: Oil saturation distribution.

Fig. 3.22 presents the oil saturation distribution at 30 days, 200 days, and 400 days. At 30 days, a lot of oil has been withdrawn from the wellbore gridblock, so the lowest oil saturation is in the wellbore gridblock, gridblock (8,1,8). At the later times (200 and 400 days), because of the gravity effect, the oil moves down to the lower layers and gas moves up to the upper layers. The lowest gridblock oil saturation is in the top layer.

Fig. 3.23 is the gas saturation distribution at different time steps. At 30 days, the biggest gas saturation is about 0.032. It is smaller than the critical gas saturation 0.05. So there is no free gas in the reservoir at this time step. Because the lowest pressure is in the wellbore gridblock, the highest gas saturation is in this gridblock. At later time (200 and 400 days), we can see the effect of gravity segregation in the reservoir. The gas moves to the top layers, so gas saturation is higher in the upper layers.

The producing gas-oil ratio decreases from 1410 scf/STB (the initial dissolved

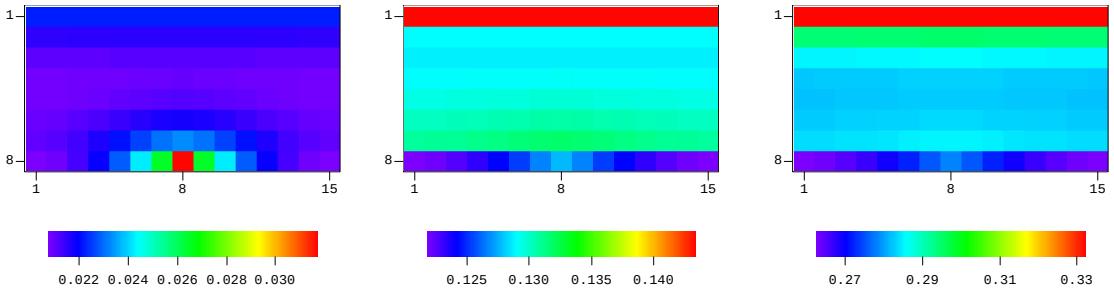

(a) 30 days . (b) 200 days. (c) 400 days.

Figure 3.23: Gas saturation distribution.

gas-oil ratio) to 1292 scf/STB at 50 days. From 50 days onward, GOR increases with time. It reaches 11,600 scf/stb at 400 days.

Sensitivities of p_{wf} and GOR to horizontal and vertical permeability, and porosity computed using the adjoint method are shown in Figs. 3.24 through 3.29. All these sensitivities have been compared with those computed from the finite difference method. We found that the match between the two methods was nearly perfect. The difference was less than 1 percent in all cases.

Sensitivity of p_{wf} to Horizontal Permeability

Fig. 3.24 shows the sensitivities of p_{wf} to the horizontal permeability. Similar to the previous example, the pressure is strongly sensitive to the horizontal permeability at the well bore gridblock. It is also quite sensitive to the horizontal permeability of other gridblocks in the bottom layer (layer 8). The pressure is much less sensitive to the horizontal permeability of other layers. At later time, the bottom hole pressure is more sensitive to the permeability of outside gridblocks and the magnitudes are bigger.

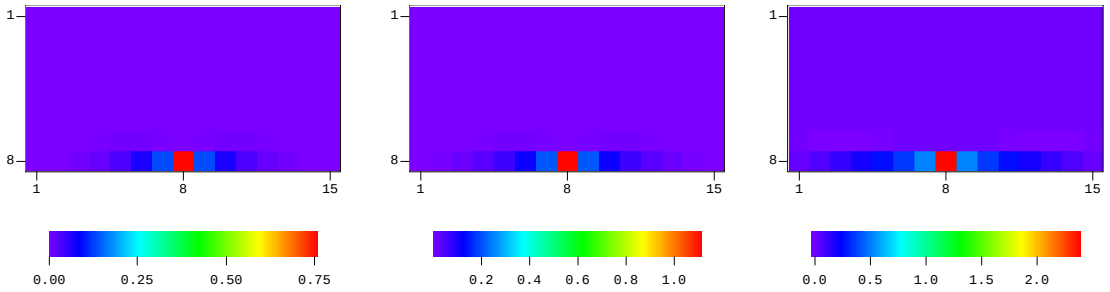

(a) 30 days . (b) 200 days. (c) 400 days.

Figure 3.24: Sensitivity of bottom-hole pressure to horizontal permeability.

Sensitivity of p_{wf} to Vertical Permeability

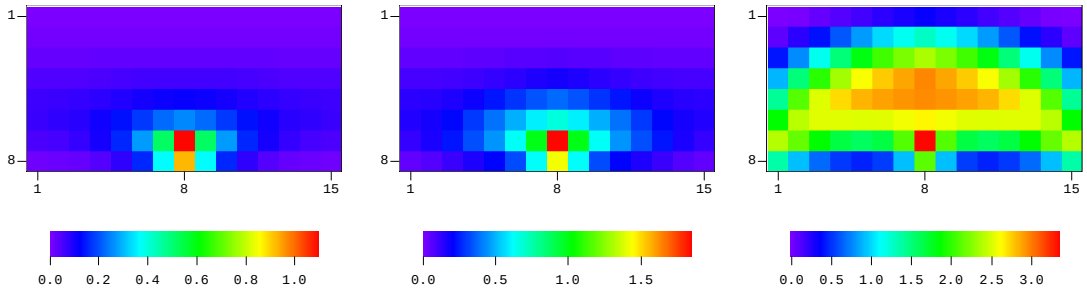

(a) 30 days . (b) 200 days. (c) 400 days.

Figure 3.25: Sensitivity of bottom-hole pressure to vertical permeability.

Fig. 3.25 presents the sensitivity of bottom-hole pressure to the vertical permeability at 30 days, 200 days, and 400 days. Since there is strong cross flow in this reservoir, vertical permeability plays an important role in the reservoir behavior. The pressure is most sensitive to the vertical permeability of the gridblock just above the wellbore gridblock. This is because most of fluid that flows to the wellbore gridblock

must pass through this gridblock. At early time (30 days), pressure is only sensitive to vertical permeability in the gridblocks near the well. At later time (200 and 400 days), it is more sensitive to vertical permeability in gridblocks far away from the well. An increase in the vertical permeability allows fluid to flow more easily to the wellbore and thus results in less pressure drop, so the sensitivity of pressure to vertical permeability is positive.

Sensitivity of p_{wf} to Porosity

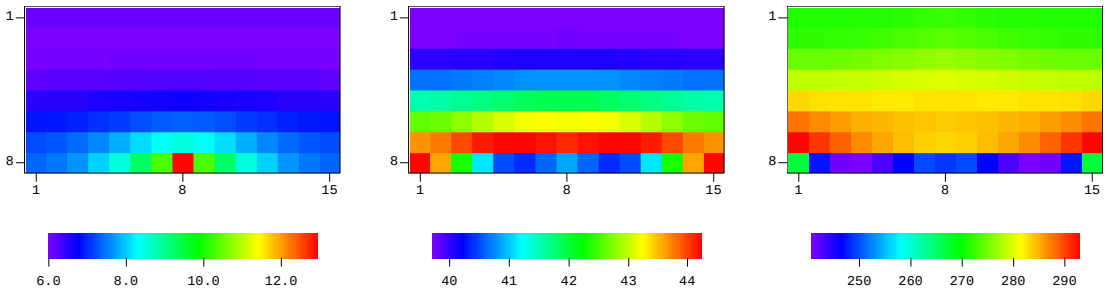

(a) 30 days . (b) 200 days. (c) 400 days.

Figure 3.26: Sensitivity of bottom-hole pressure to porosity.

Higher porosity provides additional pressure support. The pressure increases as porosity increases, so the the sensitivity of pressure to porosity is positive (Fig: 3.26). At 30 days, pressure is most sensitive to the porosity in the gridblocks near the wellbore. At later times (200 and 400 days), the pressure is more sensitive to the gridblocks far away from the wellbore gridblock.

Sensitivity of GOR to horizontal permeability

Sensitivity of the producing gas-oil ratio is more difficult to understand. Fig. 3.27 shows the sensitivity of GOR to horizontal permeability. At 30 days, there

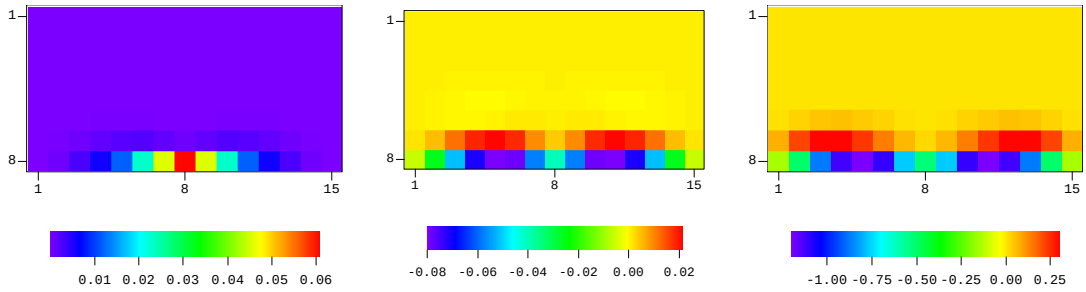

(a) 30 days . (b) 200 days. (c) 400 days.

Figure 3.27: Sensitivity of GOR to horizontal permeability.

is no free gas in the reservoir. All produced gas comes from the dissolved gas in the oil phase. An increase in the horizontal permeability results in higher pressure and more gas dissolved in the oil. As a result, more gas will be produced, so the sensitivity of GOR is positive. At later time (200 and 400 days), free gas is dominant in the reservoir, so the sensitivity of GOR to horizontal permeability is negative in the gridblocks of the bottom layer (layer 8).

Sensitivity of GOR to vertical permeability

Fig. 3.28 presents the sensitivity of gas-oil ratio to the vertical permeability. At 30 days, there is no free gas flowing, so the sensitivity to the vertical permeability is positive. At 200 days, there is mobile free gas in every gridblock, so the sensitivity to vertical permeability is negative for all gridblocks except the well gridblock.

Sensitivity of GOR to Porosity

Fig. 3.29 presents the sensitivity of gas-oil ratio to the porosity. As we discussed previously, the pressure increases as the porosity increases. At 30 days, there is no free mobile gas, so the sensitivity of GOR to porosity is positive. At later

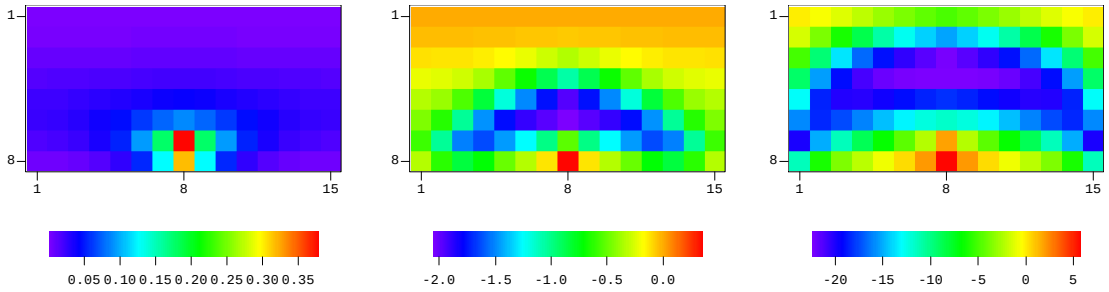

(a) 30 days . (b) 200 days. (c) 400 days.

Figure 3.28: Sensitivity of GOR to vertical permeability.

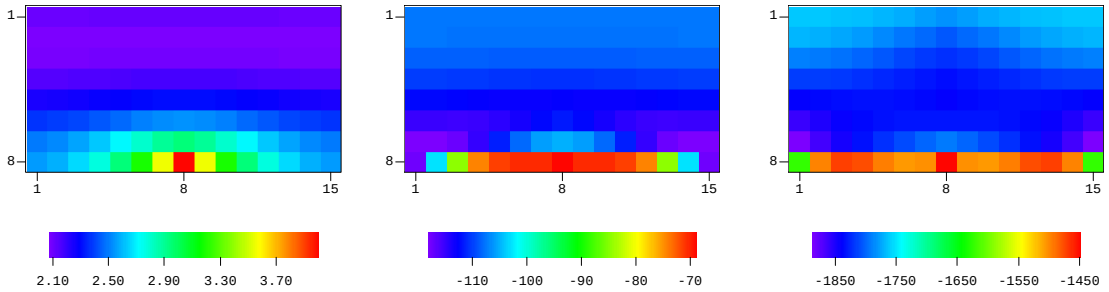

(a) 30 days . (b) 200 days. (c) 400 days.

Figure 3.29: Sensitivity of GOR to porosity.

time, free gas is dominant in the reservoir, so the sensitivity of GOR to porosity is negative.

CHAPTER IV

APPLICATIONS OF AUTOMATIC HISTORY MATCHING PROCEDURE

In this chapter, we show some computational examples of automatic history matching.

4.1 A 2D Three-Phase Reservoir

Here, we consider some simple examples to illustrate that our procedures for constructing the MAP estimate give reasonable results. We also investigate the reduction in uncertainty obtained by conditioning to various types of data.

4.1.1 The True Model and Observed Data

The true model for the 2D example is shown in Fig. 4.1. It represents a three zone reservoir. The value of log-permeability is 3.7 (40.4 mD) in the lower left quadrant, 4.3 (73.7 mD) in the lower right quadrant and 3.9 (49.4 mD) in the upper part. The porosity is constant throughout the reservoir with $\phi = 0.22$. A $21 \times 21 \times 1$ grid is used for reservoir simulation. A uniform grid is used with $\Delta x = \Delta y = 60$ ft and $\Delta z = h = 20$ ft, where throughout, h denotes reservoir thickness. There are five fully-penetrating wells completed in the reservoir. Well 5 is a water injection well which is located at the center of the reservoir i.e. in gridblock (11,11). Wells 1 through 4 are producing wells and are located, respectively, in gridblocks $(4, 4)$, $(18, 4)$, $(18, 18)$ and $(4, 18)$. At well 5, water is injected at a rate of 2100 STB/D. Each producing well produces at total fluid rate of 600 RB/D. The initial reservoir pressure is 4500 psi and the initial bubble point pressure is 4415 psi. The initial oil saturation is 0.8 and the initial water saturation is equal to the irreducible water

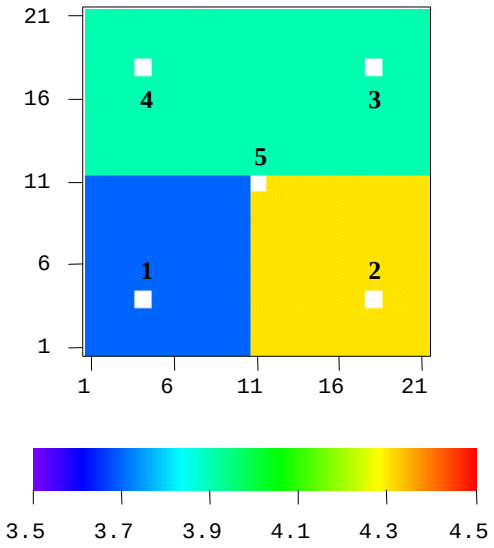

Figure 4.1: True log-permeability fields, well locations and well numbers; 2D three-phase flow.

saturation S_{wc}=0.2. In RB, the injection rate is smaller than the producing rate so the average reservoir pressure declines with time.

The observed data, p_{wf}, GOR and WOR, are generated by running the simulator with the true model rock property fields for a total time of 240 days. No noise was added to the data. The bottom-hole pressure, gas-oil ratio, and water-oil ratio, respectively, are shown in the Figs. 4.2, 4.3, and 4.4. Pressures drop at similar rates at all wells until about 140 days (Fig. 4.2) when water first breaks through at well 2 (Fig. 4.4), which is in the high permeability region. For each well, just after water breaks through, the bottom hole pressure drops sharply. GOR's begin increasing in all wells after about 80 days (Fig. 4.3). The increase is slowest in well 2, presumably because of the greater pressure support.

We selected 8 data points for each type of data at each producing well. Thus, we have 96 total data points that may be used as conditioning data. The data are uniformly distributed in the zero to 240 day time period. For the example considered

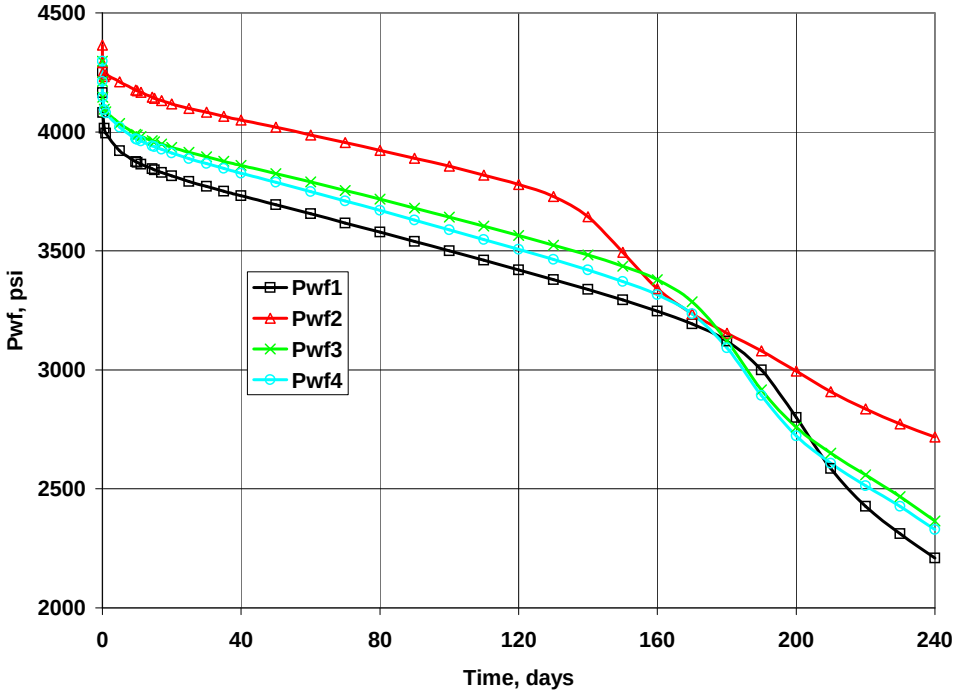

Figure 4.2: Bottom-hole pressure response of the true model.

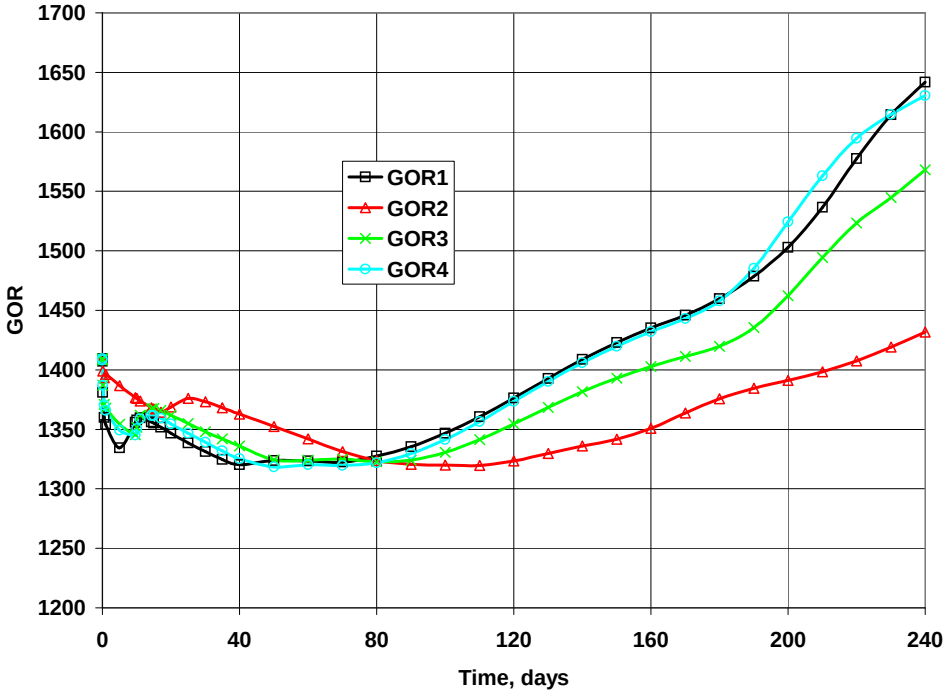

Figure 4.3: Gas-oil ratio response of the true model.

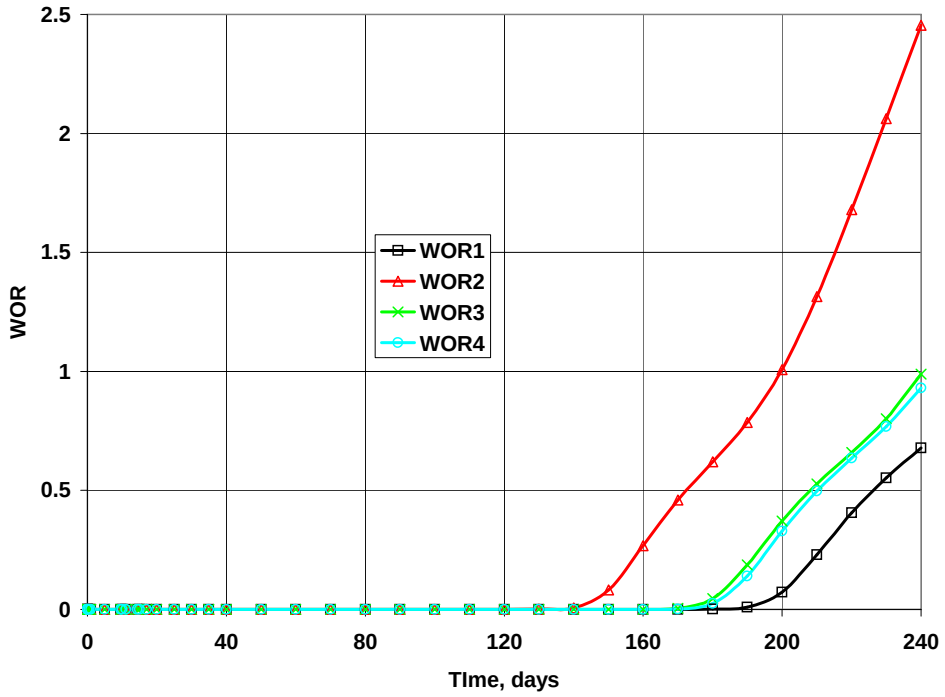

Figure 4.4: Water-oil ratio response of the true model.

here, the prior variance for bottom hole pressure measurement errors is set equal to 1.0 and the prior variance for GOR measurement errors is set equal to 10.0. (This is a small variance for GOR measurement errors. Increasing the value to 100 does not significantly alter the results presented below.) The prior variance for WOR is calculated by Eq. 2.22. we chose $\sigma^{\min}_{q_w,obs} = 2STB/D$, $\epsilon_o = 0.01$ and $\epsilon_w = 0.02$. The prior variance for the $\ln(k)$ field is 0.5 and the prior mean is 4.0. An isotropic spherical semivariogram with a range of 250 feet was used to generate the covariance matrix. Note this means that correlation range for log-permeability field is about 4 gridblocks. In generating the MAP estimate, the initial guess of log-permeability is equal to the prior mean of 4.0 throughout the reservoir.

4.1.2 MAP Estimate Results and Normalized A Posterior Variance

Fig. 4.5 shows MAP estimates of log-permeability obtained by conditioning to various data sets, (a) only wellbore pressures, (b) only to GOR data, (c) only to WOR data, (d) to both p_{wf} and GOR, (e) to both p_{wf} and WOR and (f) to all data, i.e., all wellbore pressure data, all GOR data and all WOR data. In all cases, the MAP estimate results are qualitatively correct in the sense that they give a rough approximation of the true permeability field. It is important to note that in generating the MAP estimates, we are not simply estimating three values of permeability — we are estimating the value of log-permeability at all simulator gridblocks.

Comparing Fig. 4.5(d)–4.5(f), which are conditioned to more than one type of data, to Fig. 4.5(a)–4.5(c), which are only conditioned to one type of data, we can see that the MAP estimates generated by conditioning to more that one data type give values closer to the true values (Fig. 4.1) over a broader range. However, in the case of WOR data, the resolution of the permeability field obtained by conditioning to both wellbore pressure data and WOR ratio data is about the same as that obtained by conditioning only to p_{wf} data. The best results (closest to the truth) are obtained by conditioning to all types of data. Recalling that the true log-permeability for the lower right part is 4.3 (yellow in the Fig. 4.5), we see that the MAP estimates generated by conditioning only to one type of data (Fig. 4.5(a)-4.5(c)) exhibit some $\ln(k)$ values higher than 4.3 (overshoot, red color), but the MAP estimated generated by conditioning to all three types of data or to pressure and GOR exhibit less overshoot. In this regard, conditioning to both p_{wf} and GOR data (Fig. 4.5(d)) gives better results than are obtained by conditioning only to pressure data (Fig. 4.5(a)) or only to GOR data (Fig. 4.5(b)). As noted previously, the MAP estimate obtained by conditioning to both p_{wf} and WOR is very similar to the MAP estimate obtained by conditioning only to p_{wf}. Similarly, the inversion result conditioned to all three types of data (Fig. 4.5(f)) is not significantly different from the inversion result conditioned

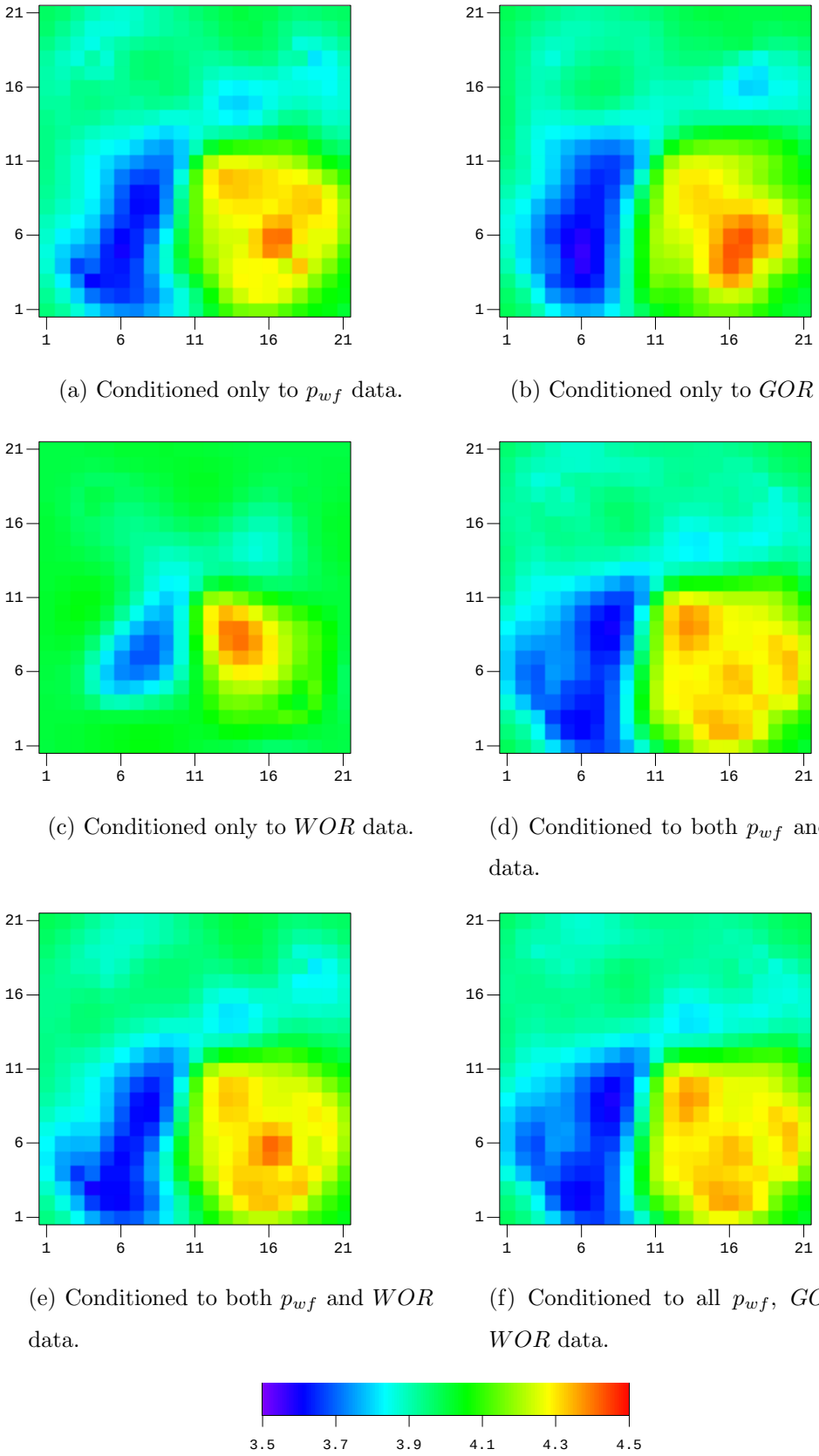

(a) Conditioned only to p_{wf} data.

(b) Conditioned only to GOR data.

(c) Conditioned only to WOR data.

(d) Conditioned to both p_{wf} and GOR data.

(e) Conditioned to both p_{wf} and WOR data.

(f) Conditioned to all p_{wf}, GOR and WOR data.

Figure 4.5: Maximum a posteriori estimate of log-permeability conditioned to p_{wf}, GOR and WOR data and their combinations.

to p_{wf} and GOR data (Fig. 4.5(d)). From above discussion, we conclude that (i) adding either p_{wf} or GOR data as conditioning data can significantly improve the inversion results. (ii) Similar to previous comments made by Landa (1997) and Wu et al. (1999) adding WOR data to another data type does not significantly improve the MAP estimate. Although results are not shown, increasing the variance of the GOR measurement error to 100 $(\text{scf/STB})^2$ does not change these conclusions. Additional support for these two conclusions can be obtained by examination of the a posteriori variances. This aspect is considered next.

The normalized a posteriori variance can be used to estimate the reduction in uncertainty obtained by conditioning to production data, see Tarantola (1987) and He et al. (1997) and the discussion of Eq. 2.25. Fig. 4.6 shows the normalized a posteriori variance of log-permeability obtained by conditioning to p_{wf}, GOR and WOR data and various combinations. The a posteriori variance has been normalized by the prior variance. Thus, if the normalized a posteriori variance is equal to 1.0, the uncertainty has not been reduced by conditioning to production data. If the normalized variance is smaller than 1.0, the uncertainty has been reduced by conditioning to production data, and the smaller the normalized a posteriori variance, the greater the reduction in uncertainty. In all cases, the uncertainty has been significantly reduced around producing wells by conditioning to production data, but close to the reservoir boundary, especially in the four corners, the normalized a posteriori variance is close to 1.0. The results of Fig. 4.6(a) indicate that the a posteriori variance for $\ln(k)$ is extremely small in the producing well gridblocks. This is because p_{wf} is extremely sensitive to the permeability in completed wellbore gridblocks, and thus, these permeabilities are resolved well by matching wellbore pressure data. (We should note, however, that well skin factors are fixed at zero for all results presented here.) Note if we condition only to one type of data, the smallest reduction in uncertainty is obtained by conditioning to WOR. Again conditioning to both wellbore pressure and WOR (Fig. 4.6(e)) does not give a significantly greater reduction in uncertainty than

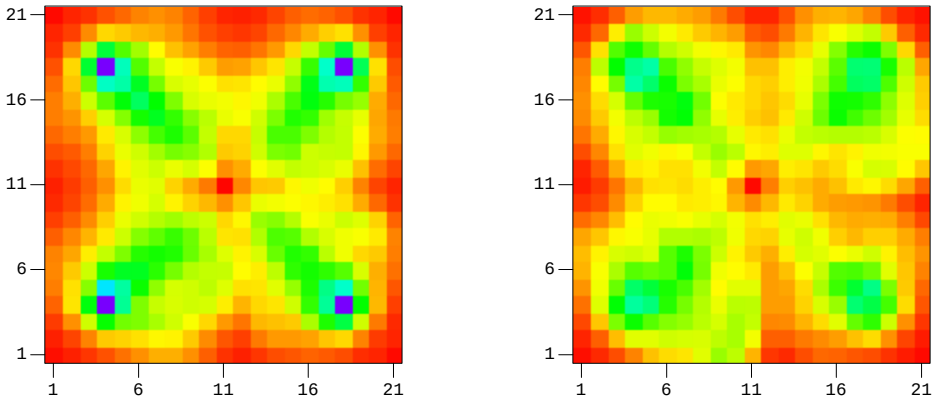

(a) Conditioned only to p_{wf} data.

(b) Conditioned only to GOR data.

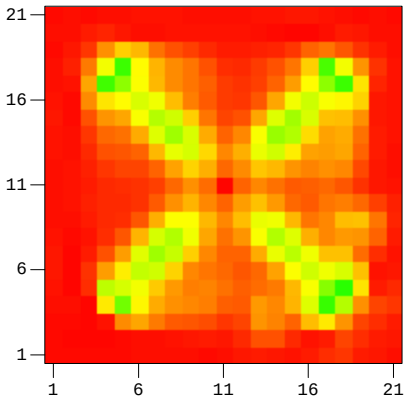

(c) Conditioned only to WOR data.

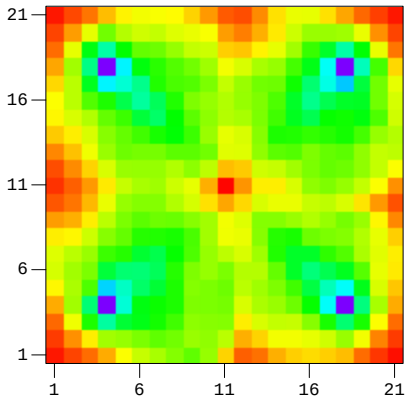

(d) Conditioned to both p_{wf} and GOR data.

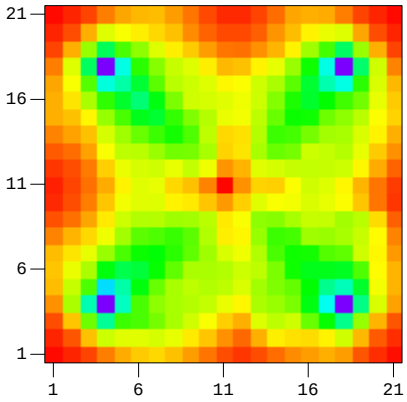

(e) Conditioned to both p_{wf} and WOR data.

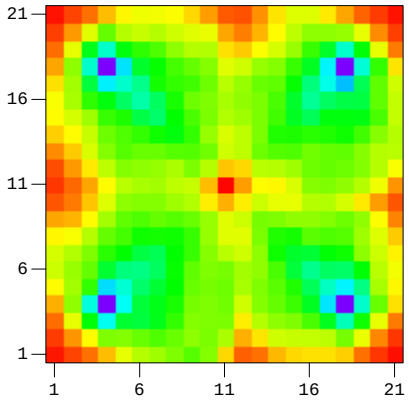

(f) Conditioned to all p_{wf}, GOR and WOR data.

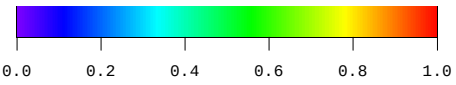

Figure 4.6: Normalized a posteriori variance of log-permeability conditioned to p_{wf}, GOR and WOR data and their combinations.

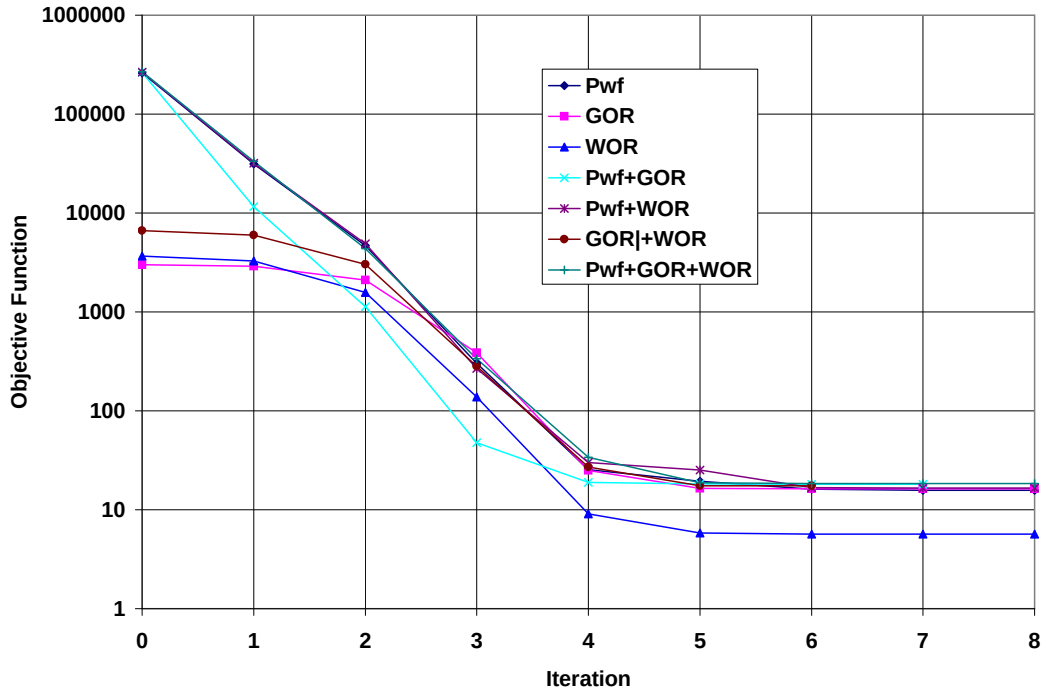

Figure 4.7: Comparison of the rate of convergence of the objective functions when conditioning to p_{wf}, GOR, WOR and their combinations.

is obtained by conditioning only to p_{wf} (Fig. 4.6(a)). However conditioning to both pressure and GOR data (Fig. 4.6(d)) yields a markedly greater reduction in uncertainty than is obtained by conditioning to only pressure data (Fig. 4.6(a)) or only to GOR data (Fig. 4.6(b)).

Each of the MAP estimates presented above was generated by minimizing the appropriate objective functions using the Levenberg-Marquardt method with initial damping factor equal to 10^5. Fig. 4.7 shows the rate of convergence of the Levenberg-Marquardt algorithm for different objectives functions, i.e., for different sets of conditioning production data. The rate of convergence is very fast requiring about six to eight iterations to obtain convergence in each case. The convergence tolerance ϵ_1 and ϵ_2 in Eq. 2.20 and 2.21 are equal to 10^{-3}.

Fig. 4.8, 4.9 and 4.10 show the matches obtained for the various types

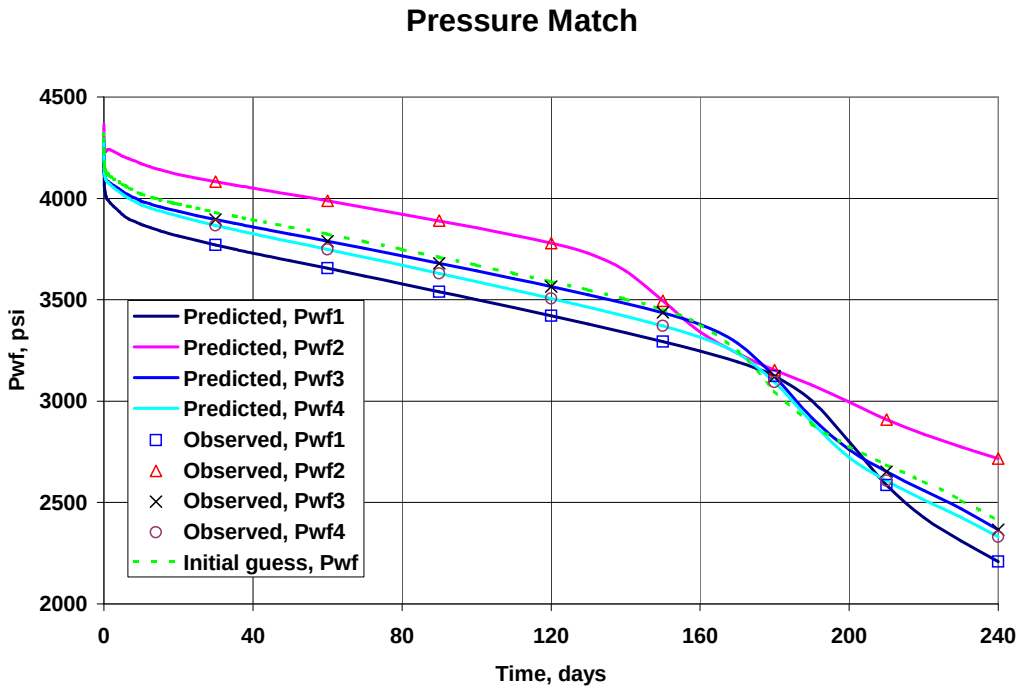

Figure 4.8: Bottom-hole pressure match after conditioning to p_{wf}, GOR and WOR data.

of conditioning data. The dashed line in each figure is the pressure, GOR, and WOR responses of the initial guess model. The MAP estimate is started from a homogeneous model, so the pressure, GOR, and WOR for the initial model are the same in all four wells. Data points represent observed data and solid curves represent production data predicted from the MAP estimates. Note we obtained an excellent history match in all cases.

4.1.3 Optimization Algorithm

As noted before, the MAP estimate that was presented was obtained using a Levenberg-Marquardt algorithm. A limited set of experiments indicates that the Levenberg-Marquardt method has better convergence properties than the standard Gauss-Newton method especially for cases where the initial data mismatch is large.

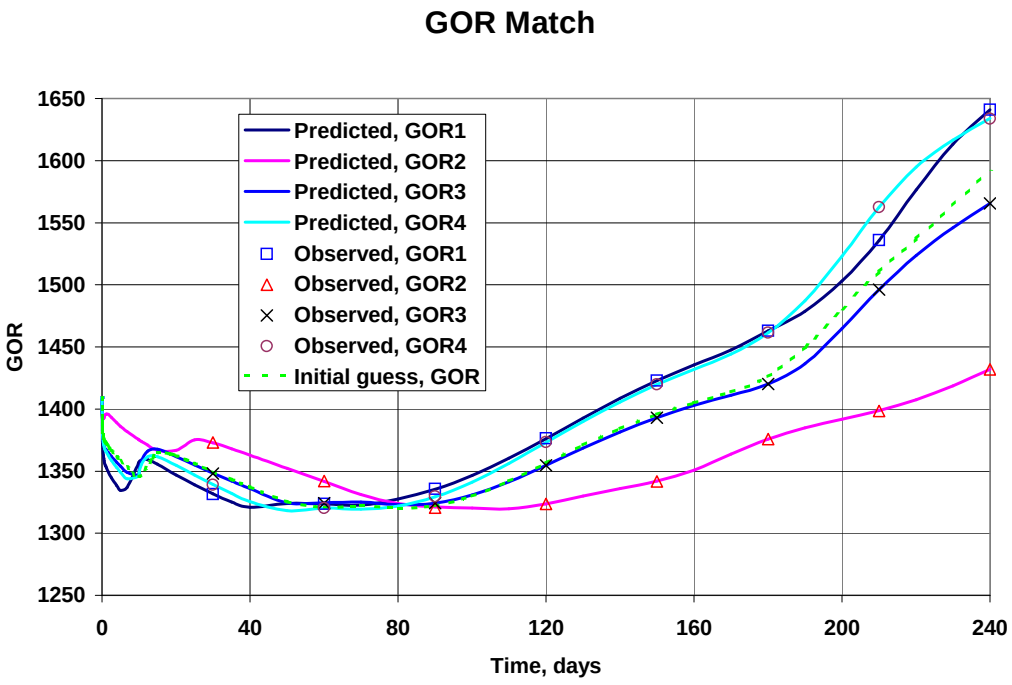

Figure 4.9: Gas-oil ratio match after conditioning to p_{wf}, GOR and WOR data.

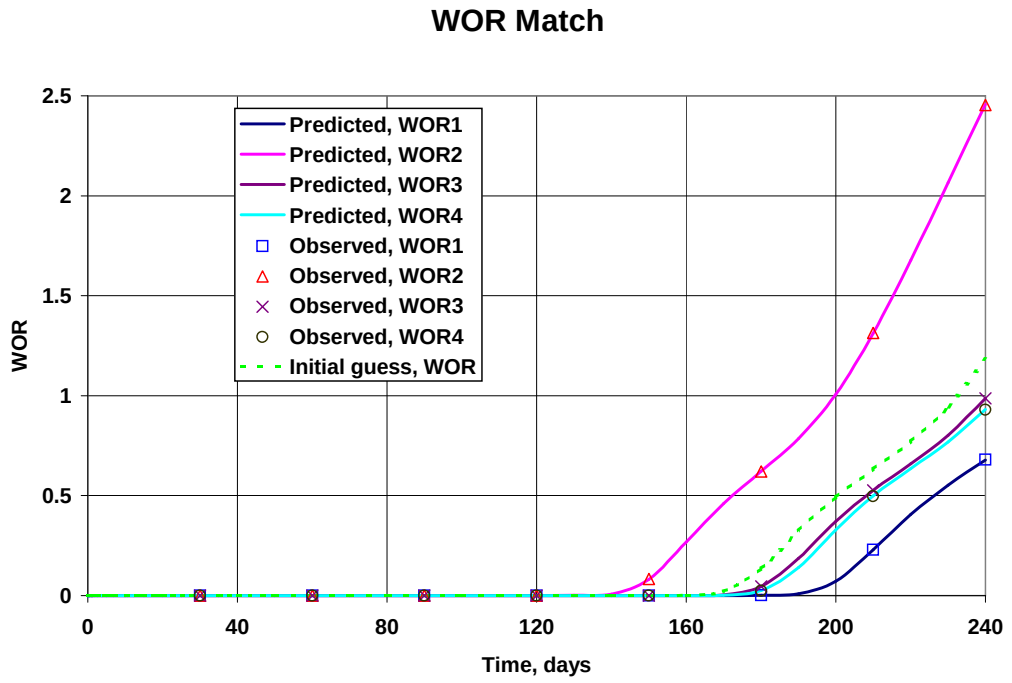

Figure 4.10: Water-oil ratio match after conditioning to p_{wf}, GOR and WOR data.

Here, we compare these two algorithms for a two-dimensional, two-phase (oil-water) flow problem. The true permeability field (Fig. 4.1), porosity, fluid properties, the prior model, the simulation grid, well constraints and well locations are the same as considered in the previous example. Each of the four producing wells produces at total rate 200 RB/d. The injection well injects water at rate 785 STB/d. We generate eight p_{wf} observed data for each producing well in a 320 days period. The MAP estimates are conditioned to the p_{wf} data only. Fig. 4.11 compares the rate of convergence of the Levenberg-Marquardt and Gauss-Newton algorithms. Note that the Gauss-Newton method converges very slowly and converges to local minimum which give a higher value of the objective function. Fig. 4.12 shows the MAP estimates. Using Levenberg-Marquardt method (Fig. 4.12(b)), we obtained a reasonable estimate of the true log-permeability field (Fig. 4.1). The MAP estimate generated from Gauss-Newton method (Fig. 4.12(a)) is very rough and far from the the true model Fig. 4.1. For example, in the lower left quadrant of the reservoir, the true value of log-permeability is 3.7, but in the results obtained from the Gauss-Newton method, gridblock values of log-pemeability range from from 2.5 to 5.0 in this quadrant.

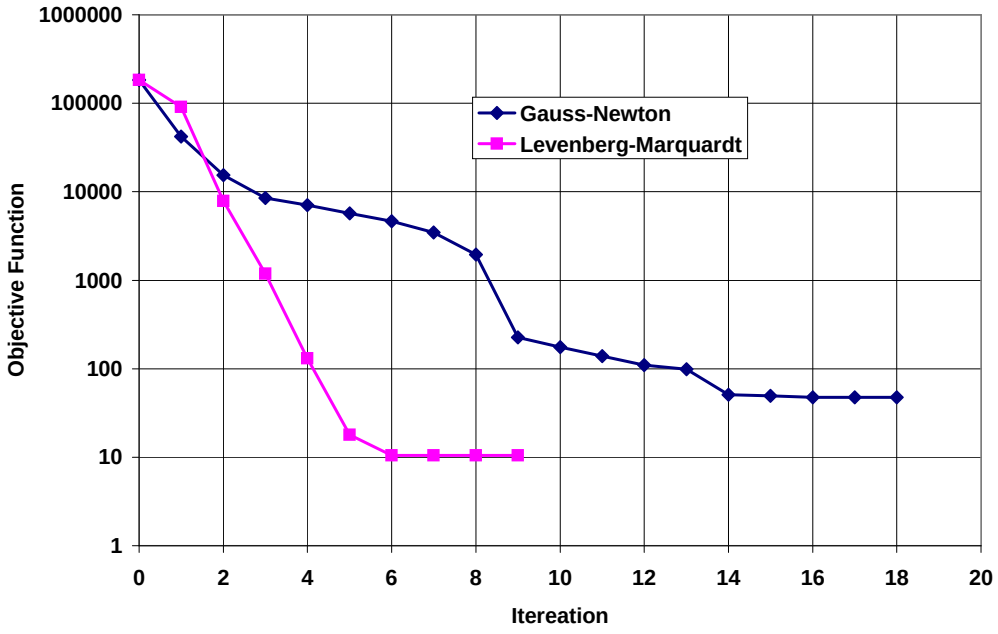

Figure 4.11: Comparison of the rate of convergence of the objective function using Gauss-Newton and Levenberg-Marquardt algorithms.

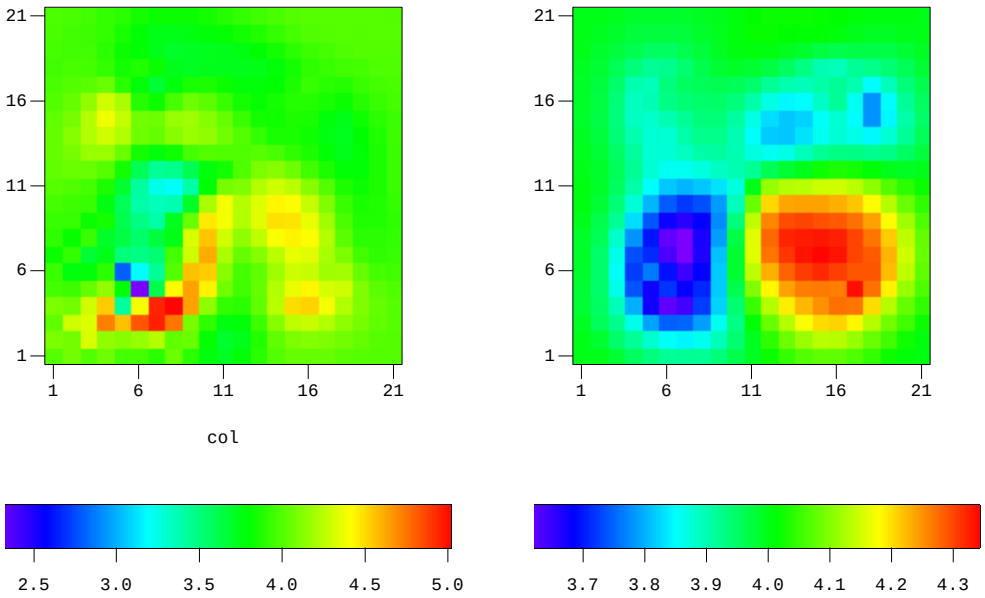

(a) Gauss-Newton method.

(b) Levenberg-Marquardt method .

Figure 4.12: Comparison of MAP estimate of log-permeability conditioned to p_{wf} data using Gauss-Newton and Levenberg-Marquardt algorithms.

4.2 3D, Three-Phase Example

The example presented here is one which is sufficiently complex to be instructive but small enough so that we were able to check the sensitivity coefficients computed by the adjoint method with those computed by the finite-difference method. Although some of the sensitivity coefficient results presented are not easy to explain from a purely physical viewpoint, all of them have been compared with results generated with the finite-difference method. (In some previous publications, the finite-difference method was referred to as the direct method, see, for example, Chu and Reynolds (1995) or He et al. (1997).) For all cases considered example, the adjoint method and finite-difference method gave results that agreed to two significant digits. The areal extent of the reservoir is 600 feet by 600 feet and contains two layers. Layer 1 refers to the top layer and layer 2 refers to the bottom layer. The thickness of each layer is uniform and equal to 30 feet. A uniform $15 \times 15 \times 2$ finite difference grid with $\Delta x = \Delta y = 40$ ft and $\Delta z = 30$ ft is used in all reservoir simulation runs.

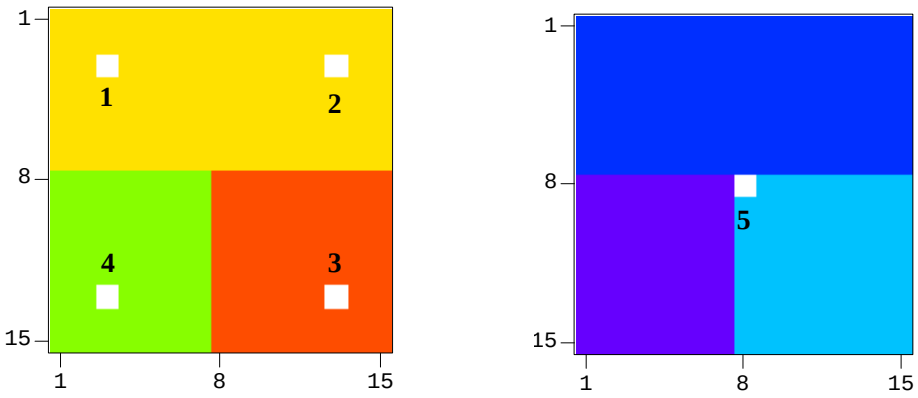

(a) True model, layer 1.

(b) True model, layer 2.

Figure 4.13: True model of horizontal log-permeability, layer 1 (left) and layer 2 (right).

Each layer of the true model consists of three permeability regions. Fig. 4.13(a) and 4.13(b) shows the distribution of values of horizontal log-permeability in layer 1 and layer 2, respectively. For layer 1, $\ln(k) = 5.2$ ($k = 181$ md) in the lower left quadrant, $\ln(k) = 5.8$ ($k = 330$ md) in the lower right quadrant and $\ln(k) = 5.5$ ($k = 245$ md) in the upper half. For layer 2, $\ln(k) = 3.7$ ($k = 40$ md) in the lower left quadrant, $\ln(k) = 4.3$ ($k = 74$ md) in the lower right quadrant and $\ln(k) = 4.0$ ($k = 55$ md) in the upper half. In the truth case, vertical permeability is equal to one-tenth horizontal permeability in the top layer and is equal to two-tenths of horizontal permeability in the bottom layer. Thus, for layer 1, $\ln(k_z) = 2.9$ ($k_z = 18$ md) in the lower left quadrant, $\ln(k_z) = 3.5$ ($k_z = 33$ md) in the lower right quadrant and $\ln(k_z) = 3.2$ ($k_z = 24.5$ md) in the upper half. For layer 2, $\ln(k_z) = 2.1$ ($k_z = 8$ md) in the lower left quadrant, $\ln(k_z) = 2.7$ ($k_z = 15$ md) in the lower right quadrant and $\ln(k_z) = 2.4$ ($k_z = 11$) in the upper half. Here reservoir porosity is assumed to be known and uniformly distributed with $\phi = 0.22$. Even though the truth case consists of zones, permeabilities of each grid cell are estimated. The simplicity of the example chosen allows one to easily visualize the quality of estimates.

Capillary effects are not included. Initial reservoir pressure at the depth corresponding to the center of the top layer is specified as $p_i = 4500$ psi. Initial bubble point pressure is set equal to 4515 psi. Initial water saturation is equal to irreducible water saturation which is equal to 0.2. Initial oil saturation is $S_{o,i} = 0.8$. As mentioned previously, Stone's second model is used to calculate the relative permeability to oil from the two sets of two-phase relative permeability curves. For the two-phase oil-water system, residual oil saturation is 0.2. For the two-phase gas-oil system, residual oil saturation is 0.3 and critical gas saturation is equal to 0.05.

The reservoir contains four producing wells which are completed only in the top layer. The white gridblocks in Fig. 4.13(a) and 4.13(b) show the location of the gridblocks that contain wells. These wells are located near the four corners

of the reservoir. Well 1 is completed in gridblock $(3, 3, 1)$, well 2 is completed is gridblock $(13, 3, 1)$, well 3 is completed in gridblock $(13, 13, 1)$ and well 4 is completed in gridblock $(3, 13, 1)$. Each of the wells is produced at total flow rate of 350 RB/D. A single water injection well (well 5) completed in gridblock $(8, 8, 2)$ is used to inject water into the bottom layer at a rate of 1100 STB/D. At initial reservoir pressure, this is equivalent to an injection rate of 1107 RB/D. Note that the injection well (well 5) is located in the lower right quadrant of the bottom layer, which corresponds to the highest permeability zone ($\ln(k) = 4.3$) of the bottom layer. The true skins factors at wells 1 through 5, respectively, are specified as 3.0, 4.0, 5.0, 2.0 and 0.0.

By running the simulator using data from the truth case as input, the production response shown in Figs. 4.14 and 4.15 were obtained. No noise was added to the data generated by the simulation. the prior variance for bottom hole pressure measurement errors is set equal to 1.0 and the prior variance for GOR measurement errors is set equal to 100. The prior variance for WOR is calculated by Eq. 2.22. As the injection rate in RB/D is less than the producing rate, the pressure at all four producing wells (not shown) continually decreases with time. Except at very early times, the pressure at the injection well also decreases with time.

Using the adjoint method, we computed the sensitivity of pressure, GOR, WOR to model parameters. Note that even though the true reservoir consists of zones, we generate the sensitivity to each gridblock permeability individually. The results we show indicate that physical intuition and an understanding of reservoir physics does not always enable one to understand how changing permeabilities will affect production data. Because of this, sensitivity coefficients can be useful even if one does not wish to fully automate the history matching process.

For the example considered, wells produce from only one gridblock so the water-oil ratio and gas-oil ratio, respectively, are given by

$$WOR = \frac{k_{rw}\mu_o B_o}{k_{ro}\mu_w B_w}, \tag{4.1}$$

and

$$GOR = R_s + \frac{k_{rg}\mu_o B_o}{k_{ro}\mu_g B_g}. \tag{4.2}$$

These equations are applied at each producing well and are evaluated using the pressure and saturations of the gridblock containing the well.

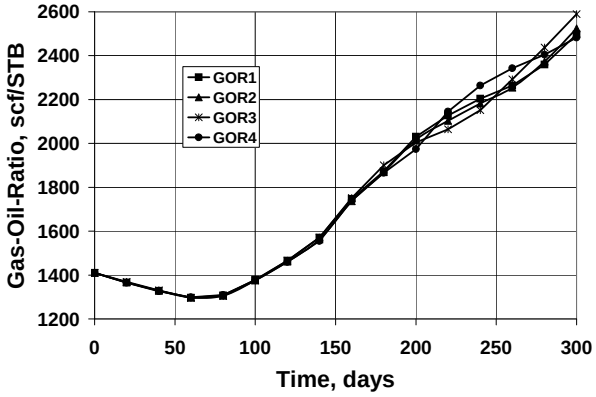

Figure 4.14: The gas-oil ratio.

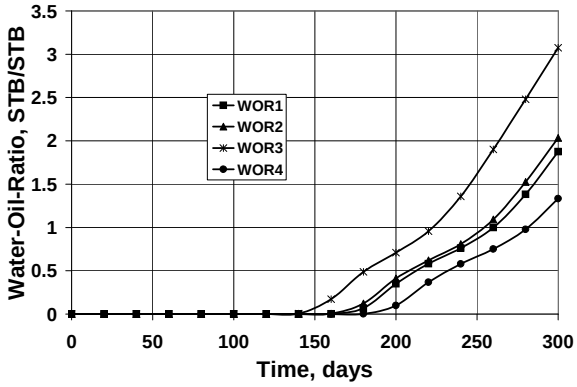

Figure 4.15: The water-oil ratio.

Fig. 4.14 shows the GOR as a function of time. The initial GOR is equal to 1400 scf/STB. As the pressure in gridblocks near producing wells drops below bubble-point pressure immediately after beginning production, a free gas phase immediately begins to form in the reservoir and R_s decreases. As gas saturation is below critical, the GOR goes down. Gas saturation first exceeds critical gas saturation at about 70 days. From about this time onwards, the ratio k_{rg}/k_{ro} increases rapidly and the contribution of this term to the producing GOR more than makes up for the decrease in R_s. Up to 140 days (the time of breakthrough in well 3) the GOR is essentially identical at all wells, but from about 165 days onward, the GOR's at the wells are somewhat different.

As shown in Fig. 4.15, water breakthrough first occurs in well 3. This is the expected result because well 3 is located in the lower right quadrant; horizontal

permeability and vertical permeability is highest is this quadrant. The fact that well 4 breaks through last is also obvious since this well is located in a quadrant of the reservoir where horizontal and vertical permeabilities are the lowest.

4.2.1 Dimensionless Sensitivity Coefficients

For three-dimensional multiphase flow problems, sensitivity coefficients are difficult to understand physically. If one wishes to perform history matching by manually adjusting parameters instead of using a fully automated procedure, the availability of a procedure to compute sensitivity coefficients should prove valuable in those cases where we are unable to apply physical intuition to predict how a change in a model parameter will change production data. The sensitivity of GOR to the permeability field is particularly hard to predict. The reason for this difficulty is that the gas production rate consists of two parts, gas dissolved in the oil phase (reflected by R_s) and the free gas flow rate which is largely controlled by gas relative permeability. If, as should be expected, an increase in permeability in the well's gridblock results in an increase in gridblock pressure, then R_s increases, but gas saturation will typically decrease resulting in a decrease in the production rate of free gas. If the incremental increase in the production rate of dissolved gas is greater than the incremental decrease in the rate of production of free gas, then the increase in permeability will result in an increase in GOR so the sensitivity of GOR to gridblock permeability is positive. On other hand if the incremental decrease in the production rate of free gas is greater than the increase in the production rate of dissolved gas, then the sensitivity will be negative. The interpretation of sensitivity coefficients is further complicated when injected water is displacing both oil and gas and flow occurs in both the horizontal and vertical directions. In this case, the sensitivity of WOR or GOR to a gridblock permeability depend on gridblock pressure, water saturation and gas saturation and changes in these variables depend on how a change in permeability affects flow of each phase in all three directions.

To understand the effect that data will have on the reduction in different types of model parameters, one should construct dimensionless sensitivity coefficients. Following F. Zhang and Oliver (2000), the dimensionless sensitivity of the ith data, g_i, to the jth model parameter is defined by

$$s_{i,j} = \frac{\partial g_i}{\partial m_j} \frac{\sigma_{m_j}}{\sigma_{d,i}}, \tag{4.3}$$

where σ_{m_j} denotes the prior variance in model parameter m_j and $\sigma_{d,i}$ denotes the variance of the measurement error for the ith observed data.

Sensitivity to Horizontal Permeability.

Fig. 4.16 shows a plot of the dimensionless sensitivity of the flowing wellbore pressure to the horizontal log-permeability field of layer 1 at four different times. In this figure, and in similar ones presented later, sensitivities are shown along a diagonal line of gridblocks from the upper left corner to the lower right corner of the reservoir as oriented in Fig. 4.13. Thus, gridblock 3 pertains to the areal location of well 1 and gridblock 8 pertains to the areal location of the injection well. As has been shown in previous work (see, for example, Wu et al. (1999)), the pressure is most sensitive to permeability in the gridblock containing the well. Increasing k in this gridblock decreases the pressure drop necessary to maintain the specified total flow rate (350 RB/D). Thus increasing k results in an increase in the flowing bottomhole pressure. It is interesting to note that sensitivities corresponding to gridblock log-permeabilities between well 1 and the injection well are negative at 210 days. From a careful examination of the simulation results, we find that increasing k in this region increases the velocity of water in this interwell region and leads to higher water saturation and lower oil and gas saturations in the gridblock containing well 1. Oil and gas saturation both decrease but these changes are such that (i) total mobility decreases (ii) k_{rg}/k_{ro} increases, (iii) k_{rw}/k_{ro} increases. Because of the decrease in total mobility, a lower flowing wellbore pressure is needed to maintain the

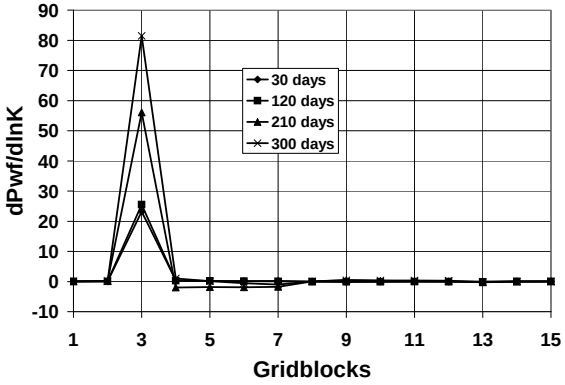

Figure 4.16: Dimensionless sensitivity of p_{wf} at well 1 to horizontal log-permeability of layer 1.

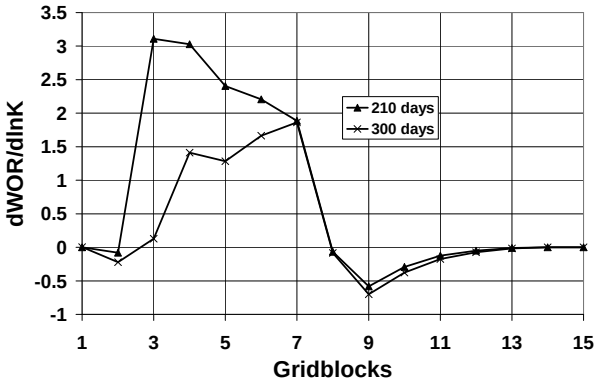

Figure 4.17: Dimensionless sensitivity of WOR at well 1 to horizontal log-permeability of layer 1.

specified production rate so the sensitivity of p_{wf} to horizontal log permeability in this interwell region is negative. Observations (ii) and (iii) explain why the sensitivity of the water-oil ratio (Fig. 4.17) and the producing gas-oil ratio (Fig. 4.18) to each gridblock log-permeability in this interwell region of layer 1 are positive.

At 300 days, the wellbore pressure at well 1 is largely insensitive to the layer 1 gridblock log-permeabilities between well 1 and the areal location of the injection well. By this time, an increase in one of these gridblock permeabilities results in a small change in total mobility. More specifically, the resulting decrease in gas mobility is small, and the increase in water mobility essentially offsets the decrease is oil mobility so that total mobility changes very little. However, the mobility ratios k_{rg}/k_{ro} and k_{rw}/k_{ro} still increase if horizontal permeability is increased and the sensitivity of the water-oil ratio (Fig. 4.17) and the producing gas-oil ratio (Fig. 4.18) to each gridblock log-permeability in this interwell region of layer 1 is still positive.

As shown in Fig. 4.17, the sensitivity of the water-oil ratio to layer 1 hori-

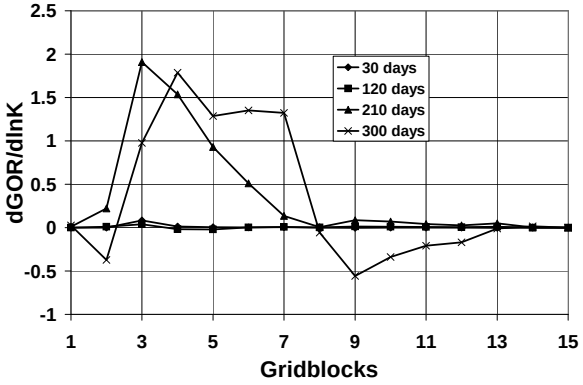

Figure 4.18: Dimensionless sensitivity of GOR at well 1 to horizontal log-permeability of layer 1.

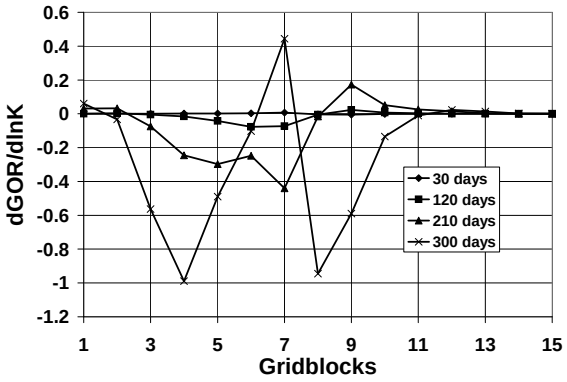

Figure 4.19: Dimensionless sensitivity of GOR at well 1 to horizontal log-permeability of layer 2.

zontal log-permeability is negative at gridblocks that are near the injection well and between well 3 and the injection well. This makes sense because increasing these permeabilities causes more of the injected water to flow towards well 3 thus decreasing the WOR at well 1. On the other hand increasing the permeability in the interwell region between well 1 and the injector causes more of the injected water to flow towards well 1 and increases the velocity of flow. Thus, the water saturation and WOR at well 1 increases. The sensitivity of the producing GOR to these permeabilities (Fig. 4.18) is not so easily explained and the behavior of the dimensionless sensitivity of GOR to horizontal log-permeability in layer 2 (Fig. 4.19) would be extremely difficult to predict a priori solely from physical intuition. The results shown in Fig. 4.19 pertain to the diagonal row of gridblocks in layer 2 that correspond to the layer 1 diagonal row of gridblocks shown in Fig. 4.18.

Figures 4.19, 4.20 and 4.21 show plots of the dimensionless sensitivity of well 1's producing GOR, WOR and flowing bottomhole pressure to layer 2 horizontal

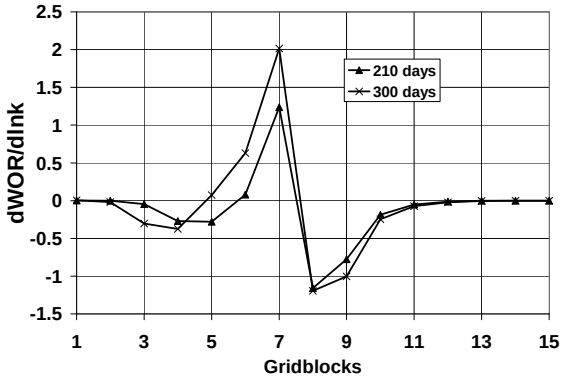

Figure 4.20: Dimensionless sensitivity of WOR at well 1 to horizontal log-permeability of layer 2.

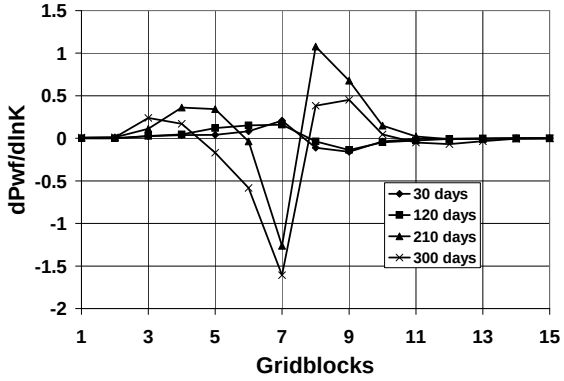

Figure 4.21: Dimensionless sensitivity of p_{wf} at well 1 to horizontal log-permeability of layer 2.

permeability at the same times considered in previous sensitivity coefficient plots. For the most part, we are unable to give a clear physical interpretation of the results.

It is interesting to note that the WOR sensitivities at 210 days and at 300 days are approximately a negative constant times the pressure sensitivity coefficients at the corresponding times. This occurs because in this specific situation, a change in a permeability that results in an increase in WOR, results in a decrease in total mobility and a decrease in the p_{wf} needed to make the specified total production rate at well 1. Similarly, a decrease in WOR due to a change in permeability corresponds to an increase in p_{wf}.

Since Eq. 2.18 indicates that the change in model parameters over a Levenberg-Marquardt iteration is determined by a linear combination of $C_M \hat{g}_i$ where $\hat{g}_i$ denotes the ith column of G_l^T, this suggests that the reduction in uncertainty in layer 2 horizontal log-permeability obtained by conditioning the model to pressure plus WOR data may be essentially the same as the reduction in uncertainty obtained by condi-

tioning only to pressure.

Sensitivity to Vertical Permeability.

Figures 4.22 and 4.23 show plots of the dimensionless sensitivity of well 1's flowing bottomhole pressure and producing GOR to layer 2 vertical permeability at the same times considered in previous sensitivity coefficient plots. Increasing k_z in gridblock 3 of Fig. 4.22 increases flow from layer 2 to layer 1 at the areal location of well 1 which produces only from layer 1. This provides pressure support, or from a well test analysis viewpoint decreases the pseudoskin factor due to restricted-entry. This effect by itself tends to result in a higher bottomhole pressure. Moreover, as this gridblock vertical permeability is increased, a greater precentage of the fluid flowing into the layer 1 gridblock containing the well comes from layer 2. At times after breakthrough, this results in a lower water saturation and higher wellblock total mobility. The higher total mobility also results in an increase in flowing bottomhole pressure. After breakthrough, which occurs at about 165 days, this second effect contributes significantly and results in a higher value of the sensitivity coefficient. A clear complete explanation of other features in Figs. 4.22 and 4.23 eludes us.

The reservoir model under consideration contains only two layers and the layer thicknesses coincide with the height of the two vertical gridblocks used in the finite-difference model. Thus, the reservoir simulator involves only the value of the harmonic average vertical permeability at the boundary between layers. Thus, even though we later present results on the estimates of layer vertical permeabilities, one should recognize that any two sets of layer vertical permeabilities that result in the same value of the harmonic average vertical permeability will yield the same production data.

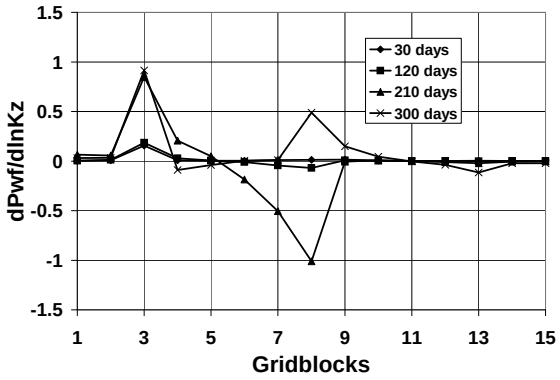

Figure 4.22: Dimensionless sensitivity of p_{wf} at well 1 to vertical log-permeability of layer 2.

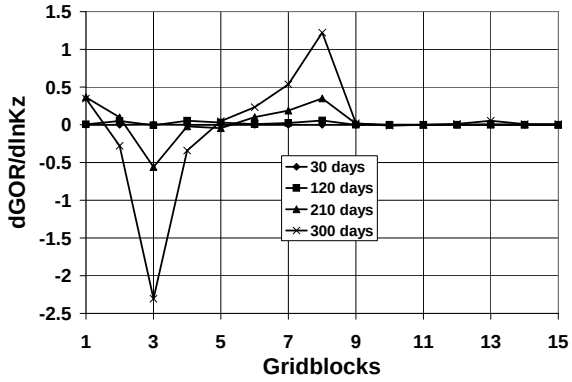

Figure 4.23: Dimensionless sensitivity of GOR at well 1 to vertical log-permeability of layer 2.

Sensitivity to Skin Factor.

The flowing wellbore pressure of producing well j is highly sensitive to the skin factor for well j but is insensitive to the skin factor at all other producing wells. Increasing the skin factor at a flowing well results in a decreased wellbore pressure ($\partial p_{wf,j}/\partial s_j < 0$), but has a negligible effect on the well's gridblock pressure. Since producing GOR and WOR are based on the well's gridblock pressure, GOR and WOR are insensitive to the wells skin factor. This indicates that history matching only to GOR or only to WOR data can not resolve well skin factors. Reasonable estimates of well skin factors can be obtained only by history matching pressure data.

Since the injection rate is fixed at the water injection well, the flow rate at the water injection well is insensitive to the skin factor at the injection well. It follows that the wellbore pressure at each producing well is insensitive to the skin factor at the injection well. (This would not be the case if the wellbore pressure was specified as the well constraint at the injection well.)

The injection wellbore pressure is highly sensitive to the skin factor at the injection well. This sensitivity coefficient is positive because as the skin factor increases, a higher wellbore pressure is required to maintain the specified injection rate. The injection well pressure is insensitive to the skin factors of all producing wells because the total flow rate is specified as a well constraint at the producing wells.

Comments.

The sensitivity of a specific production data (e.g., GOR at a specified time) to a particular model parameter (e.g., layer 1 vertical log-permeability for a gridblock containing a producing well) gives a measure of the magnitude of the change in this data that will result from a change in this model parameter. If this sensitivity is small, then we expect that the particular model parameter will not be reliably determined by the particular observed data, i.e., we expect the uncertainty in the model parameter will be not be significantly reduced by history matching the model to this single data point. However, to compare how different types of data affect the estimates of different model parameters, sensitivity results must be scaled properly. If the measurement error is very small, then the range of values of the model parameter that yield an acceptable match of the single observed data will be smaller and we expect the uncertainty in the model parameter to be smaller. Also if the prior variance is very small, then the model parameter is resolved well before history matching the data. Thus, even if the particular data is highly sensitive to the model parameter, we should not expect history matching to yield a big reduction in the uncertainty. The dimensionless sensitivity coefficients introduced by F. Zhang and Oliver (2000)(see Eq. 4.3) attempts to scale sensitivity coefficients to account for measurement errors and the prior variances in model parameters. Qualitatively, we expect that the higher dimensionless sensitivity coefficients correspond to a greater reduction in the uncertainty in model parameters. This simple concept ignores the correlation between model parameters, however. For example, if vertical permeability

were nonzero, but no vertical flow occurred in a particular region of the reservoir, production data would be insensitive to k_z in that region. If, however, k_z were strongly correlated to k in that region and the data reduced the uncertainty of k, we would expect the uncertainty in k_z to be reduced also.

4.2.2 Automatic History Matching Result

The Truth Case.

The truth case is the same one for which sensitivity coefficients were just presented. The true horizontal log permeability field is shown in Fig. 4.24(a) and 4.24(b) and the true vertical log-permeability field is shown in Fig. 4.25(a) and 4.25(b). The true skin factors at well 1 to 5, respectively, are 3.0, 4.0, 5.0, 2.0, and 0.0. The observed data consists of data obtained by running the reservoir simulator for the truth case to predict reservoir perfomance for a 300 day time period. At each producing well, we selected 10 WOR data, 10 GOR data and 10 pressure data to use as conditioning data. At the injection well, we selected 10 pressure data to use as conditioning data. The data are uniformly distributed throughout the 300 day time period with the earliest time conditioning data corresponding to $t = 30$ days. We assumed pressure measurement errors to be independent, identically-distributed, normal random variables with mean zero and variance equal to 1 psi^2. GOR measurement errors were modeled similarly except the variance was set equal to 100 (scf/STB)^2. The variances of WOR measurement errors were specified by Eq. 2.22 with $\sigma^{\min}_{q_w,\text{obs}} = 2.0$ STB/STB, $\epsilon_o = 0.01$ and $\epsilon_w = 0.02$.

For the top layer, the prior means for $\ln(k)$ and $\ln(k_z)$, respectively, were specified as 5.5 and 3.2 with the variances of both random variable equal to 0.5. For the second layer, the prior means for $\ln(k)$ and $\ln(k_z)$, respectively, were specified as 4.0 and 2.4 with the variances of both random variable equal to 0.5. The same semivariogram was used for each of the four log-permeability fields. The semivariogram

is an isotropic spherical semivariogram with range equal to 160 ft and sill equal to 0.5. As the areal dimensions of simulation gridblocks are $\Delta x = \Delta y = 40$ feet, if the distance between the centers of two gridblocks at the same elevation is greater than or equal to $4\Delta x$, permeabilities at the two gridblock are uncorrelated. There is no correlation between layer 1 permeabilities and layer 2 permeabilities. In each layer, the correlation coefficient between $\ln(k)$ and $\ln(k_z)$ is set equal to 0.7. Each well skin factor is modeled as an independent random variable with mean equal to 2.0 and variance equal to 25.

The MAP Estimate

As discussed previously, the MAP estimate was generated using the Levenberg-Marquardt algorithm to minimize the objective function of Eq. 2.8. The initial dumping factor λ is set to equal 10^5. The vector of prior means was used as the initial guess. Note even though each layer actually consists of three zones, horizontal and vertical log-permeability are estimated at each gridblock. This simple model is used only because it makes it easy to evaluate the quality of the estimate. We consider results obtained by history matching only pressure data, pressure plus WOR data, pressure plus GOR data and all three types of data.

Fig. 4.24(c) and Fig. 4.24(d) show the MAP estimate of horizontal log-permeability obtained by history-matching only pressure data and Fig. 4.24(e) and Fig. 4.24(f) show results obtained by conditioning to pressure, GOR and WOR data. Comparing results to the truth case shown in Fig. 4.24(a) and Fig. 4.24(b), we see that the MAP estimate obtained by conditioning to all three types of data is closer to the truth case. In Fig. 4.25, we can see that conditioning to pressure, WOR and GOR data gave a better estimate of the vertical log-permeability field than was obtained by conditioning only to pressure.

Fig. 4.26 confirms the preceding results and also shows results obtained by conditioning to pressure and WOR data only and pressure and GOR data only. The

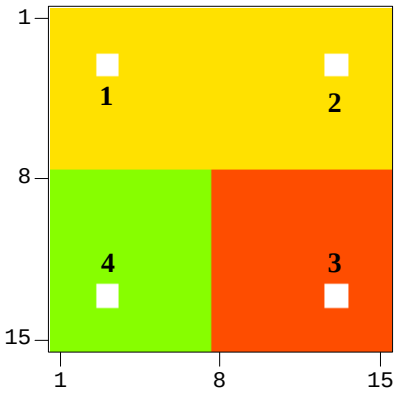

(a) True model, layer 1.

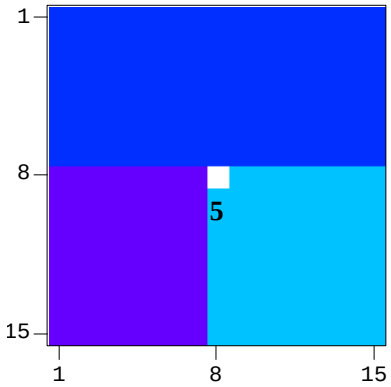

(b) True model, layer 2.

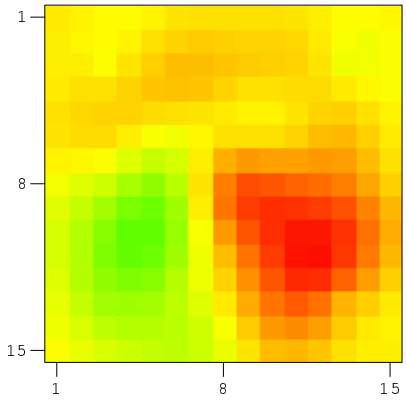

(c) Conditioned only to p_{wf} data.

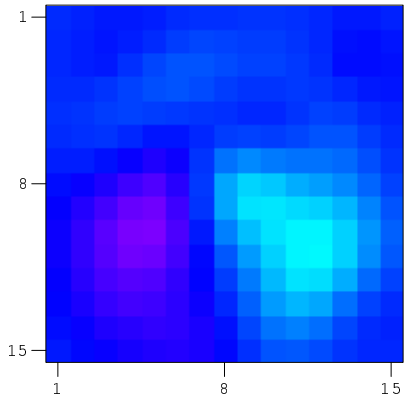

(d) Conditioned only to p_{wf}.

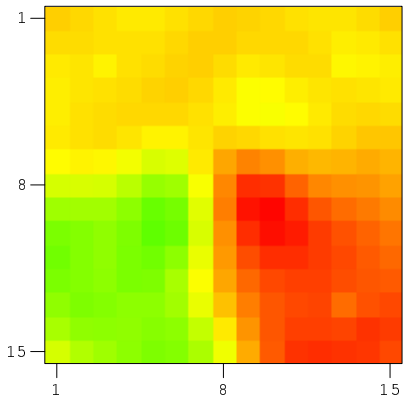

(e) Conditioned to all p_{wf}, GOR and WOR data.

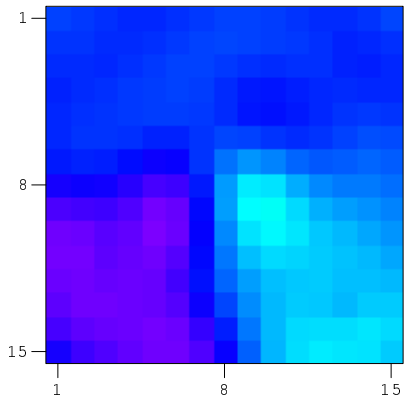

(f) Conditioned to all p_{wf}, GOR and WOR data.

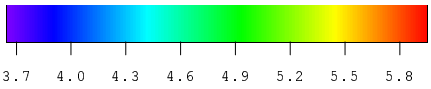

Figure 4.24: True model and maximum a posteriori estimate of horizontal log-permeability, layer 1 (left column) and layer 2 (right column).

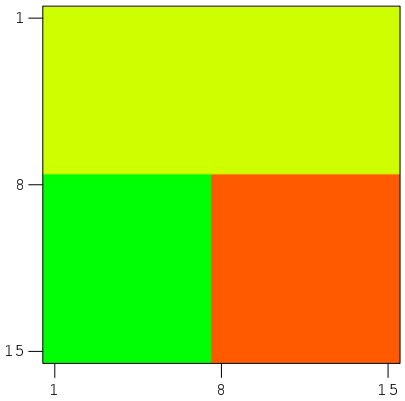

(a) True model, layer 1.

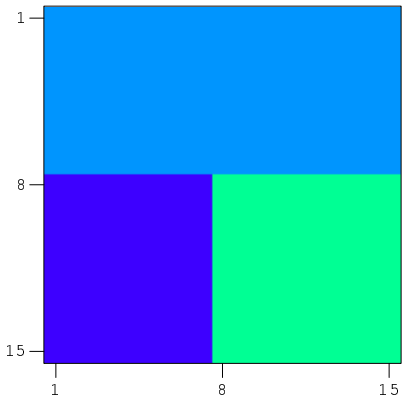

(b) True model, layer 2.

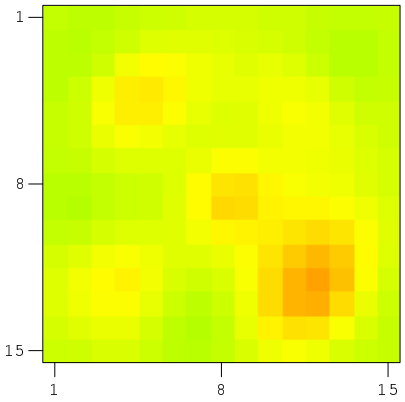

(c) Conditioned only to p_{wf} data.

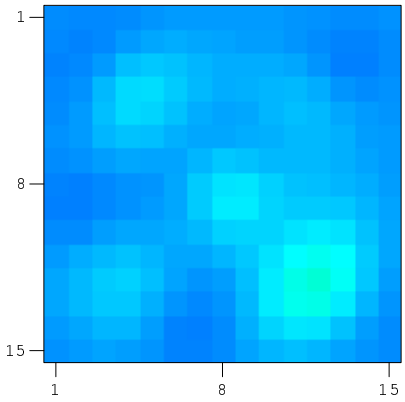

(d) Conditioned only to p_{wf}.

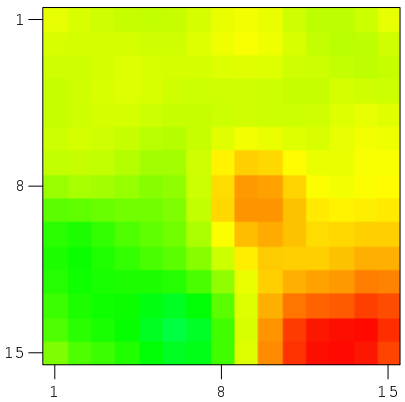

(e) Conditioned to all p_{wf}, GOR and WOR data.

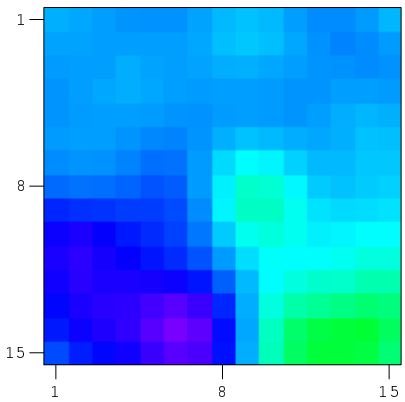

(f) Conditioned to all p_{wf}, GOR and WOR data.

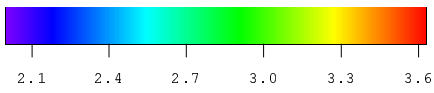

Figure 4.25: True model and maximum a posteriori estimate of vertical log-permeability, layer 1 (left column) and layer 2 (right column).

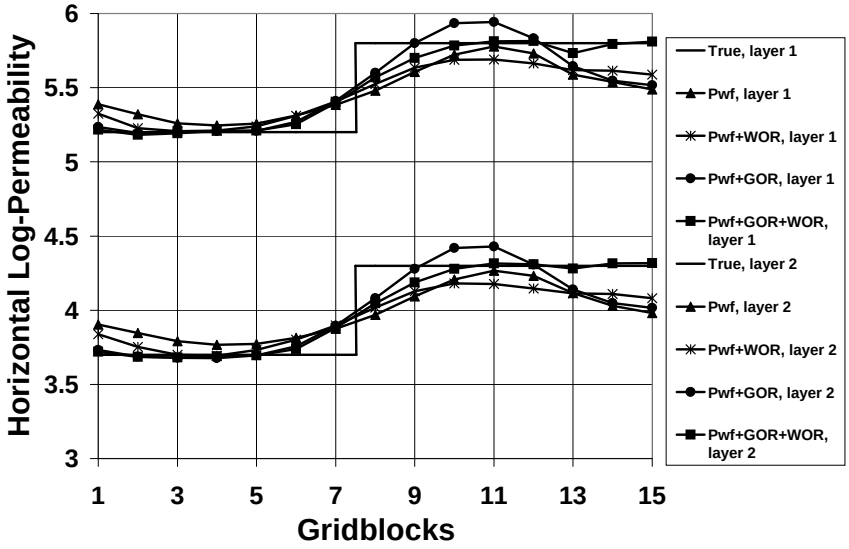

Figure 4.26: MAP estimate of horizontal log-permeability along the line from well 4 to 3.

results in Fig. 4.26 pertain to results along the line of gridblocks in layer 1 that pass through wells 3 and 4, and along the corresponding line of gridblocks in layer 2. Fig. 4.27 shows the corresponding estimates of $\ln(k_z)$. In Figs. 4.26 and 4.27 and in similar figures, curves through solid triangular data points refer to results obtained by conditioning only to pressure data, curves through data points denoted by an asterisk refer to results obtained by conditioning only to pressure and WOR data, curves through solid circular data points refer to results obtained by conditioning only to pressure and GOR data and curves through solid square data points represent results obtained by conditioning to all observed data, pressure, GOR and WOR. Considering the overall results, it is clear the worst estimates of the true permeability fields are obtained when only pressure data is history-matched and the best estimates are obtained when the estimate is obtained by history-matching all the pressure, WOR and GOR data. History matching only GOR data plus pressure data gives better

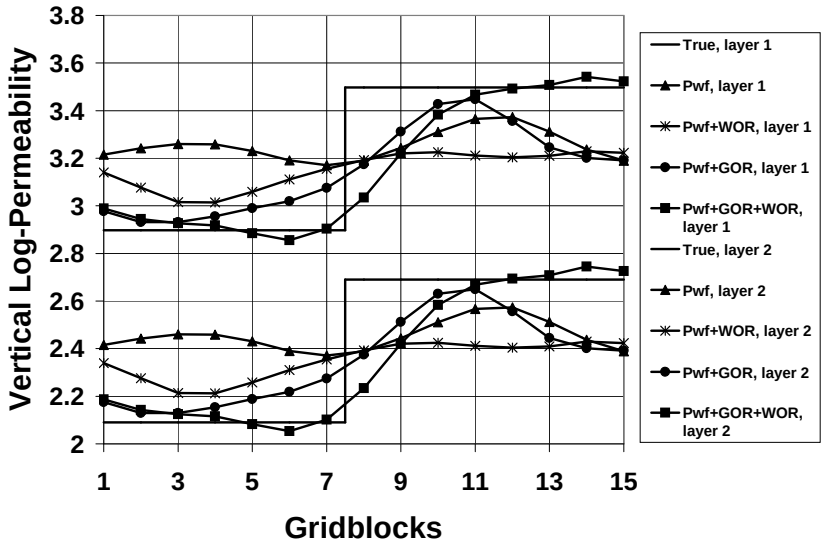

Figure 4.27: MAP estimate of vertical log-permeability along the line from well 4 to 3.

estimates of vertical permeability than history matching pressure and WOR data. On a visual basis, it does not appear that history matching pressure plus water-oil ratio data gives significantly better results than matching only pressure data. This conclusion is similar to one reported by Landa and Horne (1997) and Wu et al. (1999).

One might guess that the reasonably good estimates of $\ln(k_z)$ obtained (see Fig. 4.27) are partially due to a high correlation between the random functions $\ln(k)$ and $\ln(k_z)$ (correlation coefficient equal to 0.7) and the fact that horizontal log-permeability is fairly well resolved by the data. However, in dimensionless form, the sensitivity of production data to horizontal log-permeability and the sensitivity of production data to vertical log-permeability variables show peaks of similar magnitude; compare, for example Fig. 4.19 with Fig. 4.23. Thus, it is reasonable to conjecture that the good estimates of $\ln(k_z)$ obtained in Fig. 4.27 are not solely due to the correlation between $\ln(k)$ and $\ln(k_z)$. To investigate this conjecture, we

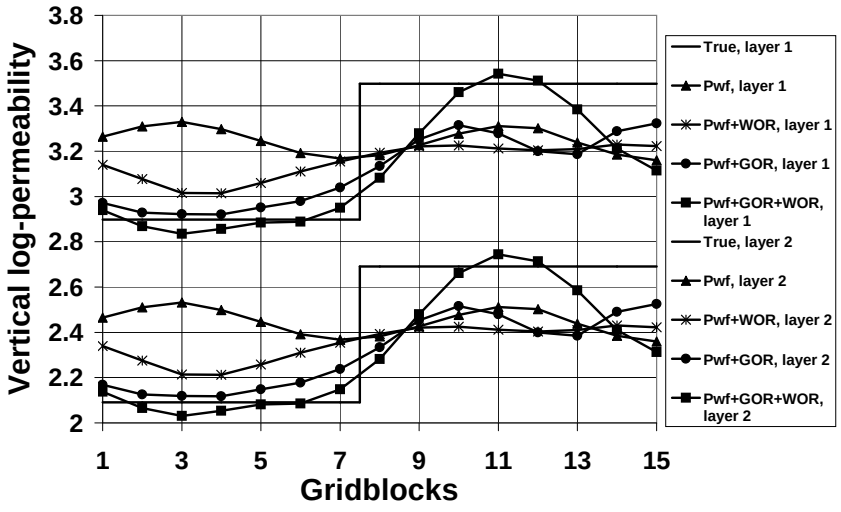

Figure 4.28: MAP estimate of vertical log-permeability along the line from well 4 to 3; no correlation between horizontal and vertical permeability.

generated the MAP estimate assuming that horizontal and vertical permeability are not correlated in the prior model (Fig. 4.28). The results obtained are shown in Fig. 4.28 are similar to the ones showed in Fig. 4.27, where the vertical permeability and horizontal permeability are correlated.

Figs. 4.29 and 4.30 show MAP estimates of horizontal and vertical log-permeability, respectively, along a diagonal line of gridblocks in layer 1 that passes through wells 1, 5 and 3 and the corresponding diagonal row of gridblocks in layer 2. The results from Figs. 4.29 and 4.30 are qualitatively similar to those shown in Figs. 4.26 and 4.27. The best estimates are obtained by history-matching all the pressure, WOR and GOR data. Figs. 4.31 and 4.32 show the corresponding normalized a posteriori variances constructed from the a posteriori covariance matrix, C_{MP}. These variances pertain to the same diagonal rows of gridblocks considered in the sensitivity coefficient plots of Figs. 4.16–4.23. In these figures, gridblock 3 pertains to the areal

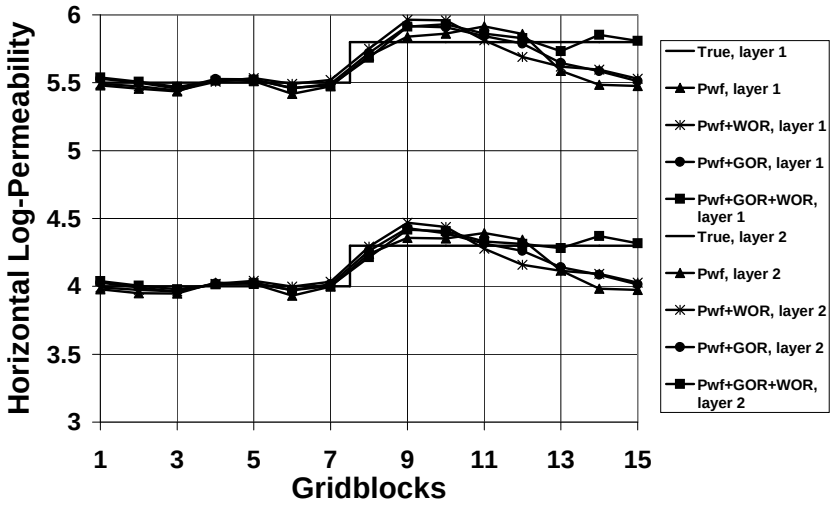

Figure 4.29: MAP estimate of horizontal log-permeability along the line from well 1 to 3.

location of well 1, gridblock 8 pertains to the areal location of well 5 and gridblock 13 represents the areal location of well 3. The normalized variances at well locations are roughly equal to 0.2 which may be interpreted to mean that we have reduced the uncertainty of these log-permeabilities by eighty percent. Except at the areal location of the injection well (gridblock 8) history matching WOR and/or GOR data plus pressure data reduced the uncertainty (as measured by the normalized a posteriori variance) below the uncertainty obtained by history matching only to pressure data. Note this occurs even at layer 1 gridblock 3 which contains well 1 (see Fig. 4.31(a)) even though the pressure at well 1 is highly sensitive to this gridblock permeability and largely insensitive to other layer 1 $\ln(k)$ values. Note, however, well gridblock $\ln(k)$ and the well skin factor are both unknown and must be resolved by the data. We believe that the fact that both the WOR (Fig. 4.17) and the GOR (Fig. 4.18) at well are highly sensitive to this gridblock $\ln(k)$ at certain times but insensitive to the

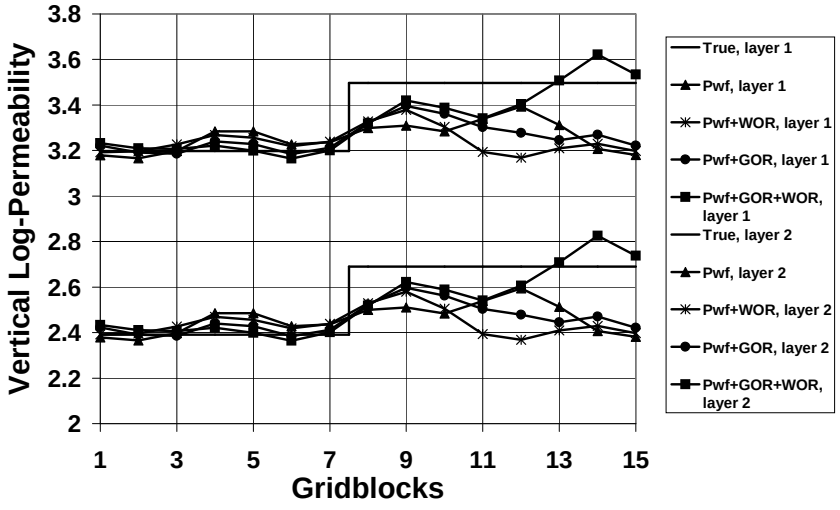

Figure 4.30: MAP estimate of vertical log-permeability along the line from well 1 to 3.

well skin factor explains why adding observed GOR and WOR data as conditioning data reduces the uncertainty in $\ln(k)$ at the gridblock containing well 1.

As the WOR and GOR at well (Figs. 4.17 and 4.18) are almost completely insensitive to the horizontal gridblock permeability for gridblock 8 of layer 1, it is not completely surprising that conditioning to WOR and/or GOR plus wellbore pressures does not significantly reduce the uncertainty below that obtained by conditioning only to pressure data. Any additional reduction in uncertainty in $\ln(k)$ obtained at this gridblock by adding WOR and/or GOR as conditioning data must come from the correlation between this $\ln(k)$ random variable and the log-permeabilities in neighboring gridblocks where the GOR and WOR sensitivity coefficients are non-negligible. It is interesting to note, however, that even though at later times, the GOR (Fig. 4.19) and WOR (Fig. 4.20) at well are relatively sensitive to $\ln(k)$ for gridblock 8 of layer 2, the reduction in uncertainty in this horizontal log-permeability

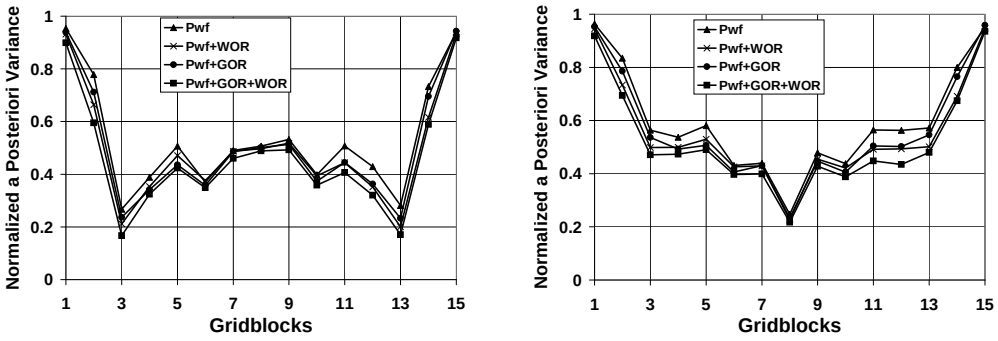

(a) Layer 1 . (b) Layer 2

Figure 4.31: The normalized a posteriori variance of horizontal log-permeability along diagonal line, well 1-3.

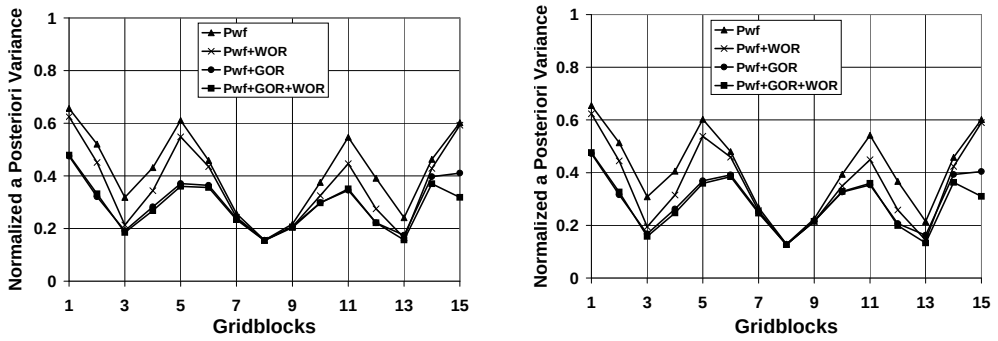

(a) Layer 1 . (b) Layer 2

Figure 4.32: The normalized a posteriori variance of vertical log-permeability along diagonal line, well 1-3.

is essentially independent of which type of data is history matched as long as pressure data is included as conditioning data. This is because the injection wellbore pressures (not shown) and flowing wellbore pressures at all producing wells are quite sensitive to this gridblock permeability but flowing wellbore pressures are insensitive to the skin factor at the injection well. Thus, using GOR and WOR data in addition to

Table 4.1: The true and estimated skin factors

Well No.	1	2	3	4	5
True skin factors	3.00	4.00	5.00	2.00	0.00
Initial guess	2.00	2.00	2.00	2.00	2.00
Conditioned to p_{wf} data	2.60	3.30	2.97	2.61	-0.19
Conditioned to p_{wf}+WOR data	2.67	3.39	3.18	2.22	0.24
Conditioned to p_{wf}+GOR data	2.73	3.39	3.54	2.07	0.00
Conditioned to p_{wf}+GOR+WOR data	2.83	3.65	4.37	1.96	-0.27

pressure data as conditioning data does not reduce the uncertainty in this gridblock $\ln(k)$ below the level obtained by conditioning only to pressure data.

Estimates of well skin factors obtained by matching various combinations of production data are shown in Table 4.1. Note that, except at the injection well, the best estimates are obtained by history matching pressure, WOR and GOR data.

The history matches of some of the observed GOR and WOR data are shown in Fig. 4.33. Solid circular and triangular data points represent the observed data used as conditioning data. Curves through the cross data points indicate the data predicted from the initial guess (m_{prior}) of the model parameters. (Some initial pressure mismatches exceeded 400 psi.) The predicted data shown is based on the model obtained by simultaneously matching pressure, WOR and GOR data. Matches of similar quality were obtained for all wells for all pressure, WOR and GOR observed data.

Fig. 4.34 shows the rate of convergence of the objective functions when conditioning to different combinations of the data. The Objective functions decrease very fast in the first 5 or 6 iterations. It is clear that it is more difficult for the objective functions to converge in a three-dimensional three-phase problem than in a

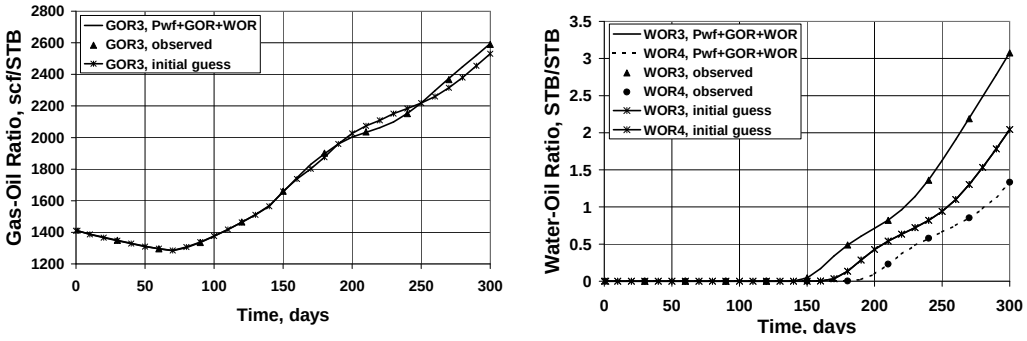

Figure 4.33: The GOR match (left)and WOR match (right) for the model conditioned to p_{wf}, GOR, and WOR data.

two-dimensional three-phase problem (Fig. 4.7).

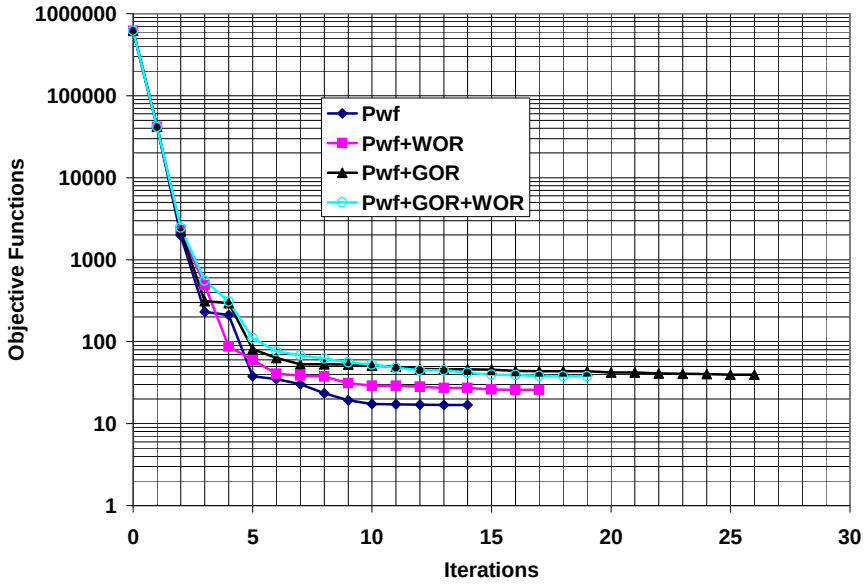

Figure 4.34: The rate of convergence of the objective functions in a three-dimensional, three-phase reservoir.

Remarks.

The results and discussion of this history matching example serves to illustrate the the following observations. If particular production data are completely insensitive to a model parameter, changing this model parameter does not change the values of production data predicted by reservoir simulation. (i) Thus, conditioning to these data can reduce the uncertainty in this model parameter only by reducing the uncertainty in the parameters which are correlated with this model parameter. The reduction in uncertainty due to either a prior correlation (determined by C_M) or a posterior correlation (determined by C_{MP}) can not be predicted by examining sensitivity coefficients. (ii) If a set of model parameters is well resolved by a given data set, adding a second set of conditioning data to the first may not give an additional reduction in uncertainty even if the second set of data is highly sensitive to the model parameters.

4.2.3 Conditional Realization of a Heterogeneous Reservoir

We present an example of a conditional realization of a 3D heterogeneous reservoir obtained by conditioning to pressure, gas-oil ratio and water-oil ratio data. The simulation grid, prior model, data measurement errors, well locations, well constraints and production rates at each well are the same as one described in the first part of section 4.2. The well skin factors in all five wells are assumed known and equal to zero. We estimate the horizontal and vertical permeability in each gridblock simultaneously. The true horizontal log-permeability field of layer 1 is shown in fig. 4.38(a). The unconditional realization (the initial model) is generated by using a Cholesky decomposition of prior covariance matrix. Fig. 4.38(b) shows the unconditional realization of horizontal log-permeability field in layer 1. We use the algorithm presented in the section 2.6.2 to generate the conditional realization by conditioning the unconditional model to p_{wf}, GOR, and WOR data. The observed data were

generated from the true model. Random noise was added to the observed data.

Figs. 4.35 to 4.37 show the data match between the observed data and the predicted data obtained by running simulator on the conditional realization model. The observed pressure data match the predicted data very well. The predicted GOR and WOR data also match the observed data reasonably well, even though it is not perfectly.

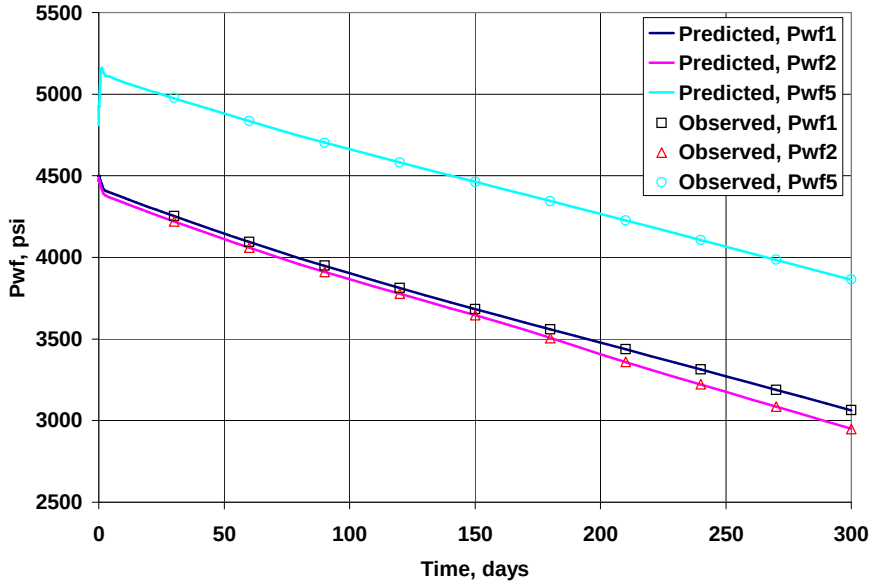

Figure 4.35: Bottom hole pressure match after conditioning to p_{wf}, GOR, and WOR Data.

Fig. 4.38 to 4.41 show the true models, unconditional and conditional realizations of horizontal and vertical permeability in both layer 1 and layer 2. In the layer 1 (Fig. 4.38 and 4.40) , we can see that the conditional realizations of both horizontal and vertical log permeability have similar feature as the true model and are significantly different from the unconditional realizations. However, it is hard to see the similarity between the true models and the conditional realizations of horizontal and vertical log permeability in the layer 2 (Fig. 4.39 and 4.41), even though the

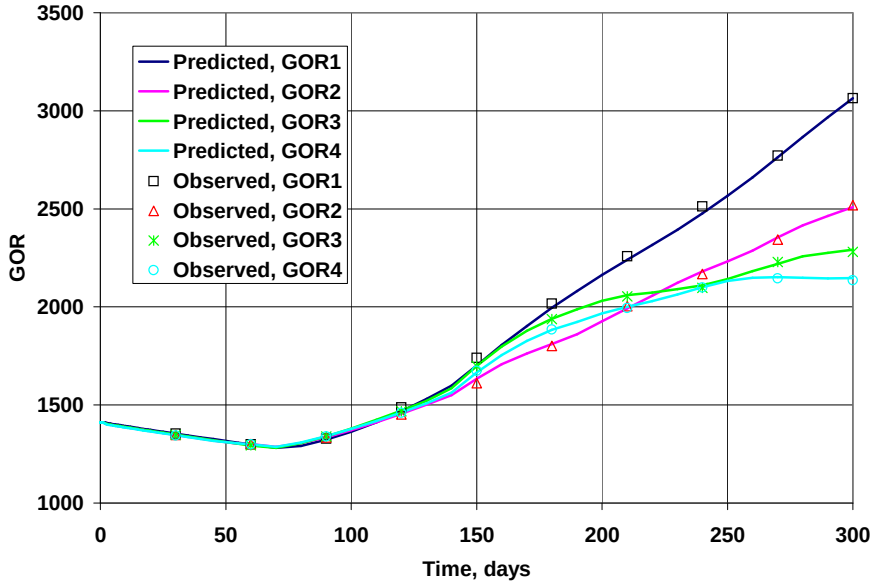

Figure 4.36: Gas-oil ratio match after conditioning to p_{wf}, GOR, and WOR Data.

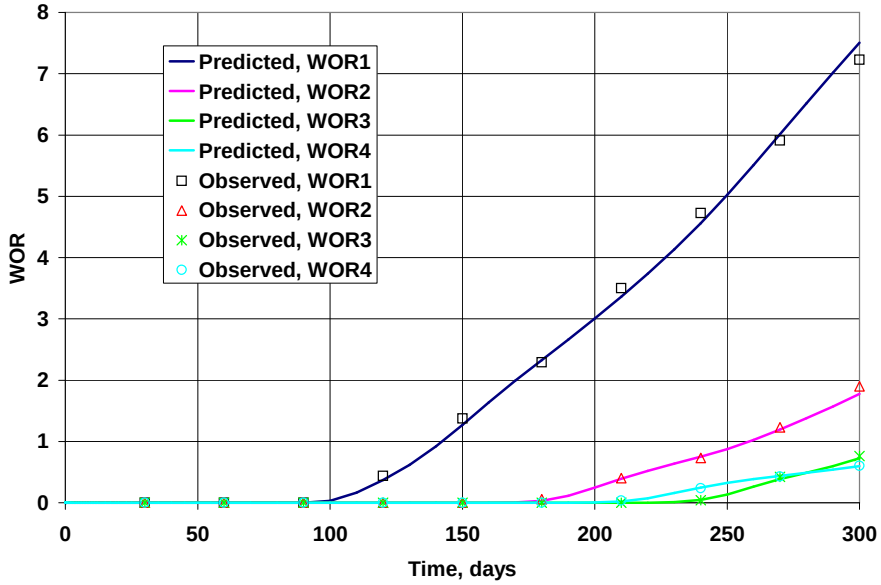

Figure 4.37: Water-oil ratio match after conditioning to p_{wf}, GOR, and WOR Data.

predicted data from the conditional realization match observed data reasonably well (Figs. 4.35 to 4.37). From the above results, we can see that even though the data

match very well, the estimated models or conditional realizations may not be similar to the true models.

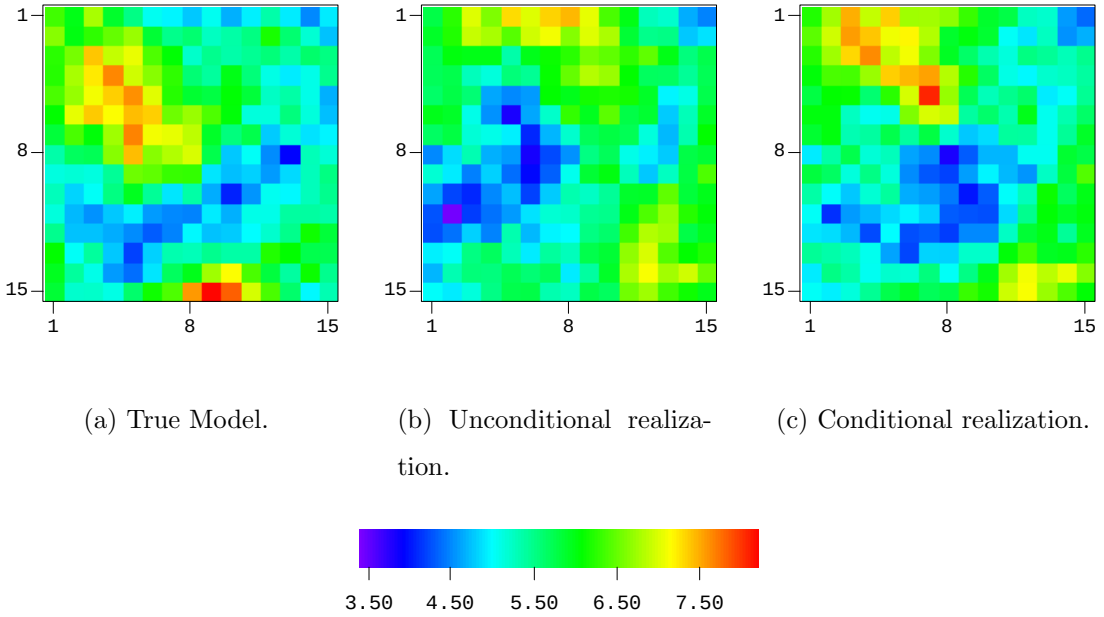

(a) True Model. (b) Unconditional realization. (c) Conditional realization.

Figure 4.38: The conditional realization of horizontal log-permeability conditioned to p_{wf}, GOR, and WOR data, layer 1.

Figs. 4.42 shows the convergence behavior of the Levenberg-Marquardt algorithm used for this heterogeneous example. The initial damping factor λ is 10^5. Note the Levenberg-Marquardt optimization algorithm converge relatively slowly and the final value of the objective function is relatively large. We also tried to estimate well skin factors along with horizontal and vertical permeability simultaneously. Unfortunately, some of the skin factors approach big negative values and the inverse procedure failed. Clearly, additional research on optimizing the optimization algorithm is needed.

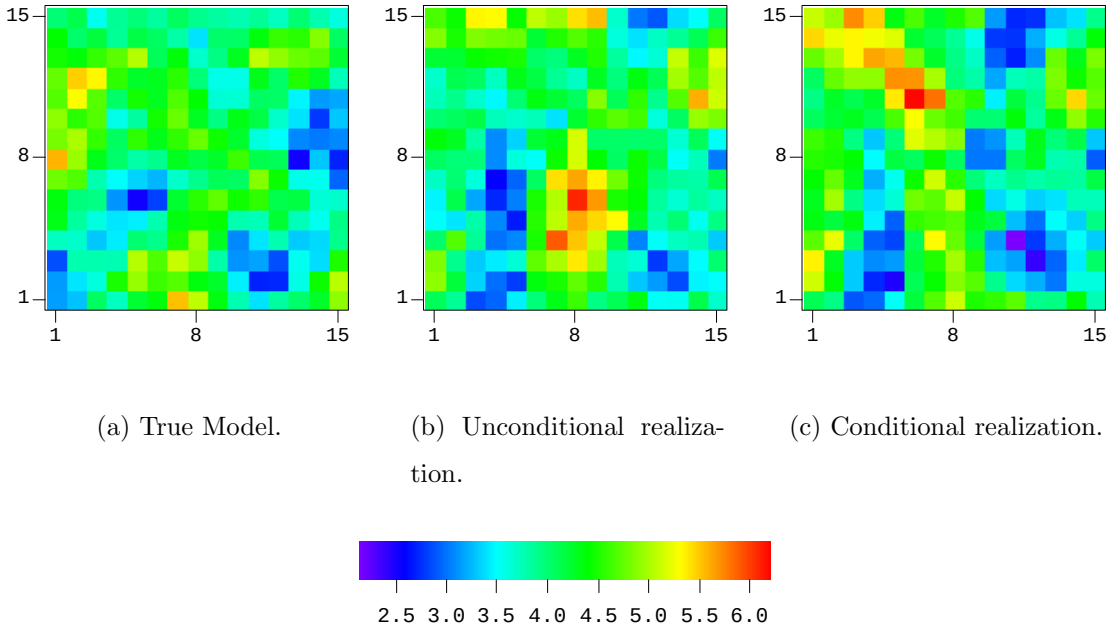

(a) True Model. (b) Unconditional realization. (c) Conditional realization.

Figure 4.39: The conditional realization of horizontal log-permeability conditioned to p_{wf}, GOR, and WOR data, layer 2.

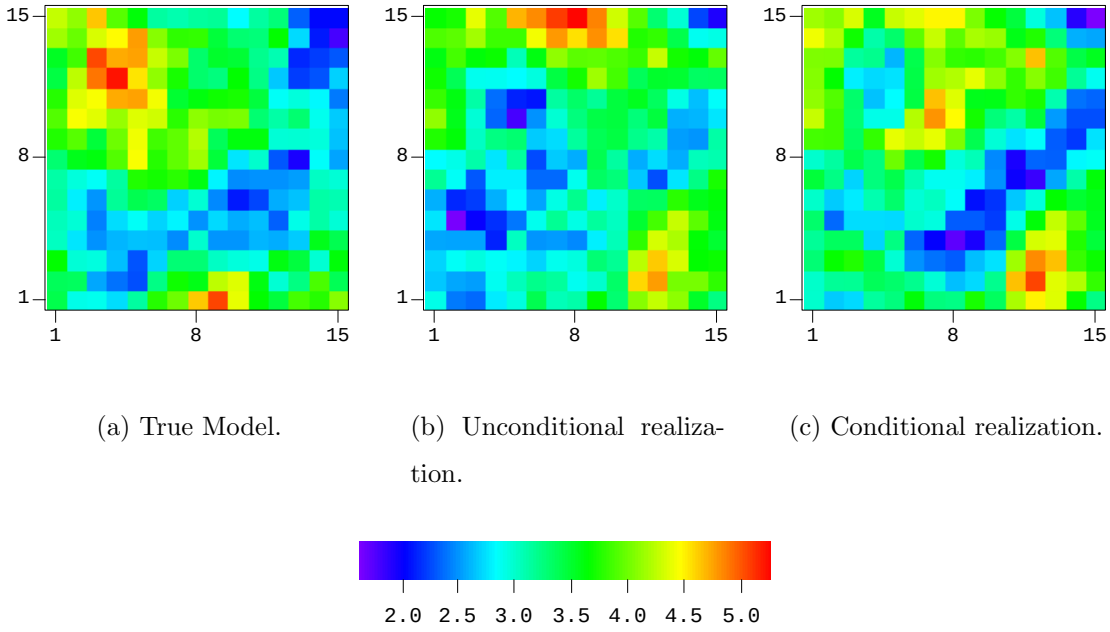

(a) True Model. (b) Unconditional realization. (c) Conditional realization.

Figure 4.40: The conditional realization of vertical log-permeability conditioned to p_{wf}, GOR, and WOR data, layer 1.

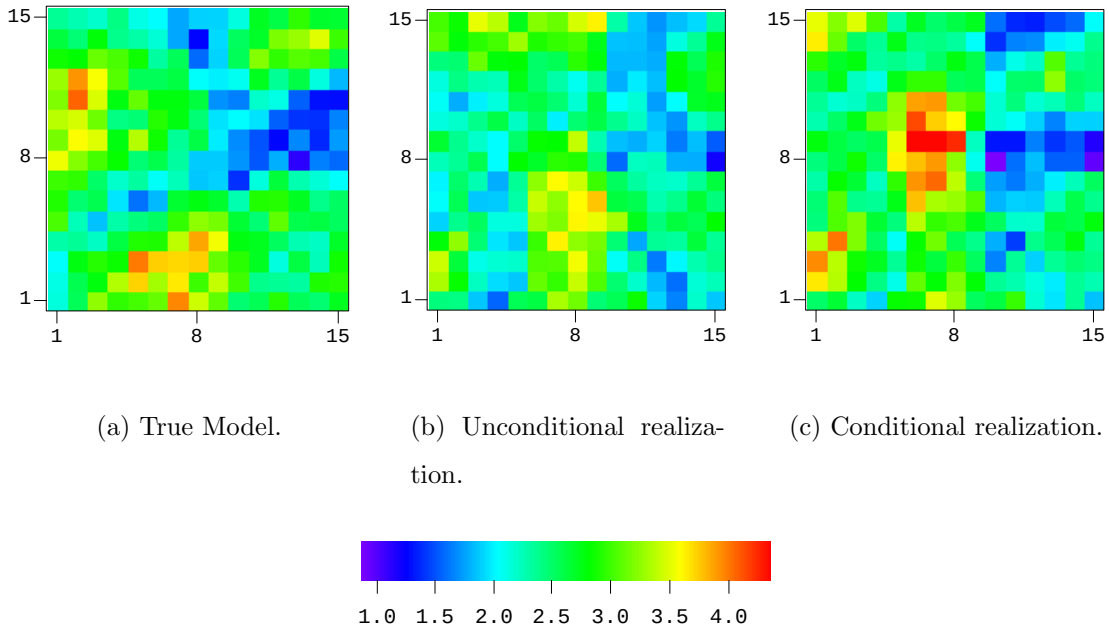

(a) True Model. (b) Unconditional realization. (c) Conditional realization.

Figure 4.41: The conditional realization of vertical log-permeability conditioned to p_{wf}, GOR, and WOR data, layer 2.

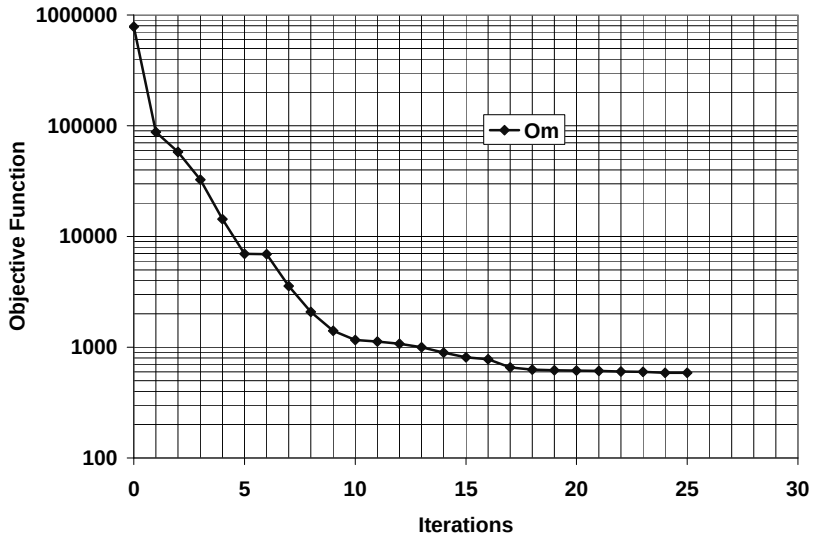

Figure 4.42: The rate of convergence of the objective function in the three-dimensional three-phase heterogeneous reservoir.

4.3 Estimation of Three-Phase Relative Permeability

4.3.1 Relative Permeability

In many cases, the relative permeability curves can be approximated by analytical functions. We can predict the relative permeability curves by estimating the parameters of the analytical function. In our approach, the three-phase relative permeability is calculated by the second model of Stone (Stone, 1973). We establish the models for two-phase water-oil and gas-oil systems, and then use the adjoint method to compute the sensitivity of production data to the parameters of the three-phase relative permeability model. Once we estimate the sensitivity coefficients, we can estimate the parameters of relative permeability model and other reservoir model parameters (k_x, k_y, k_z and ϕ) simultaneously by conditioning to production data.

For the oil-water system, we assume that relative water permeability and relative oil permeability can be modeled by the following exponential equations. If $S_w \leq S_{wc}$ then

$$k_{rw} = 0, \tag{4.4}$$

otherwise

$$k_{rw} = k_{rwcw} \left(\frac{S_w - S_{wc}}{1 - S_{orw} - S_{wc}} \right)^{n_{rw}}. \tag{4.5}$$

If $S_w \geq 1 - S_{orw}$ then

$$k_{row} = 0, \tag{4.6}$$

otherwise

$$k_{row} = k_{rocw} \left(\frac{1 - S_{orw} - S_w}{1 - S_{orw} - S_{wc}} \right)^{n_{row}}. \tag{4.7}$$

In these equations, S_{wc} is the critical water saturation, S_{orw} is residual oil saturation to waterflooding, k_{rw} is the relative water permeability when water saturation is S_w, k_{row} is the relative oil permeability in the oil-water system when water saturation is S_w, k_{rwcw} and k_{rocw} are the end points of the water and oil relative permeability curves, respectively, and n_{rw} and n_{row} are constants.

The six parameters that could be estimated for water-oil relative permeability are k_{rwcw}, k_{rocw}, n_{rw}, n_{row}, S_{wc} and S_{orw}.

Similarly, in the oil-gas system, we assume the relative gas permeability and relative oil permeability can be modeled by the exponential equations given below. If $S_w \leq S_{gc}$ then

$$k_{rg} = 0, \tag{4.8}$$

otherwise

$$k_{rg} = k_{rgcw} \left(\frac{S_g - S_{gc}}{1 - S_{org} - S_{wc} - S_{gc}} \right)^{n_{rg}}. \tag{4.9}$$

If $S_g \geq 1 - S_{wc} - S_{org}$ then

$$k_{rog} = 0, \tag{4.10}$$

otherwise

$$k_{rog} = k_{rocw} \left(\frac{1 - S_{org} - S_{wc} - S_g}{1 - S_{org} - S_{wc}} \right)^{n_{rog}}. \tag{4.11}$$

Here, S_{gc} is the critical gas saturation, S_{org} is residual oil saturation to gasflooding, k_{rg} is the relative gas permeability when gas saturation is S_g, k_{rog} is the relative oil permeability in the oil-gas system when gas saturation is S_g, k_{rgcw} and k_{rocw} are the end points of gas and oil relative permeability curves, respectively. The exponential n_{rg} and n_{rog} are constants that determine the curvature. As discussed in Appendix A, see Eq. A–12, the following equation is required when using the Stone 2 model:

$$k_{rocw} = k_{row}(S_w = S_{wc}) = k_{rog}(S_g = 0). \tag{4.12}$$

This is why the coefficients in the Eq. 4.7 and Eq. 4.11 are the same. The constraint of Eq. 4.12 reduces the number of parameters by 1.

Similar to the oil-water system, we wish to estimate the parameters k_{rgcw}, k_{rocw}, n_{rg}, n_{rog}, S_{wc}, S_{gc} and S_{org}. As discussed in Appendix A, three-phase oil relative permeability is given by

$$k_{ro} = k_{rocw} \left[([k_{row}/k_{rocw}] + k_{rw})([k_{rog}/k_{rocw}] + k_{rg}) - (k_{rw} + k_{rg}) \right]. \tag{4.13}$$

Thus, the parameters for relative permeability model under three-phase flow conditions are

$$k_r = [\ n_{rw},\quad k_{rwcw},\quad n_{rg},\quad k_{rgcw},\quad n_{row},\quad k_{rocw},\quad n_{rog},\quad S_{wc},\quad S_{orw},\quad S_{gc},\quad S_{org}\ ]^T. \tag{4.14}$$

In this work, we assume the parameters S_{wc}, S_{orw}, S_{gc}, and S_{org} are known and only estimate the following 7 relative permeability parameters,

$$k_r = [\ n_{rw},\quad k_{rwcw},\quad n_{rg},\quad k_{rgcw},\quad n_{row},\quad k_{rocw},\quad n_{rog}\ ]^T. \tag{4.15}$$

We assume that prior information on the parameters can be obtained from relative permeability curves determined by laboratory experiments. By conditioning the prior model to the production data, we integrate experimental laboratory data with production data.

In all examples presented, we estimate some or all of the parameters included in Eq. 4.15. The relative permeability curves obtained using these estimates are referred to as the estimated relative permeabilities. The objective functions are always minimized by using Levenberg-Marquardt method. The initial dumping factor α is set to 10^5. If the objective function decreases, α will be decreased by a factor of 10. Otherwise, α will be multiplied by 10. In all cases, the prior variances for pressure and GOR measurement errors are set to 1.0 and 25.0, respectively. The variance for measurement errors for WOR is calculated by Eq. 2.22. We chose $\sigma^{\min}_{q_w,obs} = 2STB/D$, $\epsilon_o = 0.01$ and $\epsilon_w = 0.02$ in the Eq. 2.22. The prior variance for absolute log permeability is 0.5. The prior variance of exponential terms (n_{rw}, n_{rg}, n_{row}, n_{rog}) is 1.0 and the variance of end point values (k_{rwcw}, k_{rgcw}, k_{rocw}) is 0.04. A spherical variogram model is used to generate the covariance matrix. The porosity in each gridblock is fixed at 0.22. In each case, the observed production data (p_{wf}, GOR, and WOR) are generated by running reservoir simulation on the true models. We condition the initial guess model to the production data to generate MAP estimates and realizations. The initial guesses of model parameters are always set equal to the

prior means. In all examples, S_{orw}=0.2, S_{wc}=0.2, S_{org}=0.1, and S_{gc}=0.05. When the pressure data are used in the examples shown in this section, the injection well pressure data are always part of the observed data.

4.3.2 Two Phase Reservoirs

We first consider a one dimensional reservoir to investigate the water-oil and gas-oil two phase flow problems. The reservoir is 11 by 1 by 1. The gridblock sizes in x, y and z direction are 40 feet, 40 feet and 30 feet, respectively. This is a homogenous reservoir with absolute log permeability in each gridblock equal to 4.61 (100 mD). The true values and initial guesses of the parameters of relative permeability are given in the second and fourth columns of table 4.2.

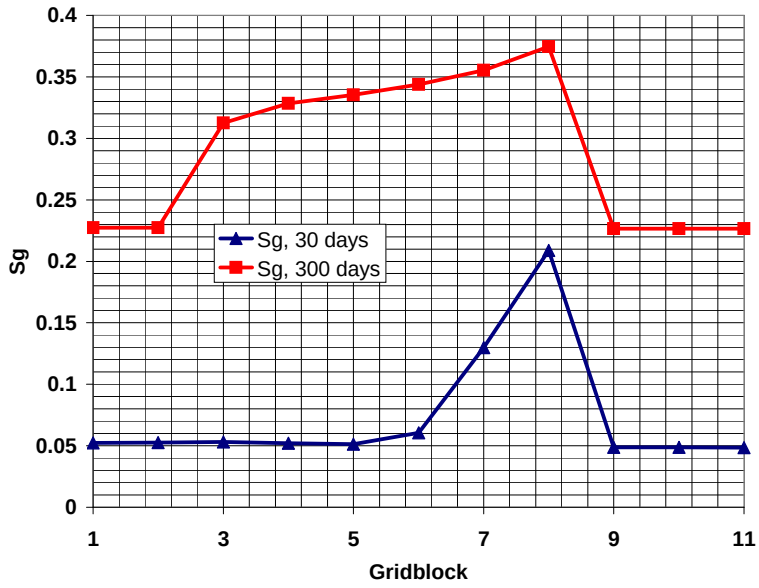

Figure 4.43: The gas saturation distribution of 1D gas injection reservoir.

In the first case, we simulate an oil reservoir with gas injection. There is a producing well at gridblock (3,1,1) produced at constant total rate 35 rb/day. An injection well is located at (8,1,1) with gas injection rate 20 scf/d. The initial reservoir

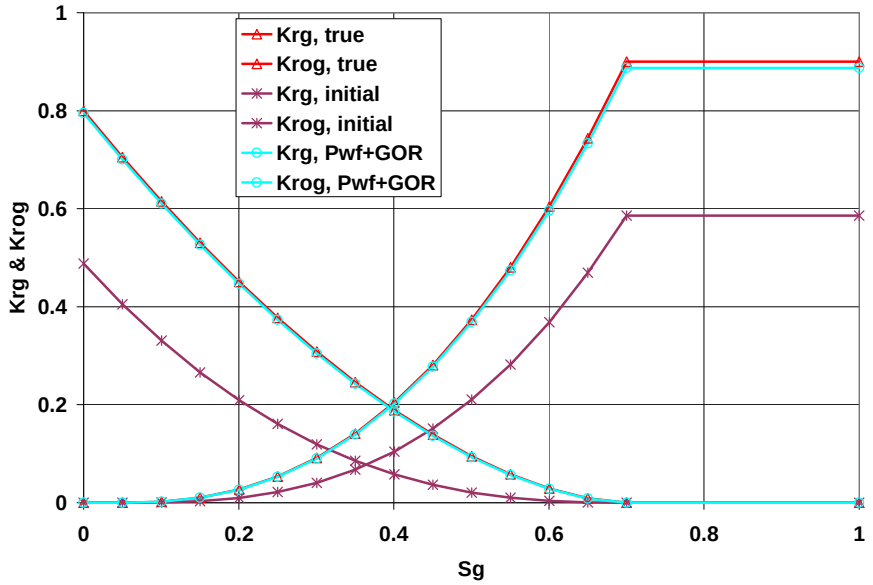

Figure 4.44: Estimated relative permeability in the gas-oil, two-phase reservoir conditioned to both p_{wf} and GOR data; estimate relative permeability only.

pressure is 4500 psi and the initial bubble point pressure is 4417. We generate 10 pressure and 10 GOR data in the production well, and 10 pressure data in the injection well by running the simulator on the true model. The data are uniformly distributed in 0 to 300 day period. There is no noise added to the observed data. The reservoir pressure declines with time. At 300 days, the bottom hole pressure at the producing well is 2665. Fig. 4.43 shows the gas saturation distribution at 30 (lower curve) and 300 (upper curve)days. Reservoir pressure drops below the bubble point pressure soon after start of the simulation run.

Fig. 4.44 shows the estimated relative permeability conditioned to both pressure and GOR data. We assume that the absolute permeability field is known and estimate relative permeability only. Here we estimate the exponential terms (n_{rg} and n_{rog}) and the end points (k_{rgcw} and k_{rocw}) in the Eqs. 4.9 and 4.11. From Fig. 4.44, we can see the estimated relative permeability curves match the true relative perme-

Table 4.2: The true and estimated parameters of relative permeability in a gas-oil two-phase reservoir.

	True	Variance	Initial Guess	Estimated Rel perm only 4 parameters	Estimated Rel+Abs Perm 4 parameters	Estimated Rel+Abs Perm 3 parameters
n_{rg}	2.4	1.0	2.795	2.396	2.396	2.395
k_{rgcw}	0.9	0.04	0.586	0.887	0.574	0.891
n_{rog}	1.7	1.0	2.514	1.711	1.712	1.712
k_{rocw}	0.8	0.04	0.488	0.795	0.515	-

ability curves very well when the model is conditioned to both pressure and GOR data. The fifth column in the table 4.2 shows the estimated values of the relative model parameters. We can see that the estimated values are very close to the true values.

In the case when absolute permeabilities are unknown, we need to estimate absolute permeability and relative permeability simultaneously. However, if all relative permeability parameters (k_{rgcw}, n_{rg}, k_{rocw}, and n_{rog}) are unknown, we only can estimate effective permeability kk_{rm} $(m = g, o)$ in the two phase flow cases. In fact, we can create two reservoir models with different values of absolute permeability, 100 and 200, but keep effective permeability kk_r constant. The pressure and GOR responses from the two different reservoirs are identical. This means that one can not resolve absolute and relative permeability simultaneously for this case. Fig. 4.45 shows the estimated relative permeability curves obtained by inversing absolute and relative permeability simultaneously. The estimated relative permeability model does not match the true model. The initial guess and prior mean on the absolute log permeability is equal to 5.00. The maximum value estimated was 5.055 at gridblock 4

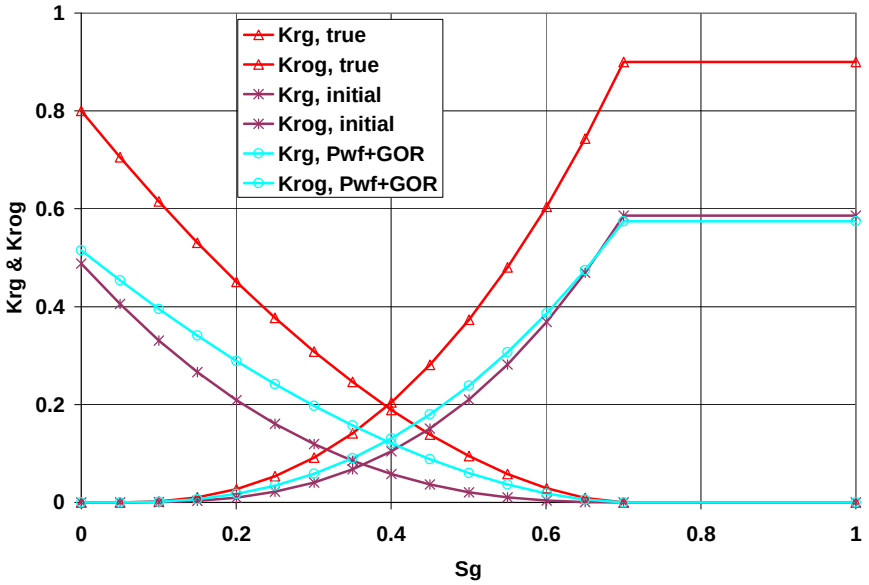

Figure 4.45: Estimated relative permeability in the gas-oil, two-phase reservoir conditioned to both p_{wf} and GOR data; estimate four relative permeability parameters (k_{rgcw}, n_{rg}, k_{rocw}, and n_{rog}) and absolute permeability at each gridblock simultaneously.

and the minimum value estimated was 5.002 at gridblock 11. The estimated absolute log permeability (5.05) at wellbore gridblock do not match the true log permeability (4.61) either, even though the predicted data match the observed data perfectly.

If the end point value k_{rocw} is known, we can separate the effect of relative and absolute permeability and estimate them simultaneously. Fig. 4.46 presents the result by estimating relative permeability (only estimate k_{rgcw}, n_{rg}, and n_{rog}) and absolute permeability simultaneously. We can see that the estimated results and the true values agree almost perfectly. At the same time, the estimated absolute permeability (4.62 at the wellbore gridblock)also matches the true absolute permeability (4.61) very well. The maximum value estimated was 4.96 at gridblock 11 and the minimum value estimated was 4.56 at gridblock 5. The estimated values of relative permeability

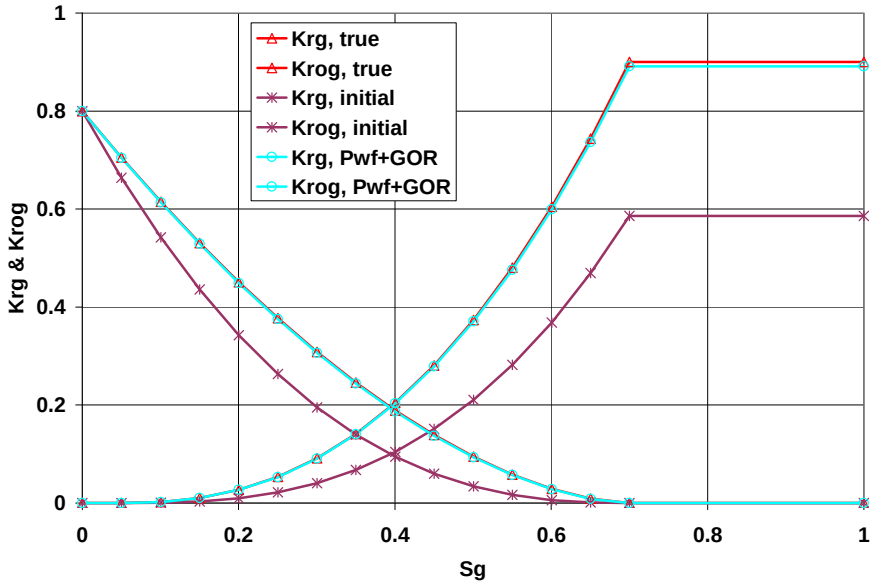

Figure 4.46: Estimated relative permeability in the gas-oil, two-phase reservoir conditioned to both p_{wf} and GOR data; estimate three relative permeability parameters (k_{rgcw}, n_{rg}, and n_{rog}) and absolute permeability at each gridblock simultaneously.

curves are shown in the table 4.2.

In the second case, we investigate a water flooding oil reservoir. The geometry in this case is the same as in the previous example. There is no free gas in the reservoir. The producing well is located at (3,1,1) with total liquid production rate 35 rb/day. The injection well is located at (8,1,1) with water injection rate equal to 34.5 stb/day. The water breaks through at about 100 days in the producing well. Fig. 4.47 shows the water saturation distribuation at 30 and 300 days.

We find that the water-oil relative permeability can be estimated very well (Fig. 4.48) if we know the absolute permeability and condition the model to both pressure and WOR data. In this case, if the model is conditioned only to pressure data, the estimated result is still very good (Fig. 4.49). However, if we only use WOR data to estimate the relative permeability curves, the estimated result is very poor

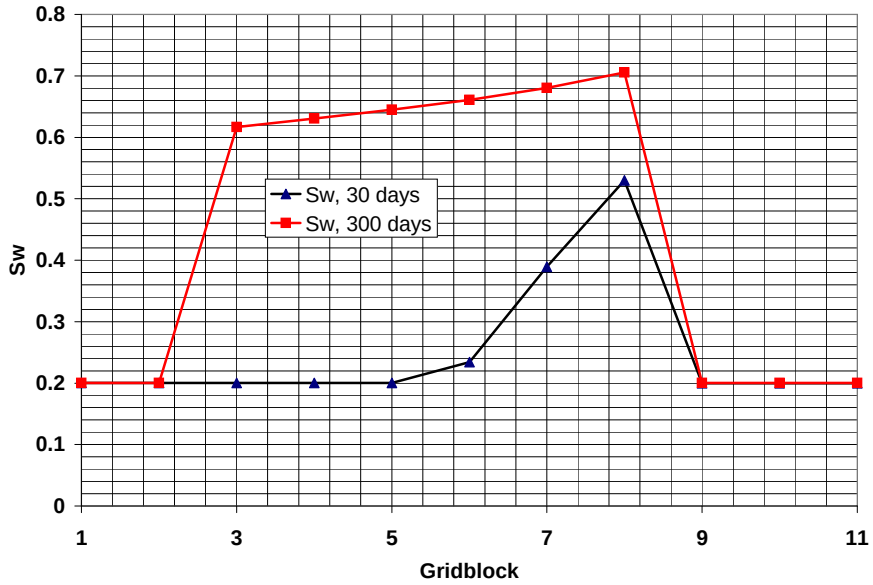

Figure 4.47: The water saturation distribution of 1D water injection reservoir.

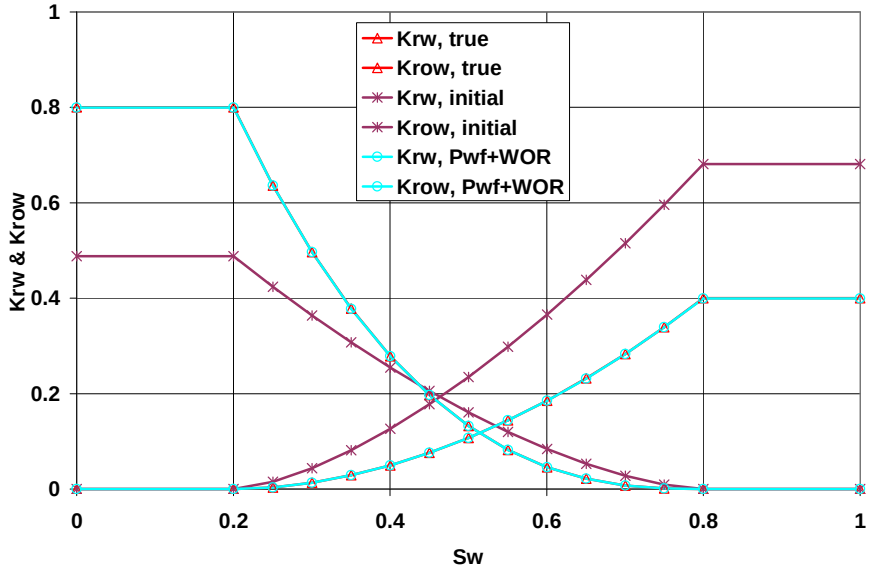

Figure 4.48: Estimated relative permeability in the water-oil, two-phase reservoir conditioned to both p_{wf} and WOR data; estimate relative permeability only.

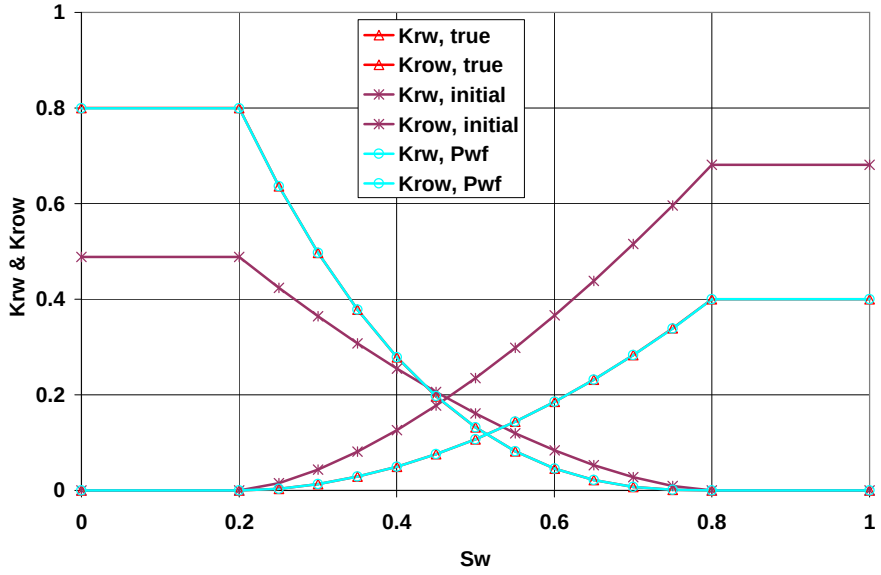

Figure 4.49: Estimated relative permeability in the water-oil, two-phase reservoir conditioned only to p_{wf} data; estimate relative permeability only.

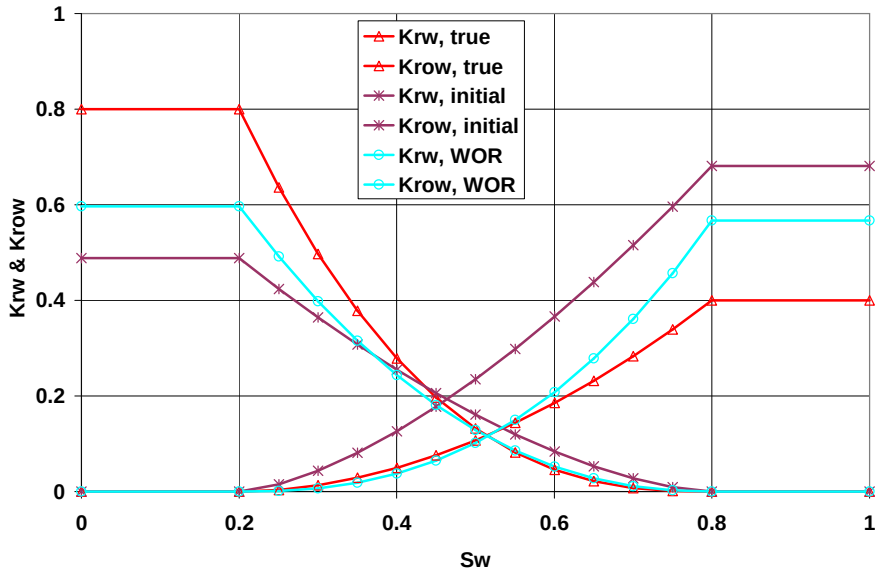

Figure 4.50: Estimated relative permeability in the water-oil, two-phase reservoir conditioned only to WOR data; estimate relative permeability only.

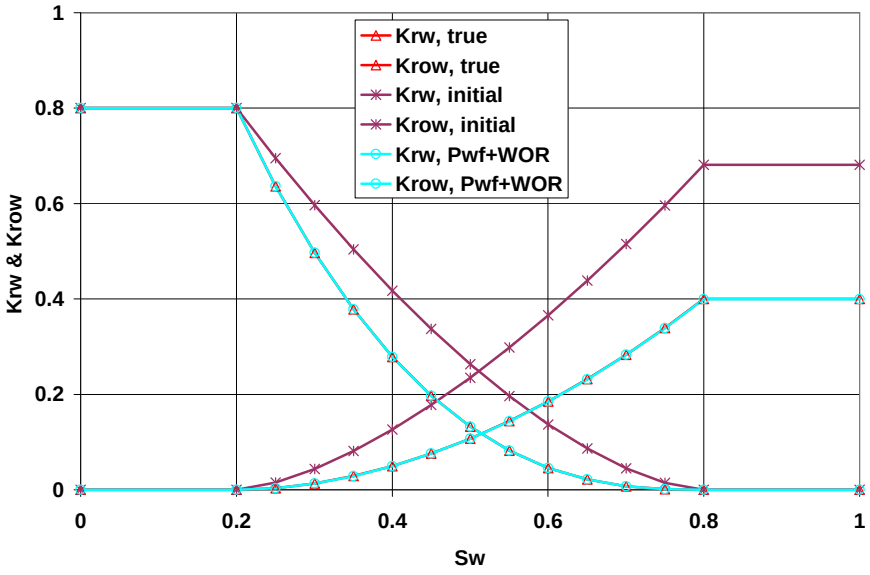

Figure 4.51: Estimated relative permeability in the water-oil, two-phase reservoir conditioned to both p_{wf} and WOR data; estimate three relative permeability parameters (k_{rwcw}, n_{rw}, and n_{row}) and absolute permeability at each gridblock simultaneously.

Table 4.3: The true and estimated parameters of relative permeability in a water-oil two-phase reservoir.

	True	Variance	Initial Guess	Estimated Rel perm only 4 parameters	Estimated Rel+Abs Perm 4 parameters	Estimated Rel+Abs Perm 3 parameters
n_{rw}	1.9	1.0	1.536	1.900	1.901	1.901
k_{rwcw}	0.4	0.04	0.681	0.400	0.364	0.400
n_{row}	2.6	1.0	1.602	2.598	2.600	2.600
k_{rocw}	0.8	0.04	0.488	0.799	0.731	-

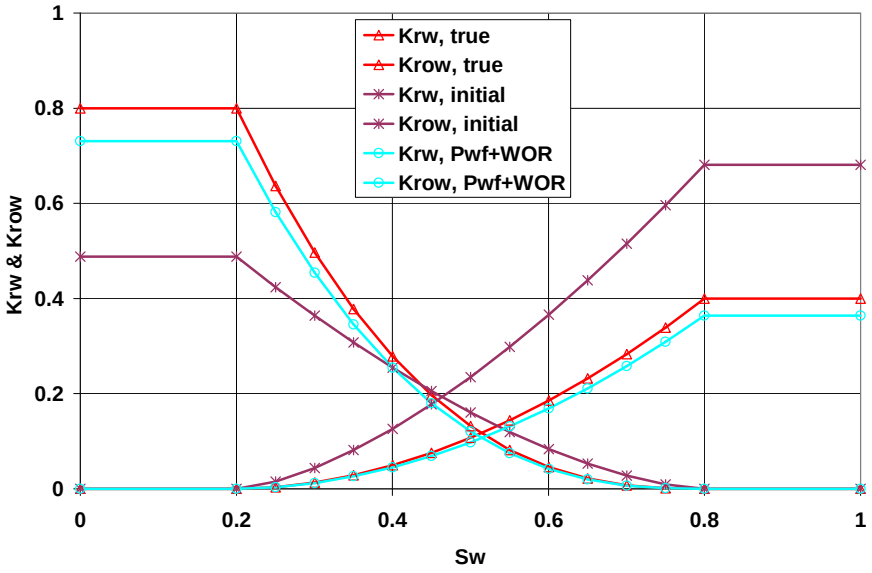

Figure 4.52: Estimated relative permeability in the water-oil, two-phase reservoir conditioned to both p_{wf} and WOR data; estimate four relative permeability parameters (k_{rwcw}, n_{rw}, k_{rocw}, and n_{row}) and absolute permeability at each gridblock simultaneously.

(Fig. 4.50). This is consistent with Watson et al. (1984).

Just like gas-oil two phase case, if one wants to estimate relative and absolute permeability simultaneously, one needs to know the end point k_{rocw}. Fig. 4.51 show the relative permeability estimates when k_{rocw} is fixed with the value of 0.8. In this case, we also estimated gridblock absolute log-permeabilities giving a initial guess of 5.00 which is equal to the prior mean. The estimated absolute permeability at the wellbore gridblock is 4.61, the same as the true value. The maximum value estimated was 4.91 at gridblock 11 and the minimum value estimated was 4.59 at gridblock 7. Otherwise, when k_{rocw} is not known, the estimated relative permeability may not match the true model (Fig. 4.52). Here, the estimated absolute log permeability at producing well gridblock is 4.71. It does not match the true value either. The maximum value estimated was 4.93 at gridblock 11 and the minimum value estimated

was 4.68 at gridblock 7. The true and estimated parameters of relative permeabilities are presented in the Table 4.3.

4.3.3 Three Phase Reservoirs

The grid used of the three phase reservoir example is 15 by 15 by 1. The gridblock sizes in x, y, and z-direction are 40 ft, 40 ft, and 30 ft, respectively. The true log-permeability field is a three zone reservoir as shown in the Fig. 4.53(a). The log-permeability is 3.7 at the lower left corner, 4.3 at the lower right corner and 3.9 at the upper part. There is one water injection well located at the center of the reservoir (gridblock(8,8,1), well 5). The water injection rate is 550 stb/day. There are four producing wells, well 1 to well 4, located at (3,3,1), (13,3,1), (13,13,1), and (3,13,1). All four wells are produced at a constant total rates of 220 rb/day. The well locations are shown in Fig. 4.53(a). The initial reservoir pressure is 4500 psi. The bubble point pressure is 4417 psi. We ran the simulation on the true model to generate the observed data. The simulation is run from 0 to 300 days. The reservoir pressure declines with time. The earliest water breakthrough happened at about 150 days in well 2 where the permeability is the highest. The last water breakthrough is at about 200 days in well 1 where the permeability is the lowest. Fig. 4.54 shows the water and gas saturation at 300 days. At 300 days, the water saturation has increased in most parts of reservoir. The producing water oil ratio at well 2 is as high as 7. There is no noise added to the observed data.

Sensitivity of Production Data to the Parameters of Relative Permeability Curves

In this work, we use the adjoint method to compute the sensitivity of the production data to absolute permeability. The sensitivity of the production data to the parameters defining relative permeability curves is also generated by the adjoint method. Fig. 4.55, 4.56, and 4.57 show the sensitivity of p_{wf}, GOR, and WOR data, respectively, at well 1 to the seven parameters of relative permeability curves at each data point. The sensitivity coefficients shown in the figures have been compared against the sensitivities generated by the finite different method. The agreement

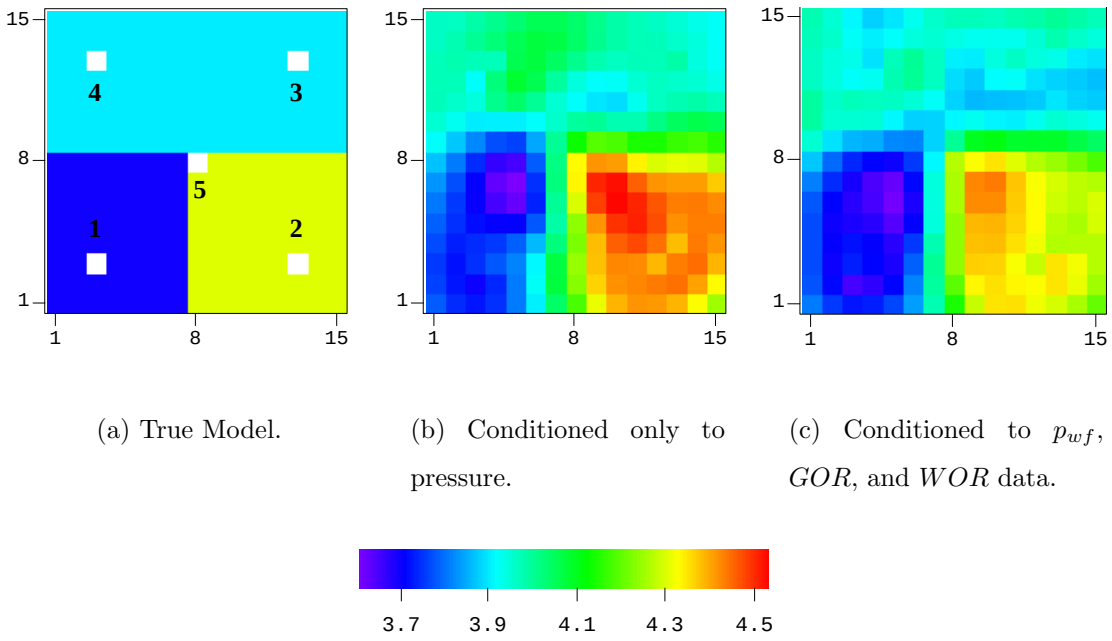

(a) True Model.

(b) Conditioned only to pressure.

(c) Conditioned to p_{wf}, GOR, and WOR data.

Figure 4.53: True and MAP estimate of absolute log-permeability field; estimate absolute and relative permeability simultaneously.

between two sets of sensitivity coefficients is excellent.

At well 1, the water breaks through at about 200 days. The sensitivity coefficients have a dramatic change around the breakthrough time, so we discuss the behavior of the sensitivity in the period before and after breakthrough. Before the breakthrough (200 days), increasing k_{rwcw} will increase the water mobility and thus increase the total mobility. We know that increasing total mobility would decrease the pressure drop across the reservoir, so the pressure is higher. This is why $\partial p_{wf}/\partial k_{rwcw}$ is positive (Fig. 4.55). On the other hand, an increase in n_{rw} will decrease the water mobility at low saturation, so $\partial p_{wf}/\partial n_{rw}$ is negative. For the gas phase, an increase in k_{rgcw} will increase the gas mobility and more gas will be produced, so $\partial GOR/\partial k_{rgcw}$ is positive. More highly expandable free gas around the wellbore also provides more pressure support and thus $\partial p_{wf}/\partial k_{rgcw}$ is positive. However, if n_{rg} increases, the gas mobility will decrease and the result is low gas production rate

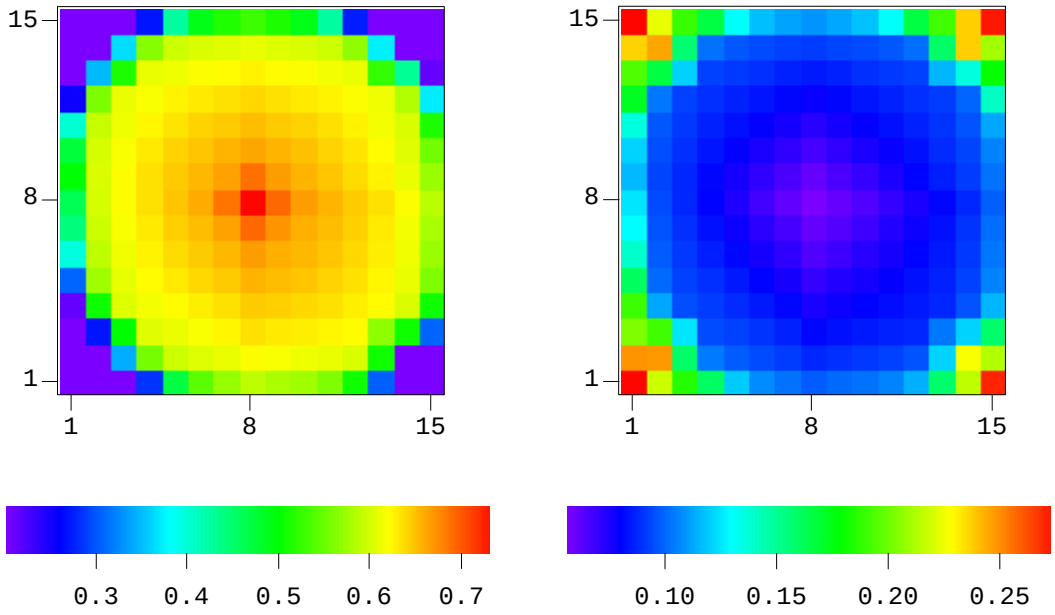

(a) Water saturation .

(b) Gas saturation.

Figure 4.54: Water and gas saturation at 300 days.

(so $\partial GOR/\partial n_{rg}$ is negative) and less pressure support ($\partial p_{wf}/\partial n_{rg}$ is negative). For the oil phase, an increase in k_{rocw} will increase the oil mobility and provides more pressure support, thus $\partial p_{wf}/\partial k_{rocw}$ is positive. When the oil mobility increases, more oil will be produced. So the gas-oil ratio is lower. This explains why $\partial GOR/\partial k_{rocw}$ is negative. The effect of the exponential terms n_{rog} and n_{row} is quite similar. They have opposite effect on p_{wf} and GOR. Increasing n_{rog} or n_{row} will reduce the oil mobility and decrease the oil rate. Thus $\partial p_{wf}/\partial n_{row}$ and $\partial p_{wf}/\partial n_{rog}$ are negative and $\partial GOR/\partial n_{row}$ and $\partial GOR/\partial n_{rog}$ are positive.

After 200 days, water appears in well 1. Water-oil ratio begins to become sensitive to the model parameters. The explanation of sensitivity of WOR to parameters of relative permeability curves (Fig. 4.57) is quite straight forward. An increase in k_{rwcw} will increase the water mobility and result in greater water production. The

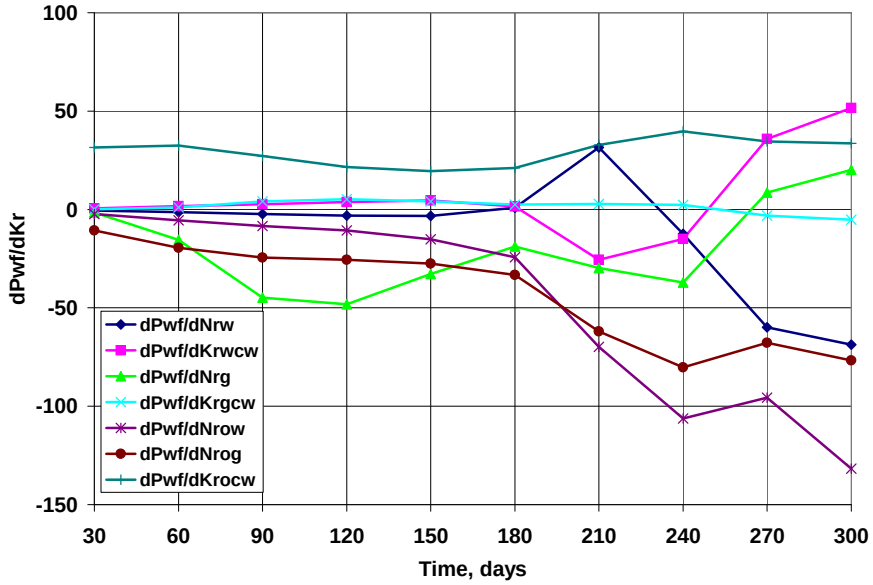

Figure 4.55: Dimensionless sensitivity of bottom hole pressure data at well 1 to the parameters of relative permeability curves.

water-oil ratio will be higher, so $\partial WOR/\partial k_{rwcw}$ is positive. Similarly, $\partial WOR/\partial n_{rw}$ is negative. If k_{rocw} or k_{rgcw} increases, the oil or gas rate will be high. Thus less water will be produced in this total rate constraint well. Thus $\partial WOR/\partial k_{rocw}$ and $\partial WOR/\partial k_{rgcw}$ are negative. For similar reason, $\partial WOR/\partial n_{row}$, $\partial WOR/\partial n_{rog}$ and $\partial WOR/\partial n_{rg}$ are positive. After breakthrough, the sensitivities of p_{wf} and GOR become more complex. Some of them still can be explained by the arguments used for the period before breakthrough. Others are more difficult to explain.

MAP Estimate of Relative and Absolute Permeability

First, we assume that the absolute permeability field is known and only estimate the relative permeability. All 7 relative permeability parameters (n_{rw}, k_{rwcw}, n_{rg}, k_{rgcw}, n_{row},, k_{rocw}, n_{rog}) are assumed unknown. The second and fourth columns of table 4.4 show the true values and initial guess, respectively, of the parameters of

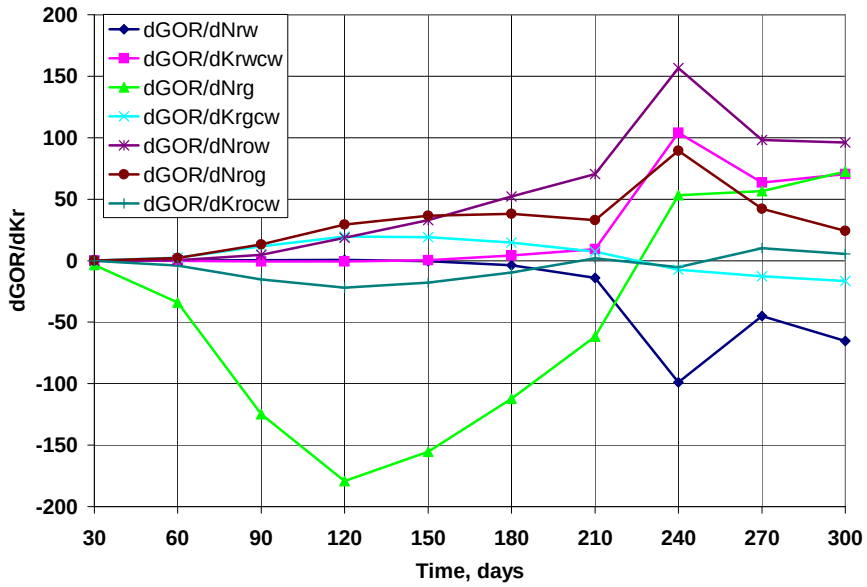

Figure 4.56: Dimensionless sensitivity of gas-oil ratio data at well 1 to the parameters of relative permeability curves.

Table 4.4: The true and estimated parameters of relative permeability in a three-phase three-zone reservoir; estimate relative permeability only.

	True	Variance	Initial Guess	Estimated p_{wf}	Estimated GOR	Estimated WOR	Estimated p_{wf}+GOR+WOR
n_{rw}	1.9	1.0	2.174	1.909	1.907	1.954	1.900
k_{rwcw}	0.4	0.04	0.580	0.401	0.392	0.342	0.400
n_{rg}	2.4	1.0	2.135	2.380	2.395	2.327	2.399
k_{rgcw}	0.9	0.04	0.492	0.862	0.870	0.544	0.899
n_{row}	2.6	1.0	2.050	2.606	2.609	2.658	2.600
n_{rog}	1.7	1.0	1.744	1.691	1.726	1.749	1.700
k_{rocw}	0.8	0.04	0.492	0.799	0.786	0.679	0.800

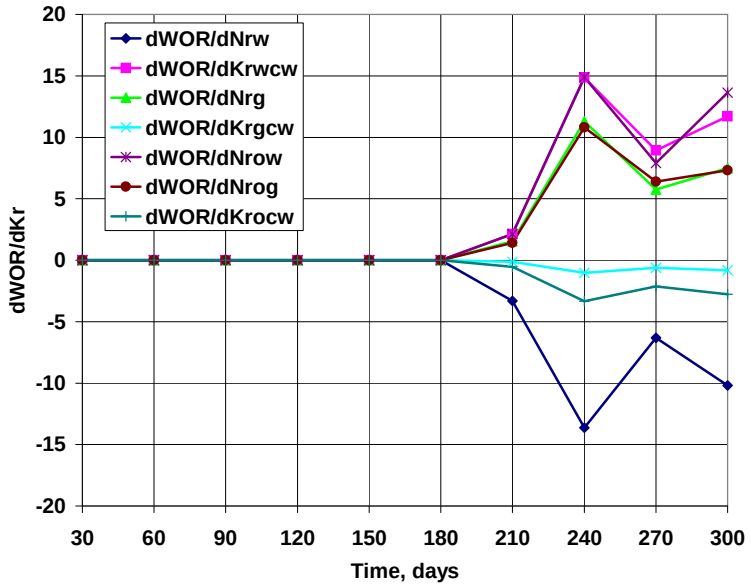

Figure 4.57: Dimensionless sensitivity of water-oil ratio data at well 1 to the parameters of relative permeability curves.

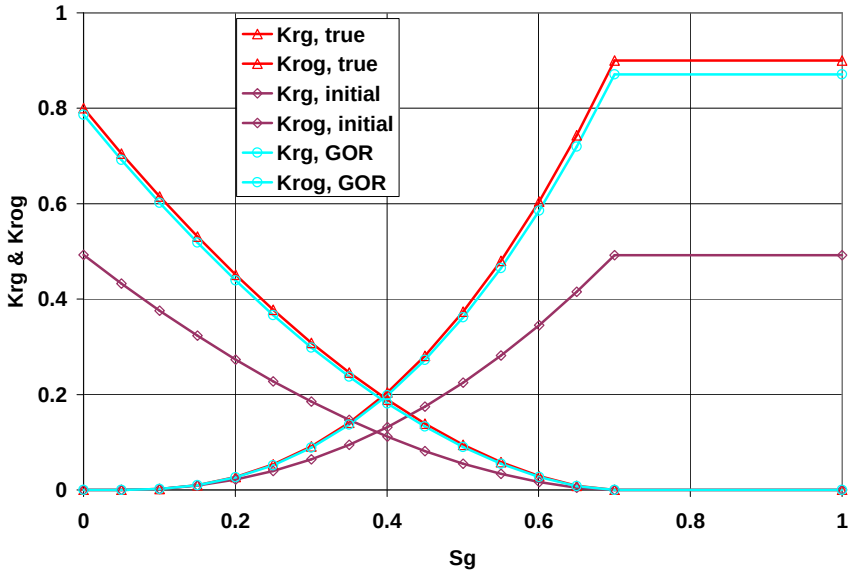

Figure 4.58: Estimated relative permeability of the gas-oil system in a three-phase reservoir conditioned only to GOR data; estimate relative permeability only.

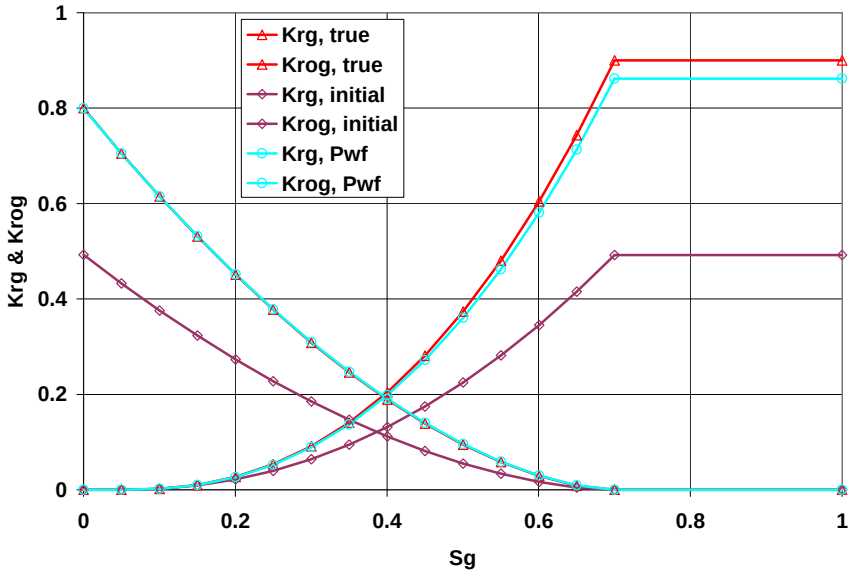

Figure 4.59: Estimated relative permeability of the gas-oil system in a three-phase reservoir conditioned only to p_{wf} data; estimate relative permeability only.

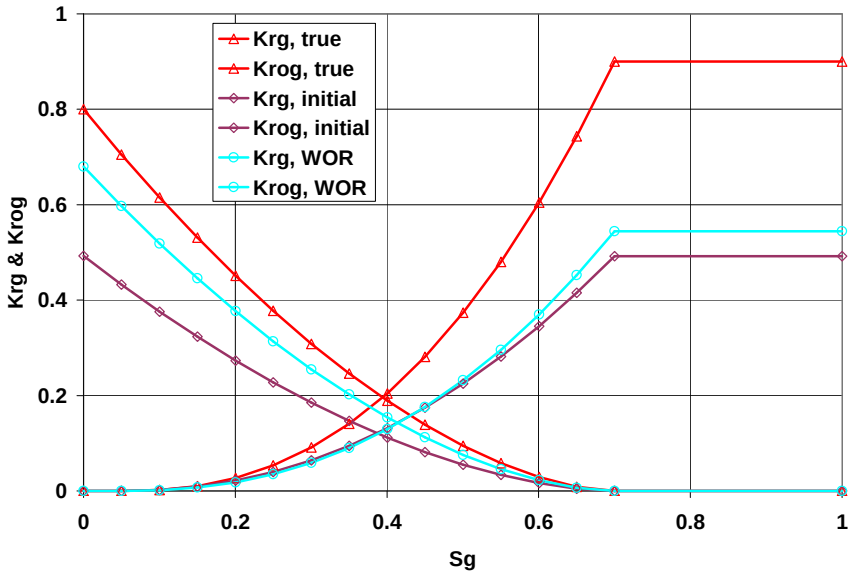

Figure 4.60: Estimated relative permeability of the gas-oil system in a three-phase reservoir conditioned only to WOR data; estimate relative permeability only.

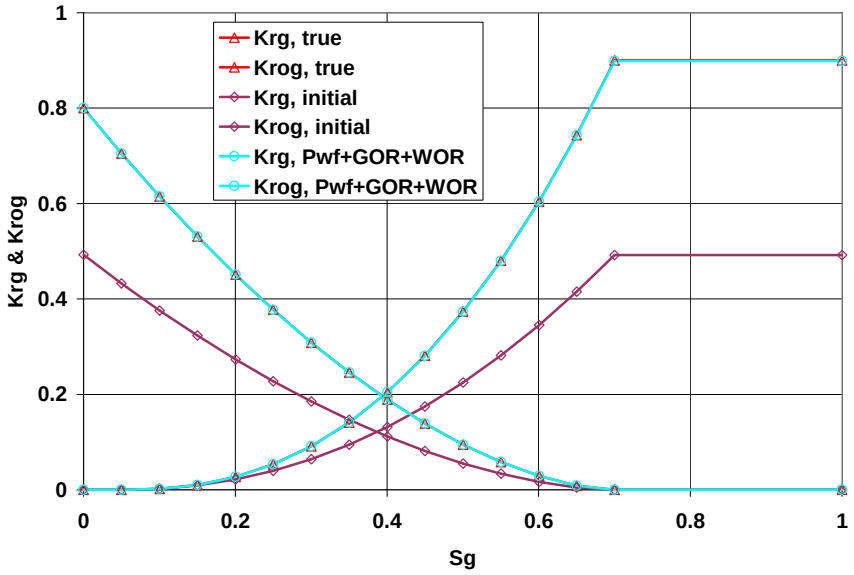

Figure 4.61: Estimated relative permeability of the gas-oil system in a three-phase reservoir conditioned to p_{wf}, GOR, and WOR data; estimate relative permeability only.

relative permeability. Figs. 4.58, 4.59, 4.60, and 4.61 show the MAP estimates of the two-phase gas-oil relative permeabilities by conditioning only to GOR, only to pressure, only to WOR, and that to all pressure, GOR and WOR data, respectively. The pressure data from the injection well are also include in the pressure data set. We can see, in this case, when conditioning only to pressure (Fig. 4.58) or only to GOR (Fig. 4.59), the estimated curves match the true curves well, but not perfectly. When conditioning only to WOR data (Fig. 4.60), the estimated curves math the true case very poorly . When conditioning to all three types of data (Fig. 4.61), the estimated model matches the true model nearly perfectly.

If the relative permeability model is only conditioned to WOR data, the MAP estimated model does not match the true model (Fig. 4.62) for the two-phase water-oil relative permeability curves. However, when conditioning only to pressure data (Fig. 4.63) or only to GOR data (Fig. 4.64), the MAP estimate matches the true

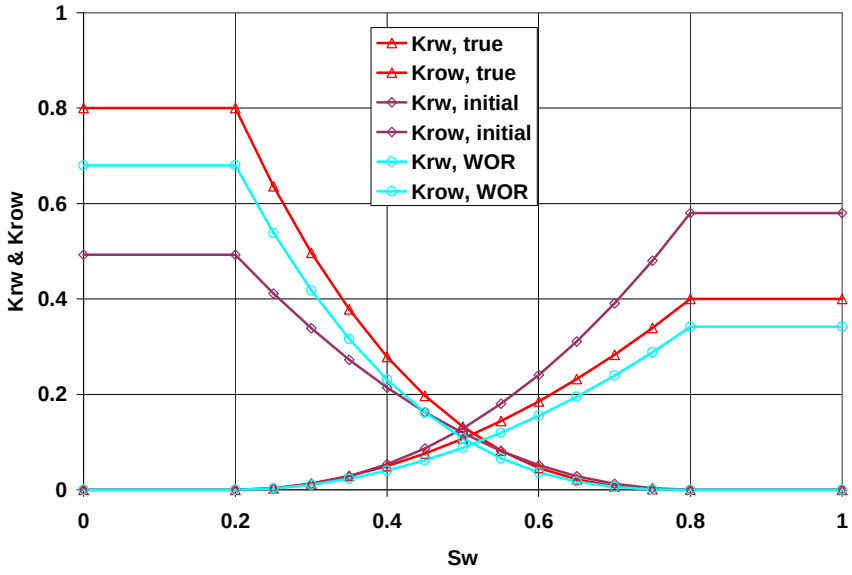

Figure 4.62: Estimated relative permeability of the water-oil system in a three-phase reservoir conditioned only to WOR data; estimate relative permeability only.

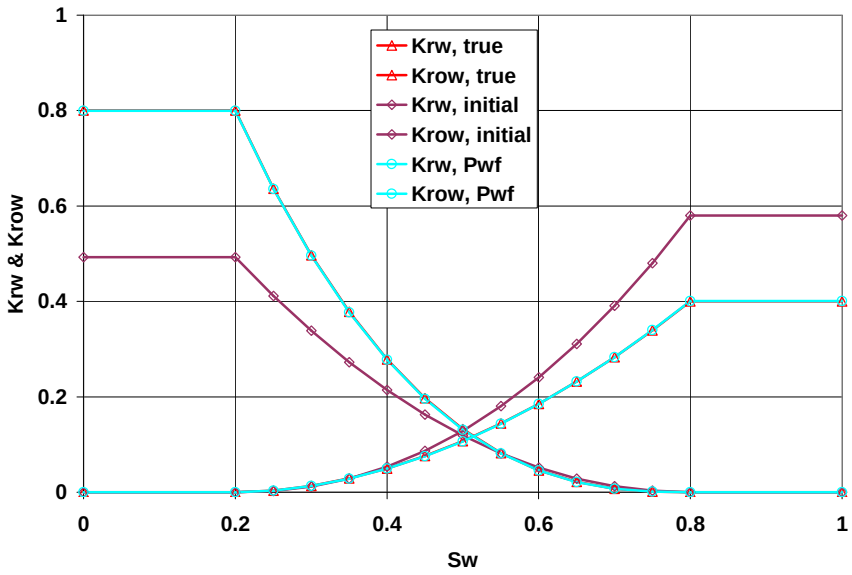

Figure 4.63: Estimated relative permeability of the water-oil system in a three-phase reservoir conditioned only to p_{wf} data; estimate relative permeability only.

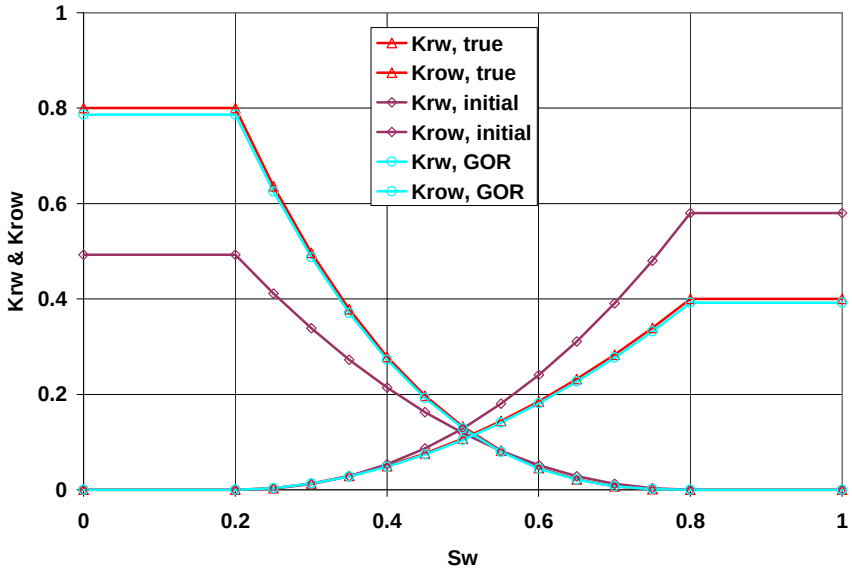

Figure 4.64: Estimated relative permeability of the water-oil system in a three-phase reservoir conditioned only to GOR data; estimate relative permeability only.

model well. Conditioning to all three types of data (Fig. 4.65) always yield the best result. Table. 4.4 gives the values of the estimated parameters of relative permeability curves. Conditioning to all three types of data yields the best results. It seems that conditioning to only WOR data always generate the worst results.

In a two-phase reservoir, an increase in absolute permeability by a factor of α os exact;u equivalent to an increase in k_{rocw} and k_{rwcw} by factors of α. Here, for two-phase reservoirs, production data can be matched by modifying either the relative permeability endpoints or the absolute permeability. When Stone 2 model for three-phase relative permeability is used to compute relative permeability, however, the effect of increasing k is not the same as increasing k_{rocw}, k_{rwcw}, and k_{rgcw}. In fact, the product of the three end points occurs in Stone's model. Because the effects are not equivalent, it is possible to estimate them separately. In another word, it is possible to estimate all 7 relative permeability parameters (n_{rw}, k_{rwcw}, n_{rg}, k_{rgcw}, $n_{row,}$, k_{rocw}, n_{rog}) and absolute permeability simultaneously in the three phase problems.

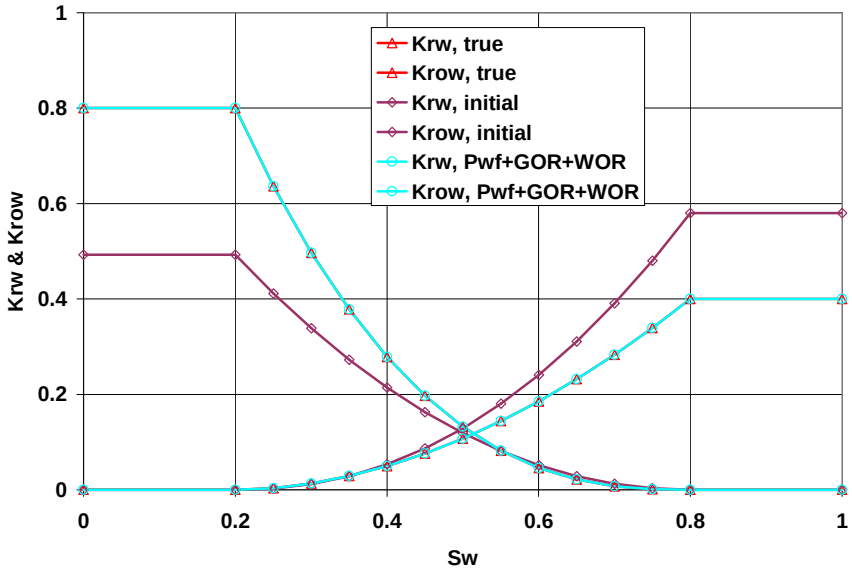

Figure 4.65: Estimated relative permeability of the water-oil system in a three-phase reservoir conditioned to p_{wf}, GOR, and WOR data; estimate relative permeability only.

Figs. 4.53(c), 4.66 and 4.67 show the MAP estimate of absolute and relative permeability obtained when estimating relative and absolute permeability simultaneously, by conditioning to all three types of data. The MAP estimate of absolute log-permeability (Fig. 4.53(c)) is quite similar to the true model. The estimated relative permeabilities in both gas-oil system (Fig. 4.66) and water-oil system (Fig. 4.67) are very close to the true model. If the model is only conditioned to pressure data (Figs. 4.53(b), 4.68 and 4.69), the estimated relative permeabilities do not match the true model (Fig. 4.68 and 4.69)). The estimated absolute log-permeability field is too high (Figs. 4.53) and the estimated relative permeability (Fig. 4.68 and 4.69)) is too low. Table 4.5 gives the true, initial and estimated values of parameters for relative permeability curves when the absolute and relative permeability are estimated simultaneously. The predicted bottom hole pressure, gas-oil ratio, and water-oil ratio computing from the MAP estimated model match the observed data very well

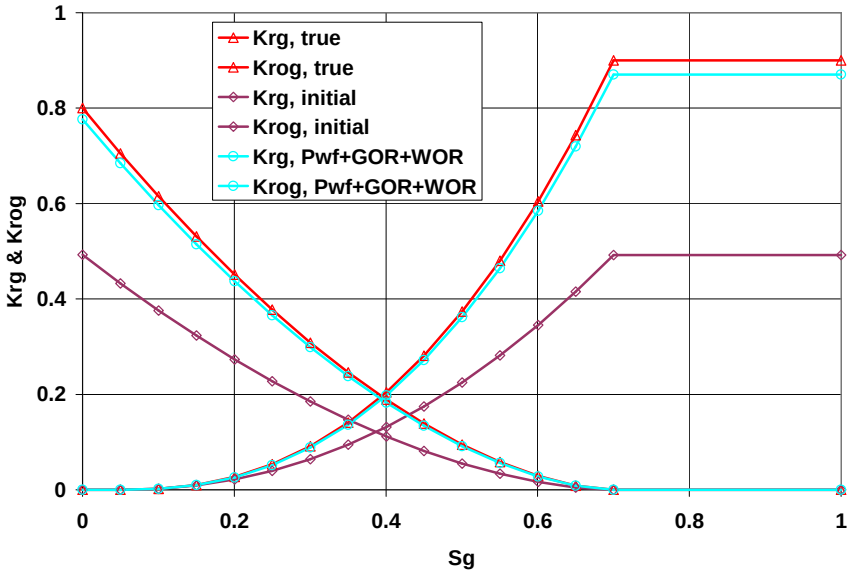

Figure 4.66: Estimated relative permeability of the gas-oil system in a three-phase reservoir conditioned to p_{wf}, GOR, and WOR data; estimate relative permeability and absolute permeability simultaneously.

(Fig. 4.70, 4.71, and 4.72). Fig. 4.73 shows the rate of the convergence of the objective functions in the 3-zone reservoir. They converge pretty fast.

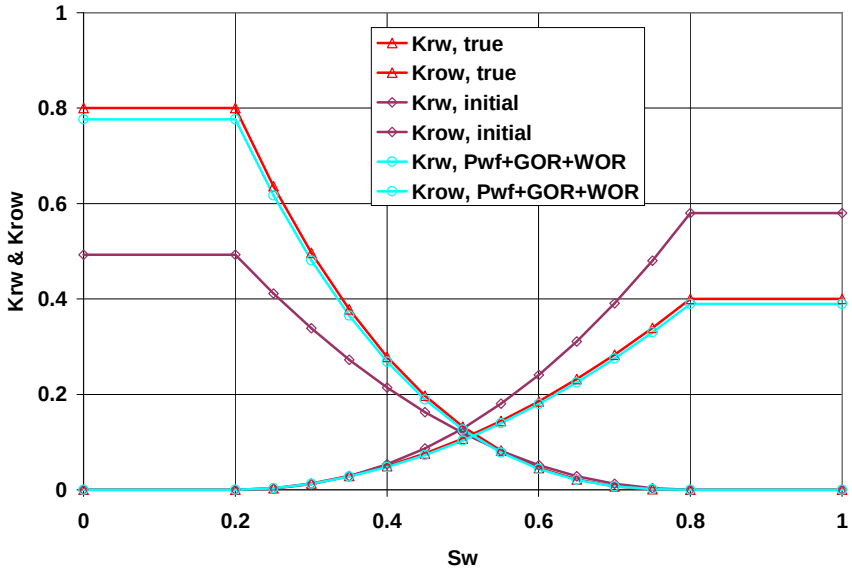

Figure 4.67: Estimated relative permeability of the water-oil system in a three phase reservoir conditioned to p_{wf}, GOR, and WOR data; estimate relative permeability and absolute permeability simultaneously.

4.3.4 Heterogeneous Reservoirs

Here, we show a conditional realization example. It is a 15 by 15 by 1 reservoir. The well location and rate constraints are the same as in the three-phase reservoir example just considered. The absolute log-permeability field of the true model is shown in Fig. 4.74(a). The mean of the realizations is 4.0. The variance of absolute log permeability field is 0.5. A spherical variogram model is used for generating the covariance matrix. The correlation range is 6 gridblock, 240 feet. Random noise has been added to the observed data based on the variance of the data. We condition the unconditional realization of absolute log permeability model (Fig. 4.74(b)) and relative permeability models to the pressure, GOR, and WOR data. The results are shown in Figs. 4.74, 4.75 and 4.76. In Fig. 4.74, the unconditional realization is quite far from the true model. However, the conditional realization is

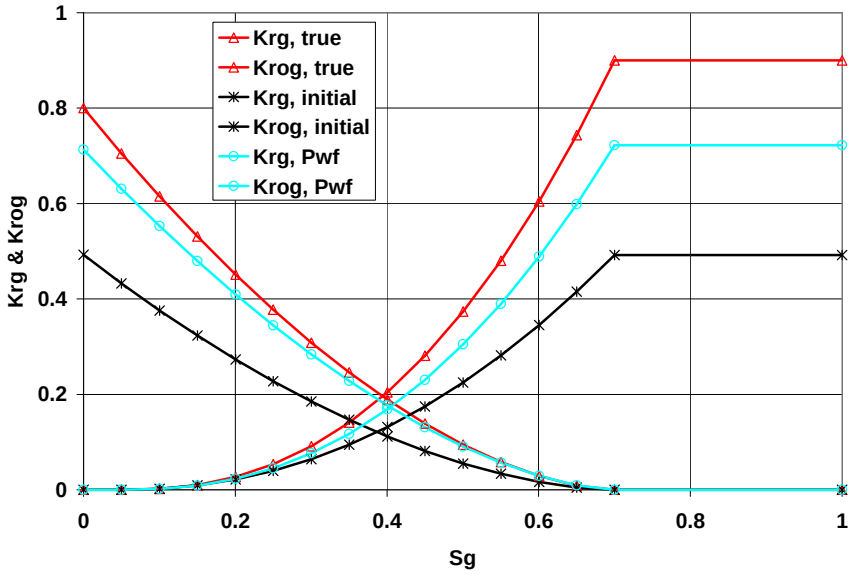

Figure 4.68: Estimated relative permeability of the gas-oil system in a three-phase reservoir conditioned only to p_{wf} data; estimate relative permeability and absolute permeability simultaneously.

very similar to the true model. The estimated relative permeability field also matches the true relative permeability model quite well. Table 4.6 shows the true, initial guess, and estimated values of the parameters for relative permeability curves.

Fig. 4.77 to 4.79 show the mismatch between the observed data and initial predicted data computed from the simulation run on the initial guess model. We see that the mismatches of all types of observed data to the predicted data generated from the unconditional realization model are very large before conditioning to the production data. After conditioning to the production data, the predicted data computing from the conditional realization model matches the observed data very well (Fig. 4.80 to 4.82).

Fig. 4.83 shows the convergence behavior of the Levenberg-Marquardt algorithm in the three-phase heterogenous reservoir. In the heterogenous cases, the objective functions normally converge relatively slowly and converge to a relative

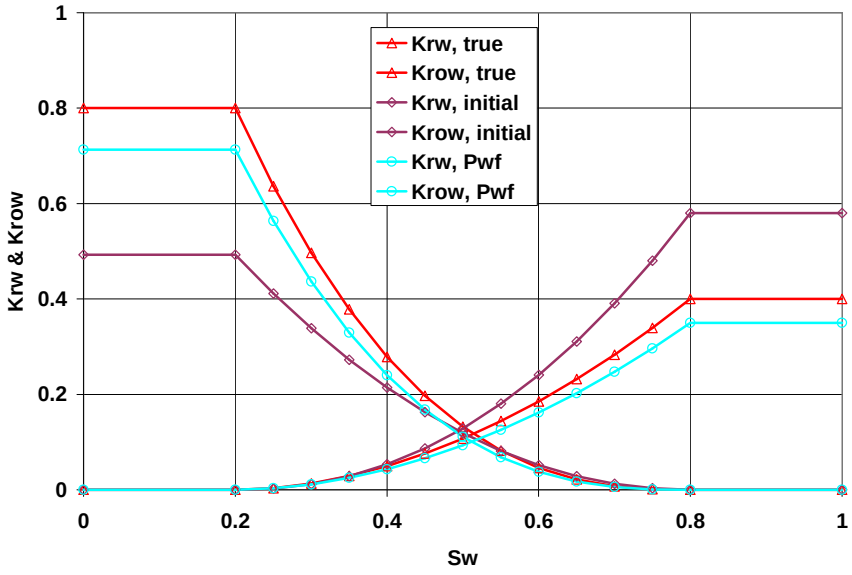

Figure 4.69: Estimated relative permeability of the water-oil system in a three-phase reservoir conditioned only to p_{wf} data; estimate relative permeability and absolute permeability simultaneously.

bigger final values of the objective functions.

Table 4.5: The true and estimated parameters of relative permeability in a three-phase three-zone reservoir; estimate relative permeability and absolute permeability simultaneously.

	True	Variance	Initial Guess	Estimated p_{wf}	Estimated p_{wf}+GOR+WOR
n_{rw}	1.9	1.0	2.174	1.908	1.912
k_{rwcw}	0.4	0.04	0.580	0.350	0.389
n_{rg}	2.4	1.0	2.135	2.355	2.399
k_{rgcw}	0.9	0.04	0.492	0.722	0.871
n_{row}	2.6	1.0	2.050	2.678	2.618
n_{rog}	1.7	1.0	1.744	1.642	1.704
k_{rocw}	0.8	0.04	0.492	0.713	0.776

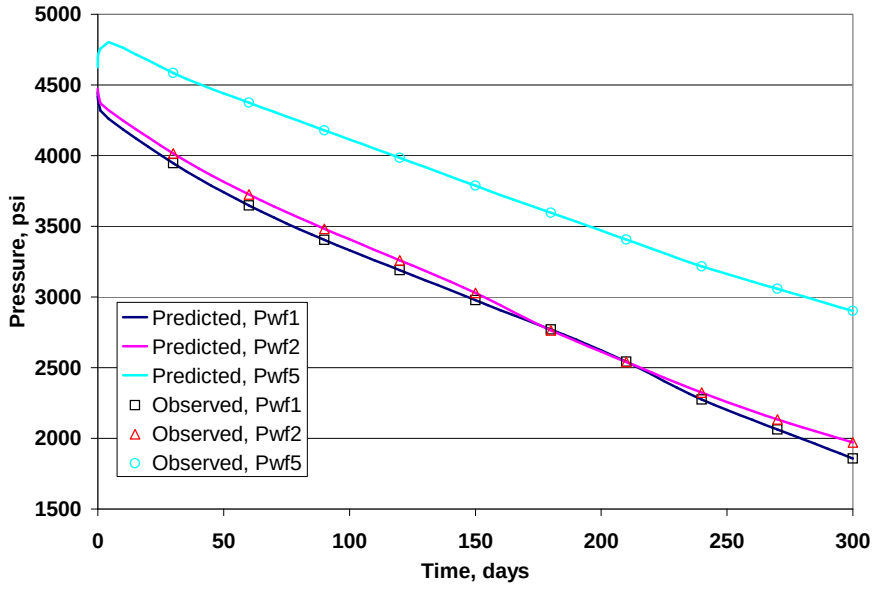

Figure 4.70: Bottom hole pressure match after conditioning to p_{wf}, GOR, and WOR in a three-phase reservoir; estimate relative permeability and absolute permeability simultaneously.

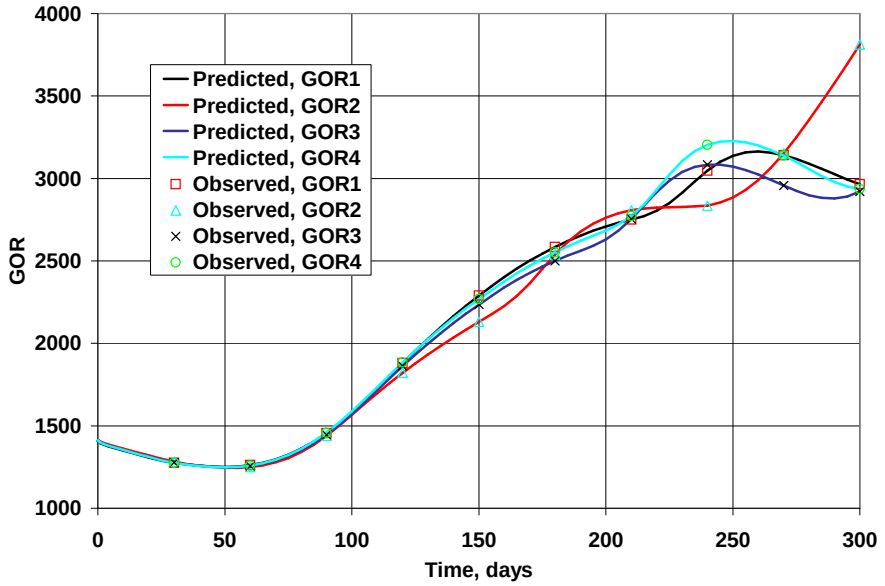

Figure 4.71: Gas-oil ratio match after conditioning to p_{wf}, GOR, and WOR in a three-phase reservoir; estimate relative permeability and absolute permeability simultaneously.

Table 4.6: The true and estimated parameters of relative permeability in a three-phase heterogeneous reservoir; estimate relative permeability and absolute permeability simultaneously.

	True	Variance	Initial Guess	Estimated Perm p_{wf}+GOR+WOR
n_{rw}	1.9	1.0	2.174	1.839
k_{rwcw}	0.4	0.04	0.580	0.404
n_{rg}	2.4	1.0	2.135	2.404
k_{rgcw}	0.9	0.04	0.492	0.963
n_{row}	2.6	1.0	2.050	2.593
n_{rog}	1.7	1.0	1.744	1.690
k_{rocw}	0.8	0.04	0.492	0.843

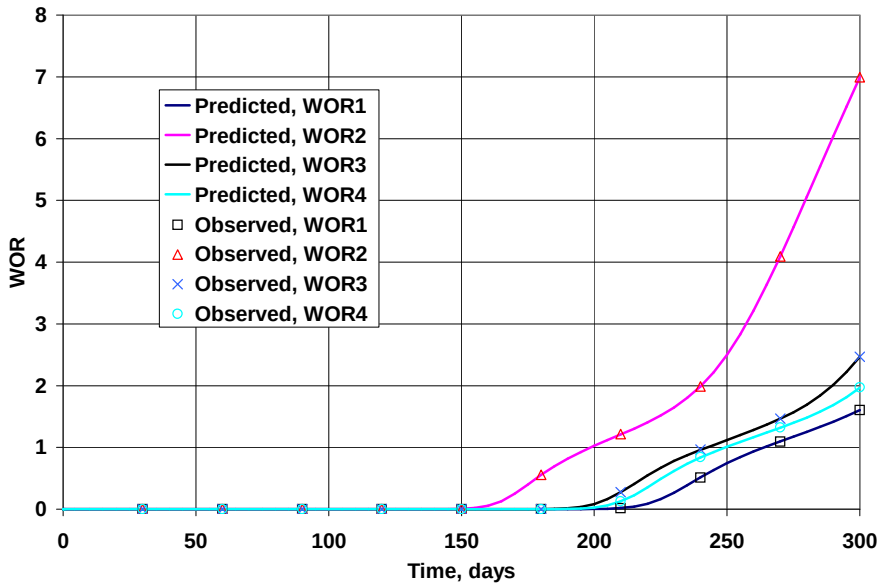

Figure 4.72: Water-oil ratio match after conditioning to p_{wf}, GOR, and WOR in a three-phase reservoir; estimate relative permeability and absolute permeability simultaneously.

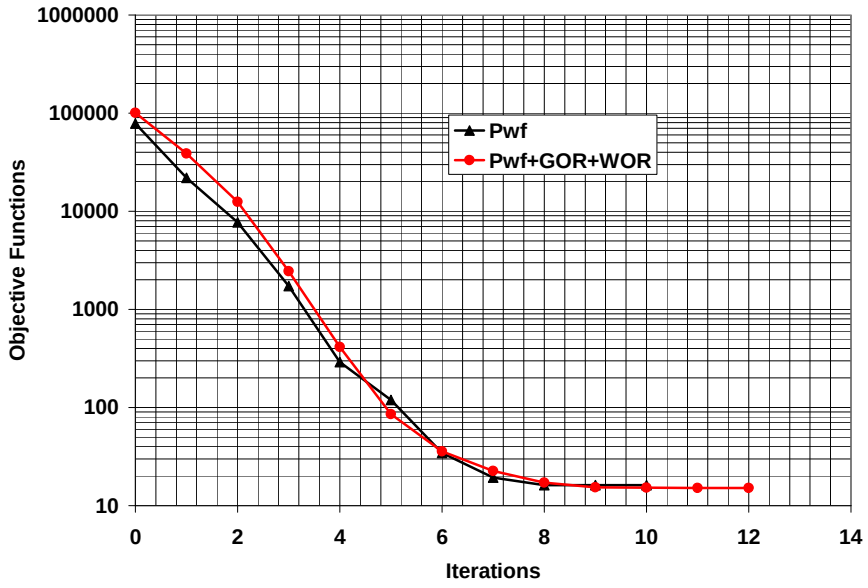

Figure 4.73: The rate of convergence of the objective functions in a three-phase reservoir.

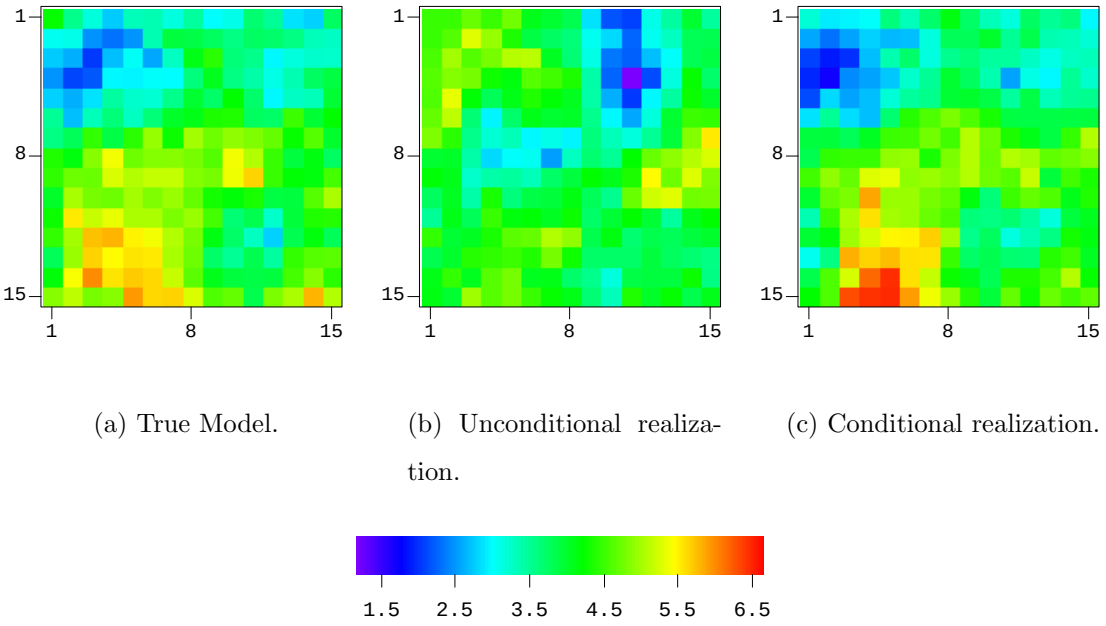

(a) True Model. (b) Unconditional realization. (c) Conditional realization.

Figure 4.74: The conditional realization of horizontal log-permeability conditioned to p_{wf}, GOR, and WOR data, layer 1.

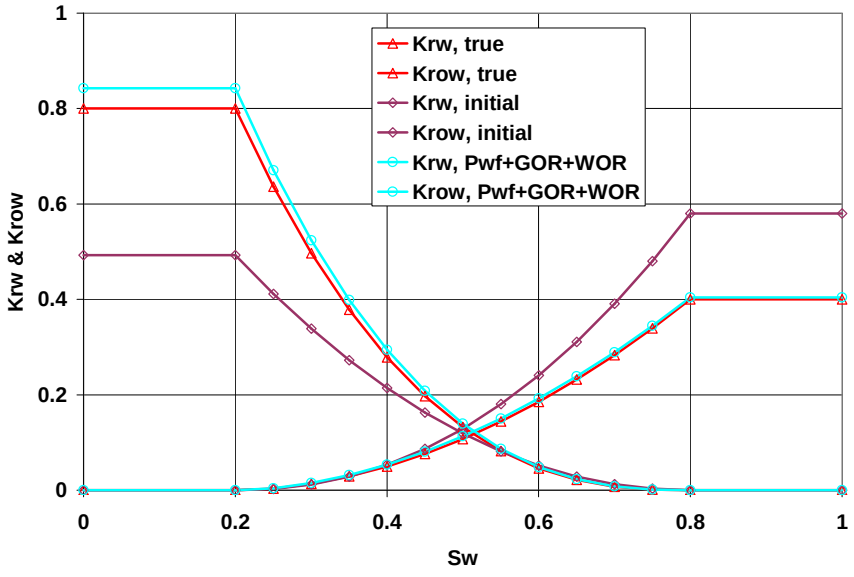

Figure 4.75: Estimated relative permeability of the water-oil system in a heterogenous reservoir conditioned to p_{wf}, GOR, and WOR data; estimate relative permeability and absolute permeability simultaneously.

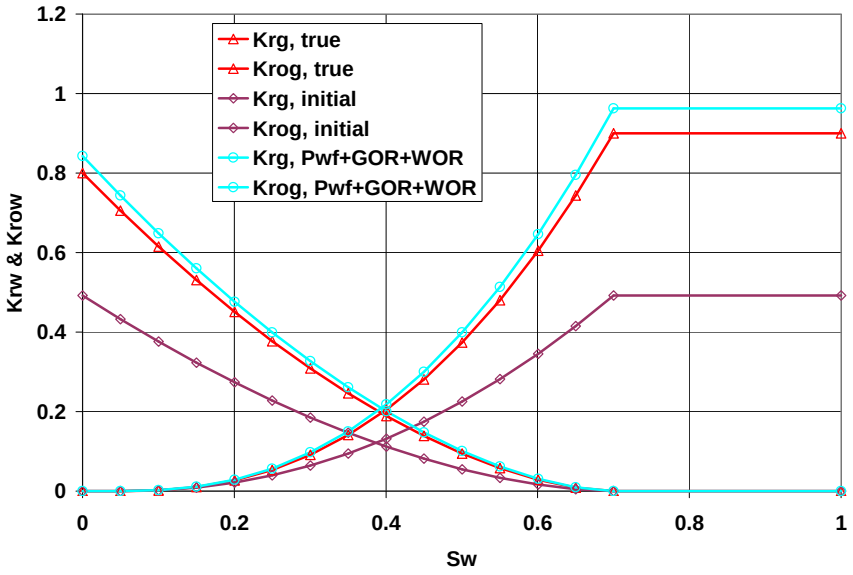

Figure 4.76: Estimated relative permeability of the gas-oil system in a heterogenous reservoir conditioned to p_{wf}, GOR, and WOR data; estimate relative permeability and absolute permeability simultaneously.

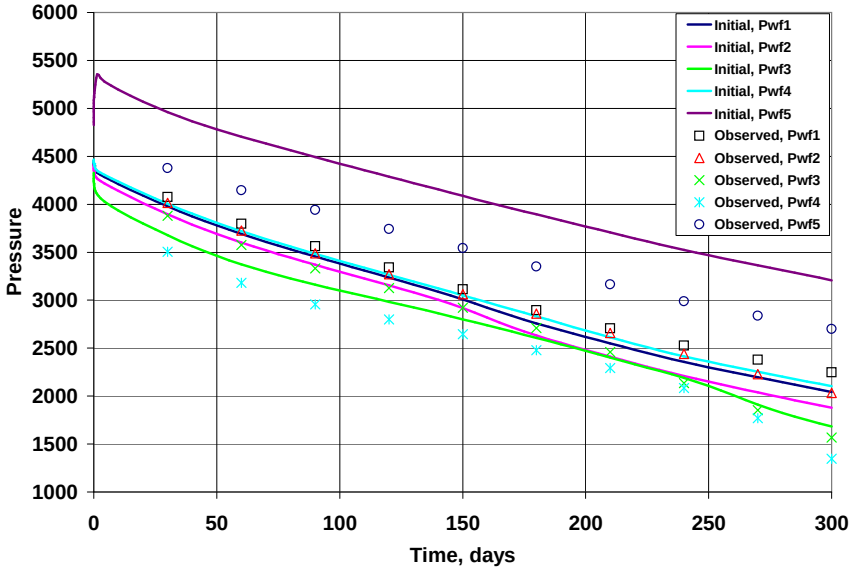

Figure 4.77: Bottom hole pressure match before conditioning to p_{wf}, GOR, and WOR in a heterogenous three-phase reservoir; estimate relative permeability and absolute permeability simultaneously.

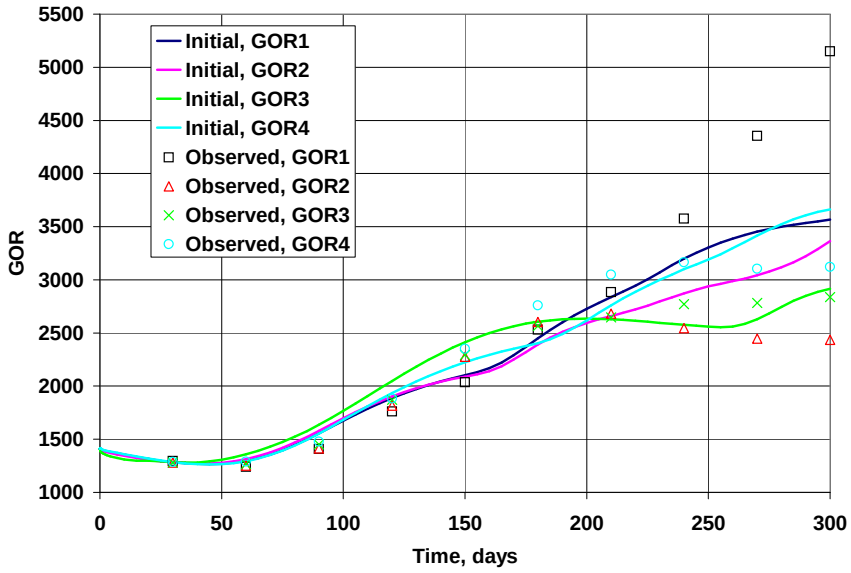

Figure 4.78: Gas-oil ratio match before conditioning to p_{wf}, GOR, and WOR in a heterogenous three-phase reservoir; estimate relative permeability and absolute permeability simultaneously.

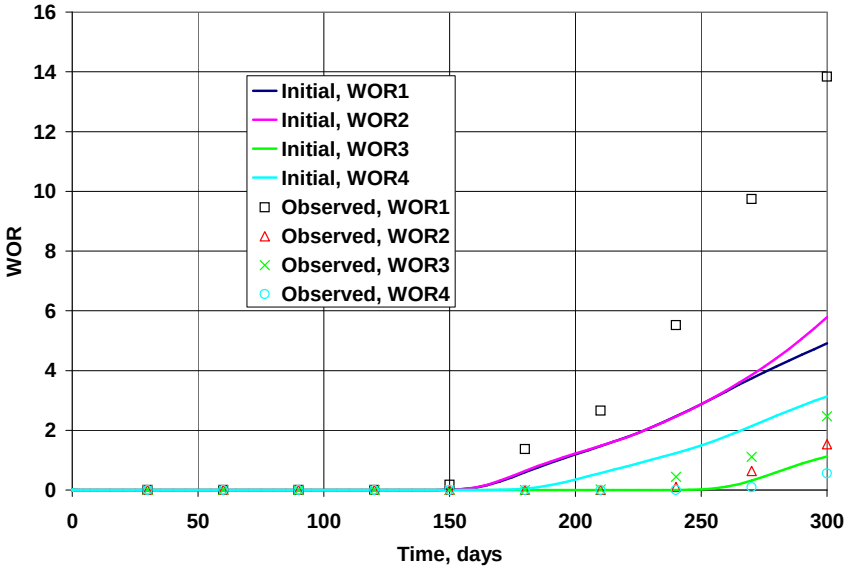

Figure 4.79: Water-oil ratio match before conditioning to p_{wf}, GOR, and WOR in a heterogenous three-phase reservoir; estimate relative permeability and absolute permeability simultaneously.

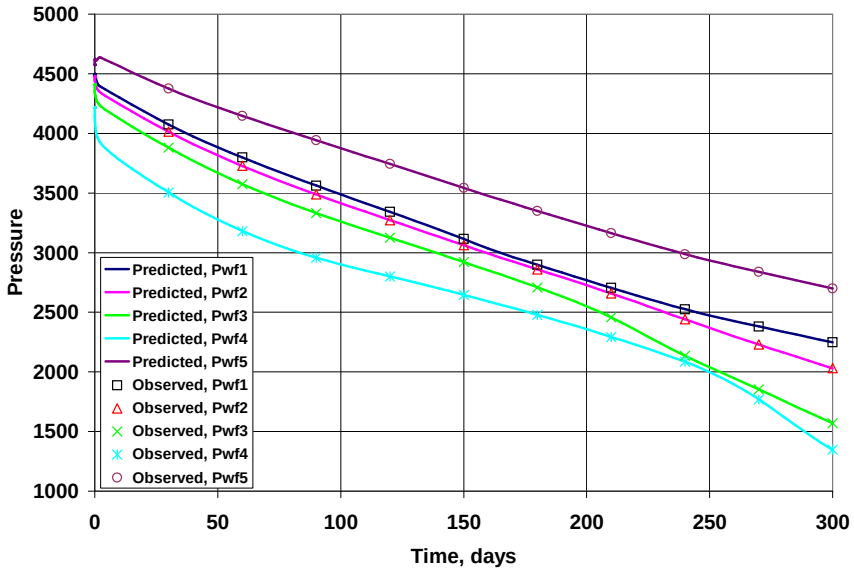

Figure 4.80: Bottom hole pressure match after conditioning to p_{wf}, GOR, and WOR in a heterogenous three-phase reservoir; estimate relative permeability and absolute permeability simultaneously.

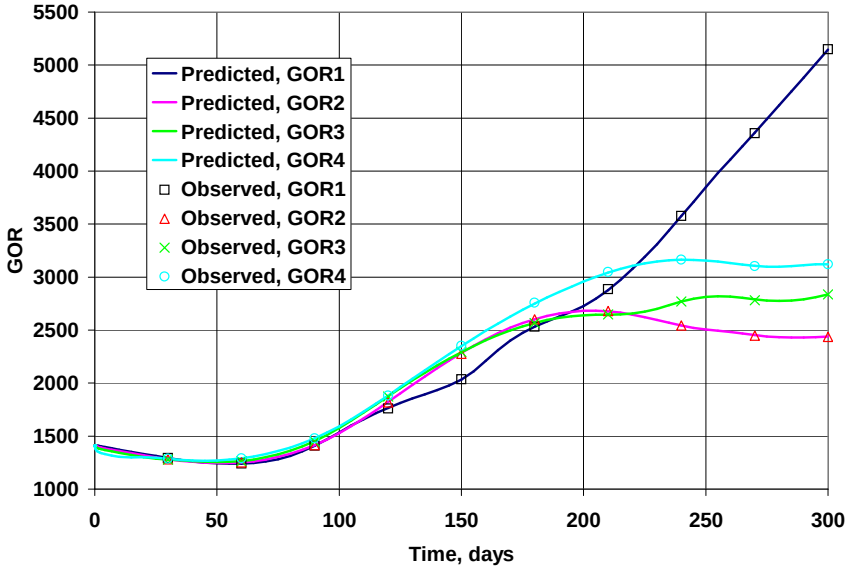

Figure 4.81: Gas-oil ratio match after conditioning to p_{wf}, GOR, and WOR in a heterogenous three-phase reservoir; estimate relative permeability and absolute permeability simultaneously.

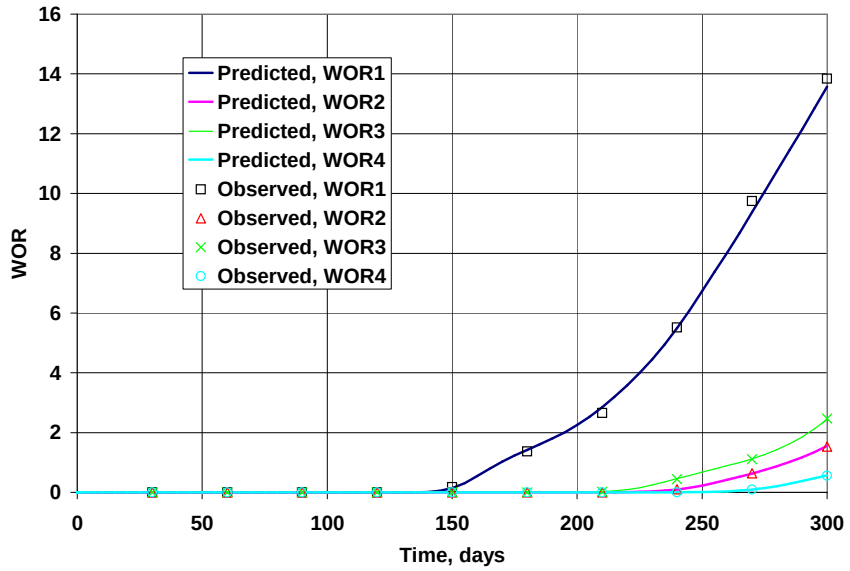

Figure 4.82: Water-oil ratio match after conditioning to p_{wf}, GOR, and WOR in a heterogenous three-phase reservoir; estimate relative permeability and absolute permeability simultaneously.

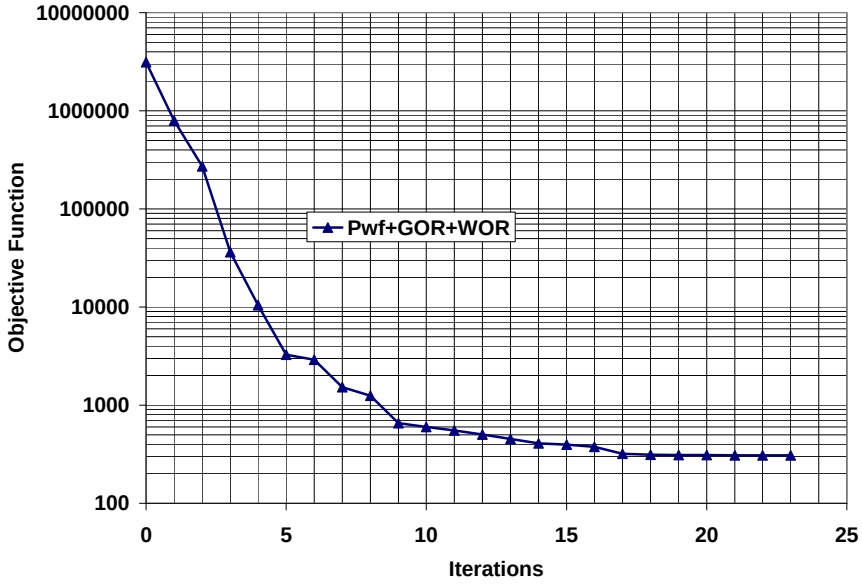

Figure 4.83: The rate of convergence of the objective functions in a three-phase heterogenous reservoir.

4.4 Estimation of porosity

In this example, we assume the absolute and relative permeabilities are known. The only unknown model parameters are porosities in each gridblock. We use production data to inverse the porosity field. The log-permeability is equal to 4.0 in each gridblock. The true porosity field is shown in the Fig. 4.84(a). The grid for reservoir simulation is 15 by 15 by 1. The gridblock sizes are 40 feet in the x- and y-directions and 30 feet in the z-direction. There is one injection well at the center (8,8,1) of the reservoir with water injection rate of 700 STB/d. Four producing wells are located at (3,3,1), (13,3,1), (13,13,1), (3,13), and (3,13,1), respectively. All four producing wells are produced with constant total reservoir volume 200 RB/d. The initial reservoir pressure is 4500 psi and the bubble point pressure is 4417 psi. The reservoir pressure decreases over the time. Fig. 4.84(b) shows the initial guess (unconditional realization). The unconditional realization is generated by Cholesky decomposition of the prior covariance matrix. The prior mean of the porosity is 0.22. The variance is 0.0016. The correlation range is 6 gridblocks (240 feet). A set of pressure, GOR, and WOR observed data were generated by running simulation on the true model. Random noise has been added to the data. Fig. 4.84(c) shows the conditional realization of the porosity field by conditioning to pressure, GOR and WOR data. The conditional realization is very close to the true porosity field. The data match is very well.

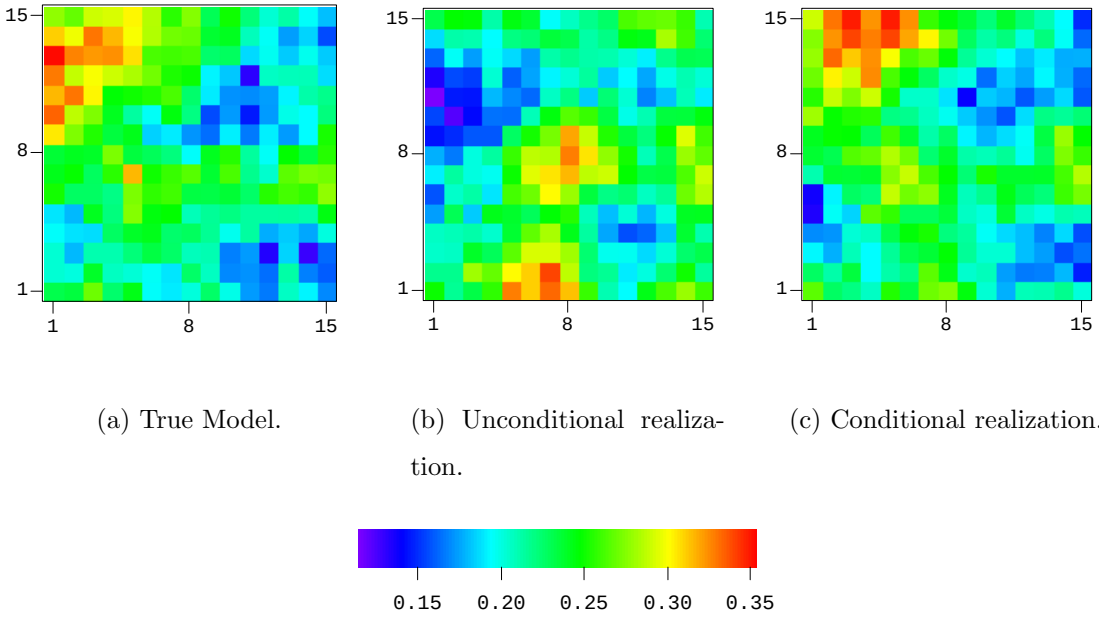

(a) True Model.

(b) Unconditional realization.

(c) Conditional realization.

Figure 4.84: The conditional realization of porosity conditioned to p_{wf}, GOR, and WOR data.

CHAPTER V

CONCLUSIONS

In this dissertation, we have described the development and implementation of a general procedure to generate maximum a posterior (MAP) estimates and realizations of reservoir model parameters conditioned to three-dimensional three-phase flow production data and prior information from static data. Using this procedure, we are able to estimate model parameters which include gridblock permeability (both horizontal and vertical permeability), gridblock porosity, well skin factors, and the parameters that describe relative permeability curves. We can condition the reservoir model to pressure, gas-oil ratio, water-oil ratio data and any combination of these three types of data. Unlike some other methods, this history matching process is applicable for problems with large numbers of model parameters and for problems with large fluid compressibility. The method presented here is quite general, however, and can also be applied to single-phase oil or gas flow or two phase flow problems. The MAP estimates or realizations are obtained by minimizing an appropriate objective function which includes both a data mismatch part and prior model part. To apply optimization procedures to minimize the objective function, one needs to calculate the sensitivity coefficients or the gradient of the objective function with respect to the model parameters. In this work, a general adjoint formulation for computing sensitivity coefficients, compatible with a fully implicit, finite-difference solution of the three-phase flow black-oil equations, has been derived and implemented in Fortran 90. The formulation given here allows one to construct the adjoint equations directly from the Jacobian matrices computed in solving the finite-difference equations using Newton-Raphson algorithm. This avoids the tedious process of directly deriving

the individual adjoint equations. Computation of sensitivity coefficients allow one to perform history matching using Newton-like methods (such as Levenberg-Marquardt or Gauss-Newton methods) which are approximately quadratically convergent as opposed to more slowly converging conjugate gradient or variable metric methods. In many cases, even in the complex two-dimensional, three-phase problems, our history matching algorithm converges whin 10 iterations. However, in some cases, especially in three-dimensional, three-phase, heterogeneous problems the history matching algorithm required 20 or more iterations to converge and given a somewhat higher value of the objective function than is expected. Clearly more work need to be done on the optimization algorithm.

The advantage of the adjoint method is that the number of matrix solution required to compute the sensitivity coefficients is independent of the number of model parameters to be estimated, so adjoint method can handle the problems with large number of model parameters. The the adjoint method is very efficient to compute sensitivity coefficients when the number of observed data is small. If only the gradient of the objective function is required to perform optimization, the adjoint method is always the best choice. The sensitivity coefficients which can be generated by this procedure include the sensitivity of wellbore pressure, GOR, WOR or any objective functions to simulator gridblock permeability and porosity, skin factor and parameters used in relative permeability curves. Because the convergence properties of the history matching procedure dependent on the accuracy of the sensitivity coefficients or gradients, it is important to obtain accurate sensitivity coefficients. We have compared the sensitivity coefficients generated by the adjoint method with these generated by the finite difference methods in various cases. The agreement is excellent. In all cases, the mismatch is less than 1%. Based on earlier experience with an IMPES simulator and a fully implicit formulation of the adjoint system, we concluded that one should always use the same flow formulation in the adjoint equations to compute sensitivity coefficients or gradients as are used in the reservoir simulator,

especially in the case where the gas phase is appear in the reservoir. Otherwise, the inconsistence of flow equations in the adjoint system and in reservoir simulator could cause significant errors in computation of sensitivity coefficients.

We have applied the history matching procedure to several 2D and 3D cases with two-phase and three-phase flow to generate MAP estimates or realizations. The results indicate that integrating more types of data improves the quality of the resulting estimate. Gas-oil ratio data tend to more useful than water-oil ratio data in resolving reservoir model parameters. With the sensitivity coefficients generated by adjoint method, we computed the approximate a posterior covariance matrix based on the Hessian. The normalized a posterior variance gives a measure of the reduction in uncertainty obtained by conditioning to production data and prior model. Based on this measure of uncertainty, conditioning to all production data (pressure, GOR and WOR) gives a greater reduction in uncertainty than is obtained by conditioning to only one or two types of data. One should bear in mind, however, that these a posterior variances only provide an approximation of the uncertainty. The best way to evaluate uncertainty is to generate a large number of realizations. However, generating multiple realizations is very expensive in computation.

For complex problems with big initial mismatch in the data, one needs to damp the updated step size of the early iterations in a history matching procedure to generate a reasonable estimate. The Levenberg-Marquardt provides a simple and efficient way to damp the step size in the first few iterations. From the examples in this work, the Levenberg-Marquardt method is more robust than regular Gauss-Newton method in term of obtaining estimates of model parameters which give acceptable matches of observed production data.

In this work, I showed that the relative permeability curves could be estimated by from observations of production data. We are have the ability to estimate the relative permeability by itself or estimate relative and absolute permeability simultaneously. Estimating absolute and relative permeability is more difficult than

estimating relative permeability only. In this work, a power law model was used to represent the relative permeability curves in the oil-gas and water-oil systems. If one only wishes to estimate relative permeability curves, one can accurately estimate both end points and exponential terms in the power law model. However, if one wants to estimate both absolute and relative permeability in a gas-oil or water-oil two phase flow problem, it was necessary to fix one end point (k_{rocw}) to obtain the reasonable estimates. Interestingly, in three-phase flow cases, it was possible to estimate absolute and relative permeability simultaneously without fixing the end points. We showed that this is a result of the use of the three-phase Stone 2 model and would not be true in general.

APPENDIX A

THE GENERAL 3D, THREE-PHASE BLACK OIL FLOW EQUATIONS

In this appendix, we present the general 3D, three-phase black oil flow equations on which the adjoint system is based.

A.1 Darcy's Law

In field units, the Darcy's Law can be written for the velocity,

$$v_m = -C_1 \frac{k_{rm}[k]}{\mu_m}(\nabla p_m - \frac{\rho_m g}{144 g_c}\nabla D), \tag{A–1}$$

where $m = o, w, g$, D points toward the center of the earth, and $C_1 = 1.127 \times 10^{-3}$. Throughout, we use Cartesian coordinate system so

$$v_m = \begin{bmatrix} v_{mx} \\ v_{my} \\ v_{mz} \end{bmatrix}, \tag{A–2}$$

and we assume that the coordinate system is aligned with the principal permeability directions so that k is a diagonal tensor given by

$$[k] = \begin{bmatrix} k_x & 0 & 0 \\ 0 & k_y & 0 \\ 0 & 0 & k_z \end{bmatrix}. \tag{A–3}$$

The components of the velocity vector v_m are in units of $RB/\text{ft}^2 - \text{day}$. The fluid density ρ_m is in units of lbm/ft^3. We define the specific weight γ_m by

$$\gamma_m = \frac{\rho_m g}{144 g_c}, \tag{A–4}$$

where $m = o, w, g$ and γ_m is in units of psi/ft. Then Darcy's Law can be written as

$$v_m = -C_1 \frac{k_{rm}[k]}{\mu_m}(\nabla p_m - \gamma_m \nabla D). \tag{A–5}$$

A.2 Three-Phase Relative Permeability

In our approach, we use the second model of Stone (1973) to calculate three-phase relative permeabilities. The oil relative permeability for three-phase flow is estimated from two sets of two-phase relative permeability data, relative permeability in an water-oil system and in an gas-oil system.

In a water-oil system, the water relative permeability k_{rw} and the oil relative permeability k_{row} only depend on water saturation S_w, i.e.,

$$k_{rw} = f(S_w), \tag{A–6}$$

and

$$k_{row} = f(S_w). \tag{A–7}$$

In a gas-oil system, the gas relative permeability k_{rg} and the oil relative permeability k_{rog} only depend on gas saturation S_g, i.e.,

$$k_{rg} = f(S_g), \tag{A–8}$$

and

$$k_{rog} = f(S_g). \tag{A–9}$$

For three-phase flow, the oil relative permeability is a function of S_w and S_g, i.e.,

$$k_{ro} = f(S_w, S_g); \tag{A–10}$$

whereas k_{rw} and K_{rg}, respectively, are still given by Eqs. A–6 and A–8. The three-phase relative oil permeability is given by the second modified Stone model,

$$k_{ro} = k_{rocw}[(k_{row}/k_{rocw} + k_{rw})(k_{rog}/k_{rocw} + k_{rg}) - (k_{rw} + k_{rg})] \tag{A–11}$$

We assume that the relative permeability data in a gas-oil system are measured in the presence of irreducible water. The term k_{rocw} in Eq. A–11 is defined by

$$k_{rocw} = k_{row}(S_{wc}) = k_{rog}(S_L = 1), \tag{A–12}$$

where $S_L = 1 - S_g = S_o + S_{wc}$ for the oil-gas system.

A.3 General Flow Equations

The adjoint procedure is based on a black-oil model. For this model, the gas component may be dissolved in oil but no oil component exists in the gas phase. In our formulation, we also assume that no gas dissolved in the water phase. However we neglect rock compressibility. From the law of mass conservation and Darcy's Law, we can obtain the following flow equations: Oil:

$$C_1 \nabla \left(\frac{k_{ro}}{\mu_o B_o} [k] (\nabla p_o(x,y,z,t) - \gamma_o \nabla D(x,y,z)) \right) = \frac{\phi}{C_2} \frac{\partial}{\partial t} \left(\frac{S_o}{B_o} \right) + \hat{q}_o(x,y,z,t); \tag{A–13}$$

Water:

$$C_1 \nabla \left(\frac{k_{rw}}{\mu_w B_w} [k] (\nabla p_w(x,y,z,t) - \gamma_w \nabla D(x,y,z)) \right) = \frac{\phi}{C_2} \frac{\partial}{\partial t} \left(\frac{S_w}{B_w} \right) + \hat{q}_w(x,y,z,t); \tag{A–14}$$

Gas:

$$\begin{aligned} C_1 \nabla \Bigg(& \frac{k_{rg}}{\mu_g B_g} [k] (\nabla p_g(x,y,z,t) - \gamma_g \nabla D(x,y,z)) \\ & + \frac{R_{so} k_{ro}}{\mu_o B_o} [k] (\nabla p_o(x,y,z,t) - \gamma_o \nabla D(x,y,z)) \Bigg) \\ & = \frac{\phi}{C_2} \frac{\partial}{\partial t} \left(\frac{S_g}{B_g} + \frac{R_{so} S_o}{B_o} \right) + \hat{q}_g(x,y,z,t). \end{aligned} \tag{A–15}$$

Throughout, $C_2 = 5.615$, the oil and water formation volume factor (B_o and B_w) are in units of RB/STB, the gas FVF (B_g) is in RB/scf, and R_{so} is the dissolved gas-oil ratio in units of scf/STB. The oil and water source/sink terms, $\hat{q}_o(x,y,z,t)$ and $\hat{q}_w(x,y,z,t)$, are in units $STB/\text{ft}^3 - \text{day}$, whereas the corresponding gas term,

$\hat{q}_g(x,y,z,t)$, is in units of $scf/\text{ft}^3 - \text{day}$. The equations are given in the form where $\hat{q}_m > 0$ corresponds to the production of phase m and $\hat{q}_m < 0$ corresponds to the injection of phase m.

The oil saturation S_o, water saturation S_w and gas saturation S_g satisfy the following constraint condition:

$$S_g + S_o + S_w = 1. \tag{A–16}$$

The two independent capillary pressure are defined by

$$p_{cow} = p_o - p_w, \tag{A–17}$$

and

$$p_{cgo} = p_g - p_o. \tag{A–18}$$

Note this means in the presence of oil and water, water is the wetting phase, whereas, in the presence of oil and gas, oil is the wetting phase. We assume that

$$p_{cow} = f(S_w), \tag{A–19}$$

and

$$p_{cgo} = f(S_g). \tag{A–20}$$

By using Eqs. A–17 and A–18, we can write Eqs. A–13 to A–15 as
Oil:

$$C_1 \nabla \left(\frac{k_{ro}}{\mu_o B_o} [k] (\nabla p_o(x,y,z,t) - \gamma_o \nabla D(x,y,z)) \right) = \frac{\phi}{C_2} \frac{\partial}{\partial t} \left(\frac{S_o}{B_o} \right) + \hat{q}_o(x,y,z,t); \tag{A–21}$$

Water:

$$C_1 \nabla \left(\frac{k_{rw}}{\mu_w B_w} [k] (\nabla p_o(x,y,z,t) - \nabla p_{cow}(x,y,z,t) - \gamma_w \nabla D(x,y,z)) \right) = \frac{\phi}{C_2} \frac{\partial}{\partial t} \left(\frac{S_w}{B_w} \right) + \hat{q}_w(x,y,z,t); \tag{A–22}$$

Gas:

$$C_1\nabla\Bigg(\frac{k_{rg}}{\mu_g B_g}[k](\nabla p_o(x,y,z,t)+\nabla p_{cgo}(x,y,z,t)-\gamma_g\nabla D(x,y,z)) + \frac{R_{so}k_{ro}}{\mu_o B_o}[k](\nabla p_o(x,y,z,t)-\gamma_o\nabla D(x,y,z))\Bigg) = \frac{\phi}{C_2}\frac{\partial}{\partial t}\left(\frac{S_g}{B_g}+\frac{R_{so}S_o}{B_o}\right)+\hat{q}_g(x,y,z,t). \tag{A–23}$$

If we neglect capillarity effects, the flow equations can be written as

Oil:

$$C_1\nabla\left(\frac{k_{ro}}{\mu_o B_o}[k](\nabla p(x,y,z,t)-\gamma_o\nabla D(x,y,z))\right)=\frac{\phi}{C_2}\frac{\partial}{\partial t}\left(\frac{S_o}{B_o}\right)+\hat{q}_o(x,y,z,t); \tag{A–24}$$

Water:

$$C_1\nabla\left(\frac{k_{rw}}{\mu_w B_w}[k](\nabla p(x,y,z,t)-\gamma_w\nabla D(x,y,z))\right)=\frac{\phi}{C_2}\frac{\partial}{\partial t}\left(\frac{S_w}{B_w}\right)+\hat{q}_w(x,y,z,t); \tag{A–25}$$

Gas:

$$C_1\nabla\Bigg(\frac{k_{rg}}{\mu_g B_g}[k](\nabla p(x,y,z,t)-\gamma_g\nabla D(x,y,z)) + \frac{R_{so}k_{ro}}{\mu_o B_o}[k](\nabla p(x,y,z,t)-\gamma_o\nabla D(x,y,z))\Bigg) = \frac{\phi}{C_2}\frac{\partial}{\partial t}\left(\frac{S_g}{B_g}+\frac{R_{so}S_o}{B_o}\right)+\hat{q}_g(x,y,z,t). \tag{A–26}$$

A.4 Discrete Flow Equations

We use a block-centered grid with gridblock centers at (x_i, y_j, z_k), $i = 1, 2, \ldots, n_x$, $j = 1, 2, \ldots, n_y$, $k = 1, 2, \ldots, n_z$. By using a fully implicit procedure to approximate spatial and time derivatives in Eqs. A–24 to A–26 multiplying the result by $V_{i,j,k} = \Delta x_i \Delta y_j \Delta z_k$ and let time $\Delta t^{n+1} = t^{n+1} - t^n$, we obtain the following equations in discrete form

Oil:

$$
\begin{aligned}
&T^{n+1}_{ox,i+1/2,j,k}[p^{n+1}_{i+1,j,k} - p^{n+1}_{i,j,k} - \gamma^{n+1}_{o,i+1/2,j,k}(D_{i+1,j,k} - D_{i,j,k})] \\
&\quad - T^{n+1}_{ox,i-1/2,j,k}[p^{n+1}_{i,j,k} - p^{n+1}_{i-1,j,k} - \gamma^{n+1}_{o,i-1/2,j,k}(D_{i,j,k} - D_{i-1,j,k})] \\
&\quad + T^{n+1}_{oy,i,j+1/2,k}[p^{n+1}_{i,j+1,k} - p^{n+1}_{i,j,k} - \gamma^{n+1}_{o,i,j+1/2,k}(D_{i,j+1,k} - D_{i,j,k})] \\
&\quad - T^{n+1}_{oy,i,j-1/2,k}[p^{n+1}_{i,j,k} - p^{n+1}_{i,j-1,k} - \gamma^{n+1}_{o,i,j-1/2,k}(D_{i,j,k} - D_{i,j-1,k})] \\
&\quad + T^{n+1}_{oz,i,,j,k+1/2}[p^{n+1}_{i,j,k+1} - p^{n+1}_{i,j,k} - \gamma^{n+1}_{o,i,j,k+1/2}(D_{i,j,k+1} - D_{i,j,k})] \\
&\quad - T^{n+1}_{oz,i,j,k-1/2}[p^{n+1}_{i,j,k} - p^{n+1}_{i,j,k-1} - \gamma^{n+1}_{o,i,j,k-1/2}(D_{i,j,k} - D_{i,j,k-1})] \\
&\qquad = \frac{V_{i,j,k}\phi_{i,j,k}}{C_2 \Delta t^{n+1}} \left[\left(\frac{S_o}{B_o} \right)^{n+1}_{i,j,k} - \left(\frac{S_o}{B_o} \right)^{n}_{i,j,k} \right] + q^{n+1}_{o,i,j,k}; \quad \text{(A–27)}
\end{aligned}
$$

Water:

$$
\begin{aligned}
&T^{n+1}_{wx,i+1/2,j,k}[p^{n+1}_{i+1,j,k} - p^{n+1}_{i,j,k} - \gamma^{n+1}_{w,i+1/2,j,k}(D_{i+1,j,k} - D_{i,j,k})] \\
&\quad - T^{n+1}_{wx,i-1/2,j,k}[p^{n+1}_{i,j,k} - p^{n+1}_{i-1,j,k} - \gamma^{n+1}_{w,i-1/2,j,k}(D_{i,j,k} - D_{i-1,j,k})] \\
&\quad + T^{n+1}_{wy,i,j+1/2,k}[p^{n+1}_{i,j+1,k} - p^{n+1}_{i,j,k} - \gamma^{n+1}_{w,i,j+1/2,k}(D_{i,j+1,k} - D_{i,j,k})] \\
&\quad - T^{n+1}_{wy,i,j-1/2,k}[p^{n+1}_{i,j,k} - p^{n+1}_{i,j-1,k} - \gamma^{n+1}_{w,i,j-1/2,k}(D_{i,j,k} - D_{i,j-1,k})] \\
&\quad + T^{n+1}_{wz,i,,j,k+1/2}[p^{n+1}_{i,j,k+1} - p^{n+1}_{i,j,k} - \gamma^{n+1}_{w,i,j,k+1/2}(D_{i,j,k+1} - D_{i,j,k})] \\
&\quad - T^{n+1}_{wz,i,j,k-1/2}[p^{n+1}_{i,j,k} - p^{n+1}_{i,j,k-1} - \gamma^{n+1}_{w,i,j,k-1/2}(D_{i,j,k} - D_{i,j,k-1})] \\
&\qquad = \frac{V_{i,j,k}\phi_{i,j,k}}{C_2 \Delta t^{n+1}} \left[\left(\frac{S_w}{B_w} \right)^{n+1}_{i,j,k} - \left(\frac{S_w}{B_w} \right)^{n}_{i,j,k} \right] + q^{n+1}_{w,i,j,k}; \quad \text{(A–28)}
\end{aligned}
$$

Gas:

$$
\begin{aligned}
&T^{n+1}_{gx,i+1/2,j,k}[p^{n+1}_{i+1,j,k} - p^{n+1}_{i,j,k} - \gamma^{n+1}_{g,i+1/2,j,k}(D_{i+1,j,k} - D_{i,j,k})] \\
&\qquad - T^{n+1}_{gx,i-1/2,j,k}[p^{n+1}_{i,j,k} - p^{n+1}_{i-1,j,k} - \gamma^{n+1}_{g,i-1/2,j,k}(D_{i,j,k} - D_{i-1,j,k})] \\
&\quad + R^{n+1}_{so,i+1/2,j,k}T^{n+1}_{ox,i+1/2,j,k}[p^{n+1}_{i+1,j,k} - p^{n+1}_{i,j,k} - \gamma^{n+1}_{o,i+1/2,j,k}(D_{i+1,j,k} - D_{i,j,k})] \\
&\quad - R^{n+1}_{so,i-1/2,j,k}T^{n+1}_{ox,i-1/2,j,k}[p^{n+1}_{i,j,k} - p^{n+1}_{i-1,j,k} - \gamma^{n+1}_{o,i-1/2,j,k}(D_{i,j,k} - D_{i-1,j,k})] \\
&\qquad + T^{n+1}_{gy,i,j+1/2,k}[p^{n+1}_{i,j+1,k} - p^{n+1}_{i,j,k} - \gamma^{n+1}_{g,i,j+1/2,k}(D_{i,j+1,k} - D_{i,j,k})] \\
&\qquad - T^{n+1}_{gy,i,j-1/2,k}[p^{n+1}_{i,j,k} - p^{n+1}_{i,j-1,k} - \gamma^{n+1}_{g,i,j-1/2,k}(D_{i,j,k} - D_{i,j-1,k})] \\
&\quad + R^{n+1}_{so,i,j+1/2,k}T^{n+1}_{oy,i,j+1/2,k}[p^{n+1}_{i,j+1,k} - p^{n+1}_{i,j,k} - \gamma^{n+1}_{o,i,j+1/2,k}(D_{i,j+1,k} - D_{i,j,k})] \\
&\quad - R^{n+1}_{so,i,j-1/2,k}T^{n+1}_{oy,i,j-1/2,k}[p^{n+1}_{i,j,k} - p^{n+1}_{i,j-1,k} - \gamma^{n+1}_{o,i,j-1/2,k}(D_{i,j,k} - D_{i,j-1,k})] \\
&\qquad + T^{n+1}_{gz,i,j,k+1/2}[p^{n+1}_{i,j,k+1} - p^{n+1}_{i,j,k} - \gamma^{n+1}_{g,i,j,k+1/2}(D_{i,j,k+1} - D_{i,j,k})] \\
&\qquad - T^{n+1}_{gz,i,j,k-1/2}[p^{n+1}_{i,j,k} - p^{n+1}_{i,j,k-1} - \gamma^{n+1}_{g,i,j,k-1/2}(D_{i,j,k} - D_{i,j,k-1})] \\
&\quad + R^{n+1}_{so,i,j,k+1/2}T^{n+1}_{oz,i,j,k+1/2}[p^{n+1}_{i,j,k+1} - p^{n+1}_{i,j,k} - \gamma^{n+1}_{o,i,j,k+1/2}(D_{i,j,k+1} - D_{i,j,k})] \\
&\quad - R^{n+1}_{so,i,j,k-1/2}T^{n+1}_{oz,i,j,k-1/2}[p^{n+1}_{o,i,j,k} - p^{n+1}_{o,i,j,k-1} - \gamma^{n+1}_{o,i,j,k-1/2}(D_{i,j,k} - D_{i,j,k-1})] \\
&\qquad = \frac{V_{i,j,k}\phi_{i,j,k}}{C_2\Delta t^{n+1}}\left[\left(\frac{S_g}{B_g} + R_{so}\frac{S_o}{B_o}\right)^{n+1}_{i,j,k} - \left(\frac{S_g}{B_g} + R_{so}\frac{S_o}{B_o}\right)^{n}_{i,j,k}\right] + q^{n+1}_{g,i,j,k}, \quad \text{(A–29)}
\end{aligned}
$$

for $i = 1, 2, \ldots, n_x, j = 1, 2, \ldots, n_y$, and $k = 1, 2, \ldots, n_z$. In the preceding three equations, the $q_{m,i,j,k}(t)$'s are defined by

$$q^{n+1}_{m,i,j,k} = \Delta x_i \Delta y_j \Delta z_k \hat{q}_{m,i,j,k}(t), \tag{A–30}$$

for $m = o, w, g$ and $V_{i,j,k} = \Delta x_i \Delta y_j \Delta z_k$. Note that the $q^{n+1}_{o,i,j,k}$ and $q^{n+1}_{w,i,j,k}$ are in units of STB/day and $q^{n+1}_{g,i,j,k}$ is in units scf/day.

The transmissibilities are given by the following equations.

$$T^{n+1}_{mx,i+1/2,j,k} = \frac{C_1 \Delta y_j \Delta z_k k_{x,i+1/2,j,k}}{x_{i+1} - x_i}\left(\frac{k_{rm}}{\mu_m B_m}\right)^{n+1}_{i+1/2,j,k}, \tag{A–31}$$

for $m = o, w, g$ and all $i = 1, 2, \ldots, n_x - 1$. The outer boundaries are no-flow, so the transmissibilities at the edges are given by

$$T^{n+1}_{mx,1/2,j,k} = T^{n+1}_{mx,n_x+1/2,j,k} = 0. \tag{A–32}$$

Similarly,

$$T^{n+1}_{my,i,j+1/2,k} = \frac{C_1 \Delta x_i \Delta z_k k_{y,i,j+1/2,k}}{y_{j+1} - y_j} \left(\frac{k_{rm}}{\mu_m B_m} \right)^{n+1}_{i,j+1/2,k}, \tag{A–33}$$

for $m = o, w, g$ and all $j = 1, 2, \ldots, n_y - 1$, and

$$T^{n+1}_{my,i,1/2,k} = T^{n+1}_{my,i,n_y+1/2,k} = 0, \tag{A–34}$$

$$T^{n+1}_{mz,i,j,k+1/2} = \frac{C_1 \Delta x_i \Delta y_j k_{z,i,j,k+1/2}}{z_{k+1} - z_k} \left(\frac{k_{rm}}{\mu_m B_m} \right)_{i,j,k+1/2}, \tag{A–35}$$

for $m = o, w, g$ and all $i = 1, 2, \ldots, n_y - 1$, and

$$T^{n+1}_{mz,i,j,1/2} = T^{n+1}_{mz,i,j,n_z+1/2} = 0. \tag{A–36}$$

The terms k_{rm}, μ_m, B_m, and R_{so} are evaluated by using upstream weightings. The specific weights γ^{n+1}_m are defined as

$$\gamma^{n+1}_{m,i\pm1/2,j,k} = \frac{g}{144 g_c} \frac{(\rho^{n+1}_{m,i,j,k} + \rho^{n+1}_{m,i\pm1,j,k})}{2}, \tag{A–37}$$

$$\gamma^{n+1}_{m,i,j\pm1/2,k} = \frac{g}{144 g_c} \frac{(\rho^{n+1}_{m,i,j,k} + \rho^{n+1}_{m,i,j\pm1,k})}{2}, \tag{A–38}$$

$$\gamma^{n+1}_{m,i,j,k\pm1/2} = \frac{g}{144 g_c} \frac{(\rho^{n+1}_{m,i,j,k} + \rho^{n+1}_{m,i,j,k\pm1})}{2}. \tag{A–39}$$

The phase density $\rho^{n+1}_{m,i,j,k}$ terms are given by

$$\rho^{n+1}_{o,i,j,k} = \frac{1}{B^{n+1}_o} (\rho_{osc} + \frac{1}{5.615} R^{n+1}_{so,i,j,k} \rho_{gsc}), \tag{A–40}$$

$$\rho^{n+1}_{w,i,j,k} = \frac{\rho_{wsc}}{B^{n+1}_w}, \tag{A–41}$$

$$\rho^{n+1}_{g,i,j,k} = \frac{\rho_{gsc}}{5.615 B^{n+1}_g}. \tag{A–42}$$

The terms ρ_{osc}, ρ_{wsc} and ρ_{gsc}, respectively, represent oil, water and gas density at the standard conditions. The units are in lbm/ft^3.

Eqs. A–27 to A–29, respectively, can be rewritten for the three phases as follows.

Oil:

$$
\begin{aligned}
f^{n+1}_{o,i,j,k} = {} & T^{n+1}_{ox,i+1/2,j,k}[p^{n+1}_{i+1,j,k} - p^{n+1}_{i,j,k} - \gamma^{n+1}_{o,i+1/2,j,k}(D_{i+1,j,k} - D_{i,j,k})] \\
& - T^{n+1}_{ox,i-1/2,j,k}[p^{n+1}_{i,j,k} - p^{n+1}_{i-1,j,k} - \gamma^{n+1}_{o,i-1/2,j,k}(D_{i,j,k} - D_{i-1,j,k})] \\
& + T^{n+1}_{oy,i,j+1/2,k}[p^{n+1}_{i,j+1,k} - p^{n+1}_{i,j,k} - \gamma^{n+1}_{o,i,j+1/2,k}(D_{i,j+1,k} - D_{i,j,k})] \\
& - T^{n+1}_{oy,i,j-1/2,k}[p^{n+1}_{i,j,k} - p^{n+1}_{i,j-1,k} - \gamma^{n+1}_{o,i,j-1/2,k}(D_{i,j,k} - D_{i,j-1,k})] \\
& + T^{n+1}_{oz,i,j,k+1/2}[p^{n+1}_{i,j,k+1} - p^{n+1}_{i,j,k} - \gamma^{n+1}_{o,i,j,k+1/2}(D_{i,j,k+1} - D_{i,j,k})] \\
& - T^{n+1}_{oz,i,j,k-1/2}[p^{n+1}_{i,j,k} - p^{n+1}_{i,j,k-1} - \gamma^{n+1}_{o,i,j,k-1/2}(D_{i,j,k} - D_{i,j,k-1})] \\
& - \frac{V_{i,j,k}\phi_{i,j,k}}{C_2 \Delta t^{n+1}} \left[\left(\frac{S_o}{B_o} \right)^{n+1}_{i,j,k} - \left(\frac{S_o}{B_o} \right)^{n}_{i,j,k} \right] - q^{n+1}_{o,i,j,k} = 0, \quad \text{(A–43)}
\end{aligned}
$$

Water:

$$
\begin{aligned}
f^{n+1}_{w,i,j,k} = {} & T^{n+1}_{wx,i+1/2,j,k}[p^{n+1}_{i+1,j,k} - p^{n+1}_{i,j,k} - \gamma^{n+1}_{w,i+1/2,j,k}(D_{i+1,j,k} - D_{i,j,k})] \\
& - T^{n+1}_{wx,i-1/2,j,k}[p^{n+1}_{i,j,k} - p^{n+1}_{i-1,j,k} - \gamma^{n+1}_{w,i-1/2,j,k}(D_{i,j,k} - D_{i-1,j,k})] \\
& + T^{n+1}_{wy,i,j+1/2,k}[p^{n+1}_{i,j+1,k} - p^{n+1}_{i,j,k} - \gamma^{n+1}_{w,i,j+1/2,k}(D_{i,j+1,k} - D_{i,j,k})] \\
& - T^{n+1}_{wy,i,j-1/2,k}[p^{n+1}_{i,j,k} - p^{n+1}_{i,j-1,k} - \gamma^{n+1}_{w,i,j-1/2,k}(D_{i,j,k} - D_{i,j-1,k})] \\
& + T^{n+1}_{wz,i,j,k+1/2}[p^{n+1}_{i,j,k+1} - p^{n+1}_{i,j,k} - \gamma^{n+1}_{w,i,j,k+1/2}(D_{i,j,k+1} - D_{i,j,k})] \\
& - T^{n+1}_{wz,i,j,k-1/2}[p^{n+1}_{i,j,k} - p^{n+1}_{i,j,k-1} - \gamma^{n+1}_{w,i,j,k-1/2}(D_{i,j,k} - D_{i,j,k-1})] \\
& - \frac{V_{i,j,k}\phi_{i,j,k}}{C_2 \Delta t^{n+1}} \left[\left(\frac{S_w}{B_w} \right)^{n+1}_{i,j,k} - \left(\frac{S_w}{B_w} \right)^{n}_{i,j,k} \right] - q^{n+1}_{w,i,j,k} = 0, \quad \text{(A–44)}
\end{aligned}
$$

Gas:

$$
\begin{aligned}
f^{n+1}_{g,i,j,k} = {} & T^{n+1}_{gx,i+1/2,j,k}[p^{n+1}_{i+1,j,k} - p^{n+1}_{i,j,k} - \gamma^{n+1}_{g,i+1/2,j,k}(D_{i+1,j,k} - D_{i,j,k})] \\
& - T^{n+1}_{gx,i-1/2,j,k}[p^{n+1}_{i,j,k} - p^{n+1}_{i-1,j,k} - \gamma^{n+1}_{g,i-1/2,j,k}(D_{i,j,k} - D_{i-1,j,k})] \\
& + R^{n+1}_{so,i+1/2,j,k} T^{n+1}_{ox,i+1/2,j,k}[p^{n+1}_{i+1,j,k} - p^{n+1}_{i,j,k} - \gamma^{n+1}_{o,i+1/2,j,k}(D_{i+1,j,k} - D_{i,j,k})] \\
& - R^{n+1}_{so,i-1/2,j,k} T^{n+1}_{ox,i-1/2,j,k}[p^{n+1}_{i,j,k} - p^{n+1}_{i-1,j,k} - \gamma^{n+1}_{o,i-1/2,j,k}(D_{i,j,k} - D_{i-1,j,k})] \\
& + T^{n+1}_{gy,i,j+1/2,k}[p^{n+1}_{i,j+1,k} - p^{n+1}_{i,j,k} - \gamma^{n+1}_{g,i,j+1/2,k}(D_{i,j+1,k} - D_{i,j,k})] \\
& - T^{n+1}_{gy,i,j-1/2,k}[p^{n+1}_{i,j,k} - p^{n+1}_{i,j-1,k} - \gamma^{n+1}_{g,i,j-1/2,k}(D_{i,j,k} - D_{i,j-1,k})] \\
& + R^{n+1}_{so,i,j+1/2,k} T^{n+1}_{oy,i,j+1/2,k}[p^{n+1}_{i,j+1,k} - p^{n+1}_{i,j,k} - \gamma^{n+1}_{o,i,j+1/2,k}(D_{i,j+1,k} - D_{i,j,k})] \\
& - R^{n+1}_{so,i,j-1/2,k} T^{n+1}_{oy,i,j-1/2,k}[p^{n+1}_{i,j,k} - p^{n+1}_{i,j-1,k} - \gamma^{n+1}_{o,i,j-1/2,k}(D_{i,j,k} - D_{i,j-1,k})] \\
& + T^{n+1}_{gz,i,j,k+1/2}[p^{n+1}_{i,j,k+1} - p^{n+1}_{i,j,k} - \gamma^{n+1}_{g,i,j,k+1/2}(D_{i,j,k+1} - D_{i,j,k})] \\
& - T^{n+1}_{gz,i,j,k-1/2}[p^{n+1}_{i,j,k} - p^{n+1}_{i,j,k-1} - \gamma^{n+1}_{g,i,j,k-1/2}(D_{i,j,k} - D_{i,j,k-1})] \\
& + R^{n+1}_{so,i,j,k+1/2} T^{n+1}_{oz,i,j,k+1/2}[p^{n+1}_{i,j,k+1} - p^{n+1}_{i,j,k} - \gamma^{n+1}_{o,i,j,k+1/2}(D_{i,j,k+1} - D_{i,j,k})] \\
& - R^{n+1}_{so,i,j,k-1/2} T^{n+1}_{oz,i,j,k-1/2}[p^{n+1}_{i,j,k} - p^{n+1}_{i,j,k-1} - \gamma^{n+1}_{o,i,j,k-1/2}(D_{i,j,k} - D_{i,j,k-1})] \\
& - \frac{V_{i,j,k}\phi_{i,j,k}}{C_2 \Delta t^{n+1}} \left[\left(\frac{S_g}{B_g} + R_{so}\frac{S_o}{B_o} \right)^{n+1}_{i,j,k} - \left(\frac{S_g}{B_g} + R_{so}\frac{S_o}{B_o} \right)^{n}_{i,j,k} \right] - q^{n+1}_{g,i,j,k} = 0, \quad \text{(A–45)}
\end{aligned}
$$

where the first equality in the preceding three equations serve to define the $f^{n+1}_{m,i,j,k}$ terms. Let

$$
f^{n+1}_f = \left[\; f^{n+1}_{o,1,1,1}, \quad f^{n+1}_{w,1,1,1}, \quad f^{n+1}_{g,1,1,1}, \quad f^{n+1}_{o,2,1,1}, \quad \ldots, \quad f^{n+1}_{g,n_x,n_y,n_z} \; \right]^T. \qquad \text{(A–46)}
$$

Then the linear system of Eqs. A–43 to A–45 can be written in vector form as

$$
f^{n+1}_f = 0. \qquad \text{(A–47)}
$$

A.5 Well Constraint Equations

In this section, we give the well constraint equations for various wellbore boundary conditions. For the producing wells, we can specify oil rate, total rate

at reservoir conditions and bottom hole pressure. For the injection wells, water or gas injection rate specified is used. The well constraints can change with time. For example, we can use a sequence of rates for the producing wells. An injection well can be changed to a producing well during the simulation run.

A.5.1 Wellbore Models

We use Peaceman's equation (Peaceman, 1983) to model the relation between wellbore pressure and gridblock pressure. The component flow rates from the perforated layer k of well l (at gridblock (i, j, k)) at time step $n+1$ can be evaluated as

$$q_{o,l,k}^{n+1} = WI_{l,k} \left(\frac{k_{ro}}{B_o \mu_o} \right)_{l,k}^{n+1} (p_{l,k}^{n+1} - p_{wf,l,k}^{n+1}), \tag{A–48}$$

$$q_{w,l,k}^{n+1} = WI_{l,k} \left(\frac{k_{rw}}{B_w \mu_w} \right)_{l,k}^{n+1} (p_{l,k}^{n+1} - p_{wf,l,k}^{n+1}), \tag{A–49}$$

and

$$\begin{aligned} q_{g,l,k}^{n+1} &= WI_{l,k} \left(\frac{k_{rg}}{B_g \mu_g} \right)_{l,k}^{n+1} (p_{l,k}^{n+1} - p_{wf,l,k}^{n+1}) + R_{so,l,k}^{n+1} q_{o,l,k}^{n+1} \\ &= WI_{l,k} \left(\frac{k_{rg}}{B_g \mu_g} + R_{so} \frac{k_{ro}}{B_o \mu_o} \right)_{l,k}^{n+1} (p_{l,k}^{n+1} - p_{wf,l,k}^{n+1}). \end{aligned} \tag{A–50}$$

The $q_{o,l,k}^{n+1}$ and $q_{w,l,k}^{n+1}$ are in units of STB/d, and the $q_{g,l,k}^{n+1}$ is in units of scf/d. Here layer k means the well-bore gridblock with z-direction gridblock index equal to k. The well index term $WI_{l,k}$ is the geometry part of productivity index and it is defined by

$$WI_{l,k} = \frac{0.00708 \triangle z_k \sqrt{k_{x,i,j,k} k_{y,i,j,k}}}{\ln(r_{o,l,k}/r_{w,l,k}) + s_{l,k}}, \tag{A–51}$$

and $r_{o,l,k}$ is defined

$$r_{o,l,k} = \frac{0.28073 \triangle x_i \sqrt{1 + \frac{k_{x,i,j,k}}{k_{y,i,j,k}} \left(\frac{\triangle y_j}{\triangle x_i} \right)^2}}{1 + \sqrt{k_{x,i,j,k}/k_{y,i,j,k}}}. \tag{A–52}$$

Here, $r_{w,l,k}$ is the wellbore radius of the well l at the layer k and the $s_{l,k}$ is the skin factor for well l at layer k.

To simplify notation, let

$$T_{o,l,k}^{n+1} = WI_{l,k}\left(\frac{k_{ro}}{B_o\mu_o}\right)_{l,k}^{n+1}, \tag{A–53}$$

$$T_{w,l,k}^{n+1} = WI_{l,k}\left(\frac{k_{rw}}{B_w\mu_w}\right)_{l,k}^{n+1}, \tag{A–54}$$

and

$$T_{g,l,k}^{n+1} = WI_{l,k}\left(\frac{k_{rg}}{B_g\mu_g} + R_{so}\frac{k_{ro}}{B_o\mu_o}\right)_{l,k}^{n+1}. \tag{A–55}$$

Then, Eqs. A–48-A–50 can be rewritten as

$$q_{o,l,k}^{n+1} = T_{o,l,k}^{n+1}(p_{l,k}^{n+1} - p_{wf,l,k}^{n+1}), \tag{A–56}$$

$$q_{w,l,k}^{n+1} = T_{w,l,k}^{n+1}(p_{l,k}^{n+1} - p_{wf,l,k}^{n+1}), \tag{A–57}$$

and

$$q_{g,l,k}^{n+1} = T_{g,l,k}^{n+1}(p_{l,k}^{n+1} - p_{wf,l,k}^{n+1}). \tag{A–58}$$

Let the $p_{wf,l}^{n+1}$ be the reference well pressure at the depth $D_{l,0}$. Assume the gravitational pressure gradient is constant ($\overline{\gamma}_l$), then the $p_{wf,l,k}^{n+1}$ at the depth $D_{l,k}$ can be expressed as

$$p_{wf,l,k}^{n+1} = p_{wf,l}^{n+1} + \overline{\gamma}_l(D_{l,k} - D_{l,0}) = p_{wf,l}^{n+1} + dp_{wf,l,k}^{n+1}, \tag{A–59}$$

where

$$dp_{wf,l,k}^{n+1} = \overline{\gamma}_l(D_{l,k} - D_{l,0}). \tag{A–60}$$

The gradient $\overline{\gamma}_l$ is evaluated from flow rates

$$\overline{\gamma}_l = \frac{\sum_k(\sum_m \gamma_{l,k}q_{m,l,k}^{n+1})}{\sum_k(\sum_m q_{m,l,k}^{n+1})}. \tag{A–61}$$

So the production rates at surface conditions for each completion gridblock can be computed by

$$q_{o,l,k}^{n+1} = T_{o,l,k}^{n+1}[p_{l,k}^{n+1} - p_{wf,l}^{n+1} - dp_{wf,l,k}^{n+1}], \tag{A–62}$$

$$q_{w,l,k}^{n+1} = T_{w,l,k}^{n+1}[p_{l,k}^{n+1} - p_{wf,l}^{n+1} - dp_{wf,l,k}^{n+1}], \tag{A–63}$$

and

$$q_{g,l,k}^{n+1} = T_{g,l,k}^{n+1}[p_{l,k}^{n+1} - p_{wf,l}^{n+1} - dp_{wf,l,k}^{n+1}]. \tag{A–64}$$

A.5.2 Well Constraints - p_{wf} Specified

Suppose the bottom hole pressure at well l, $p_{wf,l}^{n+1}$, is specified to equal $p_{wf,l,0}^{n+1}$. The well constraint equation is then simply

$$f_{wf,l}^{n+1} = p_{wf,l,0}^{n+1} - p_{wf,l}^{n+1} = 0. \tag{A–65}$$

It is necessary to Include Eq. A–65 in the reservoir simulation system equation. Through this way, the number of well constraints are always equal to the number of wells in the model. Otherwise, when the types of well constraints change, the number of well equations will change.

The production rates for each completion at surface conditions are calculated by Eqs. A–62 to A–64.

A.5.3 Well Constraints - Q_o Specified

Have $q_{o,l}^{n+1}$ denotes the oil production rate from well l at time t^{n+1} in STB/D,if we specify oil rate for well l as $q_{o,l}$, we have oil rate constraint

$$q_{o,l}^{n+1} = \sum_k q_{o,l,k}^{n+1} = \sum_k T_{o,l,k}^{n+1}(p_{l,k}^{n+1} - p_{wf,l,k}^{n+1}). \tag{A–66}$$

Substitute Eq. A–59 into Eq. A–66, and it follows that

$$\begin{aligned} q_{o,l}^{n+1} &= \sum_k T_{o,l,k}^{n+1}(p_{l,k}^{n+1} - p_{wf,l}^{n+1} - \overline{\gamma}_l(D_{l,k} - D_{l,0})) \\ &= \sum_k T_{o,l,k}^{n+1}(p_{l,k}^{n+1} - dp_{wf,l,k}^{n+1}) - \sum_k T_{o,l,k}^{n+1} p_{wf,l}^{n+1}, \end{aligned} \tag{A–67}$$

so the well l constraint equation is

$$f_{wf,l}^{n+1} = \sum_k T_{o,l,k}^{n+1}[p_{l,k}^{n+1} - p_{wf,l}^{n+1} - dp_{wf,l,k}^{n+1}] - q_{o,l}^{n+1} = 0. \tag{A–68}$$

Similarly, the production rates for each completion at surface conditions are calculated by Eqs. A–62 to A–64.

A.5.4 Well Constraints - Total Rate Q_t Specified at Reservoir Conditions

$q_{t,l}^{n+1}$ denotes the total production rate from well l at time t^{n+1} in RB/D. If we specify the total rate specified at reservoir conditions for well l , the total rate at reservoir conditions are given by

$$q_{t,l}^{n+1} = \sum_k q_{t,l,k}^{n+1} = \sum_k T_{t,l,k}^{n+1}(p_{l,k}^{n+1} - p_{wf,l,k}^{n+1}), \tag{A–69}$$

where

$$T_{t,l,k}^{n+1} = WI_{l,k}\left(\frac{k_{ro}}{\mu_o} + \frac{k_{rw}}{\mu_w} + \frac{k_{rg}}{\mu_g}\right)_{l,k}^{n+1}, \tag{A–70}$$

so the constraint equation for the well l is

$$f_{wf,l}^{n+1} = \sum_k T_{t,l,k}^{n+1}[p_{l,k}^{n+1} - p_{wf,l}^{n+1} - dp_{wf,l,k}^{n+1}] - q_{t,l}^{n+1} = 0. \tag{A–71}$$

The production rates at surface conditions are calculated by Eqs. A–62 to A–64.

A.5.5 Well Constraints - Water or Gas Injection

For the injection wells, the relative permeability of the injected phase in the Peaceman's equation is set to one. Let $q_{m,l,k}^{n+1}$ denote the injection rate of phase m at time t^{n+1}. For a water or gas injection well, the water or gas phase rate in the layer k is given by:

$$q_{m,l,k}^{n+1} = T_{inj,m,l,k}^{n+1}[p_{l,k}^{n+1} - p_{wf,l,k}^{n+1}] = T_{inj,m,l,k}^{n+1}[p_{l,k}^{n+1} - p_{wf,l}^{n+1} - dp_{wf,l,k}^{n+1}], \tag{A–72}$$

where $m = w, g$, $q_{m,l,k}^{n+1} < 0$, and

$$T_{inj,m,l,k}^{n+1} = \frac{WI_{l,k}}{(\mu_m B_m)_{l,k}^{n+1}}. \tag{A–73}$$

$WI_{l,k}$ is defined by Eq. A–51. So the well l constraint is given by

$$f_{wf,l}^{n+1} = \sum_k T_{inj,m,l,k}^{n+1}(p_{l,k}^{n+1} - p_{wf,l}^{n+1} - dp_{wf,l,k}^{n+1}) - q_{m,l}^{n+1} = 0. \tag{A–74}$$

For water injection wells, the oil and gas rates in each completion layer are set to zero, i.e.,

$$q_{g,l,k}^{n+1} = q_{o,l,k}^{n+1} = 0. \tag{A–75}$$

Similarly, for gas injection wells, the water and oil rates in each completion layer are set to zero,

$$q_{w,l,k}^{n+1} = q_{o,l,k}^{n+1} = 0. \tag{A–76}$$

A.6 Fully Implicit Simulator

Recall that $N = n_x n_y n_z$ denotes the total number of gridblocks and N_w denotes the number of wells. In this work, we solve $3N$ flow equations plus N_w well constraint equations simultaneously to get the solutions of reservoir simulation. The discrete nonlinear simulation equations can be written in the general form,

$$f(y^{n+1}, y^n, m) = 0, \tag{A–77}$$

where y^{n+1} is the vector of primary variables, p, S_w, S_g, and $p_{wf,l}$ at time step $n+1$; y^n is the vector of primary variables, at time step n; m is the vector of model parameters; f is a vector of flow equations and well constraint equations. The N gridblocks are numbered from $1, 2, ...,$ to N. Normally, the gridblocks are ordered with increasing x-direction index first, then increasing y-direction index, and finally increasing z-direction index. Actually, in our code, the order is flexible. One can increases any directions of index first. In gridblock i, the primary variables are $p_i, S_{w,i}, S_{g,i}$; All wellbore pressure are also primary variables. For three phase flow, we have three equations, water, gas and oil, in the gridblock i, which are represented in vector form by

$$f_{o,i}(y^{n+1}, y^n, m) = f_{o,i}^{n+1} = 0, \tag{A–78}$$

$$f_{w,i}(y^{n+1}, y^n, m) = f_{w,i}^{n+1} = 0, \tag{A–79}$$

and

$$f_{g,i}(y^{n+1}, y^n, m) = f_{g,i}^{n+1} = 0, \tag{A–80}$$

for $i = 1, 2, ..., N$. In each gridblock, we always put the oil equation first, and then the water equation, finally the gas equation.

The well constraints are represented by

$$f_{wf,j}(y^{n+1}, y^n, m) = f_{wf,j}^{n+1} = 0, \tag{A–81}$$

for $j = 1, 2, ..., N_w$, where N_w is the number of wells. So the simulation system, Eq. A–77, is a $3N + N_w$ dimensional vector which has the form

$$f(y^{n+1}, y^n, m) = f^{n+1} = \begin{bmatrix} f_{o,1}^{n+1} \\ f_{w,1}^{n+1} \\ f_{g,1}^{n+1} \\ f_{o,2}^{n+1} \\ \vdots \\ f_{g,N}^{n+1} \\ f_{wf,1}^{n+1} \\ \vdots \\ f_{wf,N_w}^{n+1} \end{bmatrix} = 0. \tag{A–82}$$

In Eq. A–82,

$$y^{n+1} = \begin{bmatrix} p_1^{n+1} \\ S_{w,1}^{n+1} \\ S_{g,1}^{n+1} \\ p_2^{n+1} \\ \vdots \\ S_{g,N}^{n+1} \\ p_{wf,1}^{n+1} \\ \vdots \\ p_{wf,N_w}^{n+1} \end{bmatrix}, \qquad y^n = \begin{bmatrix} p_1^n \\ S_{w,1}^n \\ S_{g,1}^n \\ p_2^n \\ \vdots \\ S_{g,N}^n \\ p_{wf,1}^n \\ \vdots \\ p_{wf,N_w}^n \end{bmatrix}, \tag{A–83}$$

and

$$m = \begin{bmatrix} m_1 \\ m_2 \\ \vdots \\ m_{N_m} \end{bmatrix}, \tag{A–84}$$

where N_m is the number of model parameters.

In the fully implicit simulator, we apply the Newton-Raphson method (Aziz, 1994) to solve the nonlinear system given by Eq. A–82. At each time step, Newton's method is applied to solve

$$J^{\nu}\delta y^{\nu+1} = -f^{\nu}, \tag{A–85}$$

for $\delta y^{\nu+1}$, where, ν is the iteration index and $J^{\nu} = [\nabla_{y^{\nu}} f^T]^T$ is the Jacobian matrix. Then the equation

$$y^{\nu+1} = y^{\nu} + \delta y^{\nu+1} \tag{A–86}$$

is used to update y (p, S_w, S_g and p_{wf}) until the procedure converges so that Eq. A–82 is satisfied to a given tolerance.

The Jacobian matrix is a $3N + N_w$ by $3N + N_w$ matrix. At time step n+1, it is given by,

$$J^{n+1} = [\nabla_{y^{n+1}}[f^{n+1}]^T]^T =$$

$$\begin{bmatrix}
\frac{\partial f_{o,1}^{n+1}}{\partial p_1^{n+1}} & \frac{\partial f_{o,1}^{n+1}}{\partial S_{w,1}^{n+1}} & \frac{\partial f_{o,1}^{n+1}}{\partial S_{g,1}^{n+1}} & \frac{\partial f_{o,1}^{n+1}}{\partial p_2^{n+1}} & \cdots & \frac{\partial f_{o,1}^{n+1}}{\partial S_{g,N}^{n+1}} & \frac{\partial f_{o,1}^{n+1}}{\partial p_{wf,1}^{n+1}} & \cdots & \frac{\partial f_{o,1}^{n+1}}{\partial p_{wf,N_w}^{n+1}} \\
\frac{\partial f_{w,1}^{n+1}}{\partial p_1^{n+1}} & \frac{\partial f_{w,1}^{n+1}}{\partial S_{w,1}^{n+1}} & \frac{\partial f_{w,1}^{n+1}}{\partial S_{g,1}^{n+1}} & \frac{\partial f_{w,1}^{n+1}}{\partial p_2^{n+1}} & \cdots & \frac{\partial f_{w,1}^{n+1}}{\partial S_{g,N}^{n+1}} & \frac{\partial f_{w,1}^{n+1}}{\partial p_{wf,1}^{n+1}} & \cdots & \frac{\partial f_{w,1}^{n+1}}{\partial p_{wf,N_w}^{n+1}} \\
\vdots & \vdots & \vdots & \vdots & \vdots & \vdots & \vdots & \vdots & \vdots \\
\frac{\partial f_{g,N}^{n+1}}{\partial p_1^{n+1}} & \frac{\partial f_{g,N}^{n+1}}{\partial S_{w,1}^{n+1}} & \frac{\partial f_{g,N}^{n+1}}{\partial S_{g,N}^{n+1}} & \frac{\partial f_{g,N}^{n+1}}{\partial p_2^{n+1}} & \cdots & \frac{\partial f_{g,N}^{n+1}}{\partial S_{g,N}^{n+1}} & \frac{\partial f_{g,N}^{n+1}}{\partial p_{wf,1}^{n+1}} & \cdots & \frac{\partial f_{g,N}^{n+1}}{\partial p_{wf,N_w}^{n+1}} \\
\frac{\partial f_{wf,1}^{n+1}}{\partial p_1^{n+1}} & \frac{\partial f_{wf,1}^{n+1}}{\partial S_{w,1}^{n+1}} & \frac{\partial f_{wf,1}^{n+1}}{\partial S_{g,1}^{n+1}} & \frac{\partial f_{wf,1}^{n+1}}{\partial p_2^{n+1}} & \cdots & \frac{\partial f_{wf,1}^{n+1}}{\partial S_{g,N}^{n+1}} & \frac{\partial f_{wf,1}^{n+1}}{\partial p_{wf,1}^{n+1}} & \cdots & \frac{\partial f_{wf,1}^{n+1}}{\partial p_{wf,N_w}^{n+1}} \\
\vdots & \vdots & \vdots & \vdots & \vdots & \vdots & \vdots & \vdots & \vdots \\
\frac{\partial f_{wf,N_w}^{n+1}}{\partial p_1^{n+1}} & \frac{\partial f_{wf,N_w}^{n+1}}{\partial S_{w,1}^{n+1}} & \frac{\partial f_{wf,N_w}^{n+1}}{\partial S_{g,1}^{n+1}} & \frac{\partial f_{wf,N_w}^{n+1}}{\partial p_2^{n+1}} & \cdots & \frac{\partial f_{wf,N_w}^{n+1}}{\partial S_{g,N}^{n+1}} & \frac{\partial f_{wf,N_w}^{n+1}}{\partial p_{wf,1}^{n+1}} & \cdots & \frac{\partial f_{wf,N_w}^{n+1}}{\partial p_{wf,N_w}^{n+1}}
\end{bmatrix}. \tag{A–87}$$

APPENDIX B

COMPUTATION OF DERIVATIVES IN THE ADJOINT SYSTEM

In chapter 3, we showed that the adjoint system of equations for our general flow equations can be written as

$$[\nabla_{y^n}(f^n)^T]\lambda^n = -[\nabla_{y^n}(f^{n+1})^T]\lambda^{n+1} - \nabla_{y^n}\beta. \tag{B–1}$$

In this appendix, we will evaluate the derivatives in Eq. B–1 for the implicit black-oil system. Recall that the state variables of the nth time step are

$$y_n = [\ p_1^n \quad S_{w,1}^n \quad S_{g,1}^n \quad p_2^n \quad \cdots \quad S_{g,N}^n \quad p_{wf,1}^n \quad \cdots \quad p_{wf,N_w}^n\ ]^T. \tag{B–2}$$

So we write the gradient of the flow equation of at time n with respect to y^n as (the transpose of Jacobian matrix)

$$\nabla_{y^n}[f^n]^T = \begin{bmatrix} \frac{\partial f_{o,1}^n}{\partial p_1^n} & \frac{\partial f_{w,1}^n}{\partial p_1^n} & \cdots & \frac{\partial f_{g,N}^n}{\partial p_1^n} & \frac{\partial f_{wf,1}^n}{\partial p_1^n} & \cdots & \frac{\partial f_{wf,N_w}^n}{\partial p_1^n} \\ \frac{\partial f_{o,1}^n}{\partial S_{w,1}^n} & \frac{\partial f_{w,1}^n}{\partial S_{w,1}^n} & \cdots & \frac{\partial f_{g,N}^n}{\partial S_{w,1}^n} & \frac{\partial f_{wf,1}^n}{\partial S_{w,1}^n} & \cdots & \frac{\partial f_{wf,N_w}^n}{\partial S_{w,1}^n} \\ \frac{\partial f_{o,1}^n}{\partial S_{g,1}^n} & \frac{\partial f_{w,1}^n}{\partial S_{g,1}^n} & \cdots & \frac{\partial f_{g,N}^n}{\partial S_{g,N}^n} & \frac{\partial f_{wf,1}^n}{\partial S_{g,1}^n} & \cdots & \frac{\partial f_{wf,N_w}^n}{\partial S_{g,1}^n} \\ \frac{\partial f_{o,1}^n}{\partial p_2^n} & \frac{\partial f_{w,1}^n}{\partial p_2^n} & \cdots & \frac{\partial f_{g,N}^n}{\partial p_2^n} & \frac{\partial f_{wf,1}^n}{\partial p_2^n} & \cdots & \frac{\partial f_{wf,N_w}^n}{\partial p_2^n} \\ \vdots & \vdots & \cdots & \vdots & \vdots & \cdots & \vdots \\ \frac{\partial f_{o,1}^n}{\partial S_{g,N}^n} & \frac{\partial f_{w,1}^n}{\partial S_{g,N}^n} & \cdots & \frac{\partial f_{g,N}^n}{\partial S_{g,N}^n} & \frac{\partial f_{wf,1}^n}{\partial S_{g,N}^n} & \cdots & \frac{\partial f_{wf,N_w}^n}{\partial S_{g,N}^n} \\ \frac{\partial f_{o,1}^n}{\partial p_{wf,1}^n} & \frac{\partial f_{w,1}^n}{\partial p_{wf,1}^n} & \cdots & \frac{\partial f_{g,N}^n}{\partial p_{wf,1}^n} & \frac{\partial f_{wf,1}^n}{\partial p_{wf,1}^n} & \cdots & \frac{\partial f_{wf,N_w}^n}{\partial p_{wf,1}^n} \\ \vdots & \vdots & \cdots & \vdots & \vdots & \cdots & \vdots \\ \frac{\partial f_{o,1}^n}{\partial p_{wf,N_w}^n} & \frac{\partial f_{w,1}^n}{\partial p_{wf,N_w}^n} & \cdots & \frac{\partial f_{g,N}^n}{\partial p_{wf,N_w}^n} & \frac{\partial f_{wf,1}^n}{\partial p_{wf,N_w}^n} & \cdots & \frac{\partial f_{wf,N_w}^n}{\partial p_{wf,N_w}^n} \end{bmatrix}. \tag{B–3}$$

A similar equation results for the gradient of the flow equations at $n+1$;

$$\nabla_{y^n}[f^{n+1}]^T = \begin{bmatrix} \frac{\partial f_{o,1}^{n+1}}{\partial p_1^n} & \frac{\partial f_{w,1}^{n+1}}{\partial p_1^n} & \cdots & \frac{\partial f_{g,N}^{n+1}}{\partial p_1^n} & \frac{\partial f_{wf,1}^{n+1}}{\partial p_1^n} & \cdots & \frac{\partial f_{wf,N_w}^{n+1}}{\partial p_1^n} \\ \frac{\partial f_{o,1}^{n+1}}{\partial S_{w,1}^n} & \frac{\partial f_{w,1}^{n+1}}{\partial S_{w,1}^n} & \cdots & \frac{\partial f_{g,N}^{n+1}}{\partial S_{w,1}^n} & \frac{\partial f_{wf,1}^{n+1}}{\partial S_{w,1}^n} & \cdots & \frac{\partial f_{wf,N_w}^{n+1}}{\partial S_{w,1}^n} \\ \frac{\partial f_{o,1}^{n+1}}{\partial S_{g,1}^n} & \frac{\partial f_{w,1}^{n+1}}{\partial S_{g,1}^n} & \cdots & \frac{\partial f_{g,N}^{n+1}}{\partial S_{g,N}^n} & \frac{\partial f_{wf,1}^{n+1}}{\partial S_{g,1}^n} & \cdots & \frac{\partial f_{wf,N_w}^{n+1}}{\partial S_{g,1}^n} \\ \frac{\partial f_{o,1}^{n+1}}{\partial p_2^n} & \frac{\partial f_{w,1}^{n+1}}{\partial p_2^n} & \cdots & \frac{\partial f_{g,N}^{n+1}}{\partial p_2^n} & \frac{\partial f_{wf,1}^{n+1}}{\partial p_2^n} & \cdots & \frac{\partial f_{wf,N_w}^{n+1}}{\partial p_2^n} \\ \vdots & \vdots & \cdots & \vdots & \vdots & \cdots & \vdots \\ \frac{\partial f_{o,1}^{n+1}}{\partial S_{g,N}^n} & \frac{\partial f_{w,1}^{n+1}}{\partial S_{g,N}^n} & \cdots & \frac{\partial f_{g,N}^{n+1}}{\partial S_{g,N}^n} & \frac{\partial f_{wf,1}^{n+1}}{\partial S_{g,N}^n} & \cdots & \frac{\partial f_{wf,N_w}^{n+1}}{\partial S_{g,N}^n} \\ \frac{\partial f_{o,1}^{n+1}}{\partial p_{wf,1}^n} & \frac{\partial f_{w,1}^{n+1}}{\partial p_{wf,1}^n} & \cdots & \frac{\partial f_{g,N}^{n+1}}{\partial p_{wf,1}^n} & \frac{\partial f_{wf,1}^{n+1}}{\partial p_{wf,1}^n} & \cdots & \frac{\partial f_{wf,N_w}^{n+1}}{\partial p_{wf,1}^n} \\ \vdots & \vdots & \cdots & \vdots & \vdots & \cdots & \vdots \\ \frac{\partial f_{o,1}^{n+1}}{\partial p_{wf,N_w}^n} & \frac{\partial f_{w,1}^{n+1}}{\partial p_{wf,N_w}^n} & \cdots & \frac{\partial f_{g,N}^{n+1}}{\partial p_{wf,N_w}^n} & \frac{\partial f_{wf,1}^{n+1}}{\partial p_{wf,N_w}^n} & \cdots & \frac{\partial f_{wf,N_w}^{n+1}}{\partial p_{wf,N_w}^n} \end{bmatrix}. \quad \text{(B–4)}$$

Finally, we must compute the gradient of the "objective function" with respect to the primary variables,

$$\nabla_{y^n}\beta = \begin{bmatrix} \frac{\partial \beta}{\partial p_1^n} \\ \frac{\partial \beta}{\partial S_{w,1}^n} \\ \frac{\partial \beta}{\partial S_{g,1}^n} \\ \frac{\partial \beta}{\partial p_2^n} \\ \vdots \\ \frac{\partial \beta}{\partial S_{g,N}^n} \\ \frac{\partial \beta}{\partial p_{wf,1}^n} \\ \vdots \\ \frac{\partial \beta}{\partial p_{wf,N_w}^n} \end{bmatrix}. \quad \text{(B–5)}$$

In order to solve the adjoint system Eq. B–1, we need to evaluate the matrices, $[\nabla_{y^n}(f^n)^T]$, $[\nabla_{y^n}(f^{n+1})^T]$ and $\nabla_{y^n}\beta$. In the following sections, we give detailed formulations for computing these derivatives. The computation of the transpose of the Jacobian matrix $[\nabla_{y^n}(f^n)^T]$ (Eq. B–3) is given in the section B.1 and B.2, the computation of diagonal band matrix $[\nabla_{y^n}(f^{n+1})^T]$ (Eq. B–4) is given in section B.3. In section B.4, we describe how to calculate the source terms $\nabla_{y^n}\beta$ in the adjoint

system.

B.1 Derivatives of Flow Equations

In this section, we compute the derivatives of flow equations Eqs. A–43 to A–45 with respect to the primary variables y^{n+1} (p, S_w, S_g, and $p_{wf,l}$).

To simplify the notation, we separate the flow equations to three parts: the flow term ($F^n_{m,i,j,k}$), the accumulation term ($A^{n+1}_{m,i,j,k}$) and the sink term ($q^{n+1}_{m,i,j,k}$). The flow equations (Eqs. A–43 to A–45) can be written

$$f^{n+1}_{m,i,j,k} = F^{n+1}_{m,i,j,k} - A^{n+1}_{m,i,j,k} - q^{n+1}_{m,i,j,k} = 0, \tag{B–6}$$

where $m = o, w, g$. The flow terms ($F^{n+1}_{m,i,j,k}$), accumulation terms ($A^{n+1}_{m,i,j,k}$), and the sink terms $q^{n+1}_{m,i,j,k}$ can be obtained from Eqs. A–43 to A–45. The flow terms are given by,

$$\begin{aligned}
F^{n+1}_{o,i,j,k} = {} & T^{n+1}_{ox,i+1/2,j,k}[p^{n+1}_{i+1,j,k} - p^{n+1}_{i,j,k} - \gamma^{n+1}_{o,i+1/2,j,k}(D_{i+1,j,k} - D_{i,j,k})] \\
& - T^{n+1}_{ox,i-1/2,j,k}[p^{n+1}_{i,j,k} - p^{n+1}_{i-1,j,k} - \gamma^{n+1}_{o,i-1/2,j,k}(D_{i,j,k} - D_{i-1,j,k})] \\
& + T^{n+1}_{oy,i,j+1/2,k}[p^{n+1}_{i,j+1,k} - p^{n+1}_{i,j,k} - \gamma^{n+1}_{o,i,j+1/2,k}(D_{i,j+1,k} - D_{i,j,k})] \\
& - T^{n+1}_{oy,i,j-1/2,k}[p^{n+1}_{i,j,k} - p^{n+1}_{i,j-1,k} - \gamma^{n+1}_{o,i,j-1/2,k}(D_{i,j,k} - D_{i,j-1,k})] \\
& + T^{n+1}_{oz,i,j,k+1/2}[p^{n+1}_{i,j,k+1} - p^{n+1}_{i,j,k} - \gamma^{n+1}_{o,i,j,k+1/2}(D_{i,j,k+1} - D_{i,j,k})] \\
& \quad - T^{n+1}_{oz,i,j,k-1/2}[p^{n+1}_{i,j,k} - p^{n+1}_{i,j,k-1} - \gamma^{n+1}_{o,i,j,k-1/2}(D_{i,j,k} - D_{i,j,k-1})],
\end{aligned} \tag{B–7}$$

$$\begin{aligned}
F^{n+1}_{w,i,j,k} = {} & T^{n+1}_{wx,i+1/2,j,k}[p^{n+1}_{i+1,j,k} - p^{n+1}_{i,j,k} - \gamma^{n+1}_{w,i+1/2,j,k}(D_{i+1,j,k} - D_{i,j,k})] \\
& - T^{n+1}_{wx,i-1/2,j,k}[p^{n+1}_{i,j,k} - p^{n+1}_{i-1,j,k} - \gamma^{n+1}_{w,i-1/2,j,k}(D_{i,j,k} - D_{i-1,j,k})] \\
& + T^{n+1}_{wy,i,j+1/2,k}[p^{n+1}_{i,j+1,k} - p^{n+1}_{i,j,k} - \gamma^{n+1}_{w,i,j+1/2,k}(D_{i,j+1,k} - D_{i,j,k})] \\
& - T^{n+1}_{wy,i,j-1/2,k}[p^{n+1}_{i,j,k} - p^{n+1}_{i,j-1,k} - \gamma^{n+1}_{w,i,j-1/2,k}(D_{i,j,k} - D_{i,j-1,k})] \\
& + T^{n+1}_{wz,i,j,k+1/2}[p^{n+1}_{i,j,k+1} - p^{n+1}_{i,j,k} - \gamma^{n+1}_{w,i,j,k+1/2}(D_{i,j,k+1} - D_{i,j,k})] \\
& \quad - T^{n+1}_{wz,i,j,k-1/2}[p^{n+1}_{i,j,k} - p^{n+1}_{i,j,k-1} - \gamma^{n+1}_{w,i,j,k-1/2}(D_{i,j,k} - D_{i,j,k-1})],
\end{aligned} \tag{B–8}$$

and

$$
\begin{aligned}
F^{n+1}_{g,i,j,k} &= T^{n+1}_{gx,i+1/2,j,k}[p^{n+1}_{i+1,j,k} - p^{n+1}_{i,j,k} - \gamma^{n+1}_{g,i+1/2,j,k}(D_{i+1,j,k} - D_{i,j,k})] \\
&\quad - T^{n+1}_{gx,i-1/2,j,k}[p^{n+1}_{i,j,k} - p^{n+1}_{i-1,j,k} - \gamma^{n+1}_{g,i-1/2,j,k}(D_{i,j,k} - D_{i-1,j,k})] \\
&\quad + R^{n+1}_{so,i+1/2,j,k}T^{n+1}_{ox,i+1/2,j,k}[p^{n+1}_{i+1,j,k} - p^{n+1}_{i,j,k} - \gamma^{n+1}_{o,i+1/2,j,k}(D_{i+1,j,k} - D_{i,j,k})] \\
&\quad - R^{n+1}_{so,i-1/2,j,k}T^{n+1}_{ox,i-1/2,j,k}[p^{n+1}_{i,j,k} - p^{n+1}_{i-1,j,k} - \gamma^{n+1}_{o,i-1/2,j,k}(D_{i,j,k} - D_{i-1,j,k})] \\
&\quad + T^{n+1}_{gy,i,j+1/2,k}[p^{n+1}_{i,j+1,k} - p^{n+1}_{i,j,k} - \gamma^{n+1}_{g,i,j+1/2,k}(D_{i,j+1,k} - D_{i,j,k})] \\
&\quad - T^{n+1}_{gy,i,j-1/2,k}[p^{n+1}_{i,j,k} - p^{n+1}_{i,j-1,k} - \gamma^{n+1}_{g,i,j-1/2,k}(D_{i,j,k} - D_{i,j-1,k})] \\
&\quad + R^{n+1}_{so,i,j+1/2,k}T^{n+1}_{oy,i,j+1/2,k}[p^{n+1}_{i,j+1,k} - p^{n+1}_{i,j,k} - \gamma^{n+1}_{o,i,j+1/2,k}(D_{i,j+1,k} - D_{i,j,k})] \\
&\quad - R^{n+1}_{so,i,j-1/2,k}T^{n+1}_{oy,i,j-1/2,k}[p^{n+1}_{i,j,k} - p^{n+1}_{i,j-1,k} - \gamma^{n+1}_{o,i,j-1/2,k}(D_{i,j,k} - D_{i,j-1,k})] \\
&\quad + T^{n+1}_{gz,i,,j,k+1/2}[p^{n+1}_{i,j,k+1} - p^{n+1}_{i,j,k} - \gamma^{n+1}_{g,i,j,k+1/2}(D_{i,j,k+1} - D_{i,j,k})] \\
&\quad - T^{n+1}_{gz,i,j,k-1/2}[p^{n+1}_{i,j,k} - p^{n+1}_{i,j,k-1} - \gamma^{n+1}_{g,i,j,k-1/2}(D_{i,j,k} - D_{i,j,k-1})] \\
&\quad + R^{n+1}_{so,i,j,k+1/2}T^{n+1}_{oz,i,,j,k+1/2}[p^{n+1}_{i,j,k+1} - p^{n+1}_{i,j,k} - \gamma^{n+1}_{o,i,j,k+1/2}(D_{i,j,k+1} - D_{i,j,k})] \\
&\quad - R^{n+1}_{so,i,j,k-1/2}T^{n+1}_{oz,i,j,k-1/2}[p^{n+1}_{i,j,k} - p^{n+1}_{i,j,k-1} - \gamma^{n+1}_{o,i,j,k-1/2}(D_{i,j,k} - D_{i,j,k-1})]. \quad \text{(B–9)}
\end{aligned}
$$

The accumulation terms are also obtained from A–43 to A–45:

$$
\begin{aligned}
A^{n+1}_{o,i,j,k} &= \frac{V_{i,j,k}\phi_{i,j,k}}{C_2\Delta t^{n+1}}\left[\left(\frac{S_o}{B_o}\right)^{n+1}_{i,j,k} - \left(\frac{S_o}{B_o}\right)^{n}_{i,j,k}\right] \\
&= \frac{V_{i,j,k}\phi_{i,j,k}}{C_2\Delta t^{n+1}}\left[\left(\frac{1-S_w-S_g}{B_o}\right)^{n+1}_{i,j,k} - \left(\frac{1-S_w-S_g}{B_o}\right)^{n}_{i,j,k}\right], \quad \text{(B–10)} \\
A^{n+1}_{w,i,j,k} &= \frac{V_{i,j,k}\phi_{i,j,k}}{C_2\Delta t^{n+1}}\left[\left(\frac{S_w}{B_w}\right)^{n+1}_{i,j,k} - \left(\frac{S_w}{B_w}\right)^{n}_{i,j,k}\right], \quad \text{(B–11)}
\end{aligned}
$$

and

$$
\begin{aligned}
A^{n+1}_{g,i,j,k} &= \frac{V_{i,j,k}\phi_{i,j,k}}{C_2\Delta t^{n+1}}\left[\left(\frac{S_g}{B_g} + R_{so}\frac{S_o}{B_o}\right)^{n+1}_{i,j,k} - \left(\frac{S_g}{B_g} + R_{so}\frac{S_o}{B_o}\right)^{n}_{i,j,k}\right] \\
&= \frac{V_{i,j,k}\phi_{i,j,k}}{C_2\Delta t^{n+1}}\left[\left(\frac{S_g}{B_g} + R_{so}\left(\frac{1-S_w-S_g}{B_o}\right)\right)^{n+1}_{i,j,k} - \left(\frac{S_g}{B_g} + R_{so}\left(\frac{1-S_w-S_g}{B_o}\right)\right)^{n}_{i,j,k}\right]. \quad \text{(B–12)}
\end{aligned}
$$

The sink terms for oil, water and gas equations are

$$q_{o,l,k}^{n+1} = WI_{l,k}\left(\frac{k_{ro}}{B_o\mu_o}\right)_{l,k}^{n+1}(p_{l,k}^{n+1} - p_{wf,l,k}^{n+1}), \tag{B–13}$$

$$q_{w,l,k}^{n+1} = WI_{l,k}\left(\frac{k_{rw}}{B_w\mu_w}\right)_{l,k}^{n+1}(p_{l,k}^{n+1} - p_{wf,l,k}^{n+1}), \tag{B–14}$$

and

$$\begin{aligned} q_{g,l,k}^{n+1} &= WI_{l,k}\left(\frac{k_{rg}}{B_g\mu_g}\right)_{l,k}^{n+1}(p_{lj,k}^{n+1} - p_{wf,l,k}^{n+1}) + R_{so,l,k}^{n+1}q_{o,l,k}^{n+1} \\ &= WI_{l,k}\left(\frac{k_{rg}}{B_g\mu_g} + R_{so}\frac{k_{ro}}{B_o\mu_o}\right)_{l,k}^{n+1}(p_{i,j,k}^{n+1} - p_{wf,l,k}^{n+1}). \end{aligned} \tag{B–15}$$

The derivative of the flow equation for component m in gridblock i, j, k with respect to an element of primary variables y_l^{n+1} is

$$\frac{\partial f_{m,i,j,k}^{n+1}}{\partial y_l^{n+1}} = \frac{\partial F_{m,i,j,k}^{n+1}}{\partial y_l^{n+1}} - \frac{\partial A_{m,i,j,k}^{n+1}}{\partial y_l^{n+1}} - \frac{\partial q_{m,i,j,k}^{n+1}}{\partial y_l^{n+1}}, \tag{B–16}$$

where $m = o, w, g$. Most of elements in the matrix $[\nabla_{y^n}(f^n)^T]$ are zero. For the primary variables $p_{i,j,k}, S_{w,i,j,k}$ and $S_{g,i,j,k}$ in gridblock (i, j, k), only the flow equations in gridblock $(i-1, j, k)$,$(i+1, j, k)$, $(i, j-1, k)$,$(i, j+1, k)$,$(i, j, k-1)$,$(i, j, k+1)$ and (i, j, k) depend on $y_{i,j,k}$. So the only components of f_m^{n+1} that have an nonzero derivatives with respect to $y_{i,j,k}^{n+1}$ are $f_{m,i-1,j,k}^{n+1}$, $f_{m,i+1,j,k}^{n+1}$, $f_{m,i,j-1k}^{n+1}$, $f_{m,i,j+1,k}^{n+1}$, $f_{m,i,j,k-1}^{n+1}$, $f_{m,i,j,k+1}^{n+1}$ and $f_{m,i,j,k}^{n+1}$.

For the primary variables $p_{wf,l}$, only sink terms depend on $p_{wf,l}$, so we have

$$\frac{\partial f_{m,i,j,k}^{n+1}}{\partial p_{wf,l}^{n+1}} = -\frac{\partial q_{m,i,j,k}^{n+1}}{\partial p_{wf,l}^{n+1}}. \tag{B–17}$$

Thus, the matrix $[\nabla_{y^n}(f^n)^T]$ is sparse.

B.1.1 Derivatives of Flow Terms

Here, we calculate the derivatives of flow terms with respect to the primary variables $p_{i,j,k}, S_{w,i,j,k}$ and $S_{g,i,j,k}$ in gridblock (i, j, k).

Derivatives of flow terms in gridblock $(i \pm 1, j, k)$

We begin by considering the derivatives of flow terms at gridblock $(i \pm 1, j, k)$ with respect to $p^n_{i,j,k}$ (for $m = o, w$)which both have the same form,

$$\frac{\partial F^n_{m,i\pm1,j,k}}{\partial p^n_{i,j,k}} = \frac{\partial T^n_{mx,i\pm1/2,j,k}}{\partial p^n_{i,j,k}}[p^n_{i,j,k} - p^n_{i\pm1,j,k} + \gamma^n_{m,i\pm1/2,j,k}(D_{i\pm1,j,k} - D_{i,j,k})] + T^n_{mx,i\pm1/2,j,k}\left[1 + \frac{\partial \gamma^n_{m,i\pm1/2,j,k}}{\partial p^n_{i,j,k}}(D_{i\pm1,j,k} - D_{i,j,k})\right], \quad \text{(B–18)}$$

for $m = o, w$. The derivatives of gas flow equation $F^n_{g,i\pm1,j,k}$ with respect to $p^n_{i,j,k}$ is

$$\begin{aligned}\frac{\partial F^n_{g,i\pm1,j,k}}{\partial p^n_{i,j,k}} &= \frac{\partial T^n_{gx,i\pm1/2,j,k}}{\partial p^n_{i,j,k}}[p^n_{i,j,k} - p^n_{i\pm1,j,k} + \gamma^n_{g,i\pm1/2,j,k}(D_{i\pm1,j,k} - D_{i,j,k})] \\ &\quad + T^n_{gx,i\pm1/2,j,k}[1 + \frac{\partial \gamma^n_{g,i\pm1/2,j,k}}{\partial p^n_{i,j,k}}(D_{i\pm1,j,k} - D_{i,j,k})] \\ &\quad + \frac{\partial (R^n_{so,i\pm1/2,j,k}T^n_{ox,i\pm1/2,j,k})}{\partial p^n_{i,j,k}}[p^n_{i,j,k} - p^n_{i\pm1,j,k} + \gamma^n_{o,i\pm1/2,j,k}(D_{i\pm1,j,k} - D_{i,j,k})] \\ &\quad + R^n_{so,i\pm1/2,j,k}T^n_{ox,i\pm1/2,j,k}[1 + \frac{\partial}{\partial p^n_{i,j,k}}\gamma^n_{o,i\pm1/2,j,k}(D_{i\pm1,j,k} - D_{i,j,k})]. \quad \text{(B–19)}\end{aligned}$$

Similarly, we evaluate the derivatives of $F^n_{m,i\pm1,j,k}$ with respect to $S^n_{w,i,j,k}$ (for $m = o, w$)

$$\frac{\partial F^n_{m,i\pm1,j,k}}{\partial S^n_{w,i,j,k}} = \frac{\partial T^n_{mx,i\pm1/2,j,k}}{\partial S^n_{w,i,j,k}}[p^n_{i,j,k} - p^n_{i\pm1,j,k} + \gamma^n_{m,i\pm1/2,j,k}(D_{i\pm1,j,k} - D_{i,j,k})], \quad \text{(B–20)}$$

for $m = o, w$. The derivatives of $F^n_{g,i\pm1,j,k}$ with respect to $S^n_{w,i,j,k}$

$$\frac{\partial F^n_{g,i\pm1,j,k}}{\partial S^n_{w,i,j,k}} = \frac{\partial T^n_{ox,i\pm1/2,j,k}}{\partial S^n_{w,i,j,k}}R^n_{so,i\pm1/2,j,k}[p^n_{i,j,k} - p^n_{i\pm1,j,k} + \gamma^n_{o,i\pm1/2,j,k}(D_{i\pm1,j,k} - D_{i,j,k})]. \quad \text{(B–21)}$$

The derivatives of $F^n_{o,i\pm1,j,k}$ with respect to $S^n_{g,i,j,k}$ are given by

$$\frac{\partial F^n_{o,i\pm1,j,k}}{\partial S^n_{g,i,j,k}} = \frac{\partial T^n_{ox,i\pm1/2,j,k}}{\partial S^n_{g,i,j,k}}[p^n_{i,j,k} - p^n_{i\pm1,j,k} + \gamma^n_{o,i\pm1/2,j,k}(D_{i\pm1,j,k} - D_{i,j,k})], \quad \text{(B–22)}$$

while the water equation does not depend on gas saturation, so

$$\frac{\partial F^n_{w,i\pm1,j,k}}{\partial S^n_{g,i,j,k}} = 0. \quad \text{(B–23)}$$

The derivatives of $F^n_{g,i\pm1,j,k}$ with respect to $S^n_{g,i,j,k}$ are

$$\frac{\partial F^n_{g,i\pm1,j,k}}{\partial S^n_{g,i,j,k}} = \frac{\partial T^n_{gx,i\pm1/2,j,k}}{\partial S^n_{g,i,j,k}}[p^n_{i,j,k} - p^n_{i\pm1,j,k} + \gamma^n_{g,i\pm1/2,j,k}(D_{i\pm1,j,k} - D_{i,j,k})] + \frac{\partial T^n_{ox,i\pm1/2,j,k}}{\partial S^n_{g,i,j,k}} R^n_{so,i\pm1/2,j,k}[p^n_{i,j,k} - p^n_{i\pm1,j,k} + \gamma^n_{o,i\pm1/2,j,k}(D_{i\pm1,j,k} - D_{i,j,k})]. \quad \text{(B–24)}$$

Derivatives of flow terms in gridblock $i, j \pm 1, k$

The derivatives of oil and water flow terms, $F^n_{m,i,j\pm1,k}$ with respect to $p^n_{i,j,k}$ (for $m = o, w$), are

$$\frac{\partial F^n_{m,i,j\pm1,k}}{\partial p^n_{i,j,k}} = \frac{\partial T^n_{my,i,j\pm1/2,k}}{\partial p^n_{i,j,k}}[p^n_{i,j,k} - p^n_{i,j\pm1,k} + \gamma^n_{m,i,j\pm1/2,k}(D_{i,j\pm1,k} - D_{i,j,k})] + T^n_{my,i,j\pm1/2,k}[1 + \frac{\partial \gamma^n_{m,i,j\pm1/2,k}}{\partial p^n_{i,j,k}}(D_{i,j\pm1,k} - D_{i,j,k})] \quad \text{(B–25)}$$

for $m = o, w$. The derivatives of the gas flow terms $F^n_{g,i,j\pm1,k}$ with respect to $p^n_{i,j,k}$ are

$$\frac{\partial F^n_{g,i,j\pm1,k}}{\partial p^n_{i,j,k}} = \frac{\partial T^n_{gy,i,j\pm1/2,k}}{\partial p^n_{i,j,k}}[p^n_{i,j,k} - p^n_{i,j\pm1,k} + \gamma^n_{g,i,j\pm1/2,k}(D_{i,j\pm1,k} - D_{i,j,k})] + T^n_{gy,i,j\pm1/2,k}[1 + \frac{\partial \gamma^n_{g,i,j\pm1/2,k}}{\partial p^n_{i,j,k}}(D_{i,j\pm1,k} - D_{i,j,k})] + \frac{\partial (R^n_{so,i,j\pm1/2,k} T^n_{oy,i,j\pm1/2,k})}{\partial p^n_{i,j,k}}[p^n_{i,j,k} - p^n_{i,j\pm1,k} + \gamma^n_{o,i,j\pm1/2,k}(D_{i,j\pm1,k} - D_{i,j,k})] + R^n_{so,i,j\pm1/2,k} T^n_{oy,i,j\pm1/2,k}[1 + \frac{\partial \gamma^n_{o,i,j\pm1/2,k}}{\partial p^n_{i,j,k}}(D_{i,j\pm1,k} - D_{i,j,k})]. \quad \text{(B–26)}$$

The derivatives of $F^n_{m,i,j\pm1,k}$ with respect to $S^n_{w,i,j,k}$ (for $m = o, w$) are

$$\frac{\partial F^n_{m,i,j\pm1,k}}{\partial S^n_{w,i,j,k}} = \frac{\partial T^n_{my,i,j\pm1/2,k}}{\partial S^n_{w,i,j,k}}[p^n_{i,j,k} - p^n_{i,j\pm1,k} + \gamma^n_{m,i,j\pm1/2,k}(D_{i,j\pm1,k} - D_{i,j,k})], \quad \text{(B–27)}$$

for $m = o, w$. The derivatives of $F^n_{g,i,j\pm1,k}$ with respect to $S^n_{w,i,j,k}$ are

$$\frac{\partial F^n_{g,i,j\pm1,k}}{\partial S^n_{w,i,j,k}} = \frac{\partial T^n_{oy,i,j\pm1/2,k}}{\partial S^n_{w,i,j,k}} R^n_{so,i,j\pm1/2,k}[p^n_{i,j,k} - p^n_{i,j\pm1,k} + \gamma^n_{o,i,j\pm1/2,k}(D_{i,j\pm1,k} - D_{i,j,k})]. \quad \text{(B–28)}$$

The derivatives of the oil flow terms, $F^n_{o,i,j\pm1,k}$ with respect to $S^n_{g,i,j,k}$ are

$$\frac{\partial F^n_{o,i,j\pm1,k}}{\partial S^n_{g,i,j,k}} = \frac{\partial T^n_{oy,i,j\pm1/2,k}}{\partial S^n_{g,i,j,k}}[p^n_{i,j,k} - p^n_{i,j\pm1,k} + \gamma^n_{o,i,j\pm1/2,k}(D_{i,j\pm1,k} - D_{i,j,k})]. \quad \text{(B–29)}$$

The water flow term does not depend on the gas saturation, so the derivatives of $F^n_{w,i,j\pm1,k}$ with respect to $S^n_{g,i,j,k}$ are

$$\frac{\partial F^n_{w,i,j\pm1,k}}{\partial S^n_{g,i,j,k}} = 0. \quad \text{(B–30)}$$

The gas saturation affects the oil and gas transmissibility, so the derivatives of $F^n_{g,i,j\pm1,k}$ with respect to $S^n_{g,i,j,k}$ are

$$\begin{aligned}\frac{\partial F^n_{g,i,j\pm1,k}}{\partial S^n_{g,i,j,k}} &= \frac{\partial T^n_{gy,i,j\pm1/2,k}}{\partial S^n_{g,i,j,k}}[p^n_{i,j,k} - p^n_{i,j\pm1,k} + \gamma^n_{g,i,j\pm1/2,k}(D_{i,j\pm1,k} - D_{i,j,k})] \\ &+ \frac{\partial T^n_{oy,i,j\pm1/2,k}}{\partial S^n_{g,i,j,k}} R^n_{so,i,j\pm1/2,k}[p^n_{i,j,k} - p^n_{i,j\pm1,k} + \gamma^n_{o,i,j\pm1/2,k}(D_{i,j\pm1,k} - D_{i,j,k})]. \quad \text{(B–31)}\end{aligned}$$

Derivatives of flow terms in gridblock $(i, j, k \pm 1)$

In this subsection, we compute the derivatives of flow terms at gridblock $(i, j, k \pm 1)$. The derivatives of $F^n_{m,i,j,k\pm1}$ with respect to $p^n_{i,j,k}$ (for $m = o, w$) are

$$\begin{aligned}\frac{\partial F^n_{m,i,j,k\pm1}}{\partial p^n_{i,j,k}} &= \frac{\partial T^n_{mz,i,j,k\pm1/2}}{\partial p^n_{i,j,k}}[p^n_{i,j,k} - p^n_{i,j,k\pm1} + \gamma^n_{m,i,j,k\pm1/2}(D_{i,j,k\pm1} - D_{i,j,k})] \\ &+ T^n_{mz,i,j,k\pm1/2}\left[1 + \frac{\partial \gamma^n_{m,i,j,k\pm1/2}}{\partial p^n_{i,j,k}}(D_{i,j,k\pm1} - D_{i,j,k})\right], \quad \text{(B–32)}\end{aligned}$$

for $m = o, w$, while the derivatives of $F^n_{g,i,j,k\pm1}$ with respect to $p^n_{i,j,k}$ are

$$\begin{aligned}\frac{\partial F^n_{g,i,j,k\pm1}}{\partial p^n_{i,j,k}} &= \frac{\partial T^n_{gz,i,j,k\pm1/2}}{\partial p^n_{i,j,k}}[p^n_{i,j,k} - p^n_{i,j,k\pm1} + \gamma^n_{g,i,j,k\pm1/2}(D_{i,j,k\pm1} - D_{i,j,k})] \\ &+ T^n_{gz,i,j,k\pm1/2}[1 + \frac{\partial \gamma^n_{g,i,j,k\pm1/2}}{\partial p^n_{i,j,k}}(D_{i,j,k\pm1} - D_{i,j,k})] \\ &+ \frac{\partial (R^n_{so,i,j,k\pm1/2} T^n_{oz,i,j,k\pm1/2})}{\partial p^n_{i,j,k}}[p^n_{i,j,k} - p^n_{i,j,k\pm1} + \gamma^n_{o,i,j,k\pm1/2}(D_{i,j,k\pm1} - D_{i,j,k})] \\ &+ R^n_{so,i,j,k\pm1/2} T^n_{oz,i,j,k\pm1/2}[1 + \frac{\partial \gamma^n_{o,i,j,k\pm1/2}}{\partial p^n_{i,j,k}}(D_{i,j,k\pm1} - D_{i,j,k})]. \quad \text{(B–33)}\end{aligned}$$

The derivatives of oil and water flow terms $F^n_{m,i,j,k\pm1}$ with respect to water saturation $S^n_{w,i,j,k}$ are

$$\frac{\partial F^n_{m,i,j,k\pm1}}{\partial S^n_{w,i,j,k}} = \frac{\partial T^n_{mz,i,j,k\pm1/2}}{\partial S^n_{w,i,j,k}}[p^n_{i,j,k} - p^n_{i,j,k\pm1} + \gamma^n_{m,i,j,k\pm1/2}(D_{i,j,k\pm1} - D_{i,j,k})], \quad \text{(B–34)}$$

for $m = o, w$. For gas, the derivatives of $F^n_{g,i,j,k\pm1}$ with respect to $S^n_{w,i,j,k}$ are

$$\frac{\partial F^n_{g,i,j,k\pm1}}{\partial S^n_{w,i,j,k}} = \frac{\partial T^n_{oz,i,j,k\pm1/2}}{\partial S^n_{w,i,j,k}} R^n_{so,i,j,k\pm1/2}[p^n_{i,j,k} - p^n_{i,j,k\pm1} + \gamma^n_{o,i,j,k\pm1/2}(D_{i,j,k\pm1} - D_{i,j,k})]. \quad \text{(B–35)}$$

The derivatives of the oil flow terms $F^n_{o,i,j,k\pm1}$ with respect to gas saturation, $S^n_{g,i,j,k}$, are

$$\frac{\partial F^n_{o,i,j,k\pm1}}{\partial S^n_{g,i,j,k}} = \frac{\partial T^n_{oz,i,j,k\pm1/2}}{\partial S^n_{g,i,j,k}}[p^n_{i,j,k} - p^n_{i,j,k\pm1} + \gamma^n_{o,i,j,k\pm1/2}(D_{i,j,k\pm1} - D_{i,j,k})]. \quad \text{(B–36)}$$

Again, the water flow terms do not depend on gas saturation, so the derivatives of $F^n_{w,i,j,k\pm1}$ with respect to $S^n_{g,i,j,k}$ are

$$\frac{\partial F^n_{w,i,j,k\pm1}}{\partial S^n_{g,i,j,k}} = 0. \quad \text{(B–37)}$$

Finally, the derivatives of $F^n_{g,i,j,k\pm1}$ with respect to $S^n_{g,i,j,k}$ are

$$\begin{aligned}\frac{\partial F^n_{g,i,j,k\pm1}}{\partial S^n_{g,i,j,k}} &= \frac{\partial T^n_{gz,i,j,k\pm1/2}}{\partial S^n_{g,i,j,k}}[p^n_{i,j,k} - p^n_{i,j,k\pm1} + \gamma^n_{g,i,j,k\pm1/2}(D_{i,j,k\pm1} - D_{i,j,k})] \\ &+ \frac{\partial T^n_{oz,i,j,k\pm1/2}}{\partial S^n_{gw,i,j,k}} R^n_{so,i,j,k\pm1/2}[p^n_{i,j,k} - p^n_{i,j,k\pm1} + \gamma^n_{o,i,j,k\pm1/2}(D_{i,j,k\pm1} - D_{i,j,k})]. \quad \text{(B–38)}\end{aligned}$$

Derivatives of flow terms in gridblock (i, j, k)

The flow terms at gridblock (i, j, k) have the derivatives,

$$\frac{\partial F^n_{m,i,j,k}}{\partial p^n_{i,j,k}} = -\left(\frac{\partial F^n_{m,i+1,j,k}}{\partial p^n_{i,j,k}} + \frac{\partial F^n_{m,i-1,j,k}}{\partial p^n_{i,j,k}} + \frac{\partial F^n_{m,i,j+1,k}}{\partial p^n_{i,j,k}} + \frac{\partial F^n_{m,i,j-1,k}}{\partial p^n_{i,j,k}} + \frac{\partial F^n_{m,i,j,k+1}}{\partial p^n_{i,j,k}} + \frac{\partial F^n_{m,i,j,k-1}}{\partial p^n_{i,j,k}}\right), \quad \text{(B–39)}$$

$$\frac{\partial F^n_{m,i,j,k}}{\partial S^n_{w,i,j,k}} = -\left(\frac{\partial F^n_{m,i+1,j,k}}{\partial S^n_{w,i,j,k}} + \frac{\partial F^n_{m,i-1,j,k}}{\partial S^n_{w,i,j,k}} + \frac{\partial F^n_{m,i,j+1,k}}{\partial S^n_{w,i,j,k}} + \frac{\partial F^n_{m,i,j-1,k}}{\partial S^n_{w,i,j,k}} + \frac{\partial F^n_{m,i,j,k+1}}{\partial S^n_{w,i,j,k}} + \frac{\partial F^n_{m,i,j,k-1}}{\partial S^n_{w,i,j,k}}\right), \quad \text{(B–40)}$$

and

$$\frac{\partial F^n_{m,i,j,k}}{\partial S^n_{g,i,j,k}} = -\left(\frac{\partial F^n_{m,i+1,j,k}}{\partial S^n_{g,i,j,k}} + \frac{\partial F^n_{m,i-1,j,k}}{\partial S^n_{g,i,j,k}} + \frac{\partial F^n_{m,i,j+1,k}}{\partial S^n_{g,i,j,k}} + \frac{\partial F^n_{m,i,j-1,k}}{\partial S^n_{g,i,j,k}} + \frac{\partial F^n_{m,i,j,k+1}}{\partial S^n_{g,i,j,k}} + \frac{\partial F^n_{m,i,j,k-1}}{\partial S^n_{g,i,j,k}}\right). \tag{B–41}$$

for $m = o, w, g$.

To calculate the derivatives of flow terms F with respect to primary variables, $p_{i,j,k}, S_{w,i,j,k}$, and $S_{g,i,j,k}$ (Eqs. B–18 to Eqs. B–41), one needs to calculate the derivatives of transmissibility terms (T) and gravity terms (γ) with respect to these primary variables. The following subsections provide the details of the calculation of these derivatives.

Derivatives of Transmissibility T Recall the transmissibilities can be written as

$$T^n_{mx,i+1/2,j,k} = \frac{C_1 \Delta y_j \Delta z_k k_{x,i+1/2,j,k}}{x_{i+1} - x_i} \frac{k^n_{rm,i+1/2,j,k}}{\mu^n_{m,i+1/2,j,k} B^n_{m,i+1/2,j,k}}, \tag{B–42}$$

for $m = o, w, g$ and $i = 1, 2, \ldots, n_x - 1$, For no-flow boundary conditions, the transmissibilities at the boundaries are

$$T^n_{mx,1/2,j,k} = T^n_{mx,n_x+1/2,j,k} = 0. \tag{B–43}$$

Similarly,

$$T^n_{my,i,j+1/2,k} = \frac{C_1 \Delta x_i \Delta z_k k_{y,i,j+1/2,k}}{y_{j+1} - y_j} \frac{k^n_{rm,i,j+1/2,k}}{\mu^n_{m,i,j+1/2,k} B^n_{m,i,j+1/2,k}}, \tag{B–44}$$

for $m = o, w, g$ and $j = 1, 2, \ldots, n_y - 1$ and

$$T^n_{my,i,1/2,k} = T^n_{my,i,n_y+1/2,k} = 0. \tag{B–45}$$

Finally, transmissibilities in the vertical direction are given by

$$T^n_{mz,i,j,k+1/2} = \frac{C_1 \Delta y_j \Delta x_i k_{z,i,j,k+1/2}}{z_{k+1} - z_k} \frac{k^n_{rm,i,j,k+1/2}}{\mu^n_{m,i,j,k+1/2} B^n_{m,i,j,k+1/2}}, \tag{B–46}$$

for $m = o, w, g$ and $k = 1, 2, \ldots, n_z - 1$ and

$$T^n_{mz,i,j,1/2} = T^n_{my,i,j,n_z+1/2} = 0. \tag{B–47}$$

In this work , the $k^n_{rm,i+1/2,j,k}$, $k^n_{rm,i,j+1/2,k}$, $k^n_{rm,i,j,k+1/2}$, $(B_m)_{i+1/2,j,k}$, $(B_m)_{i,j+1/2,k}$, $(B_m)_{i,j,k+1/2}$, $(\mu_m)_{i+1/2,j,k}$, $(\mu_m)_{i,j+1/2,k}$ and $(\mu_m)_{i,j,k+1/2}$ are evaluated by upstream weighting. For example, for k^n_{rm},

$$k^n_{rm,i+1/2,j,k} = \begin{cases} k^n_{rm,i+1,j,k} & \text{if } (i+1,j,k) \text{ is upstream} \\ k^n_{rm,i,j,k} & \text{if } (i,j,k) \text{ is upstream} \end{cases} \tag{B–48}$$

$$k^n_{rm,i,j+1/2,k} = \begin{cases} k^n_{rm,i,j+1,k} & \text{if } (i,j+1,k) \text{ is upstream} \\ k^n_{rm,i,j,k} & \text{if } (i,j,k) \text{ is upstream} \end{cases} \tag{B–49}$$

and

$$k^n_{rm,i,j,k+1/2} = \begin{cases} k^n_{rm,i,j,k+1} & \text{if } (i,j,k+1) \text{ is upstream} \\ k^n_{rm,i,j,k} & \text{if } (i,j,k) \text{ is upstream} \end{cases} \tag{B–50}$$

The derivatives of the transmissibilities with respect to pressure are

$$\begin{aligned} \frac{\partial T^n_{mx,i+1/2,j,k}}{\partial p^n_{i,j,k}} &= -\frac{C_1 \Delta y_j \Delta z_k k_{x,i+1/2,j,k}}{x_{i+1} - x_i} \times \frac{k^n_{rm,i+1/2,j,k}}{(\mu^n_{m,i+1/2,j,k} B^n_{m,i+1/2,j,k})^2} \\ &\quad \left\{ \frac{\partial B^n_{m,i+1/2,j,k}}{\partial p^n_{i,j,k}} \mu^n_{m,i+1/2,j,k} + \frac{\partial \mu^n_{m,i+1/2,j,k}}{\partial p^n_{i,j,k}} B^n_{m,i+1/2,j,k} \right\} \\ &= -\frac{T^n_{mx,i+1/2,j,k}}{\mu^n_{m,i+1/2,j,k} B^n_{m,i+1/2,j,k}} \\ &\quad \left\{ \frac{\partial B^n_{m,i+1/2,j,k}}{\partial p^n_{i,j,k}} \mu^n_{m,i+1/2,j,k} + \frac{\partial \mu^n_{m,i+1/2,j,k}}{\partial p^n_{i,j,k}} B^n_{m,i+1/2,j,k} \right\}, \end{aligned} \tag{B–51}$$

$$\begin{aligned} \frac{\partial T^n_{my,i,j+1/2,k}}{\partial p^n_{i,j,k}} &= -\frac{C_1 \Delta x_i \Delta z_k k_{y,i,j+1/2,k}}{y_{j+1} - y_j} \times \frac{k^n_{rm,i,j+1/2,k}}{(\mu^n_{m,i,j+1/2,k} B^n_{m,i,j+1/2,k})^2} \\ &\quad \left\{ \frac{\partial B^n_{m,i,j+1/2,k}}{\partial p^n_{i,j,k}} \mu^n_{m,i,j+1/2,k} + \frac{\partial \mu^n_{m,i,j+1/2,k}}{\partial p^n_{i,j,k}} B^n_{m,i,j+1/2,k} \right\} \\ &= -\frac{T^n_{my,i,j+1/2,k}}{\mu^n_{m,i,j+1/2,k} B^n_{m,i,j+1/2,k}} \\ &\quad \left\{ \frac{\partial B^n_{m,i,j+1/2,k}}{\partial p^n_{i,j,k}} \mu^n_{m,i,j+1/2,k} + \frac{\partial \mu^n_{m,i,j+1/2,k}}{\partial p^n_{i,j,k}} B^n_{m,i,j+1/2,k} \right\}, \end{aligned} \tag{B–52}$$

and

$$\frac{\partial T^n_{mz,i,j,k+1/2}}{\partial p^n_{i,j,k}} = -\frac{C_1 \Delta x_i \Delta y_j k_{z,i,j,k+1/2}}{z_{k+1} - z_k} \times \frac{k^n_{rm,i,j,k+1/2}}{(\mu^n_{m,i,j,k+1/2} B^n_{m,i,j,k+1/2})^2}$$
$$\left\{ \frac{\partial B^n_{m,i,j,k+1/2}}{\partial p^n_{i,j,k}} \mu^n_{m,i,j,k+1/2} + \frac{\partial \mu^n_{m,i,j,k+1/2}}{\partial p^n_{i,j,k}} B^n_{m,i,j,k+1/2} \right\}$$
$$= -\frac{T^n_{mz,i,j,k+1/2}}{\mu^n_{m,i,j,k+1/2} B^n_{m,i,j,k+1/2}}$$
$$\left\{ \frac{\partial B^n_{m,i,j,k+1/2}}{\partial p^n_{i,j,k}} \mu^n_{m,i,j,k+1/2} + \frac{\partial \mu^n_{m,i,j,k+1/2}}{\partial p^n_{i,j,k}} B^n_{m,i,j,k+1/2} \right\} \qquad \text{(B–53)}$$

for $m = o, w, g$. The derivatives of transmissibilities at boundaries are all equal to 0.

The formation volume factor(B), viscosity(μ), and solution gas oil ratio (R_{so}) are all evaluated by upstream weighting. So the derivatives these terms are given by

$$\frac{\partial B^n_{m,i+1/2,j,k}}{\partial p_{i,j,k}} = \frac{\partial B^n_{m,i,j+1/2,k}}{\partial p_{i,j,k}} = \frac{\partial B^n_{m,i,j,k+1/2}}{\partial p_{i,j,k}} = \begin{cases} \frac{\partial B^n_{m,i,j,k}}{\partial p_{i,j,k}} & \text{if } (i,j,k) \text{ is upstream} \\ 0 & \text{if } (i,j,k) \text{ is not upstream} \end{cases} \qquad \text{(B–54)}$$

$$\frac{\partial \mu^n_{m,i+1/2,j,k}}{\partial p_{i,j,k}} = \frac{\partial \mu^n_{m,i,j+1/2,k}}{\partial p_{i,j,k}} = \frac{\partial \mu^n_{m,i,j,k+1/2}}{\partial p_{i,j,k}} = \begin{cases} \frac{\partial \mu^n_{m,i,j,k}}{\partial p_{i,j,k}} & \text{if } (i,j,k) \text{ is upstream} \\ 0 & \text{if } (i,j,k) \text{ is not upstream} \end{cases} \qquad \text{(B–55)}$$

and

$$\frac{\partial R^n_{so,i+1/2,j,k}}{\partial p_{i,j,k}} = \frac{\partial R^n_{so,i,j+1/2,k}}{\partial p_{i,j,k}} = \frac{\partial R^n_{so,i,j,k+1/2}}{\partial p_{i,j,k}} = \begin{cases} \frac{\partial R^n_{so,i,j,k}}{\partial p_{i,j,k}} & \text{if } (i,j,k) \text{ is upstream} \\ 0 & \text{if } (i,j,k) \text{ is not upstream} \end{cases} \qquad \text{(B–56)}$$

The derivatives, $\frac{\partial B^n_{m,i,j,k}}{\partial p_{i,j,k}}$, $\frac{\partial \mu^n_{m,i,j,k}}{\partial p_{i,j,k}}$, and $\frac{\partial R^n_{so,i,j,k}}{\partial p_{i,j,k}}$ can be evaluated from the PVT tables.

Derivatives of Three Phase Relative Permeability To calculate the derivatives of transmissibility terms (T) with respect to water saturation (S_w) or gas saturation (S_g), one needs to calculate the derivatives of three-phase relative permeability

with respect to S_w and S_g. Recall that

$$k_{rw} = k_{rw}(S_w), \tag{B–57}$$

$$k_{rg} = k_{rg}(S_g), \tag{B–58}$$

and

$$\begin{aligned} k_{ro} &= k_{ro}(S_w, S_g) \\ &= k_{rocw}[([k_{row}/k_{rocw}] + k_{rw})([k_{rog}/k_{rocw}] + k_{rg}) - (k_{rw} + k_{rg})]. \end{aligned} \tag{B–59}$$

where k_{row} is the oil relative permeability in the oil-water system, with

$$k_{row} = k_{row}(S_w). \tag{B–60}$$

and the k_{rog} is the gas relative permeability in the oil-gas system

$$k_{rog} = k_{rog}(S_g). \tag{B–61}$$

We also have

$$S_o = 1 - S_g - S_w. \tag{B–62}$$

It is easy to see that only two of the variables S_g, S_o and S_w are independent. The third one can be calculated from Eq. B–62. In the adjoint system, we assume that S_g and S_w are independent variables. From Eq. B–57 and B–60 in the oil-water system, the derivatives of k_{rw} and k_{row} with respect to S_w and S_g are given by

$$\frac{\partial k_{rw}}{\partial S_w} = \frac{\partial k_{rw}(S_w)}{\partial S_w}, \tag{B–63}$$

$$\frac{\partial k_{rw}}{\partial S_g} = 0, \tag{B–64}$$

$$\frac{\partial k_{row}}{\partial S_w} = \frac{\partial k_{row}(S_w)}{\partial S_w}, \tag{B–65}$$

and,

$$\frac{\partial k_{row}}{\partial S_g} = 0. \tag{B–66}$$

Similarly, in the gas-oil system, from Eq. B–58 and B–61, the derivatives of k_{rg} and k_{rog} with respect to S_w and S_g are given by

$$\frac{\partial k_{rg}}{\partial S_w} = 0, \tag{B–67}$$

$$\frac{\partial k_{rg}}{\partial S_g} = \frac{\partial k_{rg}(S_g)}{\partial S_g}, \tag{B–68}$$

$$\frac{\partial k_{rog}}{\partial S_w} = 0, \tag{B–69}$$

and,

$$\frac{\partial k_{rog}}{\partial S_g} = \frac{\partial k_{rog}(S_g)}{\partial S_g}. \tag{B–70}$$

From Eq. B–59, we obtain derivatives of the three-phase oil relative permeability k_{ro} with respect to S_w and S_g

$$\frac{\partial k_{ro}}{\partial S_w} = k_{rocw}\left\{\left(\frac{1}{k_{rocw}}\frac{\partial k_{row}}{\partial S_w} + \frac{\partial k_{rw}}{\partial S_w}\right)\left(\frac{1}{k_{rocw}}k_{rog} + k_{rg}\right) - \frac{\partial k_{rw}}{\partial S_w}\right\}, \tag{B–71}$$

and

$$\frac{\partial k_{ro}}{\partial S_g} = k_{rocw}\left\{\left(\frac{1}{k_{rocw}}k_{row} + k_{rw}\right)\left(\frac{1}{k_{rocw}}\frac{\partial k_{rog}}{\partial S_g} + \frac{\partial k_{rg}}{\partial S_g}\right) - \frac{\partial k_{rg}}{\partial S_g}\right\}. \tag{B–72}$$

The terms $(k^n_{rm})_{i\pm1/2,j}$ and $(k^n_{rm})_{i,j\pm1/2}$ are calculated by upstream weighting. Thus, the derivative of transmissibility with respect to water saturation S_w and gas saturation S_g are

$$\frac{\partial T^n_{mx,i+1/2,j,k}}{\partial S^n_{m1,i,j,k}} = \begin{cases} \frac{C_1\Delta y_j\Delta z_k k_{x,i+1/2,j,k}}{x_{i+1}-x_i}\frac{1}{(B\mu)^n_{m,i+1/2,j,k}}\frac{\partial(k^n_{rm})_{i,j,k}}{\partial S^n_{m1,i,j,k}} & \text{if } (i,j,k) \text{ is upstream} \\ 0 & \text{if } (i,j,k) \text{ is not upstream} \end{cases} \tag{B–73}$$

$$\frac{\partial T^n_{my,i,j+1/2,k}}{\partial S^n_{m1,i,j,k}} = \begin{cases} \frac{C_1\Delta x_i\Delta z_k k_{y,i,j+1/2,k}}{y_{j+1}-y_j}\frac{1}{(B\mu)^n_{m,i,j+1/2,k}}\frac{\partial(k^n_{rm})_{i,j,k}}{\partial S^n_{m1,i,j,k}} & \text{if } (i,j,k) \text{ is upstream} \\ 0 & \text{if } (i,j,k) \text{ is not upstream} \end{cases} \tag{B–74}$$

$$\frac{\partial T^n_{mz,i,j,k+1/2}}{\partial S^n_{m1,i,j,k}} = \begin{cases} \frac{C_1\Delta x_i\Delta y_j k_{z,i,j,k+1/2}}{z_{j+1}-z_j}\frac{1}{(B\mu)^n_{m,i,j,k+1/2}}\frac{\partial(k^n_{rm})_{i,j,k}}{\partial S^n_{m1,i,j,k}} & \text{if } (i,j,k) \text{ is upstream} \\ 0 & \text{if } (i,j,k) \text{ is not upstream} \end{cases} \tag{B–75}$$

$m = o, w, g$ and $m1 = w, g$.

The derivatives of $\frac{\partial k_{rw}}{\partial S_w}$ and $\frac{\partial k_{row}}{\partial S_w}$ are computed by using the water-oil relative permeability table. The derivatives of $\frac{\partial k_{rg}}{\partial S_g}$ and $\frac{\partial k_{rog}}{\partial S_g}$ are computed by using the gas-oil relative permeability table.

Derivatives of Gravity Terms

From Eqs. A–38 to A–39, we see that the derivatives of specific weight terms are given by

$$\frac{\partial \gamma^{n+1}_{m,i\pm1/2,j,k}}{\partial p^{n+1}_{i,j,k}} = \frac{g}{288 g_c} \frac{\partial \rho^{n+1}_{m,i,j,k}}{\partial p^{n+1}_{i,j,k}}, \tag{B–76}$$

$$\frac{\partial \gamma^{n+1}_{m,i,j\pm1/2,k}}{\partial p^{n+1}_{i,j,k}} = \frac{g}{288 g_c} \frac{\partial \rho^{n+1}_{m,i,j,k}}{\partial p^{n+1}_{i,j,k}}, \tag{B–77}$$

and

$$\frac{\partial \gamma^{n+1}_{m,i,j,k\pm1/2}}{\partial p^{n+1}_{i,j,k}} = \frac{g}{288 g_c} \frac{\partial \rho^{n+1}_{m,i,j,k}}{\partial p^{n+1}_{i,j,k}}, \tag{B–78}$$

where

$$\frac{\partial \rho^{n+1}_{o,i,j,k}}{\partial p^{n+1}_{i,j,k}} = -\frac{1}{(B^{n+1}_o)^2} \frac{\partial B^{n+1}_o}{\partial p^{n+1}_{i,j,k}} (\rho_{osc} + \frac{1}{5.615} R^{n+1}_{so,i,j,k} \rho_{gsc}) + \frac{\rho_{gsc}}{5.615 B^{n+1}_o} \frac{\partial R^{n+1}_{so,i,j,k}}{\partial p^{n+1}_{i,j,k}}, \tag{B–79}$$

$$\frac{\partial \rho^{n+1}_{w,i,j,k}}{\partial p^{n+1}_{i,j,k}} = -\frac{\rho_{wsc}}{(B^{n+1}_w)^2} \frac{\partial B^{n+1}_w}{\partial p^{n+1}_{i,j,k}}, \tag{B–80}$$

and

$$\frac{\partial \rho^{n+1}_{g,i,j,k}}{\partial p^{n+1}_{i,j,k}} = -\frac{\rho_{gsc}}{5.615 (B^{n+1}_g)^2} \frac{\partial B^{n+1}_g}{\partial p^{n+1}_{i,j,k}}. \tag{B–81}$$

The derivatives of formation volume factors and the solution gas-oil ratio are calculated from the PVT table.

B.1.2 Derivatives of Accumulation Terms

From the definition of accumulation terms in Eqs. B–10 to B–12, the derivatives of $A^{n+1}_{o,i,j,k}$ are

$$\frac{\partial A^{n+1}_{o,i,j,k}}{\partial p^{n+1}_{i,j,k}} = -\frac{V_{i,j,k} \phi_{i,j,k} S^{n+1}_{o,i,j,k}}{C_2 \Delta t^{n+1} (B^{n+1}_{o,i,j,k})^2} \frac{\partial B^{n+1}_{o,i,j,k}}{\partial p^{n+1}_{i,j,k}}, \tag{B–82}$$

$$\frac{\partial A_{o,i,j,k}^{n+1}}{\partial S_{w,i,j,k}^{n+1}} = -\frac{V_{i,j,k}\phi_{i,j,k}}{C_2 \Delta t^{n+1} B_{o,i,j,k}^{n+1}}, \tag{B–83}$$

and

$$\frac{\partial A_{o,i,j,k}^{n+1}}{\partial S_{g,i,j,k}^{n+1}} = -\frac{V_{i,j,k}\phi_{i,j,k}}{C_2 \Delta t^{n+1} B_{o,i,j,k}^{n+1}}. \tag{B–84}$$

The derivatives of $A_{w,i,j,k}^{n+1}$ are

$$\frac{\partial A_{w,i,j,k}^{n+1}}{\partial p_{i,j,k}^{n+1}} = -\frac{V_{i,j,k}\phi_{i,j,k} S_{w,i,j,k}^{n+1}}{C_2 \Delta t^{n+1} (B_{w,i,j,k}^{n+1})^2} \frac{\partial B_{w,i,j,k}^{n+1}}{\partial p_{i,j,k}^{n+1}}, \tag{B–85}$$

$$\frac{\partial A_{w,i,j,k}^{n+1}}{\partial S_{w,i,j,k}^{n+1}} = \frac{V_{i,j,k}\phi_{i,j,k}}{C_2 \Delta t^{n+1} B_{w,i,j,k}^{n+1}}, \tag{B–86}$$

and

$$\frac{\partial A_{w,i,j,k}^{n+1}}{\partial S_{g,i,j,k}^{n+1}} = 0. \tag{B–87}$$

The derivatives of $A_{g,i,j,k}^{n+1}$ are

$$\frac{\partial A_{g,i,j,k}^{n+1}}{\partial p_{i,j,k}^{n+1}} = \frac{V_{i,j,k}\phi_{i,j,k}}{C_2 \Delta t^{n+1}} \left(-\frac{S_g}{(B_g)^2} \frac{\partial B_g}{\partial p} + \frac{\partial R_{so}}{\partial p} \frac{S_o}{B_o} - \frac{R_{so} S_o}{(B_o)^2} \frac{\partial B_o}{\partial p} \right)_{i,j,k}^{n+1}, \tag{B–88}$$

$$\frac{\partial A_{g,i,j,k}^{n+1}}{\partial S_{w,i,j,k}^{n+1}} = -\frac{V_{i,j,k}\phi_{i,j,k}}{C_2 \Delta t^{n+1}} \left(\frac{R_{so}}{B_o} \right)_{i,j,k}^{n+1}, \tag{B–89}$$

and

$$\frac{\partial A_{g,i,j,k}^{n+1}}{\partial S_{g,i,j,k}^{n+1}} = \frac{V_{i,j,k}\phi_{i,j,k}}{C_2 \Delta t^{n+1}} \left(\frac{1}{B_g} - \frac{R_{so}}{B_o} \right)_{i,j,k}^{n+1}. \tag{B–90}$$

For Eq. B-1, we aslo need the derivatives of sink term with respect to primary variables.

B.1.3 Derivatives of Sink Terms

In this section, we compute the derivatives of sink/source terms in the flow equations with respect to the primary variables, p, S_w, S_g, and $p_{wf,l}$.

Producing Wells (Q_o,Q_t, or p_{wf} Specified)

For the producing wells, Eqs. A–62 to A–64 indicate that production rates at layer $k0$ of well l are

$$q^{n+1}_{m,l,k0} = T^{n+1}_{m,l,k0}[p^{n+1}_{l,k0} - p^{n+1}_{wf,l} - dp^{n+1}_{wf,l,k0}], \tag{B–91}$$

for $m = o, w, g$, where,

$$T^{n+1}_{o,l,k} = WI_{l,k}\left(\frac{k_{ro}}{B_o\mu_o}\right)^{n+1}_{l,k}, \tag{B–92}$$

$$T^{n+1}_{w,l,k} = WI_{l,k}\left(\frac{k_{rw}}{B_w\mu_w}\right)^{n+1}_{l,k}, \tag{B–93}$$

and

$$T^{n+1}_{g,l,k} = WI_{l,k}\left(\frac{k_{rg}}{B_g\mu_g} + R_{so}\frac{k_{ro}}{B_o\mu_o}\right)^{n+1}_{l,k}. \tag{B–94}$$

When $k = k0$, we have the derivatives

$$\begin{aligned}\frac{\partial q^{n+1}_{m,l,k0}}{\partial p^{n+1}_{l,k}} &= \frac{\partial}{\partial p^{n+1}_{l,k0}}\{T^{n+1}_{m,l,k0}[p^{n+1}_{l,k0} - p^{n+1}_{wf,l} - dp^{n+1}_{wf,l,k}]\} \\ &= T^{n+1}_{m,l,k0} + \frac{\partial T^{n+1}_{m,l,k0}}{\partial p^{n+1}_{l,k0}}[p^{n+1}_{l,k0} - p^{n+1}_{wf,l} - dp^{n+1}_{wf,l,k}],\end{aligned} \tag{B–95}$$

and

$$\frac{\partial q^{n+1}_{m,l,k0}}{\partial S^{n+1}_{m1,l,k}} = \frac{\partial q^{n+1}_{m,l,k0}}{\partial S^{n+1}_{m1,l,k0}} = \frac{\partial T^{n+1}_{m,l,k0}}{\partial S^{n+1}_{m1,l,k0}}[p^{n+1}_{l,k0} - p^{n+1}_{wf,l} - dp^{n+1}_{wf,l,k}], \tag{B–96}$$

for $m = o, w, g$; and $m1 = w, g$.

For $k \neq k0$,

$$\frac{\partial q^{n+1}_{m,l,k0}}{\partial p^{n+1}_{l,k}} = \frac{\partial q^{n+1}_{m,l,k0}}{\partial S^{n+1}_{m1,l,k}} = 0, \tag{B–97}$$

for $m = o, w, g$; $m1 = w, g$.

The derivatives of $q^{n+1}_{m,l,k0}$ with respect to bottom hole pressure $p^{n+1}_{wf,l}$ are given by

$$\frac{\partial q^{n+1}_{m,l,k0}}{\partial p^{n+1}_{wf,l}} = -T^{n+1}_{m,l,k0}. \tag{B–98}$$

From the definition of terms $T^{n+1}_{m,l,k}$ in Eqs. B–92 to B–94, the derivatives of $T^{n+1}_{m,l,k}$ to $p^{n+1}_{l,k}$ are

$$\frac{\partial T^{n+1}_{o,l,k}}{\partial p^{n+1}_{l,k}} = -WI_{l,k}\left[\frac{k_{ro}}{(B_o\mu_o)^2}\left(\mu_o\frac{\partial B_o}{\partial p} + B_o\frac{\partial \mu_o}{\partial p}\right)\right]^{n+1}_{l,k}, \tag{B–99}$$

$$\frac{\partial T^{n+1}_{w,l,k}}{\partial p^{n+1}_{l,k}} = -WI_{l,k}\left[\frac{k_{rw}}{(B_w\mu_w)^2}\left(\mu_w\frac{\partial B_w}{\partial p} + B_w\frac{\partial \mu_w}{\partial p}\right)\right]^{n+1}_{l,k}, \tag{B–100}$$

and

$$\frac{\partial T^{n+1}_{g,l,k}}{\partial p^{n+1}_{l,k}} = WI_{l,k}\Bigg[-\frac{k_{rg}}{(B_g\mu_g)^2}\left(\mu_g\frac{\partial B_g}{\partial p} + B_g\frac{\partial \mu_g}{\partial p}\right) + \frac{k_{ro}}{(B_o\mu_o)^2}\left(B_o\mu_o\frac{\partial R_{so}}{\partial p} - R_{so}\mu_o\frac{\partial B_o}{\partial p} - R_{so}B_o\frac{\partial \mu_o}{\partial p}\right)\Bigg]^{n+1}_{l,k}. \tag{B–101}$$

The derivatives of $T^{n+1}_{m,l,k}$ to $S^{n+1}_{w,l,k}$ are

$$\frac{\partial T^{n+1}_{o,l,k}}{\partial S^{n+1}_{w,l,k}} = WI_{l,k}\left(\frac{1}{B_o\mu_o}\frac{\partial k_{ro}}{\partial S_w}\right)^{n+1}_{l,k}, \tag{B–102}$$

$$\frac{\partial T^{n+1}_{w,l,k}}{\partial S^{n+1}_{w,l,k}} = WI_{l,k}\left(\frac{1}{B_w\mu_w}\frac{\partial k_{rw}}{\partial S_w}\right)^{n+1}_{l,k}, \tag{B–103}$$

and

$$\frac{\partial T^{n+1}_{g,l,k}}{\partial S^{n+1}_{w,l,k}} = WI_{l,k}\left(\frac{R_{so}}{B_o\mu_o}\frac{\partial k_{ro}}{\partial S_w}\right)^{n+1}_{l,k}. \tag{B–104}$$

Similarly, the derivatives of $T^{n+1}_{m,l,k}$ to $S^{n+1}_{g,l,k}$ are

$$\frac{\partial T^{n+1}_{o,l,k}}{\partial S^{n+1}_{g,l,k}} = WI_{l,k}\left(\frac{1}{B_o\mu_o}\frac{\partial k_{ro}}{\partial S_g}\right)^{n+1}_{l,k}, \tag{B–105}$$

$$\frac{\partial T^{n+1}_{w,l,k}}{\partial S^{n+1}_{g,l,k}} = 0, \tag{B–106}$$

and

$$\frac{\partial T^{n+1}_{g,l,k}}{\partial S^{n+1}_{g,l,k}} = WI_{l,k}\left(\frac{1}{B_g\mu_g}\frac{\partial k_{rg}}{\partial S_g} + R_{so}\frac{1}{B_o\mu_o}\frac{\partial k_{ro}}{\partial S_g}\right)^{n+1}_{l,k}. \tag{B–107}$$

Injection Wells (Water or Gas Injection)

For water or gas injection wells, the injection rates at layer $k0$ of well l are

$$q^{n+1}_{m,l,k0} = T^{n+1}_{inj,m,l,k0}[p^{n+1}_{l,k0} - p^{n+1}_{wf,l} - dp^{n+1}_{wf,l,k}], \tag{B–108}$$

where

$$T^{n+1}_{inj,m,l,k} = \frac{WI_{l,k}}{(\mu_m B_m)^{n+1}_{l,k}}, \tag{B–109}$$

for $m = w, g$.

When $k = k0$, the derivatives of $q^{n+1}_{m,l,k0}$ with respect to $p^{n+1}_{l,k}$, $S^{n+1}_{w,l,k}$, and $S^{n+1}_{g,l,k}$ are

$$\frac{\partial q^{n+1}_{m,l,k0}}{\partial p^{n+1}_{l,k}} = \frac{\partial q^{n+1}_{m,l,k0}}{\partial p^{n+1}_{l,k0}} = T^{n+1}_{inj,m,l,k} + \frac{\partial T^{n+1}_{inj,m,l,k0}}{\partial p^{n+1}_{l,k0}}[p^{n+1}_{l,k0} - p^{n+1}_{wf,l} - dp^{n+1}_{wf,l,k}], \tag{B–110}$$

and

$$\frac{\partial q^{n+1}_{m,l,k0}}{\partial S^{n+1}_{w,l,k}} = \frac{\partial q^{n+1}_{m,l,k0}}{\partial S^{n+1}_{g,l,k}} = 0. \tag{B–111}$$

When $k \neq k0$, the derivatives of $q^{n+1}_{m,l,k0}$ to $p^{n+1}_{l,k}$, $S^{n+1}_{w,l,k}$, $S^{n+1}_{g,l,k}$ are

$$\frac{\partial q^{n+1}_{m,l,k0}}{\partial p^{n+1}_{l,k}} = \frac{\partial q^{n+1}_{m,l,k0}}{\partial S^{n+1}_{w,l,k}} = \frac{\partial q^{n+1}_{m,l,k0}}{\partial S^{n+1}_{g,l,k}} = 0. \tag{B–112}$$

The derivatives of $q^{n+1}_{m,l,k0}$ to bottom hole pressure $p^{n+1}_{wf,l,k}$ are

$$\frac{\partial q^{n+1}_{m,l,k0}}{\partial p^{n+1}_{wf,l}} = -T_{inj,m,l,k0}. \tag{B–113}$$

The derivatives of $T^{n+1}_{inj,m,l,k}$ in Eq. B–110 are given by

$$\frac{\partial T^{n+1}_{inj,m,l,k}}{\partial p^{n+1}_{l,k}} = -\frac{WI_{l,k}}{(\mu^{n+1}_{m,l,k} B^{n+1}_{m,l,k})^2}\left(B^{n+1}_{m,l,k}\frac{\partial \mu^{n+1}_{m,l,k}}{\partial p^{n+1}_{l,k}} + \mu^{n+1}_{m,l,k}\frac{\partial B^{n+1}_{m,l,k}}{\partial p^{n+1}_{l,k}}\right). \tag{B–114}$$

For water injection wells, the oil and gas rates are set to zero. Thus

$$\frac{\partial q^{n+1}_{o,l,k0}}{\partial p^{n+1}_{l,k}} = \frac{\partial q^{n+1}_{g,l,k0}}{\partial p^{n+1}_{l,k}} = \frac{\partial q^{n+1}_{o,l,k0}}{\partial S^{n+1}_{w,l,k}} = \frac{\partial q^{n+1}_{g,l,k0}}{\partial S^{n+1}_{w,l,k}} = \frac{\partial q^{n+1}_{o,l,k0}}{\partial S^{n+1}_{g,l,k}} = \frac{\partial q^{n+1}_{g,l,k0}}{\partial S^{n+1}_{g,l,k}} = 0. \tag{B–115}$$

Similarly, for gas injection wells, the water and oil rates are set to zero. So we have

$$\frac{\partial q^{n+1}_{o,l,k0}}{\partial p^{n+1}_{l,k}} = \frac{\partial q^{n+1}_{w,l,k0}}{\partial p^{n+1}_{l,k}} = \frac{\partial q^{n+1}_{o,l,k0}}{\partial S^{n+1}_{w,l,k}} = \frac{\partial q^{n+1}_{w,l,k0}}{\partial S^{n+1}_{w,l,k}} = \frac{\partial q^{n+1}_{o,l,k0}}{\partial S^{n+1}_{g,l,k}} = \frac{\partial q^{n+1}_{w,l,k0}}{\partial S^{n+1}_{g,l,k}} = 0. \tag{B–116}$$

B.2 Derivatives of Well Equations

In this section, we compute the derivatives of well constraint equations given in the section A.6 of Appendix A. For the producing wells, we consider oil rate specified, total rate specified at the reservoir conditions, and bottom hole pressure specified cases. For the injection wells, we consider both water injection and gas injection cases.

B.2.1 Q_o Specified

As shown by Eq.A–68,the well equation at well l is given by

$$f_{wf,l}^{n+1} = \sum_{k1} T_{o,l,k1}^{n+1}[p_{l,k1}^{n+1} - p_{wf,l}^{n+1} - dp_{wf,l,k1}^{n+1}] - q_{o,l}^{n+1} = 0, \tag{B–117}$$

for $m = o, w, g$, where

$$T_{o,l,k}^{n+1} = WI_{l,k}\left(\frac{k_{ro}}{B_o\mu_o}\right)_{l,k}^{n+1}. \tag{B–118}$$

The derivatives of the well constraint equations to the primary variables, p, S_w, S_g, and $p_{wf,l}$, are given by

$$\frac{\partial f_{wf,l}^{n+1}}{\partial p_{l,k}^{n+1}} = T_{o,l,k}^{n+1} + \frac{\partial T_{o,l,k}^{n+1}}{\partial p_{l,k}^{n+1}}[p_{l,k}^{n+1} - p_{wf,l}^{n+1} - dp_{wf,l,k}^{n+1}], \tag{B–119}$$

$$\frac{\partial f_{wf,l}^{n+1}}{\partial p_{wf,l}^{n+1}} = -\sum_{k1} T_{o,l,k1}^{n+1}, \tag{B–120}$$

$$\frac{\partial f_{wf,l}^{n+1}}{\partial S_{w,l,k}^{n+1}} = \frac{\partial T_{o,l,k}^{n+1}}{\partial S_{w,l,k}^{n+1}}[p_{l,k}^{n+1} - p_{wf,l}^{n+1} - dp_{wf,l,k}^{n+1}], \tag{B–121}$$

and

$$\frac{\partial f_{wf,l}^{n+1}}{\partial S_{g,l,k}^{n+1}} = \frac{\partial T_{o,l,k}^{n+1}}{\partial S_{g,l,k}^{n+1}}[p_{l,k}^{n+1} - p_{wf,l}^{n+1} - dp_{wf,l,k}^{n+1}], \tag{B–122}$$

respectively.

B.2.2 Q_t Specified at Reservoir Conditions

As indicated in Eq. A–71, when the total flow rate is specified, the well equation at well l is

$$f_{wf,l}^{n+1} = \sum_{k1} T_{t,l,k1}^{n+1}[p_{l,k1}^{n+1} - p_{wf,l}^{n+1} - dp_{wf,l,k1}^{n+1}] - q_{t,l}^{n+1} = 0, \tag{B–123}$$

for $m = o, w, g$, where the "total transmissibility" is

$$T_{t,l,k}^{n+1} = WI_{l,k}\left(\frac{k_{ro}}{\mu_o} + \frac{k_{rw}}{\mu_w} + \frac{k_{rg}}{\mu_g}\right)_{l,k}^{n+1}. \tag{B–124}$$

The derivatives of the well constraint equations to the primary variables, p, S_w, S_g, and $p_{wf,l}$, are given by

$$\frac{\partial f_{wf,l}^{n+1}}{\partial p_{l,k}^{n+1}} = T_{t,l,k}^{n+1} + \frac{\partial T_{t,l,k}^{n+1}}{\partial p_{l,k}^{n+1}}[p_{l,k}^{n+1} - p_{wf,l}^{n+1} - dp_{wf,l,k}^{n+1}], \tag{B–125}$$

$$\frac{\partial f_{wf,l}^{n+1}}{\partial p_{wf,l}^{n+1}} = -\sum_{k1} T_{t,l,k1}^{n+1}, \tag{B–126}$$

$$\frac{\partial f_{wf,l}^{n+1}}{\partial S_{w,l,k}^{n+1}} = \frac{\partial T_{t,l,k}^{n+1}}{\partial S_{w,l,k}^{n+1}}[p_{l,k}^{n+1} - p_{wf,l}^{n+1} - dp_{wf,l,k}^{n+1}], \tag{B–127}$$

and

$$\frac{\partial f_{wf,l}^{n+1}}{\partial S_{g,l,k}^{n+1}} = \frac{\partial T_{t,l,k}^{n+1}}{\partial S_{g,l,k}^{n+1}}[p_{l,k}^{n+1} - p_{wf,l}^{n+1} - dp_{wf,l,k}^{n+1}]. \tag{B–128}$$

Here, the derivatives of $T_{t,l,k}^{n+1}$ in Eqs. B–125 to B–128 are computed by

$$\frac{\partial T_{t,l,k}^{n+1}}{\partial p_{l,k}^{n+1}} = -WI_{l,k}\left(\frac{k_{ro}}{\mu_o^2}\frac{\partial \mu_o}{\partial p} + \frac{k_{rw}}{\mu_w^2}\frac{\partial \mu_w}{\partial p} + \frac{k_{rg}}{\mu_g^2}\frac{\partial \mu_g}{\partial p}\right)_{l,k}^{n+1}, \tag{B–129}$$

$$\frac{\partial T_{t,l,k}^{n+1}}{\partial S_{w,l,k}^{n+1}} = WI_{l,k}\left(\frac{1}{\mu_o}\frac{\partial k_{ro}}{\partial S_w} + \frac{1}{\mu_w}\frac{\partial k_{rw}}{\partial S_w}\right)_{l,k}^{n+1}, \tag{B–130}$$

and

$$\frac{\partial T_{t,l,k}^{n+1}}{\partial S_{g,l,k}^{n+1}} = WI_{l,k}\left(\frac{1}{\mu_o}\frac{\partial k_{ro}}{\partial S_g} + \frac{1}{\mu_g}\frac{\partial k_{rg}}{\partial S_g}\right)_{l,k}^{n+1}. \tag{B–131}$$

B.2.3 p_{wf} Specified

When the flowing pressure at the well is specified, the well equation is very simple (Eq. A–65),

$$f_{wf,l}^{n+1} = p_{wf,l,0}^{n+1} - p_{wf,l}^{n+1} = 0. \tag{B–132}$$

For the derivatives, we obtain

$$\frac{\partial f_{wf,l}^{n+1}}{\partial p_{l,k}^{n+1}} = \frac{\partial f_{wf,l}^{n+1}}{\partial S_{w,l,k}^{n+1}} = \frac{\partial f_{wf,l}^{n+1}}{\partial S_{g,l,k}^{n+1}} = 0, \tag{B–133}$$

and

$$\frac{\partial f_{wf,l}^{n+1}}{\partial p_{wf,l}^{n+1}} = -1. \tag{B–134}$$

B.2.4 Water or Gas Injection

For the water or gas injection well, the well equation at well l is given by

$$f_{wf,l}^{n+1} = \sum_{k1} T_{inj,m,l,k1}^{n+1} [p_{l,k1}^{n+1} - p_{wf,l}^{n+1} - dp_{wf,l,k1}^{n+1}] - q_{m,l}^{n+1} = 0, \tag{B–135}$$

for $m = w, g$, where $q_{m,l}^{n+1} < 0$ in the specified injection rate and

$$T_{inj,m,l,k}^{n+1} = \frac{WI_{l,k}}{(B_m \mu_m)_{l,k}^{n+1}}. \tag{B–136}$$

The derivatives of well constraint equations with respect to primary variables, p, S_w, S_g, and $p_{wf,l}$, are given by

$$\frac{\partial f_{wf,l}^{n+1}}{\partial p_{l,k}^{n+1}} = T_{inj,m,l,k}^{n+1} + \frac{\partial T_{inj,m,l,k}^{n+1}}{\partial p_{l,k}^{n+1}} [p_{l,k}^{n+1} - p_{wf,l}^{n+1} - dp_{wf,l,k}^{n+1}], \tag{B–137}$$

$$\frac{\partial f_{wf,l}^{n+1}}{\partial p_{wf,l}^{n+1}} = -\sum_{k1} T_{inj,m,l,k1}^{n+1}, \tag{B–138}$$

and

$$\frac{\partial f_{wf,l}^{n+1}}{\partial S_{w,l,k}^{n+1}} = \frac{\partial f_{wf,l}^{n+1}}{\partial S_{g,l,k}^{n+1}} = 0. \tag{B–139}$$

B.3 Computation of $[\nabla_{y^n}(f^{n+1})^T]$ in the Adjoint System

In this section, we compute the coefficient matrix $[\nabla_{y^n}(f^{n+1})^T]$ of the λ^{n+1} term which appear in the adjoint equation B–1. From the definition of f^{n+1} in Eqs. A–43 to A–45, it is to see that the matrix $[\nabla_{y^n}(f^{n+1})^T]$ only depends on the accumulation terms of the flow equations. Thus, $[\nabla_{y^n}(f^{n+1})^T]$ is a diagonal band matrix with band width equaling to 5 in the three-phase case.

For the primary variables $p^n_{i,j,k}$, $S^n_{w,i,j,k}$ and $S^n_{g,i,j,k}$ in gridblock (i,j,k), only the flow equations in gridblock (i,j,k) depend on these variables. So the only components of f^{n+1}_m that have an nonzero derivatives are $f^{n+1}_{m,i,j,k}$. The $f^{n+1}_{m,i,j,k}$ do not dependent on the primary variable $p^n_{wf,l}$, so all the derivatives of $f^{n+1}_{m,i,j,k}$ to $p^n_{wf,l}$ are equal to zero.

From the definition of flow equations in the Eqs. A–43 to A–45, the derivatives of the oil equation $f^{n+1}_{o,i,j,k}$ are given by

$$\frac{\partial f^{n+1}_{o,i,j,k}}{\partial p^n_{i,j,k}} = -\frac{V_{i,j,k}\phi_{i,j,k}S^n_{o,i,j,k}}{C_2\Delta t^{n+1}(B^n_{o,i,j,k})^2}\frac{\partial B^n_{o,i,j,k}}{\partial p^n_{i,j,k}}, \tag{B–140}$$

$$\frac{\partial f^{n+1}_{o,i,j,k}}{\partial S^n_{w,i,j,k}} = -\frac{V_{i,j,k}\phi_{i,j,k}}{C_2\Delta t^{n+1}B^n_{o,i,j,k}}, \tag{B–141}$$

and

$$\frac{\partial f^{n+1}_{o,i,j,k}}{\partial S^n_{g,i,j,k}} = -\frac{V_{i,j,k}\phi_{i,j,k}}{C_2\Delta t^{n+1}B^n_{o,i,j,k}}. \tag{B–142}$$

The derivatives of the water equation, $f^{n+1}_{w,i,j,k}$ with respect to the primary variables are

$$\frac{\partial f^{n+1}_{w,i,j,k}}{\partial p^n_{i,j,k}} = -\frac{V_{i,j,k}\phi_{i,j,k}S^{n+1}_{w,i,j,k}}{C_2\Delta t^{n+1}(B^n_{w,i,j,k})^2}\frac{\partial B^n_{w,i,j,k}}{\partial p^n_{i,j,k}}, \tag{B–143}$$

$$\frac{\partial f^{n+1}_{w,i,j,k}}{\partial S^n_{w,i,j,k}} = \frac{V_{i,j,k}\phi_{i,j,k}}{C_2\Delta t^{n+1}B^n_{w,i,j,k}}, \tag{B–144}$$

and

$$\frac{\partial f^{n+1}_{w,i,j,k}}{\partial S^n_{g,i,j,k}} = 0. \tag{B–145}$$

The derivatives of the gas equation, $f^{n+1}_{g,i,j,k}$, are

$$\frac{\partial f^{n+1}_{g,i,j,k}}{\partial p^n_{i,j,k}} = \frac{V_{i,j,k}\phi_{i,j,k}}{C_2\Delta t^{n+1}}\left(-\frac{S_g}{(B_g)^2}\frac{\partial B_g}{\partial p} + \frac{\partial R_{so}}{\partial p}\frac{S_o}{B_o} - \frac{R_{so}S_o}{(B_o)^2}\frac{\partial B_o}{\partial p}\right)^n_{i,j,k}, \tag{B–146}$$

$$\frac{\partial f^{n+1}_{g,i,j,k}}{\partial S^n_{w,i,j,k}} = -\frac{V_{i,j,k}\phi_{i,j,k}}{C_2\Delta t^{n+1}}\left(\frac{R_{so}}{B_o}\right)^n_{i,j,k}, \tag{B–147}$$

and

$$\frac{\partial f^{n+1}_{g,i,j,k}}{\partial S^n_{g,i,j,k}} = \frac{V_{i,j,k}\phi_{i,j,k}}{C_2\Delta t^{n+1}}\left(\frac{1}{B_g} - \frac{R_{so}}{B_o}\right)^n_{i,j,k}. \tag{B–148}$$

B.4 Adjoint System Source Terms $\nabla_{y^n}\beta$

To solve the adjoint system Eq. B–1, one needs to evaluate the source term $\nabla_{y^n}\beta$ in the equation. If one wants to compute the sensitivity of p_{wf}, GOR and WOR, the β will be set equal to p_{wf}, GOR and WOR, respectively.

B.4.1 Sensitivity of p_{wf} (Q_o or Q_t Specified)

If we want to compute the sensitivity of $p^r_{wf,l}$ at time t^r with respect to model parameters, then let

$$\beta = p^r_{wf,l}, \tag{B–149}$$

and we have

$$\nabla_{y^n}\beta = \nabla_{y^n} p^r_{wf,l}. \tag{B–150}$$

Recall that

$$y^n = \left[\begin{array}{ccccccccc} p^n_1 & S^n_{w,1} & S^n_{g,1} & p^n_2 & \cdots & S^n_{g,N} & p^n_{wf,1} & \cdots & p^n_{wf,N_w} \end{array}\right]. \tag{B–151}$$

We obtain the source term

$$\nabla_{y^n}\beta = \nabla_{y^n} p^r_{wf,l} = \begin{bmatrix} \frac{\partial p^r_{wf,l}}{\partial p^n_1} \\ \frac{\partial p^r_{wf,l}}{\partial S^n_{w,1}} \\ \frac{\partial p^r_{wf,l}}{\partial S^n_{g,1}} \\ \frac{\partial p^r_{wf,l}}{\partial p^n_2} \\ \vdots \\ \frac{\partial p^r_{wf,l}}{\partial S^n_{g,N}} \\ \frac{\partial p^r_{wf,l}}{\partial p^n_{wf,1}} \\ \vdots \\ \frac{\partial p^r_{wf,l}}{\partial p^n_{wf,N_w}} \end{bmatrix} = \begin{bmatrix} 0 \\ \vdots \\ 0 \\ \frac{\partial p^r_{wf,l}}{\partial p^n_{wf,l}} \\ 0 \\ \vdots \\ 0 \end{bmatrix}, \tag{B–152}$$

It follows that, for $n \neq r$,

$$\nabla_{y^n} g = 0, \tag{B–153}$$

and for $n = r$,

$$\frac{\partial p^r_{wf,l}}{\partial p^n_{wf,l}} = 1. \tag{B–154}$$

B.4.2 Sensitivity of GOR

In the case where we want to compute the sensitivity of GOR^r_l at time t^r, then

$$\beta = GOR^r_l. \tag{B–155}$$

We have

$$\nabla_{y^n}\beta = \nabla_{y^n} GOR_l^r = \begin{bmatrix} \frac{\partial GOR_l^r}{\partial p_1^n} \\ \frac{\partial GOR_l^r}{\partial S_{w,1}^n} \\ \frac{\partial GOR_l^r}{\partial S_{g,1}^n} \\ \frac{\partial GOR_l^r}{\partial p_2^n} \\ \vdots \\ \frac{\partial GOR_l^r}{\partial S_{g,N}^n} \\ \frac{\partial GOR_l^r}{\partial p_{wf,1}^n} \\ \vdots \\ \frac{\partial GOR_l^r}{\partial p_{wf,N_w}^n} \end{bmatrix}, \tag{B–156}$$

we see that

$$\nabla_{y^n} g = \nabla_{y^n} GOR_l^r = 0, \tag{B–157}$$

for $n \neq r$. If $n = r$ in the Eq. B–156, only the elements containing derivatives with respect to the primary variables $(p^n, S_w^n, S_g^n, p_{wf}^n)$ in the gridblocks where the well l is completed are nonzero. These nonzero terms are calculated by the equations presented below.

Q_o Specified In the case that oil rate is specified for well l, the gas rate at t^n is

$$q_{g,l}^n = \sum_k T_{g,l,k}^n (p_{l,k}^n - p_{wf,l,k}^n). \tag{B–158}$$

So we obtain gas-oil ratio

$$\begin{aligned} GOR_l^r &= \frac{q_{g,l}^r}{q_{o,l}^r} \\ &= \frac{1}{q_{o,l}^r} \sum_k T_{g,l,k}^r (p_{l,k}^r - p_{wf,l,k}^r) \\ &= \frac{1}{q_{o,l}^r} \sum_k T_{g,l,k}^r (p_{l,k}^r - p_{wf,l}^r - dp_{wf,l,k}^r). \end{aligned} \tag{B–159}$$

The derivatives of GOR_l^r to the primary variables, $p_{l,k}^r$, $p_{wf,l}^r$, $S_{w,l,k}^r$ and $S_{g,l,k}^r$ are given by

$$\begin{aligned}\frac{\partial GOR_l^r}{\partial p_{l,k}^r} &= \frac{1}{q_{o,l}^r}\frac{\partial}{\partial p_{l,k}^r}\sum_{k1} T_{g,l,k1}^r(p_{l,k1}^r - p_{wf,l}^r - dp_{wf,l,k}^r) \\ &= \frac{1}{q_{o,l}^r}\left[\frac{\partial T_{g,l,k}^r}{\partial p_{l,k}^r}(p_{l,k}^r - p_{wf,l}^r - dp_{wf,l,k}^r) + T_{g,l,k}^r\right],\end{aligned} \tag{B–160}$$

$$\frac{\partial GOR_l^r}{\partial p_{wf,l}^r} = -\frac{\sum_{k1} T_{g,l,k1}^r}{q_{o,l}^r}, \tag{B–161}$$

$$\begin{aligned}\frac{\partial GOR_l^r}{\partial S_{w,l,k}^r} &= \frac{1}{q_{o,l}^r}\frac{\partial}{\partial S_{w,l,k}^r}\sum_{k1} T_{g,l,k1}^r(p_{l,k1}^r - p_{wf,l}^r - dp_{wf,l,k}^r) \\ &= \frac{1}{q_{o,l}^r}\frac{\partial T_{g,l,k}^r}{\partial S_{w,l,k}^r}(p_{l,k}^r - p_{wf,l}^r - dp_{wf,l,k}^r),\end{aligned} \tag{B–162}$$

and

$$\begin{aligned}\frac{\partial GOR_l^r}{\partial S_{g,l,k}^r} &= \frac{1}{q_{o,l}^r}\frac{\partial}{\partial S_{g,l,k}^r}\sum_{k1} T_{g,l,k1}^r(p_{l,k1}^r - p_{wf,l,0}^r - dp_{wf,l,k}^r) \\ &= \frac{1}{q_{o,l}^r}\frac{\partial T_{g,l,k}^r}{\partial S_{g,l,k}^r}(p_{l,k}^r - p_{wf,l,0}^r - dp_{wf,l,k}^r).\end{aligned} \tag{B–163}$$

Q_t Specified When the total rate is specified for well l , we have (for $r = n$)

$$q_{g,l}^n = \sum_k T_{g,l,k}^n(p_{l,k}^n - p_{wf,l,k}^n), \tag{B–164}$$

$$q_{o,l}^n = \sum_k T_{o,l,k}^n(p_{l,k}^n - p_{wf,l,k}^n), \tag{B–165}$$

and

$$GOR_l^r = \frac{q_{g,l}^r}{q_{o,l}^r}. \tag{B–166}$$

Thus the derivative of GOR_l^r to the variables $p_{l,k}^n$ is

$$\begin{aligned}\frac{\partial GOR_l^r}{\partial p_{l,k}^r} = \frac{\partial}{\partial p_{l,k}^r}\left(\frac{q_{g,l}^r}{q_{o,l}^r}\right) &= \frac{1}{q_{o,l}^r}\frac{\partial q_{g,l}^r}{\partial p_{l,k}^r} - \frac{q_{g,l}^r}{(q_{o,l}^r)^2}\frac{\partial q_{o,l}^r}{\partial p_{l,k}^r} \\ &= \frac{1}{q_{o,l}^r}\left\{\frac{\partial T_{g,l,k}^r}{\partial p_{l,k}^r}(p_{l,k}^r - p_{wf,l}^r - dp_{wf,l,k}^r) + T_{g,l,k}^r\right\} \\ &\quad - \frac{q_{g,l}^r}{(q_{o,l}^r)^2}\left\{\frac{\partial T_{o,l,k}^r}{\partial p_{l,k}^r}(p_{l,k}^r - p_{wf,l}^r - dp_{wf,l,k}^r) + T_{o,l,k}^r\right\}.\end{aligned} \tag{B–167}$$

Similarly, the derivatives of GOR_l^r to the primary variables, $p_{wf,l}^r$, $S_{w,l,k}^r$ and $S_{g,l,k}^r$ are given by

$$\begin{aligned}\frac{\partial GOR_l^r}{\partial p_{wf,l}^r} &= \frac{1}{q_{o,l}^r}\frac{\partial q_{g,l}^r}{\partial p_{wf,l}^r} - \frac{q_{g,l}^r}{(q_{o,l}^r)^2}\frac{\partial q_{o,l}^r}{\partial p_{wf,l}^r} \\ &= -\frac{\sum_{k1} T_{g,l,k1}^r}{q_{o,l}^r} + \frac{q_{g,l}^r}{(q_{o,l}^r)^2}\sum_{k1} T_{o,l,k1}^r,\end{aligned} \tag{B–168}$$

$$\begin{aligned}\frac{\partial GOR_l^r}{\partial S_{w,l,k}^r} &= \frac{1}{q_{o,l}^r}\frac{\partial q_{g,l}^r}{\partial S_{w,l,k}^r} - \frac{q_{g,l}^r}{(q_{o,l}^r)^2}\frac{\partial q_{o,l}^r}{\partial S_{w,l,k}^r} \\ &= \frac{1}{q_{o,l}^r}\{\frac{\partial T_{g,l,k}^r}{\partial S_{w,l,k}^r}(p_{l,k}^r - p_{wf,l}^r - dp_{wf,l,k}^r)\} - \frac{q_{g,l}^r}{(q_{o,l}^r)^2}\{\frac{\partial T_{o,l,k}^r}{\partial S_{w,l,k}^r}(p_{l,k}^r - p_{wf,l}^r - dp_{wf,l,k}^r)\},\end{aligned} \tag{B–169}$$

and

$$\begin{aligned}\frac{\partial GOR_l^r}{\partial S_{g,l,k}^r} &= \frac{1}{q_{o,l}^r}\frac{\partial q_{g,l}^r}{\partial S_{g,l,k}^r} - \frac{q_{g,l}^r}{(q_{o,l}^r)^2}\frac{\partial q_{o,l}^r}{\partial S_{w,l,k}^r} \\ &= \frac{1}{q_{o,l}^r}\frac{\partial T_{g,l,k}^r}{\partial S_{g,l,k}^r}(p_{l,k}^r - p_{wf,l}^r - dp_{wf,l,k}^r) - \frac{q_{g,l}^r}{(q_{o,l}^r)^2}\{\frac{\partial T_{o,l,k}^r}{\partial S_{g,l,k}^r}(p_{l,k}^r - p_{wf,l}^r - dp_{wf,l,k}^r)\}.\end{aligned} \tag{B–170}$$

B.4.3 Sensitivity of WOR

If we want to compute the sensitivity of WOR_l^r at time t^r, then

$$\beta = WOR_l^r. \tag{B–171}$$

We have

$$\nabla_{y^n}\beta = \nabla_{y^n} WOR_l^r = \begin{bmatrix} \frac{\partial WOR_l^r}{\partial p_1^n} \\ \frac{\partial WOR_l^r}{\partial S_{w,1}^n} \\ \frac{\partial WOR_l^r}{\partial S_{g,1}^n} \\ \frac{\partial WOR_l^r}{\partial p_2^n} \\ \vdots \\ \frac{\partial WOR_l^r}{\partial S_{g,N}^n} \\ \frac{\partial WOR_l^r}{\partial p_{wf,1}^n} \\ \vdots \\ \frac{\partial WOR_l^r}{\partial p_{wf,N_w}^n} \end{bmatrix}. \tag{B–172}$$

It follows that for $n \neq r$,

$$\nabla_{y^n}\beta = \nabla_{y^n} WOR_l^r = 0. \tag{B–173}$$

For $n = r$, only the elements containing derivatives with respect to the primary variables $(p^n, S_w^n, S_g^n, p_{wf}^n)$ in the gridblocks where the well l is completed are nonzero. These nonzero terms are calculated by the equations presented below.

Q_o Specified If we use oil rate specified for well l , we have

$$q_{w,l}^n = \sum_k T_{w,l,k}^n (p_{l,k}^n - p_{wf,l,k}^n). \tag{B–174}$$

So the water-oil ratio is

$$\begin{aligned} WOR^r = \frac{q_{w,l}^r}{q_{o,l}^r} &= \frac{1}{q_{o,l}^r} \sum_k T_{w,l,k}^r (p_{l,k}^r - p_{wf,l,k}^r) \\ &= \frac{1}{q_{o,l}^r} \sum_k T_{w,l,k}^r (p_{l,k}^r - p_{wf,l}^r - dp_{wf,l,k}^r). \end{aligned} \tag{B–175}$$

The derivatives of WOR to $(p^r, p_{wf}^r, S_w^r, S_g^r)$ are

$$\begin{aligned} \frac{\partial WOR^r}{\partial p_{l,k}^r} &= \frac{1}{q_{o,l}^r} \frac{\partial}{\partial p_{l,k}^r} \sum_{k1} T_{w,l,k1}^r (p_{l,k1}^r - p_{wf,l}^r - dp_{wf,l,k}^r) \\ &= \frac{1}{q_{o,l}^r} \left[\frac{\partial T_{w,l,k1}^r}{\partial p_{l,k}^r} (p_{l,k}^r - p_{wf,l}^r - dp_{wf,l,k}^r) + T_{w,l,k1}^r \right], \end{aligned} \tag{B–176}$$

$$\frac{\partial WOR^r}{\partial p^r_{wf,l}} = -\frac{\sum_{k1} T^r_{w,l,k1}}{q^r_{o,l}}, \tag{B–177}$$

$$\begin{aligned}\frac{\partial WOR^r}{\partial S^r_{w,l,k}} &= \frac{1}{q^r_{o,l}} \frac{\partial}{\partial S^r_{w,l,k}} \sum_{k1} T^r_{w,l,k1}(p^r_{l,k1} - p^r_{wf,l} - dp^r_{wf,l,k}) \\ &= \frac{1}{q^r_{o,l}} \frac{\partial T^r_{w,l,k}}{\partial S^r_{w,l,k}}(p^r_{l,k} - p^r_{wf,l} - dp^r_{wf,l,k}),\end{aligned} \tag{B–178}$$

and

$$\begin{aligned}\frac{\partial WOR^r}{\partial S^r_{g,l,k}} &= \frac{1}{q^r_{o,l}} \frac{\partial}{\partial S^r_{g,l,k}} \sum_{k1} T^r_{w,l,k1}(p^r_{l,k1} - p^r_{wf,l} - dp^r_{wf,l,k}) \\ &= \frac{1}{q^r_{o,l}} \frac{\partial T^r_{w,l,k}}{\partial S^r_{g,l,k}}(p^r_{l,k} - p^r_{wf,l} - dp^r_{wf,l,k}).\end{aligned} \tag{B–179}$$

Q_t or p_{wf} Specified If we use total rate specified for well l , we have the water rate given by

$$q^n_{w,l} = \sum_k T^n_{w,l,k}(p^n_{l,k} - p^n_{wf,l,k}), \tag{B–180}$$

and the oil rate by

$$q^n_{o,l} = \sum_k T^n_{o,l,k}(p^n_{l,k} - p^n_{wf,l,k}). \tag{B–181}$$

So the water-oil ratio is

$$WOR^r = \frac{q^r_{w,l}}{q^r_{o,l}}. \tag{B–182}$$

The derivatives of WOR are

$$\begin{aligned}\frac{\partial WOR^r}{\partial p^r_{l,k}} &= \frac{\partial}{\partial p^r_{l,k}}(\frac{q^r_{w,l}}{q^r_{o,l}}) \\ &= \frac{1}{q^r_{o,l}} \frac{\partial q^r_{w,l}}{\partial p^r_{l,k}} - \frac{q^r_{w,l}}{(q^r_{o,l})^2} \frac{\partial q^r_{o,l}}{\partial p^r_{l,k}} \\ &= \frac{1}{q^r_{o,l}} \left[\frac{\partial T^r_{w,l,k}}{\partial p^r_{l,k}}(p^r_{l,k} - p^r_{wf,l} - dp^r_{wf,l,k}) + T^r_{w,l,k} \right] \\ &\quad - \frac{q^r_{w,l}}{(q^r_{o,l})^2} \left[\frac{\partial T^r_{o,l,k}}{\partial p^r_{l,k}}(p^r_{l,k} - p^r_{wf,l} - dp^r_{wf,l,k}) + T^r_{o,l,k} \right],\end{aligned} \tag{B–183}$$

Similarly,

$$\begin{aligned}\frac{\partial WOR^r}{\partial p^r_{wf,l}} &= \frac{1}{q^r_{o,l}}\frac{\partial q^r_{w,l}}{\partial p^r_{wf,l}} - \frac{q^r_{w,l}}{(q^r_{o,l})^2}\frac{\partial q^r_{o,l}}{\partial p^r_{wf,l}} \\ &= -\frac{\sum_{k1} T^r_{w,l,k1}}{q^r_{o,l}} + \frac{q^r_{w,l}}{(q^r_{o,l})^2}\sum_{k1} T^r_{o,l,k1},\end{aligned} \tag{B–184}$$

$$\begin{aligned}\frac{\partial WOR^r}{\partial S^r_{w,l,k}} &= \frac{1}{q^r_{o,l}}\frac{\partial q^r_{w,l}}{\partial S^r_{w,l,k}} - \frac{q^r_{w,l}}{(q^r_{o,l})^2}\frac{\partial q^r_{o,l}}{\partial S^r_{w,l,k}} \\ &= \frac{1}{q^r_{o,l}}\left[\frac{\partial T^r_{w,l,k}}{\partial S^r_{w,l,k}}(p^r_{l,k} - p^r_{wf,l} - dp^r_{wf,l,k})\right] \\ &\quad - \frac{q^r_{w,l}}{(q^r_{o,l})^2}\left[\frac{\partial T^r_{o,l,k}}{\partial S^r_{w,l,k}}(p^r_{l,k} - p^r_{wf,l} - dp^r_{wf,l,k})\right],\end{aligned} \tag{B–185}$$

and

$$\begin{aligned}\frac{\partial WOR^r}{\partial S^r_{g,l,k}} &= \frac{1}{q^r_{o,l}}\frac{\partial q^r_{w,l}}{\partial S^r_{g,l,k}} - \frac{q^r_{w,l}}{(q^r_{o,l})^2}\frac{\partial q^r_{o,l}}{\partial S^r_{w,l,k}} \\ &= \frac{1}{q^r_{o,l}}\left[\frac{\partial T^r_{w,l,k}}{\partial S^r_{g,l,k}}(p^r_{l,k} - p^r_{wf,l} - dp^r_{wf,l,k})\right] \\ &\quad - \frac{q^r_{w,l}}{(q^r_{o,l})^2}\left[\frac{\partial T^r_{o,l,k}}{\partial S^r_{g,l,k}}(p^r_{l,k} - p^r_{wf,l} - dp^r_{wf,l,k})\right] \\ &= -\frac{q^r_{w,l}}{(q^r_{o,l})^2}\left[\frac{\partial T^r_{o,l,k}}{\partial S^r_{g,l,k}}(p^r_{l,k} - p^r_{wf,l} - dp^r_{wf,l,k})\right].\end{aligned} \tag{B–186}$$

APPENDIX C

COMPUTATION OF SENSITIVITY COEFFICIENTS

The sensitivity of some function J to the model parameters m can be computed using Eq. 3.26, which is repeated here,

$$\nabla_m J = \nabla_m \beta + \sum_{n=1}^{L} [\nabla_m (f^n)^T](\lambda^n) \tag{C–1}$$

where

$$\nabla_m [f^n]^T = \begin{bmatrix} \frac{\partial f^n_{o,1}}{\partial m_1} & \frac{\partial f^n_{w,1}}{\partial m_1} & \frac{\partial f^n_{g,1}}{\partial m_1} & \frac{\partial f^n_{o,2}}{\partial m_1} & \cdots & \frac{\partial f^n_{g,N}}{\partial m_1} & \frac{\partial f^n_{wf,1}}{\partial m_1} & \cdots & \frac{\partial f^n_{wf,N_w}}{\partial m_1} \\ \frac{\partial f^n_{o,1}}{\partial m_2} & \frac{\partial f^n_{w,1}}{\partial m_2} & \frac{\partial f^n_{o,1}}{\partial m_2} & \frac{\partial f^n_{o,2}}{\partial m_2} & \cdots & \frac{\partial f^n_{g,N}}{\partial m_2} & \frac{\partial f^n_{wf,1}}{\partial m_2} & \cdots & \frac{\partial f^n_{wf,N_w}}{\partial m_2} \\ \vdots & \vdots & \vdots & \vdots & \vdots & \vdots & \vdots & \vdots & \vdots \\ \frac{\partial f^n_{o,1}}{\partial m_{N_m}} & \frac{\partial f^n_{w,1}}{\partial m_{N_m}} & \frac{\partial f^n_{o,1}}{\partial m_{N_m}} & \frac{\partial f^n_{o,2}}{\partial m_{N_m}} & \cdots & \frac{\partial f^n_{g,N}}{\partial m_{N_m}} & \frac{\partial f^n_{wf,1}}{\partial m_{N_m}} & \cdots & \frac{\partial f^n_{wf,N_w}}{\partial m_{N_m}} \end{bmatrix}, \tag{C–2}$$

and

$$\nabla_m \beta = \begin{bmatrix} \frac{\partial \beta}{\partial m_1} \\ \frac{\partial \beta}{\partial m_2} \\ \vdots \\ \frac{\partial \beta}{\partial m_{N_m}} \end{bmatrix}. \tag{C–3}$$

Once we obtain the solution for adjoint variables λ from the adjoint Eq. 3.21, we can use the formula given in Eq. C–1 to calculate sensitivity coefficients. In this appendix, we give the details of equations for computing the matrix $\nabla_m (f^n)^T$ (Eq. C–2) and the vector $\nabla_m \beta$ (Eq. C–3) which appear in Eq. C–1 for various cases. The specific cases considered here include the sensitivities of p_{wf}, GOR and WOR to horizontal and vertical permeability, porosity (Section C.1 and C.2), skin factor (Section C.3), and relative permeability (Section C.4). In the section C.5, we briefly

describe how to compute the gradient of the total objective function by using the adjoint method.

C.1 Sensitivity of p_{wf}, GOR and WOR to Permeabilities and Porosity

From Eq. C–1, the sensitivity to x-direction permeability(k_x), y-direction permeability (k_y), and z-direction permeability (k_z) and porosity (ϕ) are given by

$$\nabla_{k_x} J = \nabla_{k_x} \beta + \sum_{n=1}^{L} [\nabla_{k_x} (f^n)^T](\lambda^n), \tag{C–4}$$

$$\nabla_{k_y} J = \nabla_{k_y} \beta + \sum_{n=1}^{L} [\nabla_{k_y} (f^n)^T](\lambda^n), \tag{C–5}$$

$$\nabla_{k_z} J = \nabla_{k_z} \beta + \sum_{n=1}^{L} [\nabla_{k_z} (f^n)^T](\lambda^n), \tag{C–6}$$

and

$$\nabla_{\phi} J = \nabla_{\phi} \beta + \sum_{n=1}^{L} [\nabla_{\phi} (f^n)^T](\lambda^n). \tag{C–7}$$

where J may be p_{wf}, GOR or WOR at time step t^L. Here, the vectors k_x, k_y, k_z and ϕ are defined by

$$k_x = [\ k_{x,1} \quad k_{x,2} \quad \cdots \quad k_{x,M}\ ]^T, \tag{C–8}$$

$$k_y = [\ k_{y,1} \quad k_{y,2} \quad \cdots \quad k_{y,M}\ ]^T, \tag{C–9}$$

$$k_z = [\ k_{z,1} \quad k_{z,2} \quad \cdots \quad k_{z,M}\ ]^T, \tag{C–10}$$

and

$$\phi = [\ \phi_1 \quad \phi_2 \quad \cdots \quad \phi_M\ ]^T. \tag{C–11}$$

To calculate sensitivity coefficients, we need to evaluate the matrix $\nabla_m [f^n]^T$ and vector $\nabla_m \beta$ ($m = k_x, k_y, k_z$ and ϕ) in Eqs. C–4 to C–7. In this part, we use the definition in Eqs. B–7 to B–12. Only flow terms and sink/source terms depend on permeability k (k_x, k_y or k_z), so we have

$$\frac{\partial f^{n+1}_{m,i,j,k}}{\partial k} = \frac{\partial F^{n+1}_{m,i,j,k}}{\partial k} - \frac{\partial q^{n+1}_{m,i,j,k}}{\partial k}. \tag{C–12}$$

For calculating sensitivity to porosity, only accumulation terms in the flow equations depend on ϕ, so

$$\frac{\partial f^{n+1}_{m,i,j,k}}{\partial \phi} = -\frac{\partial A^{n+1}_{m,i,j,k}}{\partial \phi}. \tag{C–13}$$

If the horizontal permeability is isotropic, i.e. $k_x = k_y$, the sensitivity to horizontal permeability k_h can be evaluated by

$$\nabla_{k_h} J = \nabla_{k_x} J + \nabla_{k_y} J. \tag{C–14}$$

C.1.1 Derivatives of Flow Terms

We calculate the derivatives of flow terms with respect to the model parameters k_x, k_y, k_z and ϕ at gridblock (i, j, k). Only the flow terms at gridblocks $(i+1, j, k)$, (i, j, k) and $(i-1, j, k)$ depend on $k_{x,i,j,k}$; only the flow terms at gridblocks $(i, j+1, k)$, (i, j, k) and $(i, j-1, k)$ depend on $k_{y,i,j,k}$; and only the flow terms at gridblocks $(i, j, k+1)$, (i, j, k) and $(i, j, k-1)$ depend on $k_{z,i,j,k}$.

The derivatives of flow terms at gridblock $(i \pm 1, j, k)$ with respect to $k_{x,i,j,k}$:

$$\frac{\partial F^n_{o,i\pm1,j,k}}{\partial k_{x,i,j,k}} = \frac{\partial T^n_{ox,i\pm1/2,j,k}}{\partial k_{x,i,j,k}}[p^n_{i,j,k} - p^n_{i\pm1,j,k} + \gamma^n_{o,i\pm1/2,j,k}(D_{i\pm1,j,k} - D_{i,j,k})], \tag{C–15}$$

$$\frac{\partial F^n_{w,i\pm1,j,k}}{\partial k_{x,i,j,k}} = \frac{\partial T^n_{wx,i\pm1/2,j,k}}{\partial k_{x,i,j,k}}[p^n_{i,j,k} - p^n_{i\pm1,j,k} + \gamma^n_{w,i\pm1/2,j,k}(D_{i\pm1,j,k} - D_{i,j,k})], \tag{C–16}$$

$$\begin{aligned}\frac{\partial F^n_{g,i\pm1,j,k}}{\partial k_{x,i,j,k}} &= \frac{\partial T^n_{gx,i\pm1/2,j,k}}{\partial k_{x,i,j,k}}[p^n_{i,j,k} - p^n_{i\pm1,j,k} + \gamma^n_{g,i\pm1/2,j,k}(D_{i\pm1,j,k} - D_{i,j,k})] \\ &\quad + R^n_{so,i\pm1/2,j,k}\frac{\partial T^n_{ox,i\pm1/2,j,k}}{\partial k_{x,i,j,k}}[p^n_{i,j,k} - p^n_{i\pm1,j,k} + \gamma^n_{o,i\pm1/2,j,k}(D_{i\pm1,j,k} - D_{i,j,k})],\end{aligned} \tag{C–17}$$

and

$$\frac{\partial F^n_{o,i\pm1,j,k}}{\partial k_{y,i,j,k}} = \frac{\partial F^n_{o,i\pm1,j,k}}{\partial k_{z,i,j,k}} = \frac{\partial F^n_{w,i\pm1,j,k}}{\partial k_{y,i,j,k}} = \frac{\partial F^n_{w,i\pm1,j,k}}{\partial k_{z,i,j,k}} = \frac{\partial F^n_{g,i\pm1,j,k}}{\partial k_{y,i,j,k}} = \frac{\partial F^n_{g,i\pm1,j,k}}{\partial k_{z,i,j,k}} = 0. \tag{C–18}$$

The derivatives of flow terms at gridblock $(i, j \pm 1, k)$ with respect to $k_{y,i,j,k}$:

$$\frac{\partial F^n_{o,i,j\pm1,k}}{\partial k_{y,i,j,k}} = \frac{\partial T^n_{oy,i,j\pm1/2,k}}{\partial k_{y,i,j,k}}[p^n_{i,j,k} - p^n_{i,j\pm1,k} + \gamma^n_{o,i,j\pm1/2,k}(D_{i,j\pm1,k} - D_{i,j,k})], \tag{C–19}$$

$$\frac{\partial F^n_{w,i,j\pm1,k}}{\partial k_{y,i,j,k}} = \frac{\partial T^n_{wy,i,j\pm1/2,k}}{\partial k_{y,i,j,k}}[p^n_{i,j,k} - p^n_{i,j\pm1,k} + \gamma^n_{w,i,j\pm1/2,k}(D_{i,j\pm1,k} - D_{i,j,k})], \quad \text{(C–20)}$$

and

$$\frac{\partial F^n_{g,i,j\pm1,k}}{\partial k_{y,i,j,k}} = \frac{\partial T^n_{gy,i,j\pm1/2,k}}{\partial k_{y,i,j,k}}[p^n_{i,j,k} - p^n_{i,j\pm1,k} + \gamma^n_{g,i,j\pm1/2,k}(D_{i,j\pm1,k} - D_{i,j,k})] + \frac{\partial T^n_{oy,i,j\pm1/2,k}}{\partial k_{y,i,j,k}} R^n_{so,i,j\pm1/2,k}[p^n_{i,j,k} - p^n_{i,j\pm1,k} + \gamma^n_{o,i,j\pm1/2,k}(D_{i,j\pm1,k} - D_{i,j,k})]. \quad \text{(C–21)}$$

The derivatives of flow terms at gridblock $(i, j, k \pm 1)$ with respect to $k_{z,i,j,k}$:

$$\frac{\partial F^n_{o,i,j,k\pm1}}{\partial k_{z,i,j,k}} = \frac{\partial T^n_{oz,i,j,k\pm1/2}}{\partial k_{z,i,j,k}}[p^n_{i,j,k} - p^n_{i,j,k\pm1} + \gamma^n_{o,i,j,k\pm1/2}(D_{i,j,k\pm1} - D_{i,j,k})], \quad \text{(C–22)}$$

$$\frac{\partial F^n_{w,i,j,k\pm1}}{\partial k_{z,i,j,k}} = \frac{\partial T^n_{wz,i,j,k\pm1/2}}{\partial k_{z,i,j,k}}[p^n_{i,j,k} - p^n_{i,j,k\pm1} + \gamma^n_{w,i,j,k\pm1/2}(D_{i,j,k\pm1} - D_{i,j,k})], \quad \text{(C–23)}$$

and

$$\frac{\partial F^n_{g,i,j,k\pm1}}{\partial k_{z,i,j,k}} = \frac{\partial T^n_{gz,i,j,k\pm1/2}}{\partial k_{z,i,j,k}}[p^n_{i,j,k} - p^n_{i,j,k\pm1} + \gamma^n_{g,i,j,k\pm1/2}(D_{i,j,k\pm1} - D_{i,j,k})] + \frac{\partial T^n_{oz,i,j,k\pm1/2}}{\partial k_{z,i,j,k}} R^n_{so,i,j,k\pm1/2}[p^n_{i,j,k} - p^n_{i,j,k\pm1} + \gamma^n_{o,i,j,k\pm1/2}(D_{i,j,k\pm1} - D_{i,j,k})]. \quad \text{(C–24)}$$

The derivatives of flow terms at gridblock (i, j, k) with respect to $k_{x,i,j,k}$, $k_{y,i,j,k}$, $k_{z,i,j,k}$:

$$\frac{\partial F^n_{m,i,j,k}}{\partial k_{x,i,j,k}} = -\left(\frac{\partial F^n_{m,i+1,j,k}}{\partial k_{x,i,j,k}} + \frac{\partial F^n_{m,i-1,j,k}}{\partial k_{x,i,j,k}}\right), \quad \text{(C–25)}$$

$$\frac{\partial F^n_{m,i,j,k}}{\partial k_{y,i,j,k}} = -\left(\frac{\partial F^n_{m,i,j+1,k}}{\partial k_{y,i,j,k}} + \frac{\partial F^n_{m,i,j-1,k}}{\partial k_{y,i,j,k}}\right), \quad \text{(C–26)}$$

and

$$\frac{\partial F^n_{m,i,j,k}}{\partial k_{z,i,j,k}} = -\left(\frac{\partial F^n_{m,i,j,k+1}}{\partial k_{z,i,j,k}} + \frac{\partial F^n_{m,i,j,k-1}}{\partial k_{z,i,j,k}}\right). \quad \text{(C–27)}$$

for $m = o, w, g$.

The derivatives of transmissibility T to permeabilities are given in the next subsection.

Because only accumulation terms involve porosity ϕ, it is easy to see that the derivatives of oil, water and gas flow equations with respect to porosity are given

by

$$\frac{\partial f_{o,i,j,k}^{n+1}}{\partial \phi_{i,j,k}} = -\frac{V_{i,j,k}}{C_2 \Delta t^{n+1}} \left[\left(\frac{S_o}{B_o} \right)_{i,j,k}^{n+1} - \left(\frac{S_o}{B_o} \right)_{i,j,k}^{n} \right], \tag{C–28}$$

$$\frac{\partial f_{w,i,j,k}^{n+1}}{\partial \phi_{i,j,k}} = -\frac{V_{i,j,k}}{C_2 \Delta t^{n+1}} \left[\left(\frac{S_w}{B_w} \right)_{i,j,k}^{n+1} - \left(\frac{S_w}{B_w} \right)_{i,j,k}^{n} \right], \tag{C–29}$$

and

$$\frac{\partial f_{g,i,j,k}^{n+1}}{\partial \phi_{i,j,k}} = -\frac{V_{i,j,k}}{C_2 \Delta t^{n+1}} \left[\left(\frac{S_g}{B_g} + R_{so} \frac{S_o}{B_o} \right)_{i,j,k}^{n+1} - \left(\frac{S_g}{B_g} + R_{so} \frac{S_o}{B_o} \right)_{i,j,k}^{n} \right], \tag{C–30}$$

respectively.

Computing the Partial Derivatives of Transmissibility T

Recall the transmissibilities can be written as

$$T_{mx,i+1/2,j,k}^{n} = \frac{C_1 \Delta y_j \Delta z_k k_{x,i+1/2,j,k}}{x_{i+1} - x_i} \frac{k_{rm,i+1/2,j,k}^{n}}{\mu_{m,i+1/2,j,k}^{n} B_{m,i+1/2,j,k}^{n}}, \tag{C–31}$$

for $m = o, w, g$ and $i = 1, 2, \ldots, n_x - 1$, and

$$T_{mx,1/2,j,k}^{n} = T_{mx,n_x+1/2,j,k}^{n} = 0. \tag{C–32}$$

Similarly,

$$T_{my,i,j+1/2,k}^{n} = \frac{C_1 \Delta x_i \Delta z_k k_{y,i,j+1/2,k}}{y_{j+1} - y_j} \frac{k_{rm,i,j+1/2,k}^{n}}{\mu_{m,i,j+1/2,k}^{n} B_{m,i,j+1/2,k}^{n}}, \tag{C–33}$$

for $m = o, w, g$ and $j = 1, 2, \ldots, n_y - 1$, and

$$T_{my,i,1/2,k}^{n} = T_{my,i,n_y+1/2,k}^{n} = 0. \tag{C–34}$$

Finally,

$$T_{mz,i,j,k+1/2}^{n} = \frac{C_1 \Delta y_j \Delta x_i k_{z,i,j,k+1/2}}{z_{k+1} - z_k} \frac{k_{rm,i,j,k+1/2}^{n}}{\mu_{m,i,j,k+1/2}^{n} B_{m,i,j,k+1/2}^{n}}, \tag{C–35}$$

for $m = o, w, g$ and $k = 1, 2, \ldots, n_z - 1$. and

$$T_{mz,i,j,1/2}^{n} = T_{mz,i,j,n_z+1/2}^{n} = 0. \tag{C–36}$$

The permeabilities at gridblock interfaces are computed as harmonic averages. For all j and k such that $1 \le j \le n_y$ and $1 \le k \le n_z$,

$$k_{x,i+1/2,j,k} = \frac{(\triangle x_i + \triangle x_{i+1}) k_{x,i,j,k} k_{x,i+1,j,k}}{\triangle x_i k_{x,i+1,j,k} + \triangle x_{i+1} k_{x,i,j,k}}, \tag{C–37}$$

for $i = 1, 2, \ldots, n_x - 1$,

$$k_{x,1/2,j,k} = k_{x,1,j,k}, \tag{C–38}$$

and

$$k_{x,n_x+1/2,j,k} = k_{x,n_x,j,k}. \tag{C–39}$$

It follows that

$$\begin{aligned}
&\frac{\partial k_{x,i+1/2,j,k}}{\partial k_{x,i,j,k}} \\
&= \frac{(\triangle x_i + \triangle x_{i+1}) k_{x,i+1,j,k} (\triangle x_i k_{x,i+1,j,k} + \triangle x_{i+1} k_{x,i,j,k}) - (\triangle x_i + \triangle x_{i+1}) k_{x,i,j,k} k_{x,i+1,j,k} \triangle x_{i+1}}{(\triangle x_i k_{x,i+1,j,k} + \triangle x_{i+1} k_{x,i,j,k})^2} \\
&= \frac{(\triangle x_i + \triangle x_{i+1}) \triangle x_i k_{x,i+1,j,k}^2}{(\triangle x_i k_{x,i+1,j,k} + \triangle x_{i+1} k_{x,i,j,k})^2} \\
&= \frac{\triangle x_i k_{x,i+1,j,k}}{k_{x,i,j,k} (\triangle x_i k_{x,i+1,j,k} + \triangle x_{i+1} k_{x,i,j,k})} k_{x,i+1/2,j,k},
\end{aligned} \tag{C–40}$$

for $i = 1, 2, \ldots, n_x - 1$, and

$$\frac{\partial k_{x,1/2,j,k}}{\partial k_{x,1,j,k}} = \frac{\partial k_{x,n_x+1/2,j,k}}{\partial k_{x,n_x,j,k}} = 1. \tag{C–41}$$

The derivative of the term

$$k_{x,i-1/2,j,k} = \frac{(\triangle x_{i-1} + \triangle x_i) k_{x,i-1,j,k} k_{x,i,j,k}}{\triangle x_{i-1} k_{x,i,j,k} + \triangle x_i k_{x,i-1,j,k}}, \tag{C–42}$$

for $i = 2, 3, ..., n_x$, is given by

$$\begin{aligned}
&\frac{\partial k_{x,i-1/2,j,k}}{\partial k_{x,i,j,k}} \\
&= \frac{(\triangle x_{i-1} + \triangle x_i)k_{x,i-1,j,k}(\triangle x_{i-1}k_{x,i,j,k} + \triangle x_i k_{x,i-1,j,k}) - (\triangle x_{i-1} + \triangle x_i)k_{x,i-1,j,k}k_{x,i,j,k}\triangle x_{i-1}}{(\triangle x_{i-1}k_{x,i,j,k} + \triangle x_i k_{x,i-1,j,k})^2} \\
&= \frac{(\triangle x_{i-1} + \triangle x_i)\triangle x_i k_{x,i-1,j,k}^2}{(\triangle x_{i-1}k_{x,i,j,k} + \triangle x_i k_{x,i-1,j,k})^2} \\
&= \frac{\triangle x_i k_{x,i-1,j,k}}{k_{x,i,j,k}(\triangle x_{i-1}k_{x,i,j,k} + \triangle x_i k_{x,i-1,j,k})} k_{x,i-1/2,j,k}.
\end{aligned} \tag{C–43}$$

Similarly, the derivatives of $k_{y,i,j+1/2,k}$ and $k_{y,i,j-1/2,k}$ with respect to $k_{y,i,j,k}$ are

$$\frac{\partial k_{y,i,j+1/2,k}}{\partial k_{y,i,j,k}} = \frac{\triangle y_j k_{y,i,j+1,k}}{k_{y,i,j,k}(\triangle y_j k_{y,i,j+1,k} + \triangle y_{j+1}k_{y,i,j,k})} k_{y,i,j+1/2,k}, \tag{C–44}$$

and

$$\frac{\partial k_{y,i,j-1/2,k}}{\partial k_{y,i,j,k}} = \frac{\triangle y_j k_{y,i,j-1,k}}{k_{y,i,j,k}(\triangle y_{j-1}k_{y,i,j,k} + \triangle y_j k_{y,i,j-1,k})} k_{y,i,j-1/2,k}. \tag{C–45}$$

The derivatives of $k_{z,i,j,k+1/2}$ and $k_{z,i,j,k-1/2}$ with respect to $k_{z,i,j,k}$ are

$$\frac{\partial k_{z,i,j,k+1/2}}{\partial k_{z,i,j,k}} = \frac{\triangle z_k k_{z,i,j,k+1}}{k_{z,i,j,k}(\triangle z_k k_{z,i,j,k+1} + \triangle z_{k+1}k_{z,i,j,k})} k_{z,i,j,k+1/2}, \tag{C–46}$$

and

$$\frac{\partial k_{z,i,j,k-1/2}}{\partial k_{z,i,j,k}} = \frac{\triangle z_k k_{z,i,j,k-1}}{k_{z,i,j,k}(\triangle z_{k-1}k_{z,i,j,k} + \triangle z_k k_{z,i,j,k-1})} k_{z,i,j,k-1/2}. \tag{C–47}$$

The derivative of the x-direction transmissibility can now be obtained as follows,

$$\begin{aligned}
\frac{\partial T^n_{mx,i+1/2,j,k}}{\partial k_{x,i,j,k}} &= \frac{\partial k_{x,i+1/2,j,k}}{\partial k_{x,i,j,k}} \frac{C_1 \Delta y_j \Delta z_k}{x_{i+1} - x_i} \frac{k^n_{rm,i+1/2,j,k}}{(B\mu)^n_{m,i+1/2,j,k}} \\
&= \frac{\triangle x_i k_{x,i+1,j,k}}{k_{x,i,j,k}(\triangle x_i k_{x,i+1,j,k} + \triangle x_{i+1}k_{x,i,j,k})} \frac{C_1 \Delta y_j \Delta z_k k_{x,i+1/2,j,k}}{x_{i+1} - x_i} \frac{k^n_{rm,i+1/2,j,k}}{(B\mu)^n_{m,i+1/2,j,k}} \\
&= \frac{\triangle x_i k_{x,i+1,j,k}}{k_{x,i,j,k}(\triangle x_i k_{x,i+1,j,k} + \triangle x_{i+1}k_{x,i,j,k})} T^n_{mx,i+1/2,j,k},
\end{aligned} \tag{C–48}$$

$$\frac{\partial T^n_{mx,i-1/2,j,k}}{\partial k_{x,i,j,k}} = \frac{\triangle x_i k_{x,i-1,j,k}}{k_{x,i,j,k}(\triangle x_{i-1}k_{x,i,j,k} + \triangle x_i k_{x,i-1,j,k})} T^n_{mx,i-1/2,j,k}. \tag{C–49}$$

Similar results are obtained from the y and z direction transmissibility derivatives,

$$\frac{\partial T^n_{my,i,j+1/2,k}}{\partial k_{y,i,j,k}} = \frac{\triangle y_j k_{y,i,j+1,k}}{k_{y,i,j,k}(\triangle y_j k_{y,i,j+1,k} + \triangle y_{j+1} k_{y,i,j,k})} T^n_{my,i,j+1/2,k}, \tag{C–50}$$

$$\frac{\partial T^n_{my,i,j-1/2,k}}{\partial k_{y,i,j,k}} = \frac{\triangle y_j k_{y,i,j-1,k}}{k_{x,i,j,k}(\triangle y_{j-1} k_{y,i,j,k} + \triangle y_j k_{y,i,j-1,k})} T^n_{my,i,j-1/2,k}, \tag{C–51}$$

$$\frac{\partial T^n_{mz,i,j,k+1/2}}{\partial k_{z,i,j,k}} = \frac{\triangle z_k k_{z,i,j,k+1}}{k_{z,i,j,k}(\triangle z_k k_{z,i,j,k+1} + \triangle z_{k+1} k_{z,i,j,k})} T^n_{mz,i,j,k+1/2}, \tag{C–52}$$

and

$$\frac{\partial T^n_{mz,i,j,k-1/2}}{\partial k_{z,i,j,k}} = \frac{\triangle z_k k_{z,i,j,k-1}}{k_{z,i,j,k}(\triangle z_{k-1} k_{z,i,j,k} + \triangle z_k k_{z,i,j,k-1})} T^n_{mz,i,j,k-1/2}, \tag{C–53}$$

for $m = o, w, g$. At the boundaries, transmissibilities are zero, so the derivatives of transmissibility are equal to zero, i.e.,

$$\begin{aligned} \frac{\partial T^n_{mx,1/2,j,k}}{\partial k^n_{i,j,k}} &= \frac{\partial T^n_{mx,n_x+1/2,j,k}}{\partial k^n_{i,j,k}} = \frac{\partial T^n_{my,i,1/2,k}}{\partial k^n_{i,j,k}} \\ &= \frac{\partial T^n_{my,i,n_y+1/2,k}}{\partial k^n_{i,j,k}} = \frac{\partial T^n_{mz,i,j,1/2}}{\partial k^n_{i,j,k}} = \frac{\partial T^n_{mz,i,j,n_z+1/2}}{\partial k^n_{i,j,k}} = 0. \end{aligned} \tag{C–54}$$

C.1.2 Derivatives of Sink Terms

In this section, we calculate the derivatives of sink/source terms in Eq. C–12,i.e., we present formulas for $\partial q^{n+1}_{m,i,j,k}/\partial k$.

Producing wells (Q_o, Q_t or p_{wf} Specified)

In the producing wells, the production rates from layer $k0$ at well l are given by

$$q^{n+1}_{m,l,k0} = T^{n+1}_{m,l,k0}[p^{n+1}_{l,k0} - p^{n+1}_{wf,l} - dp^{n+1}_{wf,l,k0}], \tag{C–55}$$

for $m = o, w, g$, where,

$$T^{n+1}_{o,l,k} = WI_{l,k} \left(\frac{k_{ro}}{B_o \mu_o} \right)^{n+1}_{l,k}, \tag{C–56}$$

$$T^{n+1}_{w,l,k} = WI_{l,k} \left(\frac{k_{rw}}{B_w \mu_w} \right)^{n+1}_{l,k}, \tag{C–57}$$

and

$$T_{g,l,k}^{n+1} = WI_{l,k}\left(\frac{k_{rg}}{B_g\mu_g} + R_{so}\frac{k_{ro}}{B_o\mu_o}\right)_{l,k}^{n+1}. \tag{C–58}$$

The layer production rates, $q_{m,l,k0}^{n+1}$, do not explicitly dependent on the vertical permeability k_z, so the derivatives of $q_{m,l,k0}^{n+1}$ with respect to k_z are equal to zero,i.e.,

$$\frac{\partial q_{m,l,k0}^{n+1}}{\partial k_z} = 0, \tag{C–59}$$

for $k = k0$ and all gridblock k_z's, we have

$$\frac{\partial q_{m,l,k0}^{n+1}}{\partial k_{x,l,k}} = \frac{\partial T_{m,l,k}^{n+1}}{\partial k_{x,l,k}}[p_{l,k}^{n+1} - p_{wf,l}^{n+1} - dp_{wf,l,k}^{n+1}], \tag{C–60}$$

$$\frac{\partial q_{m,l,k0}^{n+1}}{\partial k_{y,l,k}} = \frac{\partial T_{m,l,k}^{n+1}}{\partial k_{y,l,k}}[p_{l,k}^{n+1} - p_{wf,l}^{n+1} - dp_{wf,l,k}^{n+1}], \tag{C–61}$$

for $m = o, w, g$. For $k \neq k0$

$$\frac{\partial q_{m,l,k0}^{n+1}}{\partial k_{x,l,k}} = \frac{\partial q_{m,l,k0}^{n+1}}{\partial k_{y,l,k}} = 0, \tag{C–62}$$

for $m = o, w, g$.

The derivatives of $T_{m,l,k}^{n+1}$ with respect to $k_{x,l,k}$ can be calculated as

$$\frac{\partial T_{o,l,k}^{n+1}}{\partial k_{x,l,k}} = \frac{\partial WI_{l,k}}{\partial k_{x,l,k}}\left(\frac{k_{ro}}{B_o\mu_o}\right)_{l,k}^{n+1}, \tag{C–63}$$

$$\frac{\partial T_{w,l,k}^{n+1}}{\partial k_{x,l,k}} = \frac{\partial WI_{l,k}}{\partial k_{x,l,k}}\left(\frac{k_{rw}}{B_w\mu_w}\right)_{l,k}^{n+1}, \tag{C–64}$$

and

$$\frac{\partial T_{g,l,k}^{n+1}}{\partial k_{x,l,k}} = \frac{\partial WI_{l,k}}{\partial k_{x,l,k}}\left(\frac{k_{rg}}{B_g\mu_g} + R_{so}\frac{k_{ro}}{B_o\mu_o}\right)_{l,k}^{n+1}. \tag{C–65}$$

The derivatives of $T_{m,l,k}^{n+1}$ with respect to $k_{y,l,k}$ can be calculated as

$$\frac{\partial T_{o,l,k}^{n+1}}{\partial k_{y,l,k}} = \frac{\partial WI_{l,k}}{\partial k_{y,l,k}}\left(\frac{k_{ro}}{B_o\mu_o}\right)_{l,k}^{n+1}, \tag{C–66}$$

$$\frac{\partial T_{w,l,k}^{n+1}}{\partial k_{y,l,k}} = \frac{\partial WI_{l,k}}{\partial k_{y,l,k}}\left(\frac{k_{rw}}{B_w\mu_w}\right)_{l,k}^{n+1}, \tag{C–67}$$

and

$$\frac{\partial T_{g,l,k}^{n+1}}{\partial k_{y,l,k}} = \frac{\partial WI_{l,k}}{\partial k_{y,l,k}} \left(\frac{k_{rg}}{B_g \mu_g} + R_{so} \frac{k_{ro}}{B_o \mu_o} \right)_{l,k}^{n+1}. \tag{C–68}$$

From a previous TUPREP report,

$$\frac{\partial WI_{l,k}}{\partial k_{x,l,k}} = \frac{0.00708 \triangle z}{2[\ln(r_{o,l,k}/r_{w,l,k}) + s_{l,k}]} \times \left[\frac{\sqrt{k_{y,l,k}}}{\sqrt{k_{x,l,k}}} - \left(\frac{1}{\ln(r_{o,l,k}/r_{w,l,k}) + s_{l,k}} \right) \left(\frac{\triangle y_{l,k}^2 \sqrt{k_{x,l,k} k_{y,l,k}}}{\triangle x_{l,k}^2 k_{y,l,k} + \triangle y_{l,k}^2 k_{x,l,k}} - \frac{\sqrt{k_{y,l,k}}}{\sqrt{k_{x,l,k}} + \sqrt{k_{y,l,k}}} \right) \right], \tag{C–69}$$

and

$$\frac{\partial WI_{l,k}}{\partial k_{y,l,k}} = \frac{0.00708 \triangle z}{2[\ln(r_{o,l,k}/r_{w,l,k}) + s_{l,k}]} \times \left[\frac{\sqrt{k_{x,l,k}}}{\sqrt{k_{y,l,k}}} + \left(\frac{1}{\ln(r_{o,l,k}/r_{w,l,k}) + s_{l,k}} \right) \times \left(\frac{\triangle y_{l,k}^2 k_{x,l,k} \sqrt{k_{x,l,k}}}{\triangle x_{l,k}^2 k_{y,l,k} \sqrt{k_{y,l,k}} + \triangle y_{l,k}^2 k_{x,l,k} \sqrt{k_{y,l,k}}} - \frac{k_{x,l,k}}{k_{y,l,k} + \sqrt{k_{y,l,k} k_{x,l,k}}} \right) \right]. \tag{C–70}$$

Injection Wells (Water or Gas injection)

For water or gas injection wells, the injection rates at layer $k0$ of well l are

$$q_{m,l,k0}^{n+1} = T_{inj,m,l,k0}^{n+1} [p_{l,k0}^{n+1} - p_{wf,l}^{n+1} - dp_{wf,l,k0}^{n+1}], \tag{C–71}$$

for $m = w, g$, where

$$T_{inj,m,l,k}^{n+1} = \frac{WI_{l,k}}{\mu_{m,l,k}^{n+1} B_{m,l,k}^{n+1}}. \tag{C–72}$$

For $k = k0$, the derivatives of $q_{m,l,k0}^{n+1}$ with respect to horizontal permeabilities are

$$\frac{\partial q_{m,l,k0}^{n+1}}{\partial k_{x,l,k}} = \frac{\partial T_{inj,m,l,k}^{n+1}}{\partial k_{x,l,k}} [p_{l,k}^{n+1} - p_{wf,l}^{n+1} - dp_{wf,l,k}^{n+1}], \tag{C–73}$$

and

$$\frac{\partial q_{m,l,k0}^{n+1}}{\partial k_{y,l,k}} = \frac{\partial T_{inj,m,l,k}^{n+1}}{\partial k_{y,l,k}} [p_{l,k}^{n+1} - p_{wf,l}^{n+1} - dp_{wf,l,k}^{n+1}]. \tag{C–74}$$

For $k \neq k0$, it is easy to see that

$$\frac{\partial q_{m,l,k0}^{n+1}}{\partial k_{x,l,k}} = \frac{\partial q_{m,l,k0}^{n+1}}{\partial k_{y,l,k}} = 0. \tag{C–75}$$

For $k = k_0$, the derivatives of $T^{n+1}_{inj,m,l,k}$ can be calculated as

$$\frac{\partial T^{n+1}_{inj,m,l,k}}{\partial k_{x,l,k}} = \frac{\partial WI_{l,k}}{\partial k_{x,l,k}} \frac{1}{\mu^{n+1}_{m,l,k} B^{n+1}_{m,l,k}}, \tag{C–76}$$

and

$$\frac{\partial T^{n+1}_{inj,m,l,k}}{\partial k_{y,l,k}} = \frac{\partial WI_{l,k}}{\partial k_{y,l,k}} \frac{1}{\mu^{n+1}_{m,l,k} B^{n+1}_{m,l,k}}. \tag{C–77}$$

The term $q^{n+1}_{m,l,k0}$ does not explicitly depend on k_z or ϕ, so the derivatives of $q^{n+1}_{m,l,k0}$ with respect to these two model parameters are equal to zero, i.e.

$$\frac{\partial q^{n+1}_{m,l,k0}}{\partial k_z} = \frac{\partial q^{n+1}_{m,l,k0}}{\partial \phi} = 0, \tag{C–78}$$

for $m = o, w, g$ and all gridblock k_z's and ϕ's.

In the water injection wells, the gas and oil rates are set to zero. So the derivatives of these rates are zero,i.e.,

$$\frac{\partial q^{n+1}_{o,l,k0}}{\partial k_x} = \frac{\partial q^{n+1}_{o,l,k0}}{\partial k_y} = \frac{\partial q^{n+1}_{g,l,k0}}{\partial k_x} = \frac{\partial q^{n+1}_{g,l,k0}}{\partial k_y} = 0. \tag{C–79}$$

In the gas injection wells, the water and oil rates are set to zero. So the derivatives of water or oil rates are equal to zero,i.e.,

$$\frac{\partial q^{n+1}_{o,l,k0}}{\partial k_x} = \frac{\partial q^{n+1}_{o,l,k0}}{\partial k_y} = \frac{\partial q^{n+1}_{w,l,k0}}{\partial k_x} = \frac{\partial q^{n+1}_{w,l,k0}}{\partial k_y} = 0. \tag{C–80}$$

C.1.3 Derivatives of Well Equations

Here, we give the details how to compute the derivatives of well constraint equation $f^{n+1}_{wf,l}$ with respect to permeabilities and porosity.

Q_o Specified

In the case where oil rate is specified, the well equation at well l is

$$f^{n+1}_{wf,l} = \sum_{k1} T^{n+1}_{o,l,k1} [p^{n+1}_{l,k1} - p^{n+1}_{wf,l} - dp^{n+1}_{wf,l,k1}] - q^{n+1}_{o,l} = 0, \tag{C–81}$$

for $m = o, w, g$, where

$$T_{o,l,k}^{n+1} = WI_{l,k} \left(\frac{k_{ro}}{B_o \mu_o} \right)_{l,k}^{n+1}. \tag{C–82}$$

Thus, the derivatives of well equations are

$$\frac{\partial f_{wf,l}^{n+1}}{\partial k_{x,l,k}} = \frac{\partial T_{o,l,k}^{n+1}}{\partial k_{x,l,k}} [p_{l,k}^{n+1} - p_{wf,l}^{n+1} - dp_{wf,l,k}^{n+1}], \tag{C–83}$$

$$\frac{\partial f_{wf,l}^{n+1}}{\partial k_{y,l,k}} = \frac{\partial T_{o,l,k}^{n+1}}{\partial k_{y,l,k}} [p_{l,k}^{n+1} - p_{wf,l}^{n+1} - dp_{wf,l,k}^{n+1}], \tag{C–84}$$

and

$$\frac{\partial f_{wf,l}^{n+1}}{\partial k_{z,l,k}} = \frac{\partial f_{wf,l}^{n+1}}{\partial \phi} = 0. \tag{C–85}$$

The derivatives $\frac{\partial T_{o,l,k}^{n+1}}{\partial k_{x,l,k}}$ and $\frac{\partial T_{o,l,k}^{n+1}}{\partial k_{y,l,k}}$ are given by Eqs. C–63 and C–66.

$\underline{Q_t \text{ Specified}}$

In the case where the total rate is specified at reservoir conditions, the well equation at well l is

$$f_{wf,l}^{n+1} = \sum_{k1} T_{t,l,k1}^{n+1} [p_{l,k1}^{n+1} - p_{wf,l}^{n+1} - dp_{wf,l,k1}^{n+1}] - q_{t,l}^{n+1} = 0, \tag{C–86}$$

for $m = o, w, g$, where,

$$T_{t,l,k}^{n+1} = WI_{l,k} \left(\frac{k_{ro}}{\mu_o} + \frac{k_{rw}}{\mu_w} + \frac{k_{rg}}{\mu_g} \right)_{l,k}^{n+1}. \tag{C–87}$$

We obtain

$$\frac{\partial f_{wf,l}^{n+1}}{\partial k_{x,l,k}} = \frac{\partial T_{t,l,k}^{n+1}}{\partial k_{x,l,k}} [p_{l,k}^{n+1} - p_{wf,l}^{n+1} - dp_{wf,l,k}^{n+1}], \tag{C–88}$$

$$\frac{\partial f_{wf,l}^{n+1}}{\partial k_{y,l,k}} = \frac{\partial T_{t,l,k}^{n+1}}{\partial k_{y,l,k}} [p_{l,k}^{n+1} - p_{wf,l}^{n+1} - dp_{wf,l,k}^{n+1}], \tag{C–89}$$

and

$$\frac{\partial f_{wf,l}^{n+1}}{\partial k_{z,l,k}} = \frac{\partial f_{wf,l}^{n+1}}{\partial \phi} = 0, \tag{C–90}$$

where the derivative of $T_{t,l,k}^{n+1}$ are computed by

$$\frac{\partial T_{t,l,k}^{n+1}}{\partial k_{x,l,k}} = \frac{\partial WI_{l,k}}{\partial k_{x,l,k}} \left(\frac{k_{ro}}{\mu_o} + \frac{k_{rw}}{\mu_w} + \frac{k_{rg}}{\mu_g} \right)_{l,k}^{n+1}, \tag{C–91}$$

and

$$\frac{\partial T_{t,l,k}^{n+1}}{\partial k_{y,l,k}} = \frac{\partial WI_{l,k}}{\partial k_{y,l,k}} \left(\frac{k_{ro}}{\mu_o} + \frac{k_{rw}}{\mu_w} + \frac{k_{rg}}{\mu_g} \right)_{l,k}^{n+1}. \tag{C–92}$$

$\underline{p_{wf} \text{ Specified}}$

In the p_{wf} specified case, the well equation at well l is (Eq. A–65)

$$f_{wf,l}^{n+1} = p_{wf,l,0}^{n+1} - p_{wf,l}^{n+1} = 0. \tag{C–93}$$

There is no k_x, k_y, k_z, and ϕ appearing in Eq. C–93, so the derivatives of the well equations are zero. We have

$$\frac{\partial f_{wf,l}^{n+1}}{\partial k_{x,l,k}} = \frac{\partial f_{wf,l}^{n+1}}{\partial k_{y,l,k}} = \frac{\partial f_{wf,l}^{n+1}}{\partial k_{z,l,k}} = \frac{\partial f_{wf,l}^{n+1}}{\partial \phi} = 0. \tag{C–94}$$

$\underline{\text{Water or Gas Injection}}$

In the injection wells, the well equation at well l is

$$f_{wf,l}^{n+1} = \sum_{k1} T_{inlm,l,k1}^{n+1} [p_{l,k1}^{n+1} - p_{wf,l}^{n+1} - dp_{wf,l,k1}^{n+1}] - q_{m,l}^{n+1} = 0, \tag{C–95}$$

for $m = w, g$, where

$$T_{inj,m,l,k}^{n+1} = \frac{WI_{l,k}}{(B_m \mu_m)_{l,k}^{n+1}}. \tag{C–96}$$

We obtain the derivatives of $f_{wf,l}^{n+1}$ with respect to model parameters as

$$\frac{\partial f_{wf,l}^{n+1}}{\partial k_{x,l,k}} = \frac{\partial T_{inj,m,l,k}^{n+1}}{\partial k_{x,l,k}} [p_{l,k}^{n+1} - p_{wf,l}^{n+1} - dp_{wf,l,k}^{n+1}], \tag{C–97}$$

$$\frac{\partial f_{wf,l}^{n+1}}{\partial k_{y,l,k}} = \frac{\partial T_{inj,m,l,k}^{n+1}}{\partial k_{y,l,k}} [p_{l,k}^{n+1} - p_{wf,l}^{n+1} - dp_{wf,l,k}^{n+1}], \tag{C–98}$$

and

$$\frac{\partial f_{wf,l}^{n+1}}{\partial k_{z,l,k}} = \frac{\partial f_{wf,l}^{n+1}}{\partial \phi_{l,k}} = 0. \tag{C–99}$$

The derivatives $\partial T_{inj,m,l,k}^{n+1}/\partial k_{x,l,k}$ and $\partial T_{inj,m,l,k}^{n+1}/\partial k_{y,l,k}$ are given in Eqs. C–76 and C–77.

C.1.4 The Vector $\nabla_m \beta$ in Equations for Sensitivity Coefficients

In this section, the model parameters (m) we want to estimate are

$$k_x = [\ k_{x,1} \quad k_{x,2} \quad \cdots \quad k_{x,M}\ ]^T, \tag{C–100}$$

$$k_y = [\ k_{y,1} \quad k_{y,2} \quad \cdots \quad k_{y,M}\ ]^T, \tag{C–101}$$

$$k_z = [\ k_{z,1} \quad k_{z,2} \quad \cdots \quad k_{z,M}\ ]^T, \tag{C–102}$$

and

$$\phi = [\ \phi_1 \quad \phi_2 \quad \cdots \quad \phi_M\ ]^T. \tag{C–103}$$

Here, we give the equations for computing $\nabla_m \beta$ in the sensitivity equation (Eq. C-1) for various cases. We wish to calculate the sensitivity of p_{wf}, GOR, and WOR, so we set β equal to p_{wf}, GOR, and WOR and compute the gradient of p_{wf}, GOR, and WOR. Gradient $\nabla_m \beta$ are nonzero only when the model parameter m explicitly appear in the expression of β.

Gradient of p_{wf}

In this case,

$$\beta = p_{wf}^r. \tag{C–104}$$

Because p_{wf}^r does not explicitly dependent on the model parameters, k_x, k_y, k_z, or ϕ, we have

$$\nabla_m \beta = \nabla_m p_{wf}^r = 0. \tag{C–105}$$

Derivatives of GOR

The gradient of GOR with respect to m at well l at time step t^r is formally given by the expression,

$$\nabla_m \beta = \nabla_m GOR_l^r = \begin{bmatrix} \frac{\partial GOR_l^r}{\partial m_1} \\ \frac{\partial GOR_l^r}{\partial m_2} \\ \vdots \\ \frac{\partial GOR_l^r}{\partial m_M} \end{bmatrix}. \tag{C–106}$$

In all cases (Q_o, Q_t, or p_{wf} specified), we have for porosity

$$\nabla_\phi \beta = \nabla_\phi GOR_l^r = 0. \tag{C–107}$$

Q_o Specified If the oil rate is specified for well l , the gas rate is given by

$$q_{g,l}^r = \sum_{k1} T_{g,l,k1}^r (p_{l,k1}^r - p_{wf,l,k1}^r), \tag{C–108}$$

so the gas-oil ratio is

$$\begin{aligned} GOR_l^r &= \frac{q_{g,l}^r}{q_{o,l}^r} \\ &= \frac{1}{q_{o,l}^r} \sum_{k1} T_{g,l,k}^r (p_{l,k1}^r - p_{wf,l,k1}^r) \\ &= \frac{1}{q_{o,l}^r} \sum_{k1} T_{g,l,k1}^r (p_{l,k1}^r - p_{wf,l}^r - dp_{wf,l,k1}^r). \end{aligned} \tag{C–109}$$

The relevant derivatives are

$$\begin{aligned} \frac{\partial GOR_l^r}{\partial k_{x,l,k}} &= \frac{1}{q_{o,l}^r} \frac{\partial}{\partial k_{x,l,k}} \sum_{k1} T_{g,l,k1}^r (p_{l,k1}^r - p_{wf,l}^r - dp_{wf,l,k1}^r) \\ &= \frac{1}{q_{o,l}^r} \frac{\partial T_{g,l,k}^r}{\partial k_{x,l,k}} (p_{l,k}^r - p_{wf,l}^r - dp_{wf,l,k}^r), \end{aligned} \tag{C–110}$$

$$\begin{aligned} \frac{\partial GOR_l^r}{\partial k_{y,l,k}} &= \frac{1}{q_{o,l}^r} \frac{\partial}{\partial k_{y,l,k}} \sum_{k1} T_{g,l,k1}^r (p_{l,k1}^r - p_{wf,l}^r - dp_{wf,l,k1}^r) \\ &= \frac{1}{q_{o,l}^r} \frac{\partial T_{g,l,k}^r}{\partial k_{y,l,k}} (p_{l,k}^r - p_{wf,l}^r - dp_{wf,l,k}^r), \end{aligned} \tag{C–111}$$

and

$$\frac{\partial GOR_l^r}{\partial k_{z,l,k}} = 0. \tag{C–112}$$

Q_t or p_{wf} Specified In the case where the total rate is specified or bottom hole pressure is specified at well l, the gas rate and oil rate are computed by

$$q_{g,l}^r = \sum_{k1} T_{g,l,k1}^r (p_{l,k1}^r - p_{wf,l,k1}^r), \tag{C–113}$$

and

$$q_{o,l}^r = \sum_{k1} T_{o,l,k1}^r (p_{l,k1}^r - p_{wf,l,k1}^r), \tag{C–114}$$

respectively, and the gas-oil ratio is defined as

$$GOR_l^r = \frac{q_{g,l}^r}{q_{o,l}^r}. \tag{C–115}$$

The derivatives of GOR with respect to permeabilities are given by

$$\begin{aligned}\frac{\partial GOR_l^r}{\partial k_{x,l,k}} &= \frac{1}{q_{o,l}^r}\frac{\partial q_{g,l}^r}{\partial k_{x,l,k}} - \frac{q_{g,l}^r}{(q_{o,l}^r)^2}\frac{\partial q_{o,l}^r}{\partial k_{x,l,k}} \\ &= \frac{1}{q_{o,l}^r}\frac{\partial T_{g,l,k}^r}{\partial k_{x,l,k}}(p_{l,k}^r - p_{wf,l}^r - dp_{wf,l,k}^r) - \frac{q_{g,l}^r}{(q_{o,l}^r)^2}\frac{\partial T_{o,l,k}^r}{\partial k_{x,l,k}}(p_{l,k}^r - p_{wf,l}^r - dp_{wf,l,k}^r),\end{aligned} \tag{C–116}$$

$$\begin{aligned}\frac{\partial GOR_l^r}{\partial k_{y,l,k}} &= \frac{1}{q_{o,l}^r}\frac{\partial q_{g,l}^r}{\partial k_{y,l,k}} - \frac{q_{g,l}^r}{(q_{o,l}^r)^2}\frac{\partial q_{o,l}^r}{\partial k_{y,l,k}} \\ &= \frac{1}{q_{o,l}^r}\frac{\partial T_{g,l,k}^r}{\partial k_{y,l,k}}(p_{l,k}^r - p_{wf,l}^r - dp_{wf,l,k}^r) - \frac{q_{g,l}^r}{(q_{o,l}^r)^2}\frac{\partial T_{o,l,k}^r}{\partial k_{y,l,k}}(p_{l,k}^r - p_{wf,l}^r - dp_{wf,l,k}^r),\end{aligned} \tag{C–117}$$

and

$$\frac{\partial GOR_l^r}{\partial k_{z,l,k}} = 0. \tag{C–118}$$

derivatives of WOR

The gradient of WOR at well l at time step t^r is given by

$$\nabla_m \beta = \nabla_m WOR_l^r = \begin{bmatrix} \frac{\partial WOR_l^r}{\partial m_1} \\ \frac{\partial WOR_l^r}{\partial m_2} \\ \vdots \\ \frac{\partial WOR_l^r}{\partial m_M} \end{bmatrix}. \tag{C–119}$$

The WOR does not depend explicitly on porosity, so

$$\nabla_\phi \beta = \nabla_\phi WOR_l^r = 0. \tag{C–120}$$

Q_o specified If the oil rate is specified for well l, we have

$$q_{w,l}^r = \sum_{k1} T_{w,l,k1}^r (p_{l,k1}^r - p_{wf,l,k1}^r). \tag{C–121}$$

so the water-oil ratio is given by

$$\begin{aligned} WOR_l^r &= \frac{q_{w,l}^r}{q_{o,l}^r} \\ &= \frac{1}{q_{o,l}^r} \sum_{k1} T_{w,l,k1}^r (p_{l,k1}^r - p_{wf,l,k1}^r) \\ &= \frac{1}{q_{o,l}^r} \sum_{k1} T_{w,l,k1}^r (p_{l,k1}^r - p_{wf,l}^r - dp_{wf,l,k1}^r). \end{aligned} \tag{C–122}$$

The derivatives with respect to permeability are

$$\begin{aligned} \frac{\partial WOR_l^r}{\partial k_{x,l,k}} &= \frac{1}{q_{o,l}^r} \frac{\partial}{\partial k_{x,l,k}} \sum_{k1} T_{w,l,k1}^r (p_{l,k1}^r - p_{wf,l}^r - dp_{wf,l,k1}^r) \\ &= \frac{1}{q_{o,l}^r} \frac{\partial T_{w,l,k}^r}{\partial k_{x,l,k}} (p_{l,k}^r - p_{wf,l}^r - dp_{wf,l,k}^r), \end{aligned} \tag{C–123}$$

$$\begin{aligned} \frac{\partial WOR_l^r}{\partial k_{y,l,k}} &= \frac{1}{q_{o,l}^r} \frac{\partial}{\partial k_{y,l,k}} \sum_{k1} T_{w,l,k1}^r (p_{l,k1}^r - p_{wf,l}^r - dp_{wf,l,k1}^r) \\ &= \frac{1}{q_{o,l}^r} \frac{\partial T_{w,l,k}^r}{\partial k_{y,l,k}} (p_{l,k}^r - p_{wf,l}^r - dp_{wf,l,k}^r), \end{aligned} \tag{C–124}$$

and

$$\frac{\partial WOR_l^r}{\partial k_{z,l,k}} = 0. \tag{C–125}$$

Q_t or p_{wf} Specified In the case where the total rate or bottom hole pressure is specified for well l, the water rate and oil rate are given by

$$q^r_{w,l} = \sum_k T^r_{w,l,k}(p^r_{l,k} - p^r_{wf,l,k}), \tag{C–126}$$

and

$$q^r_{o,l} = \sum_k T^r_{o,l,k}(p^r_{l,k} - p^r_{wf,l,k}), \tag{C–127}$$

and the water-oil ratio is defined as

$$WOR^r_l = \frac{q^r_{w,l}}{q^r_{o,l}}. \tag{C–128}$$

We have

$$\begin{aligned}\frac{\partial WOR^r_l}{\partial k_{x,l,k}} &= \frac{1}{q^r_{o,l}}\frac{\partial q^r_{w,l}}{\partial k_{x,l,k}} - \frac{q^r_{w,l}}{(q^r_{o,l})^2}\frac{\partial q^r_{o,l}}{\partial k_{x,l,k}} \\ &= \frac{1}{q^r_{o,l}}\frac{\partial T^r_{w,l,k}}{\partial k_{x,l,k}}(p^r_{l,k} - p^r_{wf,l} - dp^r_{wf,l,k}) - \frac{q^r_{w,l}}{(q^r_{o,l})^2}\frac{\partial T^r_{o,l,k}}{\partial k_{x,l,k}}(p^r_{l,k} - p^r_{wf,l} - dp^r_{wf,l,k}),\end{aligned} \tag{C–129}$$

$$\begin{aligned}\frac{\partial WOR^r_l}{\partial k_{y,l,k}} &= \frac{1}{q^r_{o,l}}\frac{\partial q^r_{w,l}}{\partial k_{y,l,k}} - \frac{q^r_{w,l}}{(q^r_{o,l})^2}\frac{\partial q^r_{o,l}}{\partial k_{y,l,k}} \\ &= \frac{1}{q^r_{o,l}}\frac{\partial T^r_{w,l,k}}{\partial k_{y,l,k}}(p^r_{l,k} - p^r_{wf,l} - dp^r_{wf,l,k}) - \frac{q^r_{w,l}}{(q^r_{o,l})^2}\frac{\partial T^r_{o,l,k}}{\partial k_{y,l,k}}(p^r_{l,k} - p^r_{wf,l} - dp^r_{wf,l,k}),\end{aligned} \tag{C–130}$$

and

$$\frac{\partial WOR^r_l}{\partial k_{z,l,k}} = 0. \tag{C–131}$$

C.2 Sensitivity for Case $k_z = a\sqrt{k_x k_y}$

For some reservoirs, we may wish to assume that

$$k_z = a\sqrt{k_x k_y}, \tag{C–132}$$

where a is a constant scalar value for the reservoir. In this case, the independent variables of permeability fields are k_x, k_y and a (instead of k_x, k_y and k_z). The

computation of the derivatives for the adjoint equation (Eq. C–1) is very similar to what we presented in section C.1. The only difference is in the derivatives of the flow terms. Here we give details how to calculate derivatives of flow terms for this case. The transmissibilities are given by

$$T^{n+1}_{mx,i+1/2,j,k} = \frac{C_1 \Delta y_j \Delta z_k k_{x,i+1/2,j,k}}{x_{i+1} - x_i} \left(\frac{k_{rm}}{\mu_m B_m} \right)^{n+1}_{i+1/2,j,k}, \tag{C–133}$$

$$T^{n+1}_{my,i,j+1/2,k} = \frac{C_1 \Delta x_i \Delta z_k k_{y,i,j+1/2,k}}{y_{j+1} - y_j} \left(\frac{k_{rm}}{\mu_m B_m} \right)^{n+1}_{i,j+1/2,k}, \tag{C–134}$$

and

$$T^{n+1}_{mz,i,j,k+1/2} = \frac{C_1 \Delta x_i \Delta y_j k_{z,i,j,k+1/2}}{z_{k+1} - z_k} \left(\frac{k_{rm}}{\mu_m B_m} \right)_{i,j,k+1/2}, \tag{C–135}$$

where

$$\begin{aligned} k_{z,i,j,k+1/2} &= \frac{(\triangle z_k + \triangle z_{k+1}) k_{z,i,j,k} k_{z,i,j,k+1}}{\triangle z_k k_{z,i,j,k+1} + \triangle z_{k+1} k_{z,i,j,k}} \\ &= \frac{a(\triangle z_k + \triangle z_{k+1}) \sqrt{k_{x,i,j,k} k_{y,i,j,k}} \sqrt{k_{x,i,j,k+1} k_{y,i,j,k+1}}}{\triangle z_k \sqrt{k_{x,i,j,k+1} k_{y,i,j,k+1}} + \triangle z_{k+1} \sqrt{k_{x,i,j,k} k_{y,i,j,k}}}. \end{aligned} \tag{C–136}$$

Normally, the transmissibility in z-direction, $T^{n+1}_{mz,i,j,k+1/2}$, dependents only on the k_z. However, in this case, it is easy to see that $T^{n+1}_{mz,i,j,k+1/2}$ is a function of k_x, k_y, and a. We need to calculate the derivatives of $T^{n+1}_{mz,i,j,k+1/2}$ with respect to k_x, k_y, and a.

C.2.1 The Derivatives of Flow Terms

We calculate the derivatives of flow terms with respect to the model parameters at gridblock (i, j, k). For the flow terms at gridblock $(i+1, j, k)$, $(i-1, j, k)$, $(i, j+1, k)$ and $(i, j-1, k)$, we use Eqs. C–15 to C–21 to calculate derivatives. The derivatives of flow terms at gridblock $(i, j, k \pm 1)$ to permeability are

$$\frac{\partial F^n_{o,i,j,k\pm1}}{\partial k_{i,j,k}} = \frac{\partial T^n_{oz,i,j,k\pm1/2}}{\partial k_{i,j,k}} [p^n_{i,j,k} - p^n_{i,j,k\pm1} + \gamma^n_{o,i,j,k\pm1/2}(D_{i,j,k\pm1} - D_{i,j,k})], \tag{C–137}$$

$$\frac{\partial F^n_{w,i,j,k\pm1}}{\partial k_{i,j,k}} = \frac{\partial T^n_{wz,i,j,k\pm1/2}}{\partial k_{i,j,k}} [p^n_{i,j,k} - p^n_{i,j,k\pm1} + \gamma^n_{w,i,j,k\pm1/2}(D_{i,j,k\pm1} - D_{i,j,k})], \tag{C–138}$$

and

$$\frac{\partial F^n_{g,i,j,k\pm1}}{\partial k_{i,j,k}} = \frac{\partial T^n_{gz,i,j,k\pm1/2}}{\partial k_{i,j,k}}[p^n_{i,j,k} - p^n_{i,j,k\pm1} + \gamma^n_{g,i,j,k\pm1/2}(D_{i,j,k\pm1} - D_{i,j,k})]$$
$$+ \frac{\partial T^n_{oz,i,j,k\pm1/2}}{\partial k_{i,j,k}} R^n_{so,i,j,k\pm1/2}[p^n_{i,j,k} - p^n_{i,j,k\pm1} + \gamma^n_{o,i,j,k\pm1/2}(D_{i,j,k\pm1} - D_{i,j,k})], \quad \text{(C–139)}$$

where $k_{i,j,k} = k_{x,i,j,k}$ or $k_{y,i,j,k}$.

The derivatives of flow terms at gridblock (i, j, k) are given by

$$\frac{\partial F^n_{m,i,j,k}}{\partial k_{x,i,j,k}} = -\left(\frac{\partial F^n_{m,i+1,j,k}}{\partial k_{x,i,j,k}} + \frac{\partial F^n_{m,i-1,j,k}}{\partial k_{x,i,j,k}} + \frac{\partial F^n_{m,i,j,k\pm1}}{\partial k_{x,i,j,k}} + \frac{\partial F^n_{m,i,j,k-1}}{\partial k_{x,i,j,k}}\right), \quad \text{(C–140)}$$

and

$$\frac{\partial F^n_{m,i,j,k}}{\partial k_{y,i,j,k}} = -\left(\frac{\partial F^n_{m,i,j+1,k}}{\partial k_{y,i,j,k}} + \frac{\partial F^n_{m,i,j-1,k}}{\partial k_{y,i,j,k}} + \frac{\partial F^n_{m,i,j,k\pm1}}{\partial k_{y,i,j,k}} + \frac{\partial F^n_{m,i,j,k-1}}{\partial k_{y,i,j,k}}\right). \quad \text{(C–141)}$$

Because all flow terms, $F^n_{m,i,j,k}$, involve the z-direction transmissibility $T^n_{mz,i,j,k\pm1/2}$, all $F^n_{m,i,j,k}$'s are functions of a. The derivatives of flow terms with respect to the parameter a are given by

$$\frac{\partial F^n_{o,i,j,k}}{\partial a} = -\frac{\partial T^n_{oz,i,j,k+1/2}}{\partial a}[p^n_{i,j,k} - p^n_{i,j,k+1} + \gamma^n_{o,i,j,k+1/2}(D_{i,j,k+1} - D_{i,j,k})]$$
$$- \frac{\partial T^n_{oz,i,j,k-1/2}}{\partial a}[p^n_{i,j,k} - p^n_{i,j,k-1} + \gamma^n_{o,i,j,k-1/2}(D_{i,j,k-1} - D_{i,j,k})], \quad \text{(C–142)}$$

$$\frac{\partial F^n_{w,i,j,k}}{\partial a} = -\frac{\partial T^n_{wz,i,j,k+1/2}}{\partial a}[p^n_{i,j,k} - p^n_{i,j,k+1} + \gamma^n_{w,i,j,k+1/2}(D_{i,j,k+1} - D_{i,j,k})]$$
$$- \frac{\partial T^n_{wz,i,j,k-1/2}}{\partial a}[p^n_{i,j,k} - p^n_{i,j,k-1} + \gamma^n_{w,i,j,k-1/2}(D_{i,j,k-1} - D_{i,j,k})], \quad \text{(C–143)}$$

and

$$\frac{\partial F^n_{g,i,j,k}}{\partial a} = -\frac{\partial T^n_{gz,i,j,k+1/2}}{\partial a}[p^n_{i,j,k} - p^n_{i,j,k+1} + \gamma^n_{g,i,j,k+1/2}(D_{i,j,k+1} - D_{i,j,k})]$$
$$- \frac{\partial T^n_{gz,i,j,k-1/2}}{\partial a}[p^n_{i,j,k} - p^n_{i,j,k-1} + \gamma^n_{g,i,j,k-1/2}(D_{i,j,k-1} - D_{i,j,k})]$$
$$- \frac{\partial T^n_{oz,i,j,k+1/2}}{\partial a} R^n_{so,i,j,k+1/2}[p^n_{i,j,k} - p^n_{i,j,k+1} + \gamma^n_{o,i,j,k+1/2}(D_{i,j,k+1} - D_{i,j,k})]$$
$$- \frac{\partial T^n_{oz,i,j,k-1/2}}{\partial a} R^n_{so,i,j,k-1/2}[p^n_{i,j,k} - p^n_{i,j,k-1} + \gamma^n_{o,i,j,k-1/2}(D_{i,j,k-1} - D_{i,j,k})]. \quad \text{(C–144)}$$

Compute Partial Derivatives of Transmissibility T

From section B.1, we have

$$\frac{\partial T^n_{mx,i+1/2,j,k}}{\partial k_{x,i,j,k}} = \frac{\triangle x_i k_{x,i+1,j,k}}{k_{x,i,j,k}(\triangle x_i k_{x,i+1,j,k} + \triangle x_{i+1} k_{x,i,j,k})} T^n_{mx,i+1/2,j,k}, \tag{C–145}$$

$$\frac{\partial T^n_{mx,i-1/2,j,k}}{\partial k_{x,i,j,k}} = \frac{\triangle x_i k_{x,i-1,j,k}}{k_{x,i,j,k}(\triangle x_{i-1} k_{x,i,j,k} + \triangle x_i k_{x,i-1,j,k})} T^n_{mx,i-1/2,j,k}, \tag{C–146}$$

$$\frac{\partial T^n_{my,i,j+1/2,k}}{\partial k_{y,i,j,k}} = \frac{\triangle y_j k_{y,i,j+1,k}}{k_{y,i,j,k}(\triangle y_j k_{y,i,j+1,k} + \triangle y_{j+1} k_{y,i,j,k})} T^n_{my,i,j+1/2,k}, \tag{C–147}$$

and

$$\frac{\partial T^n_{my,i,j-1/2,k}}{\partial k_{y,i,j,k}} = \frac{\triangle y_j k_{y,i-1,j,k}}{k_{y,i,j,k}(\triangle y_{j-1} k_{y,i,j,k} + \triangle y_j k_{y,i,j-1,k})} T^n_{my,i,j-1/2,k}, \tag{C–148}$$

for $m = ow, g$.

In this case, the model parameters are k_x, k_y, and a instead of k_x, k_y, and k_z in the regular cases. k_z depends on k_x, k_y, and a. We need to compute derivatives of k_z with respect to k_x, k_y, and a and use chain rule to find the derivatives of transmissibilities. From Eq. C–136, the term $k_{z,i,j,k+1/2}$ is

$$\begin{aligned} k_{z,i,j,k+1/2} &= \frac{(\triangle z_k + \triangle z_{k+1}) k_{z,i,j,k} k_{z,i,j,k+1}}{\triangle z_k k_{z,i,j,k+1} + \triangle z_{k+1} k_{z,i,j,k}} \\ &= \frac{a(\triangle z_k + \triangle z_{k+1}) \sqrt{k_{x,i,j,k} k_{y,i,j,k}} \sqrt{k_{x,i,j,k+1} k_{y,i,j,k+1}}}{\triangle z_k \sqrt{k_{x,i,j,k+1} k_{y,i,j,k+1}} + \triangle z_{k+1} \sqrt{k_{x,i,j,k} k_{y,i,j,k}}}, \end{aligned} \tag{C–149}$$

so the derivatives of $k_{z,i,j,k+1/2}$ with respect to $k_{x,i,j,k}$ are

$$\begin{aligned}
\frac{\partial k_{z,i,j,k+1/2}}{\partial k_{x,i,j,k}} &= \frac{a(\triangle z_k + \triangle z_{k+1})}{2(\triangle z_k\sqrt{k_{x,i,j,k+1}k_{y,i,j,k+1}} + \triangle z_{k+1}\sqrt{k_{x,i,j,k}k_{y,i,j,k}})^2}\times \\
&\quad\Bigg[(\triangle z_k\sqrt{k_{x,i,j,k+1}k_{y,i,j,k+1}} + \triangle z_{k+1}\sqrt{k_{x,i,j,k}k_{y,i,j,k}})\sqrt{\frac{k_{y,i,j,k}}{k_{x,i,j,k}}}\sqrt{k_{x,i,j,k+1}k_{y,i,j,k+1}} \\
&\quad - \triangle z_{k+1}\sqrt{\frac{k_{y,i,j,k}}{k_{x,i,j,k}}}\sqrt{k_{x,i,j,k}k_{y,i,j,k}}\sqrt{k_{x,i,j,k+1}k_{y,i,j,k+1}}\Bigg] \\
&= \frac{a(\triangle z_k + \triangle z_{k+1})}{2(\triangle z_k\sqrt{k_{x,i,j,k+1}k_{y,i,j,k+1}} + \triangle z_{k+1}\sqrt{k_{x,i,j,k}k_{y,i,j,k}})^2}\times \\
&\quad(\triangle z_k\sqrt{k_{x,i,j,k+1}k_{y,i,j,k+1}}\sqrt{\frac{k_{y,i,j,k}}{k_{x,i,j,k}}}\sqrt{k_{x,i,j,k+1}k_{y,i,j,k+1}} \\
&= \frac{1}{2}\sqrt{\frac{k_{y,i,j,k}}{k_{x,i,j,k}}}\frac{\triangle z_k\sqrt{k_{x,i,j,k+1}k_{y,i,j,k+1}}}{\sqrt{k_{x,i,j,k}k_{y,i,j,k}}(\triangle z_k\sqrt{k_{x,i,j,k+1}k_{y,i,j,k+1}} + \triangle z_{k+1}\sqrt{k_{x,i,j,k}k_{y,i,j,k}})} \\
&\quad\frac{a(\triangle z_k + \triangle z_{k+1})\sqrt{k_{x,i,j,k}k_{y,i,j,k}}\sqrt{k_{x,i,j,k+1}k_{y,i,j,k+1}}}{(\triangle z_k\sqrt{k_{x,i,j,k+1}k_{y,i,j,k+1}} + \triangle z_{k+1}\sqrt{k_{x,i,j,k}k_{y,i,j,k}})} \\
&= \frac{\triangle z_k\sqrt{k_{x,i,j,k+1}k_{y,i,j,k+1}}}{2k_{x,i,j,k}(\triangle z_k\sqrt{k_{x,i,j,k+1}k_{y,i,j,k+1}} + \triangle z_{k+1}\sqrt{k_{x,i,j,k}k_{y,i,j,k}})}k_{z,i,j,k+1/2}.
\end{aligned} \tag{C–150}$$

Similarly, we obtain the other derivatives

$$\frac{\partial k_{z,i,j,k-1/2}}{\partial k_{x,i,j,k}} = \frac{\triangle z_k\sqrt{k_{x,i,j,k-1}k_{y,i,j,k-1}}}{2k_{x,i,j,k}(\triangle z_k\sqrt{k_{x,i,j,k-1}k_{y,i,j,k-1}} + \triangle z_{k-1}\sqrt{k_{x,i,j,k}k_{y,i,j,k}})}k_{z,i,j,k-1/2}, \tag{C–151}$$

and

$$\frac{\partial k_{z,i,j,k\pm1/2}}{\partial k_{y,i,j,k}} = \frac{\triangle z_k\sqrt{k_{x,i,j,k\pm1}k_{y,i,j,k\pm1}}}{2k_{y,i,j,k}(\triangle z_k\sqrt{k_{x,i,j,k\pm1}k_{y,i,j,k\pm1}} + \triangle z_{k\pm1}\sqrt{k_{x,i,j,k}k_{y,i,j,k}})}k_{z,i,j,k\pm1/2}. \tag{C–152}$$

The derivatives of transmissibilities with respect to permeability are

$$\begin{aligned}\frac{\partial T^n_{mz,i,j,k\pm1/2}}{\partial k_{x,i,j,k}} &= \frac{\partial T^n_{mz,i,j,k\pm1/2}}{\partial k_{z,i,j,k\pm1/2}}\frac{\partial k^n_{z,i,j,k\pm1/2}}{\partial k_{x,i,j,k}} \\ &= \frac{T^n_{mz,i,j,k\pm1/2}}{2k_{x,i,j,k}(1+(\triangle z_{k\pm1}/\triangle z_k)\sqrt{(k_{x,i,j,k}k_{y,i,j,k})/(k_{x,i,j,k\pm1}k_{y,i,j,k\pm1})})} \\ &= \frac{T^n_{mz,i,j,k\pm1/2}}{2k_{x,i,j,k}(1+(\triangle z_{k\pm1}/\triangle z_k)(k_{z,i,j,k}/k_{z,i,j,k\pm1}))},\end{aligned} \tag{C–153}$$

and

$$\begin{aligned}\frac{\partial T^n_{mz,i,j,k\pm1/2}}{\partial k_{y,i,j,k}} &= \frac{\partial T^n_{mz,i,j,k\pm1/2}}{\partial k_{z,i,j,k\pm1/2}}\frac{\partial k^n_{z,i,j,k\pm1/2}}{\partial k_{y,i,j,k}} \\ &= \frac{T^n_{mz,i,j,k\pm1/2}}{2k_{y,i,j,k}(1+(\triangle z_{k\pm1}/\triangle z_k)\sqrt{(k_{x,i,j,k}k_{y,i,j,k})/(k_{x,i,j,k\pm1}k_{y,i,j,k\pm1})})} \\ &= \frac{T^n_{mz,i,j,k\pm1/2}}{2k_{y,i,j,k}(1+(\triangle z_{k\pm1}/\triangle z_k)(k_{z,i,j,k}/k_{z,i,j,k\pm1}))}.\end{aligned} \tag{C–154}$$

From Eq. C–136,

$$\begin{aligned}\frac{\partial k_{z,i,j,k\pm1/2}}{\partial a} &= \frac{(\triangle z_k+\triangle z_{k\pm1})\sqrt{k_{x,i,j,k}k_{y,i,j,k}}\sqrt{k_{x,i,j,k\pm1}k_{y,i,j,k\pm1}}}{\triangle z_k\sqrt{k_{x,i,j,k\pm1}k_{y,i,j,k\pm1}}+\triangle z_{k\pm1}\sqrt{k_{x,i,j,k}k_{y,i,j,k}}} \\ &= \frac{1}{a}k_{z,i,j,k\pm1/2}.\end{aligned} \tag{C–155}$$

So we have the derivatives of transmissibility with respect to the parameter a,

$$\begin{aligned}\frac{\partial T^n_{mz,i,j,k\pm1/2}}{\partial a} &= \frac{\partial T^n_{mz,i,j,k\pm1/2}}{\partial k_{z,i,j,k\pm1/2}}\frac{\partial k_{z,i,j,k\pm1/2}}{\partial a} \\ &= \frac{1}{a}T^n_{mz,i,j,k\pm1/2},\end{aligned} \tag{C–156}$$

for $m = o, w, g$.

At the boundaries, the derivatives of the transmissibility are zero, i.e.,

$$\begin{aligned}\frac{\partial T^n_{mx,1/2,j,k}}{\partial k^n_{i,j,k}} &= \frac{\partial T^n_{mx,n_x+1/2,j,k}}{\partial k^n_{i,j,k}} = \frac{\partial T^n_{my,i,1/2,k}}{\partial k^n_{i,j,k}} \\ &= \frac{\partial T^n_{my,i,n_y+1/2,k}}{\partial k^n_{i,j,k}} = \frac{\partial T^n_{mz,i,j,1/2}}{\partial k^n_{i,j,k}} = \frac{\partial T^n_{mz,i,j,n_z+1/2}}{\partial k^n_{i,j,k}} = 0\end{aligned} \tag{C–157}$$

C.3 Derivatives with respect to Skin Factors

In order to estimate the skin factors, one need compute the sensitivities to skin factors. Therefore, one need calculate the derivatives with respect to skin factors in Eq. C-1. Because only the sink terms in the flow equations involve skin factors, the derivatives of flow terms and accumulation terms with respect to the skin factor are zero. Only the derivatives of sink terms in flow equations and well equations have nonzero derivatives with respect to skin factors.

In this section, we give the formulas to compute the sensitivities to the skin factors in each completion. If one wishes to use one skin factor per well, one only need to simply add up the sensitivity coefficients of all completion in the given well. For example, the skin factor at layer k of well l is $s_{l,k}$ and the sensitivity coefficient is $\partial J/\partial s_{l,k}$. Assume that all skin factors in well l are equal to s_l, i.e., $s_l = s_{l,k}$, for all k, we have

$$\frac{\partial J}{\partial s_l} = \sum_{k1} \frac{\partial J}{\partial s_{l,k1}}. \tag{C–158}$$

C.3.1 Derivatives of Sink Terms in the Flow Equations

Producing Wells (Q_o, Q_t, or p_{wf} Specified)

For a producing well, the layer k_0 production rates at well l are

$$q^{n+1}_{m,l,k0} = T^{n+1}_{m,l,k0}[p^{n+1}_{l,k0} - p^{n+1}_{wf,l} - dp^{n+1}_{wf,l,k0}], \tag{C–159}$$

for $m = o, w, g$, where

$$T^{n+1}_{o,l,k0} = WI_{l,k0}\left(\frac{k_{ro}}{B_o\mu_o}\right)^{n+1}_{l,k0}, \tag{C–160}$$

$$T^{n+1}_{w,l,k0} = WI_{l,k0}\left(\frac{k_{rw}}{B_w\mu_w}\right)^{n+1}_{l,k0}, \tag{C–161}$$

and

$$T_{g,l,k0}^{n+1} = WI_{l,k0}\left(\frac{k_{rg}}{B_g\mu_g} + R_{so}\frac{k_{ro}}{B_o\mu_o}\right)_{l,k0}^{n+1}. \tag{C–162}$$

It is easy to see that for $k = k0$

$$\frac{\partial q_{m,l,k0}^{n+1}}{\partial s_{l,k}} = \frac{\partial q_{m,l,k0}^{n+1}}{\partial s_{l,k0}} = \frac{\partial T_{m,l,k0}^{n+1}}{\partial s_{l,k0}}[p_{l,k0}^{n+1} - p_{wf,l}^{n+1} - dp_{wf,l,k0}^{n+1}], \tag{C–163}$$

for $m = o, w, g$. For $k \neq k0$

$$\frac{\partial q_{m,l,k0}^{n+1}}{\partial s_{l,k}} = 0, \tag{C–164}$$

for all three phases.

Recall that

$$WI_{l,k0} = \frac{0.00708\triangle z\sqrt{k_{x,l,k0}k_{y,l,k0}}}{\ln(r_{o,l,k0}/r_{w,l,k0}) + s_{l,k0}}, \tag{C–165}$$

and

$$r_{o,l,k0} = \frac{0.28073\triangle x_i\sqrt{1 + \frac{k_{x,l,k0}}{k_{y,l,k0}}\left(\frac{\triangle y_j}{\triangle x_i}\right)^2}}{1 + \sqrt{k_{x,l,k0}/k_{y,l,k0}}}. \tag{C–166}$$

So we have

$$\begin{aligned}\frac{\partial WI_{l,k0}}{\partial s_{l,k0}} &= \frac{\partial}{\partial s_{l,k0}}\left(\frac{0.00708\triangle z\sqrt{k_{x,l,k0}k_{y,l,k0}}}{\ln(r_{o,l,k0}/r_{w,l,k0}) + s_{l,k0}}\right) \\ &= -\frac{0.00708\triangle z\sqrt{k_{x,l,k0}k_{y,l,k0}}}{(\ln(r_{o,l,k0}/r_{w,l,k0}) + s_{l,k0})^2} \\ &= -\frac{WI_{l,k0}}{\ln(r_{o,l,k0}/r_{w,l,k0}) + s_{l,k0}}.\end{aligned} \tag{C–167}$$

The derivatives of $T_{m,l,k0}^{n+1}$ with respect to skin factor $s_{l,k0}$ are

$$\frac{\partial T_{m,l,k0}^{n+1}}{\partial s_{l,k0}} = -\frac{T_{m,l,k0}^{n+1}}{\ln(r_{o,l,k0}/r_{w,l,k0}) + s_{l,k0}}, \tag{C–168}$$

where $m = o, w, g$. So the derivatives of the sink/source terms with respect to the skin factor $s_{l,k0}$ are

$$\frac{\partial q_{m,l,k00}^{n+1}}{\partial s_{l,k0}} = -\frac{q_{m,l,k0}^{n+1}}{\ln(r_{o,l,k0}/r_{w,l,k0}) + s_{l,k0}}, \tag{C–169}$$

for each of the three phases.

Injection Wells (Water or Gas Injection)

For the injection wells, the water or gas injection rates at layer $k0$ of well l are given by

$$q^{n+1}_{m,l,k0} = T^{n+1}_{inj,m,l,k0}[p^{n+1}_{l,k0} - p^{n+1}_{wf,l} - dp^{n+1}_{wf,l,k0}], \tag{C–170}$$

for $m = w, g$, where

$$T^{n+1}_{inj,m,l,k0} = \frac{WI_{l,k0}}{\mu^{n+1}_{m,l,k0} B^{n+1}_{m,l,k0}}. \tag{C–171}$$

For $k = k0$, the derivatives are

$$\frac{\partial q^{n+1}_{m,l,k0}}{\partial s_{l,k}} = \frac{\partial q^{n+1}_{m,l,k0}}{\partial s_{l,k0}} = -\frac{q^{n+1}_{m,l,k0}}{\ln(r_{o,l,k0}/r_{w,l,k0}) + s_{l,k0}} \tag{C–172}$$

for $m = o, w, g$.

In the water injection case, the oil rates and gas rates are set to zero, so the derivatives are

$$\frac{\partial q^{n+1}_{o,l,k0}}{\partial s_{l,k}} = \frac{\partial q^{n+1}_{g,l,k0}}{\partial s_{l,k}} = 0, \tag{C–173}$$

and in the gas injection case, the oil rates and water rates are set to zero, so the derivatives are

$$\frac{\partial q^{n+1}_{o,l,k0}}{\partial s_{l,k}} = \frac{\partial q^{n+1}_{w,l,k0}}{\partial s_{l,k}} = 0, \tag{C–174}$$

for all k.

If p_{wf} is specified, all the equations are still the same.

C.3.2 Derivatives of Well Equations

In this section, we compute the derivatives of well constraint equations to the skin factors.

Q_o Specified

In the case that oil rate is specified, the well equation at well l is

$$f^{n+1}_{wf,l} = \sum_{k1} T^{n+1}_{o,l,k1}[p^{n+1}_{l,k1} - p^{n+1}_{wf,l} - dp^{n+1}_{wf,l,k1}] - q^{n+1}_{o,l} = 0, \tag{C–175}$$

where

$$T^{n+1}_{o,l,k1} = WI_{l,k1}\left(\frac{k_{ro}}{B_o\mu_o}\right)^{n+1}_{l,k1}. \tag{C–176}$$

We obtain the derivatives

$$\begin{aligned}\frac{\partial f^{n+1}_{wf,l}}{\partial s_{l,k}} &= \frac{\partial T^{n+1}_{o,l,k}}{\partial s_{l,k}}[p^{n+1}_{l,k} - p^{n+1}_{wf,l} - dp^{n+1}_{wf,l,k}] \\ &= -\frac{T^{n+1}_{o,l,k}[p^{n+1}_{l,k} - p^{n+1}_{wf,l} - dp^{n+1}_{wf,l,k}]}{\ln(r_{o,l,k}/r_{w,l,k}) + s_{l,k}} \\ &= -\frac{q^{n+1}_{o,l,k}}{\ln(r_{o,l,k}/r_{w,l,k}) + s_{l,k}}.\end{aligned} \tag{C–177}$$

<u>Q_t Specified</u>

In the case where total rate is specified at reservoir condition, the well equation at well l is

$$f^{n+1}_{wf,l} = \sum_{k1} T^{n+1}_{t,l,k1}[p^{n+1}_{l,k1} - p^{n+1}_{wf,l} - dp^{n+1}_{wf,l,k1}] - q^{n+1}_{t,l} = 0, \tag{C–178}$$

where

$$T^{n+1}_{t,l,k1} = WI_{l,k}\left(\frac{k_{ro}}{\mu_o} + \frac{k_{rw}}{\mu_w} + \frac{k_{rg}}{\mu_g}\right)^{n+1}_{l,k1}. \tag{C–179}$$

We obtain the derivatives.

$$\begin{aligned}\frac{\partial f^{n+1}_{wf,l}}{\partial s_{l,k}} &= \frac{\partial T^{n+1}_{t,l,k}}{\partial s_{l,k}}[p^{n+1}_{l,k} - p^{n+1}_{wf,l} - dp^{n+1}_{wf,l,k}] \\ &= -\frac{T^{n+1}_{t,l,k}[p^{n+1}_{l,k} - p^{n+1}_{wf,l} - dp^{n+1}_{wf,l,k}]}{\ln(r_{o,l,k}/r_{w,l,k}) + s_{l,k}}.\end{aligned} \tag{C–180}$$

<u>Water or Gas Injection</u>

In the water or gas injection case, the well equation for well l is

$$f^{n+1}_{wf,l} = \sum_{k1} T^{n+1}_{inj,m,l,k1}[p^{n+1}_{l,k1} - p^{n+1}_{wf,l} - dp^{n+1}_{wf,l,k1}] - q^{n+1}_{m,l} = 0, \tag{C–181}$$

for $m = w, g$, where

$$T^{n+1}_{inj,m,l,k1} = \frac{WI_{l,k1}}{(B_m\mu_m)^{n+1}_{l,k1}}. \tag{C–182}$$

The derivatives of the flow equations are then

$$\begin{aligned}\frac{\partial f_{wf,l}^{n+1}}{\partial s_{l,k}} &= \frac{\partial T_{inj,m,l,k}^{n+1}}{\partial s_{l,k}}[p_{l,k}^{n+1} - p_{wf,l}^{n+1} - dp_{wf,l,k}^{n+1}] \\ &= -\frac{T_{inj,m,l,k}^{n+1}[p_{l,k}^{n+1} - p_{wf,l}^{n+1} - dp_{wf,l,k}^{n+1}]}{\ln(r_{o,l,k}/r_{w,l,k}) + s_{l,k}}.\end{aligned} \tag{C–183}$$

For the p_{wf} specified cases, we also use the same equations presented above.

C.3.3 Computation of the Vector $\nabla_m \beta$

In this part, we compute the vector $\nabla_m \beta$ in the sensitivity equation.

Derivatives of p_{wf}

If one wants to compute the sensitivity of p_{wf} to model parameter m, we set $\beta = p_{wf}$. Since p_{wf} does not explicitly dependent on skin factors, we have

$$\nabla_m \beta = 0. \tag{C–184}$$

Derivatives of GOR

Q_o Specified In the case where the oil rate is specified at well l, the gas rate is

$$q_{g,l}^{n+1} = \sum_{k1} T_{g,l,k1}^{n+1}(p_{l,k1}^{n+1} - p_{wf,l,k1}^{n+1}), \tag{C–185}$$

so the gas oil-ratio is

$$\begin{aligned}GOR_l^{n+1} &= \frac{q_{g,l}^{n+1}}{q_{o,l}^{n+1}} \\ &= \frac{1}{q_{o,l}^{n+1}} \sum_{k1} T_{g,l,k}^{n+1}(p_{l,k1}^{n+1} - p_{wf,l,k1}^{n+1}) \\ &= \frac{1}{q_{o,l}^{n+1}} \sum_{k1} T_{g,l,k1}^{n+1}(p_{l,k1}^{n+1} - p_{wf,l}^{n+1} - dp_{wf,l,k1}^{n+1}).\end{aligned} \tag{C–186}$$

The derivatives of gas-oil ratio with respect to skin are

$$\begin{aligned}\frac{\partial GOR_l^{n+1}}{\partial s_{l,k}} &= \frac{1}{q_{o,l}^{n+1}}\frac{\partial}{\partial s_{l,k}}\sum_{k1} T_{g,l,k1}^{n+1}(p_{l,k1}^{n+1} - p_{wf,l}^{n+1} - dp_{wf,l,k}^{n+1}) \\ &= \frac{1}{q_{o,l}^{n+1}}\frac{\partial T_{g,l,k}^{n+1}}{\partial s_{l,k}}(p_{l,k}^{n+1} - p_{wf,l}^{n+1} - dp_{wf,l,k}^{n+1}) \\ &= -\frac{1}{q_{o,l}^{n+1}}\frac{T_{g,l,k}^{n+1}(p_{l,k}^{n+1} - p_{wf,l}^{n+1} - dp_{wf,l,k}^{n+1})}{\ln(r_{o,l,k}/r_{w,l,k}) + s_{l,k}} \\ &= -\frac{1}{q_{o,l}^{n+1}}\frac{q_{g,l,k}^{n+1}}{\ln(r_{o,l,k}/r_{w,l,k}) + s_{l,k}}.\end{aligned} \tag{C–187}$$

Q_t or p_{wf} Specified When the total rate is specified for well l , the gas rate and oil rate are given by

$$q_{g,l}^{n+1} = \sum_{k1} T_{g,l,k1}^{n+1}(p_{l,k1}^{n+1} - p_{wf,l,k1}^{n+1}), \tag{C–188}$$

$$q_{o,l}^{n+1} = \sum_{k1} T_{o,l,k1}^{n+1}(p_{l,k1}^{n+1} - p_{wf,l,k1}^{n+1}), \tag{C–189}$$

and the gas-oil ratio is

$$GOR_l^{n+1} = \frac{q_{g,l}^{n+1}}{q_{o,l}^{n+1}}. \tag{C–190}$$

We therefore have the derivatives

$$\begin{aligned}\frac{\partial GOR}{\partial s_{l,k}} &= \frac{1}{q_{o,l}^{n+1}}\frac{\partial q_{g,l}^{n+1}}{\partial s_{l,k}} - \frac{q_{g,l}^{n+1}}{(q_{o,l}^{n+1})^2}\frac{\partial q_{o,l}^{n+1}}{\partial s_{l,k}} \\ &= \frac{1}{q_{o,l}^{n+1}}\frac{\partial T_{g,l,k}^{n+1}}{\partial s_{l,k}}(p_{l,k}^{n+1} - p_{wf,l}^{n+1} - dp_{wf,l,k}^{n+1}) - \frac{q_{g,l}^{n+1}}{(q_{o,l}^{n+1})^2}\frac{\partial T_{o,l,k}^{n+1}}{\partial s_{l,k}}(p_{l,k}^{n+1} - p_{wf,l}^{n+1} - dp_{wf,l,k}^{n+1}) \\ &= -\frac{1}{(\ln(r_{o,l,k}/r_{w,l,k}) + s_{l,k})}\left[\frac{1}{q_{o,l}^{n+1}}T_{g,l,k}^{n+1}(p_{l,k}^{n+1} - p_{wf,l}^{n+1} - dp_{wf,l,k}^{n+1})\right. \\ &\quad \left. - \frac{q_{g,l}^{n+1}}{(q_{o,l}^{n+1})^2}T_{o,l,k}^{n+1}(p_{l,k}^{n+1} - p_{wf,l}^{n+1} - dp_{wf,l,k}^{n+1})\right] \\ &= -\frac{1}{q_{o,l}^{n+1}}\frac{q_{g,l,k}^{n+1}}{(\ln(r_{o,l,k}/r_{w,l,k}) + s_{l,k})} + \frac{q_{g,l}^{n+1}}{(q_{o,l}^{n+1})^2}\frac{q_{o,l,k}^{n+1}}{(\ln(r_{o,l,k}/r_{w,l,k}) + s_{l,k})}.\end{aligned} \tag{C–191}$$

Derivatives of WOR

Q_o Specified If the oil rate is specified at well l, the water rate is

$$q_{w,l}^{n+1} = \sum_{k1} T_{w,l,k1}^{n+1}(p_{l,k1}^{n+1} - p_{wf,l,k1}^{n+1}), \tag{C–192}$$

and water-oil ratio is

$$\begin{aligned} WOR_l^{n+1} &= \frac{q_{w,l}^{n+1}}{q_{o,l}^{n+1}} \\ &= \frac{1}{q_{o,l}^{n+1}} \sum_{k1} T_{w,l,k}^{n+1}(p_{l,k1}^{n+1} - p_{wf,l,k1}^{n+1}) \\ &= \frac{1}{q_{o,l}^{n+1}} \sum_{k1} T_{w,l,k1}^{n+1}(p_{l,k1}^{n+1} - p_{wf,l}^{n+1} - dp_{wf,l,k1}^{n+1}). \end{aligned} \tag{C–193}$$

The derivatives are

$$\begin{aligned} \frac{\partial WOR_l^{n+1}}{\partial s_{l,k}} &= \frac{1}{q_{o,l}^{n+1}} \frac{\partial}{\partial s_{l,k}} \sum_{k1} T_{w,l,k1}^{n+1}(p_{l,k1}^{n+1} - p_{wf,l}^{n+1} - dp_{wf,l,k}^{n+1}) \\ &= \frac{1}{q_{o,l}^{n+1}} \frac{\partial T_{w,l,k}^{n+1}}{\partial s_{l,k}}(p_{l,k}^{n+1} - p_{wf,l}^{n+1} - dp_{wf,l,k}^{n+1}) \\ &= -\frac{1}{q_{o,l}^{n+1}} \frac{T_{w,l,k}^{n+1}(p_{l,k}^{n+1} - p_{wf,l}^{n+1} - dp_{wf,l,k}^{n+1})}{\ln(r_{o,l,k}/r_{w,l,k}) + s_{l,k}} \\ &= -\frac{1}{q_{o,l}^{n+1}} \frac{q_{w,l,k}^{n+1}}{\ln(r_{o,l,k}/r_{w,l,k}) + s_{l,k}}. \end{aligned} \tag{C–194}$$

Q_t or p_{wf} Specified When the total rate is specified at well l, the water and oil rates are given by

$$q_{w,l}^{n+1} = \sum_{k1} T_{w,l,k}^{n+1}(p_{l,k1}^{n+1} - p_{wf,l,k1}^{n+1}), \tag{C–195}$$

$$q_{o,l}^{n+1} = \sum_{k1} T_{o,l,k}^{n+1}(p_{l,k1}^{n+1} - p_{wf,l,k1}^{n+1}), \tag{C–196}$$

and the water oil ratio is

$$WOR = \frac{q_{w,l}^{n+1}}{q_{o,l}^{n+1}}. \tag{C–197}$$

We have the derivatives

$$\begin{aligned}
\frac{\partial WOR_l^{n+1}}{\partial s_{l,k}} &= \frac{1}{q_{o,l}^{n+1}}\frac{\partial q_{w,l}^{n+1}}{\partial s_{l,k}} - \frac{q_{w,l}^{n+1}}{(q_{o,l}^{n+1})^2}\frac{\partial q_{o,l}^{n+1}}{\partial s_{l,k}} \\
&= \frac{1}{q_{o,l}^{n+1}}\frac{\partial T_{w,l,k}^{n+1}}{\partial s_{l,k}}(p_{l,k}^{n+1} - p_{wf,l}^{n+1} - dp_{wf,l,k}^{n+1}) \\
&\quad - \frac{q_{w,l}^{n+1}}{(q_{o,l}^{n+1})^2}\frac{\partial T_{o,l,k}^{n+1}}{\partial s_{l,k}}(p_{l,k}^{n+1} - p_{wf,l}^{n+1} - dp_{wf,l,k}^{n+1}) \\
&= -\frac{1}{\ln(r_{o,l,k}/r_{w,l,k}) + s_{l,k}}\left[\frac{1}{q_{o,l}^{n+1}}T_{w,l,k}^{n+1}(p_{l,k}^{n+1} - p_{wf,l}^{n+1} - dp_{wf,l,k}^{n+1})\right. \\
&\quad \left. - \frac{q_{w,l}^{n+1}}{(q_{o,l}^{n+1})^2}T_{o,l,k}^{n+1}(p_{l,k}^{n+1} - p_{wf,l}^{n+1} - dp_{wf,l,k}^{n+1})\right] \\
&= -\frac{1}{q_{o,l}^{n+1}}\frac{q_{w,l,k}^{n+1}}{\ln(r_{o,l,k}/r_{w,l,k}) + s_{l,k}} + \frac{q_{w,l}^{n+1}}{(q_{o,l}^{n+1})^2}\frac{q_{o,l,k}^{n+1}}{\ln(r_{o,l,k}/r_{w,l,k}) + s_{l,k}}.
\end{aligned} \tag{C–198}$$

C.4 Computation of Sensitivity to the Parameters of Relative Permeability

Recall that the parameters for relative permeability model in the three-phase flow are

$$k_r = [\ n_{rw},\quad k_{rwcw},\quad n_{rg},\quad k_{rgcw},\quad n_{row},\quad k_{rocw},\quad n_{rog},\quad S_{wc},\quad S_{orw},\quad S_{gc},\quad S_{org}\ ]^T. \tag{C–199}$$

We use the adjoint equation to calculate the adjoint variables λ. The formulation to calculate sensitivity of β to relative permeability parameters is

$$\nabla_{k_r} J = \nabla_{k_r}\beta + \sum_{n=1}^{N}[\nabla_{k_r}(f^n)^T](\lambda^n). \tag{C–200}$$

The $\nabla_m[f^n]^T$ matrix is defined by

$$\nabla_m[f^n]^T = \begin{bmatrix}
\frac{\partial f_{o,1}^n}{\partial m_1} & \frac{\partial f_{w,1}^n}{\partial m_1} & \frac{\partial f_{g,1}^n}{\partial m_1} & \frac{\partial f_{o,2}^n}{\partial m_1} & \cdots & \frac{\partial f_{g,N}^n}{\partial m_1} & \frac{\partial f_{wf,1}^n}{\partial m_1} & \cdots & \frac{\partial f_{wf,N_w}^n}{\partial m_1} \\
\frac{\partial f_{o,1}^n}{\partial m_2} & \frac{\partial f_{w,1}^n}{\partial m_2} & \frac{\partial f_{o,1}^n}{\partial m_2} & \frac{\partial f_{o,2}^n}{\partial m_2} & \cdots & \frac{\partial f_{g,N}^n}{\partial m_2} & \frac{\partial f_{wf,1}^n}{\partial m_2} & \cdots & \frac{\partial f_{wf,N_w}^n}{\partial m_2} \\
\vdots & \vdots & \vdots & \vdots & \vdots & \vdots & \vdots & \vdots & \vdots \\
\frac{\partial f_{o,1}^n}{\partial m_M} & \frac{\partial f_{w,1}^n}{\partial m_M} & \frac{\partial f_{o,1}^n}{\partial m_M} & \frac{\partial f_{o,2}^n}{\partial m_M} & \cdots & \frac{\partial f_{g,N}^n}{\partial m_M} & \frac{\partial f_{wf,1}^n}{\partial m_M} & \cdots & \frac{\partial f_{wf,N_w}^n}{\partial m_M}
\end{bmatrix}. \tag{C–201}$$

where $m = k_r$. Actually, we do not have to use the functions shown above to model relative permeability curves. We can use any other appropriate analytical functions to approximate the relative permeability curves.

C.4.1 The Derivatives of Relative Permeability

Here, we present formulas to compute the derivatives of relative permeability with respect to any of the model parameters which define relative permeability. Here, I simply list the derivatives of the relative permeability for each phase with respect to the eleven model parameters.

The derivatives of k_{rw} with respect to k_r

$$\begin{aligned}\frac{\partial k_{rw}}{\partial n_{rw}} &= k_{rwcw}\left(\frac{S_w - S_{wc}}{1 - S_{orw} - S_{wc}}\right)^{n_{rw}} \ln\left(\frac{S_w - S_{wc}}{1 - S_{orw} - S_{wc}}\right) \\ &= k_{rw} \ln\left(\frac{S_w - S_{wc}}{1 - S_{orw} - S_{wc}}\right),\end{aligned} \tag{C–202}$$

$$\frac{\partial k_{rw}}{\partial k_{rwcw}} = \left(\frac{S_w - S_{wc}}{1 - S_{orw} - S_{wc}}\right)^{n_{rw}} = \frac{k_{rw}}{k_{rwcw}}, \tag{C–203}$$

$$\begin{aligned}\frac{\partial k_{rw}}{\partial S_{wc}} &= n_{rw} k_{rwcw}\left(\frac{S_w - S_{wc}}{1 - S_{orw} - S_{wc}}\right)^{n_{rw}-1} \frac{(S_w - 1 + S_{orw})}{(1 - S_{orw} - S_{wc})^2} \\ &= k_{rw} \frac{n_{rw}(S_w - 1 + S_{orw})}{(1 - S_{orw} - S_{wc})(S_w - S_{wc})},\end{aligned} \tag{C–204}$$

$$\begin{aligned}\frac{\partial k_{rw}}{\partial S_{orw}} &= n_{rw} k_{rwcw}\left(\frac{S_w - S_{wc}}{1 - S_{orw} - S_{wc}}\right)^{n_{rw}-1} \frac{(S_w - S_{wc})}{(1 - S_{orw} - S_{wc})^2} \\ &= k_{rw} \frac{n_{rw}}{(1 - S_{orw} - S_{wc})},\end{aligned} \tag{C–205}$$

and

$$\frac{\partial k_{rw}}{\partial n_{row}} = \frac{\partial k_{rw}}{\partial n_{rg}} = \frac{\partial k_{rw}}{\partial n_{rog}} = \frac{\partial k_{rw}}{\partial k_{rocw}} = \frac{\partial k_{rw}}{\partial k_{rgcw}} = \frac{\partial k_{rw}}{\partial S_{gc}} = \frac{\partial k_{rw}}{\partial S_{org}} = 0. \tag{C–206}$$

The derivatives of k_{row} with respect to k_r

$$\begin{aligned}\frac{\partial k_{row}}{\partial n_{row}} &= k_{rocw}\left(\frac{1-S_{orw}-S_w}{1-S_{orw}-S_{wc}}\right)^{n_{row}}\ln\left(\frac{1-S_{orw}-S_w}{1-S_{orw}-S_{wc}}\right)\\ &= k_{row}\ln\left(\frac{1-S_{orw}-S_w}{1-S_{orw}-S_{wc}}\right),\end{aligned} \tag{C–207}$$

$$\frac{\partial k_{row}}{\partial k_{rocw}} = \left(\frac{1-S_{orw}-S_w}{1-S_{orw}-S_{wc}}\right)^{n_{row}} = \frac{k_{row}}{k_{rocw}}, \tag{C–208}$$

$$\begin{aligned}\frac{\partial k_{row}}{\partial S_{wc}} &= n_{row}k_{rocw}\left(\frac{1-S_{orw}-S_w}{1-S_{orw}-S_{wc}}\right)^{n_{row}-1}\frac{(1-S_{orw}-S_w)}{(1-S_{orw}-S_{wc})^2}\\ &= \frac{k_{row}n_{row}}{(1-S_{orw}-S_{wc})},\end{aligned} \tag{C–209}$$

$$\begin{aligned}\frac{\partial k_{row}}{\partial S_{orw}} &= -n_{row}k_{rocw}\left(\frac{1-S_{orw}-S_w}{1-S_{orw}-S_{wc}}\right)^{n_{row}-1}\frac{(S_w-S_{wc})}{(1-S_{orw}-S_{wc})^2}\\ &= -k_{row}\frac{n_{row}(S_w-S_{wc})}{(1-S_{orw}-S_{wc})(1-S_{orw}-S_w)},\end{aligned} \tag{C–210}$$

and

$$\frac{\partial k_{row}}{\partial n_{rw}} = \frac{\partial k_{row}}{\partial n_{rg}} = \frac{\partial k_{rw}}{\partial n_{rog}} = \frac{\partial k_{row}}{\partial k_{rwcw}} = \frac{\partial k_{row}}{\partial k_{rgcw}} = \frac{\partial k_{row}}{\partial S_{gc}} = \frac{\partial k_{row}}{\partial S_{org}} = 0. \tag{C–211}$$

The derivatives of k_{rg} with respect to k_r

$$\begin{aligned}\frac{\partial k_{rg}}{\partial n_{rg}} &= k_{rgcw}\left(\frac{S_g-S_{gc}}{1-S_{org}-S_{wc}-S_{gc}}\right)^{n_{rg}}\ln\left(\frac{S_g-S_{gc}}{1-S_{org}-S_{wc}-S_{gc}}\right)\\ &= k_{rg}\ln\left(\frac{S_g-S_{gc}}{1-S_{org}-S_{wc}-S_{gc}}\right),\end{aligned} \tag{C–212}$$

$$\frac{\partial k_{rg}}{\partial k_{rgcw}} = \left(\frac{S_g-S_{gc}}{1-S_{org}-S_{wc}-S_{gc}}\right)^{n_{rg}} = \frac{k_{rg}}{k_{rgcw}}, \tag{C–213}$$

$$\begin{aligned}\frac{\partial k_{rg}}{\partial S_{gc}} &= n_{rg}k_{rgcw}\left(\frac{S_g-S_{gc}}{1-S_{org}-S_{wc}-S_{gc}}\right)^{n_{rg}-1}\frac{S_g-(1-S_{org}-S_{wc})}{(1-S_{org}-S_{wc}-S_{gc})^2}\\ &= k_{rg}\frac{n_{rg}(S_g-(1-S_{org}-S_{wc}))}{(1-S_{org}-S_{wc}-S_{gc})(S_g-S_{gc})},\end{aligned} \tag{C–214}$$

$$\frac{\partial k_{rg}}{\partial S_{org}} = n_{rg} k_{rgcw} \left(\frac{S_g - S_{gc}}{1 - S_{org} - S_{wc} - S_{gc}} \right)^{n_{rg}-1} \frac{(S_g - S_{gc})}{(1 - S_{org} - S_{wc} - S_{gc})^2} = k_{rg} \frac{n_{rg}}{(1 - S_{org} - S_{wc} - S_{gc})} \tag{C–215}$$

$$\frac{\partial k_{rg}}{\partial S_{wc}} = n_{rg} k_{rgcw} \left(\frac{S_g - S_{gc}}{1 - S_{org} - S_{wc} - S_{gc}} \right)^{n_{rg}-1} \frac{(S_g - S_{gc})}{(1 - S_{org} - S_{wc} - S_{gc})^2} = k_{rg} \frac{n_{rg}}{(1 - S_{org} - S_{wc} - S_{gc})}, \tag{C–216}$$

and

$$\frac{\partial k_{rg}}{\partial n_{row}} = \frac{\partial k_{rg}}{\partial n_{rw}} = \frac{\partial k_{rg}}{\partial n_{rog}} = \frac{\partial k_{rg}}{\partial k_{rocw}} = \frac{\partial k_{rg}}{\partial k_{rwcw}} = \frac{\partial k_{rg}}{\partial S_{orw}} = 0. \tag{C–217}$$

The derivatives of k_{rog} with respect to k_r

$$\frac{\partial k_{rog}}{\partial n_{rog}} = k_{rgcw} \left(\frac{1 - S_{org} - S_{wc} - S_g}{1 - S_{org} - S_{wc}} \right)^{n_{rog}} \ln \left(\frac{1 - S_{org} - S_{wc} - S_g}{1 - S_{org} - S_{wc}} \right) = k_{rog} \ln \left(\frac{1 - S_{org} - S_{wc} - S_g}{1 - S_{org} - S_{wc}} \right), \tag{C–218}$$

$$\frac{\partial k_{rog}}{\partial k_{rocw}} = \left(\frac{1 - S_{org} - S_{wc} - S_g}{1 - S_{org} - S_{wc}} \right)^{n_{rog}} = \frac{k_{rog}}{k_{rocw}}, \tag{C–219}$$

$$\frac{\partial k_{rog}}{\partial S_{org}} = n_{rog} k_{rgcw} \left(\frac{1 - S_{org} - S_{wc} - S_g}{1 - S_{org} - S_{wc}} \right)^{n_{rog}-1} \frac{-S_g}{(1 - S_{org} - S_{wc})^2} = -k_{rog} \frac{n_{rog} S_g}{(1 - S_{org} - S_{wc})(1 - S_{org} - S_{wc} - S_g)}, \tag{C–220}$$

$$\frac{\partial k_{rog}}{\partial S_{wc}} = n_{rog} k_{rgcw} \left(\frac{1 - S_{org} - S_{wc} - S_g}{1 - S_{org} - S_{wc}} \right)^{n_{rog}-1} \frac{-S_g}{(1 - S_{org} - S_{wc})^2} = -k_{rog} \frac{n_{rog} S_g}{(1 - S_{org} - S_{wc})(1 - S_{org} - S_{wc} - S_g)}, \tag{C–221}$$

and

$$\frac{\partial k_{rog}}{\partial n_{row}} = \frac{\partial k_{rog}}{\partial n_{rg}} = \frac{\partial k_{rog}}{\partial n_{rw}} = \frac{\partial k_{rog}}{\partial k_{rwcw}} = \frac{\partial k_{rog}}{\partial k_{rgcw}} = \frac{\partial k_{rog}}{\partial S_{gc}} = \frac{\partial k_{rog}}{\partial S_{orw}} = 0. \tag{C–222}$$

The derivatives of k_{ro} with respect to k_r

From Stone's equation (Eq. **??**), we have

$$\frac{\partial k_{ro}}{\partial k_r} = k_{rocw}\left[\left(\frac{\partial k_{row}}{\partial k_r}\frac{1}{k_{rocw}} + \frac{\partial k_{rw}}{\partial k_r}\right)\left(\frac{k_{rog}}{k_{rocw}} + k_{rg}\right) + \left(\frac{k_{row}}{k_{rocw}} + k_{rw}\right)\left(\frac{\partial k_{rog}}{\partial k_r}\frac{1}{k_{rocw}} + \frac{\partial k_{rg}}{\partial k_r}\right) - \left(\frac{\partial k_{rw}}{\partial k_r} + \frac{\partial k_{rg}}{\partial k_r}\right)\right], \tag{C–223}$$

for $k_r \neq k_{rocw}$, and for $k_r = k_{rocw}$

$$\frac{\partial k_{ro}}{\partial k_r} = \frac{\partial k_{ro}}{\partial k_{rocw}} = \frac{k_{ro}}{k_{rocw}}. \tag{C–224}$$

C.4.2 The Derivatives of Flow Equations

The derivatives of the flow terms with respect to the parameter k_r are

$$\begin{aligned}\frac{\partial F^n_{o,i,j,k}}{\partial k_r} = {} & \frac{\partial T^n_{ox,i+1/2,j,k}}{\partial k_r}[p^n_{i+1,j,k} - p^n_{i,j,k} - \gamma^n_{o,i+1/2,j,k}(D_{i+1,j,k} - D_{i,j,k})] \\ & - \frac{\partial T^n_{ox,i-1/2,j,k}}{\partial k_r}[p^n_{i,j,k} - p^n_{i-1,j,k} - \gamma^n_{o,i-1/2,j,k}(D_{i,j,k} - D_{i-1,j,k})] \\ & + \frac{\partial T^n_{oy,i,j+1/2,k}}{\partial k_r}[p^n_{i,j+1,k} - p^n_{i,j,k} - \gamma^n_{o,i,j+1/2,k}(D_{i,j+1,k} - D_{i,j,k})] \\ & - \frac{\partial T^n_{oy,i,j-1/2,k}}{\partial k_r}[p^n_{i,j,k} - p^n_{i,j-1,k} - \gamma^n_{o,i,j-1/2,k}(D_{i,j,k} - D_{i,j-1,k})] \\ & + \frac{\partial T^n_{oz,i,,j,k+1/2}}{\partial k_r}[p^n_{i,j,k+1} - p^n_{i,j,k} - \gamma^n_{o,i,j,k+1/2}(D_{i,j,k+1} - D_{i,j,k})] \\ & - \frac{\partial T^n_{oz,i,j,k-1/2}}{\partial k_r}[p^n_{i,j,k} - p^n_{i,j,k-1} - \gamma^n_{o,i,j,k-1/2}(D_{i,j,k} - D_{i,j,k-1})],\end{aligned} \tag{C–225}$$

$$\begin{aligned}\frac{\partial F^n_{w,i,j,k}}{\partial k_r} &= \frac{\partial T^n_{wx,i+1/2,j,k}}{\partial k_r}[p^n_{i+1,j,k} - p^n_{i,j,k} - \gamma^n_{w,i+1/2,j,k}(D_{i+1,j,k} - D_{i,j,k})] \\ &- \frac{\partial T^n_{wx,i-1/2,j,k}}{\partial k_r}[p^n_{i,j,k} - p^n_{i-1,j,k} - \gamma^n_{w,i-1/2,j,k}(D_{i,j,k} - D_{i-1,j,k})] \\ &+ \frac{\partial T^n_{wy,i,j+1/2,k}}{\partial k_r}[p^n_{i,j+1,k} - p^n_{i,j,k} - \gamma^n_{w,i,j+1/2,k}(D_{i,j+1,k} - D_{i,j,k})] \\ &- \frac{\partial T^n_{wy,i,j-1/2,k}}{\partial k_r}[p^n_{i,j,k} - p^n_{i,j-1,k} - \gamma^n_{w,i,j-1/2,k}(D_{i,j,k} - D_{i,j-1,k})] \\ &+ \frac{\partial T^n_{wz,i,,j,k+1/2}}{\partial k_r}[p^n_{i,j,k+1} - p^n_{i,j,k} - \gamma^n_{w,i,j,k+1/2}(D_{i,j,k+1} - D_{i,j,k})] \\ &- \frac{\partial T^n_{wz,i,j,k-1/2}}{\partial k_r}[p^n_{i,j,k} - p^n_{i,j,k-1} - \gamma^n_{w,i,j,k-1/2}(D_{i,j,k} - D_{i,j,k-1})], \quad \text{(C–226)}\end{aligned}$$

and

$$\begin{aligned}
\frac{\partial F^n_{g,i,j,k}}{\partial k_r} &= \frac{\partial T^n_{gx,i+1/2,j,k}}{\partial k_r}[p^n_{i+1,j,k} - p^n_{i,j,k} - \gamma^n_{g,i+1/2,j,k}(D_{i+1,j,k} - D_{i,j,k})] \\
&\quad - \frac{\partial T^n_{gx,i-1/2,j,k}}{\partial k_r}[p^n_{i,j,k} - p^n_{i-1,j,k} - \gamma^n_{g,i-1/2,j,k}(D_{i,j,k} - D_{i-1,j,k})] \\
&\quad + R^n_{so,i+1/2,j,k}\frac{\partial T^n_{ox,i+1/2,j,k}}{\partial k_r}[p^n_{i+1,j,k} - p^n_{i,j,k} - \gamma^n_{o,i+1/2,j,k}(D_{i+1,j,k} - D_{i,j,k})] \\
&\quad - R^n_{so,i-1/2,j,k}\frac{\partial T^n_{ox,i-1/2,j,k}}{\partial k_r}[p^n_{i,j,k} - p^n_{i-1,j,k} - \gamma^n_{o,i-1/2,j,k}(D_{i,j,k} - D_{i-1,j,k})] \\
&\quad + \frac{T^n_{gy,i,j+1/2,k}\partial}{\partial k_r}[p^n_{i,j+1,k} - p^n_{i,j,k} - \gamma^n_{g,i,j+1/2,k}(D_{i,j+1,k} - D_{i,j,k})] \\
&\quad - \frac{\partial T^n_{gy,i,j-1/2,k}}{\partial k_r}[p^n_{i,j,k} - p^n_{i,j-1,k} - \gamma^n_{g,i,j-1/2,k}(D_{i,j,k} - D_{i,j-1,k})] \\
&\quad + R^n_{so,i,j+1/2,k}\frac{\partial T^n_{oy,i,j+1/2,k}}{\partial k_r}[p^n_{i,j+1,k} - p^n_{i,j,k} - \gamma^n_{o,i,j+1/2,k}(D_{i,j+1,k} - D_{i,j,k})] \\
&\quad - R^n_{so,i,j-1/2,k}\frac{\partial T^n_{oy,i,j-1/2,k}}{\partial k_r}[p^n_{i,j,k} - p^n_{i,j-1,k} - \gamma^n_{o,i,j-1/2,k}(D_{i,j,k} - D_{i,j-1,k})] \\
&\quad + \frac{\partial T^n_{gz,i,,j,k+1/2}}{\partial k_r}[p^n_{i,j,k+1} - p^n_{i,j,k} - \gamma^n_{g,i,j,k+1/2}(D_{i,j,k+1} - D_{i,j,k})] \\
&\quad - \frac{\partial T^n_{gz,i,j,k-1/2}}{\partial k_r}[p^n_{i,j,k} - p^n_{i,j,k-1} - \gamma^n_{g,i,j,k-1/2}(D_{i,j,k} - D_{i,j,k-1})] \\
&\quad + R^n_{so,i,j,k+1/2}\frac{\partial T^n_{oz,i,,j,k+1/2}}{\partial k_r}[p^n_{i,j,k+1} - p^n_{i,j,k} - \gamma^n_{o,i,j,k+1/2}(D_{i,j,k+1} - D_{i,j,k})] \\
&\quad - R^n_{so,i,j,k-1/2}\frac{\partial T^n_{oz,i,j,k-1/2}}{\partial k_r}[p^n_{i,j,k} - p^n_{i,j,k-1} - \gamma^n_{o,i,j,k-1/2}(D_{i,j,k} - D_{i,j,k-1})]. \quad \text{(C–227)}
\end{aligned}$$

Compute Partial Derivatives of Transmissibility T

The transmissibilities can be written as

$$T^n_{mx,i+1/2,j,k} = \frac{C_1 \Delta y_j \Delta z_k k_{x,i+1/2,j,k}}{x_{i+1} - x_i}\frac{k^n_{rm,i+1/2,j,k}}{\mu^n_{m,i+1/2,j,k} B^n_{m,i+1/2,j,k}}, \quad \text{(C–228)}$$

for $m = o, w, g$ and all $i = 1, 2, \ldots, n_x - 1$, and

$$T^n_{mx,1/2,j,k} = T^n_{mx,n_x+1/2,j,k} = 0. \quad \text{(C–229)}$$

Similarly,

$$T^n_{my,i,j+1/2,k} = \frac{C_1 \Delta x_i \Delta z_k k_{y,i,j+1/2,k}}{y_{j+1} - y_j} \frac{k^n_{rm,i,j+1/2,k}}{\mu^n_{m,i,j+1/2,k} B^n_{m,i,j+1/2,k}}, \tag{C–230}$$

for $m = o, w, g$ and all $j = 1, 2, \ldots, n_y - 1$ and

$$T^n_{my,i,1/2,k} = T^n_{my,i,n_y+1/2,k} = 0. \tag{C–231}$$

Finally,

$$T^n_{mz,i,j,k+1/2} = \frac{C_1 \Delta y_j \Delta x_i k_{z,i,j,k+1/2}}{z_{k+1} - z_k} \frac{k^n_{rm,i,j,k+1/2}}{\mu^n_{m,i,j,k+1/2} B^n_{m,i,j,k+1/2}}, \tag{C–232}$$

for $m = o, w, g$ and all $k = 1, 2, \ldots, n_z - 1$ and

$$T^n_{mz,i,j,1/2} = T^n_{my,i,j,n_z+1/2} = 0. \tag{C–233}$$

In this work, the $k^n_{rm,i,j,k+1/2}$, $(B_m)_{i+1/2,j,k}$ and $(\mu_m)_{i+1/2,j,k}$ are evaluated by the upstream weighting, i.e.

$$k^n_{rm,i,j,k+1/2} = \begin{cases} k^n_{rm,i,j,k+1} & \text{if } (i,j,k+1) \text{ is upstream} \\ k^n_{rm,i,j,k} & \text{if } (i,j,k) \text{ is upstream} \end{cases} \tag{C–234}$$

$$B^n_{m,i,j,k+1/2} = \begin{cases} B^n_{m,i,j,k+1} & \text{if } (i,j,k+1) \text{ is upstream} \\ B^n_{m,i,j,k} & \text{if } (i,j,k) \text{ is upstream} \end{cases} \tag{C–235}$$

and

$$\mu^n_{m,i,j,k+1/2} = \begin{cases} \mu^n_{m,i,j,k+1} & \text{if } (i,j,k+1) \text{ is upstream} \\ \mu^n_{m,i,j,k} & \text{if } (i,j,k) \text{ is upstream} \end{cases} \tag{C–236}$$

The derivatives required to estimate the parameters k_r are given by

$$\frac{\partial T^n_{mx,i+1/2,j,k}}{\partial k_r} = \frac{C_1 \Delta y_j \Delta z_k k_{x,i+1/2,j,k}}{x_{i+1} - x_i} \frac{1}{\mu^n_{m,i+1/2,j,k} B^n_{m,i+1/2,j,k}} \frac{\partial k^n_{rm,i+1/2,j,k}}{\partial k_r}, \tag{C–237}$$

$$\frac{\partial T^n_{my,i,j+1/2,k}}{\partial k_r} = \frac{C_1 \Delta x_i \Delta z_k k_{y,i,j+1/2,k}}{y_{j+1} - y_j} \frac{1}{\mu^n_{m,i,j+1/2,k} B^n_{m,i,j+1/2,k}} \frac{\partial k^n_{rm,i,j+1/2,k}}{\partial k_r}, \tag{C–238}$$

and

$$\frac{\partial T^n_{mz,i,j,k+1/2}}{\partial k_r} = \frac{C_1 \Delta y_j \Delta x_i k_{z,i,j,k+1/2}}{z_{k+1} - z_k} \frac{1}{\mu^n_{m,i,j,k+1/2} B^n_{m,i,j,k+1/2}} \frac{\partial k^n_{rm,i,j,k+1/2}}{\partial k_r}. \quad \text{(C–239)}$$

The derivatives of relative permeabilities with respect to the parameters k_r are computed by the Eqs. C–202 to C–224.

C.4.3 Derivatives of Sink Terms of Flow Equations

Production Wells (Q_o, Q_t or p_{wf} Specified)

In the producing wells, the layer k production rates at well l are given by

$$q^{n+1}_{m,l,k} = T^{n+1}_{m,l,k}[p^{n+1}_{l,k} - p^{n+1}_{wf,l} - dp^{n+1}_{wf,l,k}], \quad \text{(C–240)}$$

for $m = o, w, g$, where

$$T^{n+1}_{o,l,k} = WI_{l,k} \left(\frac{k_{ro}}{B_o \mu_o} \right)^{n+1}_{l,k}, \quad \text{(C–241)}$$

$$T^{n+1}_{w,l,k} = WI_{l,k} \left(\frac{k_{rw}}{B_w \mu_w} \right)^{n+1}_{l,k}, \quad \text{(C–242)}$$

and

$$T^{n+1}_{g,l,k} = WI_{l,k} \left(\frac{k_{rg}}{B_g \mu_g} + R_{so} \frac{k_{ro}}{B_o \mu_o} \right)^{n+1}_{l,k}. \quad \text{(C–243)}$$

The derivatives of flow rates to the parameter of relative permeability k_r are

$$\frac{\partial q^{n+1}_{m,l,k}}{\partial k_r} = \frac{\partial T^{n+1}_{m,l,k}}{\partial k_r}[p^{n+1}_{l,k} - p^{n+1}_{wf,l} - dp^{n+1}_{wf,l,k}], \quad \text{(C–244)}$$

for $m = o, w, g$.

The derivatives of $T^{n+1}_{m,l,k}$ can be calculated as

$$\frac{\partial T^{n+1}_{o,l,k}}{\partial k_r} = WI_{l,k} \left(\frac{1}{B_o \mu_o} \frac{\partial k_{ro}}{\partial k_r} \right)^{n+1}_{l,k}, \quad \text{(C–245)}$$

$$\frac{\partial T^{n+1}_{w,l,k}}{\partial k_r} = WI_{l,k} \left(\frac{1}{B_w \mu_w} \frac{\partial k_{rw}}{\partial k_r} \right)^{n+1}_{l,k}, \quad \text{(C–246)}$$

and

$$\frac{\partial T^{n+1}_{g,l,k}}{\partial k_r} = WI_{l,k} \left(\frac{1}{B_g \mu_g} \frac{\partial k_{rg}}{\partial k_r} + R_{so} \frac{1}{B_o \mu_o} \frac{\partial k_{ro}}{\partial k_r} \right)^{n+1}_{l,k}. \quad \text{(C–247)}$$

Injection Wells (Water or Gas Injection)

For water or gas injection wells, the water or gas injection rate at layer k of well l is given by

$$q_{m,l,k}^{n+1} = T_{inj,m,l,k}^{n+1}[p_{l,k}^{n+1} - p_{wf,l}^{n+1} - dp_{wf,l,k}^{n+1}], \tag{C–248}$$

for $m = w, g$, where

$$T_{inj,m,l,k}^{n+1} = \frac{WI_{l,k}}{\mu_{w,l,k}^{n+1} B_{w,l,k}^{n+1}}. \tag{C–249}$$

There is no k_r in the $q_{m,l,k}^{n+1}$, so the derivative of $q_{m,l,k}^{n+1}$ to k_r is zero, i.e.

$$\frac{\partial q_{m,l,k}^{n+1}}{\partial k_r} = 0. \tag{C–250}$$

C.4.4 Derivatives of Well Equations

Q_o specified

In the oil rate specified case, the well equation at well l is

$$f_{wf,l}^{n+1} = \sum_{k1} T_{o,l,k1}^{n+1}[p_{l,k1}^{n+1} - p_{wf,l}^{n+1} - dp_{wf,l,k1}^{n+1}] - q_{o,l}^{n+1} = 0, \tag{C–251}$$

where

$$T_{o,l,k1}^{n+1} = WI_{l,k1} \left(\frac{k_{ro}}{B_o \mu_o} \right)_{l,k1}^{n+1}. \tag{C–252}$$

We obtain the derivative

$$\frac{\partial f_{wf,l}^{n+1}}{\partial k_r} = \sum_{k1} \frac{\partial T_{o,l,k1}^{n+1}}{\partial k_r}[p_{l,k1}^{n+1} - p_{wf,l}^{n+1} - dp_{wf,l,k1}^{n+1}]. \tag{C–253}$$

Q_t Specified

In the case the total rate is specified at reservoir conditions, the well equation at well l is

$$f_{wf,l}^{n+1} = \sum_{k1} T_{t,l,k1}^{n+1}[p_{l,k1}^{n+1} - p_{wf,l}^{n+1} - dp_{wf,l,k1}^{n+1}] - q_{t,l}^{n+1} = 0, \tag{C–254}$$

where

$$T^{n+1}_{t,l,k1} = WI_{l,k1}\left(\frac{k_{ro}}{\mu_o} + \frac{k_{rw}}{\mu_w} + \frac{k_{rg}}{\mu_g}\right)^{n+1}_{l,k1}. \tag{C–255}$$

We obtain the derivative

$$\frac{\partial f^{n+1}_{wf,l}}{\partial k_r} = \sum_{k1} \frac{\partial T^{n+1}_{t,l,k1}}{\partial k_r}[p^{n+1}_{l,k1} - p^{n+1}_{wf,l} - dp^{n+1}_{wf,l,k1}]. \tag{C–256}$$

It is easy to see

$$\frac{\partial T^{n+1}_{t,l,k}}{\partial k_r} = WI_{l,k}\left(\frac{1}{\mu_o}\frac{\partial k_{ro}}{\partial k_r} + \frac{1}{\mu_w}\frac{\partial k_{rw}}{\partial k_r} + \frac{1}{\mu_g}\frac{\partial k_{rg}}{\partial k_r}\right)^{n+1}_{l,k}. \tag{C–257}$$

Water or Gas Injection

In the water or gas injection case, the well equation at well l is

$$f^{n+1}_{wf,l} = \sum_{k1} T^{n+1}_{inj,m,l,k1}[p^{n+1}_{l,k1} - p^{n+1}_{wf,l} - dp^{n+1}_{wf,l,k1}] - q^{n+1}_{o,l} = 0, \tag{C–258}$$

where

$$T^{n+1}_{o,l,k} = \frac{WI_{l,k}}{(B_w\mu_w)^{n+1}_{l,k}}. \tag{C–259}$$

We obtain

$$\frac{\partial f^{n+1}_{wf,l}}{\partial k_r} = 0. \tag{C–260}$$

C.4.5 Computation of $\nabla_{k_r}\beta$

In this part, we compute the vector $\nabla_{k_r}\beta$ for the cases $\beta = p_{wf}$, $\beta = GOR$, and $\beta = WOR$.

Gradient of p_{wf}

Since p_{wf} does not explicitly depend on the parameters k_r, it is clear that

$$\nabla_{k_r}\beta = \nabla_{k_r}p_{wf} = 0. \tag{C–261}$$

Gradient of GOR

Q_o Specified When the oil rate is specified for well l, the gas rate is

$$q_{g,l}^{n+1} = \sum_k T_{g,l,k}^{n+1}(p_{l,k}^{n+1} - p_{wf,l,k}^{n+1}). \tag{C–262}$$

The gas-oil ratio is therefore:

$$\begin{aligned} GOR_l^{n+1} &= \frac{q_{g,l}^{n+1}}{q_{o,l}^{n+1}} \\ &= \frac{1}{q_{o,l}^{n+1}} \sum_k T_{g,l,k}^{n+1}(p_{l,k}^{n+1} - p_{wf,l,k}^{n+1}) \\ &= \frac{1}{q_{o,l}^{n+1}} \sum_k T_{g,l,k}^{n+1}(p_{l,k}^{n+1} - p_{wf,l}^{n+1} - dp_{wf,l,k}^{n+1}), \end{aligned} \tag{C–263}$$

The derivatives of this expression is

$$\frac{\partial GOR_l^{n+1}}{\partial k_r} = \frac{1}{q_{o,l}^{n+1}} \sum_k \frac{\partial T_{g,l,k}^{n+1}}{\partial k_r}(p_{l,k}^{n+1} - p_{wf,l}^{n+1} - dp_{wf,l,k}^{n+1}). \tag{C–264}$$

Q_t or p_{wf} Specified. When the total rate is specified for well l, the gas rate and oil rate are

$$q_{g,l}^{n+1} = \sum_k T_{g,l,k}^{n+1}(p_{l,k}^{n+1} - p_{wf,l,k}^{n+1}), \tag{C–265}$$

$$q_{o,l}^{n+1} = \sum_k T_{o,l,k}^{n+1}(p_{l,k}^{n+1} - p_{wf,l,k}^{n+1}), \tag{C–266}$$

and gas-oil ratio is

$$GOR_l^{n+1} = \frac{q_{g,l}^{n+1}}{q_{o,l}^{n+1}}. \tag{C–267}$$

We have the derivatives

$$\begin{aligned} \frac{\partial GOR_l^{n+1}}{\partial k_r} &= \frac{1}{q_{o,l}^{n+1}} \frac{\partial q_{g,l}^{n+1}}{\partial k_r} - \frac{q_{g,l}^{n+1}}{(q_{o,l}^{n+1})^2} \frac{\partial q_{o,l}^{n+1}}{\partial k_r} \\ &= \frac{1}{q_{o,l}^{n+1}} \sum_k \frac{\partial T_{g,l,k}^{n+1}}{\partial k_r}(p_{l,k}^{n+1} - p_{wf,l}^{n+1} - dp_{wf,l,k}^{n+1}) \\ &\quad - \frac{q_{g,l}^{n+1}}{(q_{o,l}^{n+1})^2} \sum_k \frac{\partial T_{o,l,k}^{n+1}}{\partial k_r}(p_{l,k}^{n+1} - p_{wf,l}^{n+1} - dp_{wf,l,k}^{n+1}). \end{aligned} \tag{C–268}$$

Gradient of WOR

Q_o Specified When the oil rate is specified at well l, we have

$$q_{w,l}^{n+1} = \sum_k T_{w,l,k}^{n+1}(p_{l,k}^{n+1} - p_{wf,l,k}^{n+1}), \tag{C–269}$$

so

$$\begin{aligned} WOR_l^{n+1} &= \frac{q_{w,l}^{n+1}}{q_{o,l}^{n+1}} \\ &= \frac{1}{q_{o,l}^{n+1}} \sum_k T_{w,l,k}^{n+1}(p_{l,k}^{n+1} - p_{wf,l,k}^{n+1}) \\ &= \frac{1}{q_{o,l}^{n+1}} \sum_k T_{w,l,k}^{n+1}(p_{l,k}^{n+1} - p_{wf,l}^{n+1} - dp_{wf,l,k}^{n+1}). \end{aligned} \tag{C–270}$$

The derivatives are

$$\frac{\partial WOR_l^{n+1}}{\partial k_r} = \frac{1}{q_{o,l}^{n+1}} \sum_k \frac{\partial T_{w,l,k}^{n+1}}{\partial k_r}(p_{l,k}^{n+1} - p_{wf,l}^{n+1} - dp_{wf,l,k}^{n+1}). \tag{C–271}$$

Q_t or p_{wf} Specified When total rate is specified for well l, we have

$$q_{w,l}^{n+1} = \sum_k T_{w,l,k}^{n+1}(p_{l,k}^{n+1} - p_{wf,l,k}^{n+1}), \tag{C–272}$$

$$q_{o,l}^{n+1} = \sum_k T_{o,l,k}^{n+1}(p_{l,k}^{n+1} - p_{wf,l,k}^{n+1}), \tag{C–273}$$

and

$$WOR_l^{n+1} = \frac{q_{w,l}^{n+1}}{q_{o,l}^{n+1}}. \tag{C–274}$$

We have

$$\begin{aligned} \frac{\partial WOR_l^{n+1}}{\partial k_r} &= \frac{1}{q_{o,l}^{n+1}} \frac{\partial q_{w,l}^{n+1}}{\partial k_r} - \frac{q_{w,l}^{n+1}}{(q_{o,l}^{n+1})^2} \frac{\partial q_{o,l}^{n+1}}{\partial k_r} \\ &= \frac{1}{q_{o,l}^{n+1}} \sum_k \frac{\partial T_{w,l,k}^{n+1}}{\partial k_r}(p_{l,k}^{n+1} - p_{wf,l}^{n+1} - dp_{wf,l,k}^{n+1}) \\ &\quad - \frac{q_{w,l}^{n+1}}{(q_{o,l}^{n+1})^2} \sum_k \frac{\partial T_{o,l,k}^{n+1}}{\partial k_r}(p_{l,k}^{n+1} - p_{wf,l}^{n+1} - dp_{wf,l,k}^{n+1}). \end{aligned} \tag{C–275}$$

C.5 Sensitivity of Objective Function

In some practical problems, both the number of observed data and number of model parameters are large. It is computationally expensive to use the adjoint method to calculate sensitivity coefficients for problems that have large amounts of data. In this case, one can consider using a preconditioned conjugate gradient method to minimize the objective function. To apply the conjugate gradient algorithm, one only needs to calculate the gradient of the objective function and does not need to calculate sensitivity coefficients. It is very fast to use the adjoint method to calculate the gradient of a objective function. One only need solve the adjoint system equation once to get the gradient, regardless of the number of data and parameters. Even though the conjugate gradient method tends to converge slower than the Gauss-Newton method, the whole automatic history matching procedure could be efficient because one does not need to calculate sensitivity coefficients. Moreover, if an efficient preconditioner can be found, convergence could be significantly accelerated. Assume the objective function is

$$O(m) = \frac{1}{2}(m-m_{prior})^T C_M^{-1}(m-m_{prior}) + \frac{1}{2}(g(m)-d_{\text{obs}})^T C_D^{-1}(g(m)-d_{\text{obs}}), \quad \text{(C–276)}$$

where m is the vector of model parameters; m_{prior} is prior means of model parameters; C_M^{-1} is the prior covariance matrix computed from the prior covariance function (or variogram); C_D is the data covariance matrix; d_{obs} is observed production data vector that are used to condition the model; and $g(m)$ is the calculated production data based on the model parameter m. The $g(m)$ vector is given by

$$g(m) = \begin{bmatrix} g_1 & g_2 & \cdots & g_{N_d} \end{bmatrix}^T. \quad \text{(C–277)}$$

To apply the adjoint method to calculate the gradient of the objective function, we need to evaluate the source term $\nabla_{y^n}\beta$ in the adjoint Eq. 3.21 and the derivative term $\nabla_m\beta$ in the sensitivity Eq. C–1.

C.5.1 Compute Source Term $\nabla_{y^n}\beta$

Here we choose

$$\beta = O(m) = \frac{1}{2}(m - m_{prior})^T C_M^{-1}(m - m_{prior}) + \frac{1}{2}(g(m) - d_{\text{obs}})^T C_D^{-1}(g(m) - d_{\text{obs}}), \tag{C–278}$$

thus

$$\begin{aligned}\nabla_{y^n}\beta = \nabla_{y^n}O(m) &= \nabla_{y^n}\{\frac{1}{2}(m-m_{prior})^T C_M^{-1}(m-m_{prior})+\frac{1}{2}(g(m)-d_{\text{obs}})^T C_D^{-1}(g(m)-d_{\text{obs}})\} \\ &= \frac{1}{2}\nabla_{y^n}\{(g(m) - d_{\text{obs}})^T C_D^{-1}(g(m) - d_{\text{obs}})\} \\ &= [\nabla_{y^n}(g(m) - d_{\text{obs}})^T]C_D^{-1}(g(m) - d_{\text{obs}}). \end{aligned} \tag{C–279}$$

So we obtain

$$\nabla_{y^n}\beta = \nabla_{y^n}[g(m)]^T C_D^{-1}(g(m) - d_{\text{obs}}). \tag{C–280}$$

The matrix $\nabla_{y^n}[g(m)]^T$ is a $3N_M + N_w$ by N_d matrix and defined as

$$\nabla_{y^n}[g(m)]^T = \begin{bmatrix} \frac{\partial g_1}{\partial p_1^n} & \frac{\partial g_2}{\partial p_1^n} & \cdots & \frac{\partial g_{N_d}}{\partial p_1^n} \\ \frac{\partial g_1}{\partial S_{w,1}^n} & \frac{\partial g_2}{\partial S_{w,1}^n} & \cdots & \frac{\partial g_{N_d}}{\partial S_{w,1}^n} \\ \frac{\partial g_1}{\partial S_{g,1}^n} & \frac{\partial g_2}{\partial S_{g,1}^n} & \cdots & \frac{\partial g_{N_d}}{\partial S_{g,N}^n} \\ \frac{\partial g_1}{\partial p_2^n} & \frac{\partial g_2}{\partial p_2^n} & \cdots & \frac{\partial g_{N_d}}{\partial p_2^n} \\ \vdots & \vdots & \cdots & \vdots \\ \frac{\partial g_1}{\partial S_{g,N}^n} & \frac{\partial g_2}{\partial S_{g,N}^n} & \cdots & \frac{\partial g_{N_d}}{\partial S_{g,N}^n} \\ \frac{\partial g_1}{\partial p_{wf,1}^n} & \frac{\partial g_2}{\partial p_{wf,1}^n} & \cdots & \frac{\partial g_{N_d}}{\partial p_{wf,1}^n} \\ \vdots & \vdots & \cdots & \vdots \\ \frac{\partial g_1}{\partial p_{wf,N_w}^n} & \frac{\partial g_2}{\partial p_{wf,N_w}^n} & \cdots & \frac{\partial g_{N_d}}{\partial p_{wf,N_w}^n} \end{bmatrix}. \tag{C–281}$$

The $g(m)$ is production data vector. It could be p_{wf}, GOR and WOR or any combination of these three kinds of production data. The matrix $\nabla_{y^n}[g(m)]^T$ can be calculated by using the formulas in appendix B.

C.5.2 Compute Derivative $\nabla_m \beta$

From the definition of the objective function, we have

$$\begin{aligned}\nabla_m \beta &= \nabla_m O(m) \\ &= \nabla_m \left\{ \frac{1}{2}(m - m_{prior})^T C_M^{-1}(m - m_{prior}) + \frac{1}{2}(g(m) - d_{\text{obs}})^T C_D^{-1}(g(m) - d_{\text{obs}}) \right\} \\ &= C_M^{-1}(m - m_{prior}) + [\nabla_m (g(m) - d_{\text{obs}})^T] C_D^{-1}(g(m) - d_{\text{obs}})\end{aligned} \tag{C–282}$$

So we obtain

$$\nabla_m \beta = C_M^{-1}(m - m_{prior}) + \nabla_m [g(m)]^T C_D^{-1}(g(m) - d_{\text{obs}}) \tag{C–283}$$

The matrix $\nabla_m [g(m)]^T$ is a M by N_d matrix and defined as

$$\nabla_m [g(m)]^T = \begin{bmatrix} \frac{\partial g_1}{\partial m_1} & \frac{\partial g_2}{\partial m_1} & \cdots & \frac{\partial g_{N_d}}{\partial m_1} \\ \frac{\partial g_1}{\partial m_2} & \frac{\partial g_2}{\partial m_2} & \cdots & \frac{\partial g_{N_d}}{\partial m_2} \\ \vdots & \vdots & \cdots & \vdots \\ \frac{\partial g_1}{\partial m_M} & \frac{\partial g_2}{\partial m_M} & \cdots & \frac{\partial g_{N_d}}{\partial m_M} \end{bmatrix} \tag{C–284}$$

The vector $g(m)$ is the calculated production data vector. It could be p_{wf}, GOR and WOR or any combination of these three kinds of production data. The elements in matrix $\nabla_m [g(m)]^T$ can be calculated by using the formulations in appendix C. For example, if one wants to use the p_{wf}, GOR, and/or WOR data to estimate the permeability and/or porosity field, one can use the equations in the section C.1.4 to compute the elements in the matrix $\nabla_m [g(m)]^T$.

Bibliography

Y. Abacioglu, D. S. Oliver, and A. C. Reynolds. Efficient history-matching using subspace vectors. In *TUPREP Research Report 17 (May 22, 2000)*, pages 69–90, 2000.

F. Anterion, B. Karcher, and R. Eymard. Use of parameter gradients for reservoir history matching, SPE-18433. In *10th SPE Reservoir Simulation Symp.*, pages 339–354, 1989.

K. Aziz and A. Settaari. *Petroleum Reservoir Simulation*. Elsevier Applied Science Publishers, New York, 1979.

Khalid Aziz. *Notes for Petroleum Reservoir Simulation*. Stanford University, 1994.

James V. Beck and Kenneth J. Arnold. *Parameter Estimation in Engineering and Science*. John Wiley & Sons, Chichester, England, 1977.

Zhuoxin Bi, D. S. Oliver, and A. C. Reynolds. Conditioning 3D stochastic channels to pressure data, SPE-56682. In *1999 SPE Annual Technical Conference and Exhibition*, 1999.

Robert Bissell. Calculating optimal parameters for history matching. In *4th European Conference on the Mathematics of Oil Recovery*, 1994.

Robert Bissell, Yogeshwar Sharma, and J. E. Killough. History matching using the method of gradients: Two case studies. *SPE 69th Annual Technical Conference and Exhibition*, SPE 28590:275–289, 1994.

R. D. Carter, L. F. Kemp, A. C. Pierce, and D. L. Williams. Performance matching with constraints. *Soc. Petrol. Eng. J.*, 14(4):187–196, 1974.

Guy M. Chavent, M. Dupuy, and P. Lemonnier. History matching by use of optimal control theory. *Soc. Petrol. Eng. J.*, 15(1):74–86, 1975.

W. H. Chen, G. R. Gavalas, John H. Seinfeld, and Mel L. Wasserman. A new algorithm for automatic history matching. *Soc. Petrol. Eng. J.*, pages 593–608, 1974.

L. Chu and A. C. Reynolds. A general efficient method for generating sensitivity coefficients. In *Well Testing, Reservoir Characterization and Reservoir Simulation*, Petroleum Reservoir Exploitation Projects, pages 100–133. University of Tulsa, 1995.

Luciane Bonet Cunha. *Sampling From the a Posteriori Probability Density Function for Permeability Fields Conditioned to Variogram and Well-Test Pressure Data*. Ph.D. dissertation, University of Tulsa, Tulsa, Oklahoma, 1996.

A. C. Reynolds F. Zhang and D. S. Oliver. Evaluation of the reduction in uncertainty obtained by conditioning a 3d channel to multiwell pressure data. *Mathematical Geology*, submitted, 2000.

G. R. Gavalas, P. C. Shah, and John H. Seinfeld. Reservoir history matching by Bayesian estimation. *Soc. Petrol. Eng. J.*, 16(6):337–350, 1976.

N. He, A. C. Reynolds, and D. S. Oliver. Three-dimensional reservoir description from multiwell pressure data and prior information. *Soc. Pet. Eng. J.*, pages 312–327, 1997.

Nanqun He. *Three Dimensional Reservoir Description by Inverse Theory using Well-Test Pressure and Geostatistical Data*. PhD thesis, University of Tulsa, 1997.

Bjørn Kåre Hegstad and Henning Omre. A comparison of rejection sampling and Metropolis-Hastings algorithm. Technical report, Norwegian University of Science and Technology, 1997.

P. Jacquard. Théorie de l'interprétation des mesures de pression. *Revue de L'Institut Français du Pétrole*, 19(3):297–334, 1964.

P. Jacquard and C. Jain. Permeability distribution from field pressure data. *Soc. Petrol. Eng. J.*, 5(4):281–294, 1965.

Hans O. Jahns. A rapid method for obtaining a two-dimensional reservoir description from well pressure response data. *Soc. Petrol. Eng. J.*, 6(12):315–327, 1966.

J. E. Killough, Yogeshwar Sharma, Alain Dupuy, Robert Bissell, and John Wallis. A multiple right hand side iterative solver for history matching SPE 29119. In *Proceedings of the 13th SPE Symposium on Reservoir Simulation*, pages 249–255, 1995.

Peter K. Kitanidis. Quasi-linear geostatistical theory for inversing. *Water Resour. Res.*, 31(10):2411–2419, 1995.

K. N. Kulkarni and Akhil Datta-Gupta. Estimating relative permeability from production data: A streamline approach. *SPE Journal*, 5(4):402–411, 2000.

Jorge L. Landa. *Reservoir Parameter Estimation Constrained to Pressure Transients, Performance History and Distributed Saturation Data*. Ph.D. thesis, Stanford University, Stanford, California, 1997.

Jorge L. Landa and Roland N. Horne. A procedure to integrate well test data, reservoir performance history and 4-D seismic information into a reservoir description (SPE-38653). In *1997 SPE Annual Technical Conference and Exhibition*, 1997.

T. Y. Lee and John H. Seinfeld. Estimation of two-phase petroleum reservoir properties by regularization. *J. Computational Physics*, 69:397–419, 1987a.

Tai-Yong Lee and John H. Seinfeld. Estimation of absolute and relative permeabilities in petroleum reservoirs. *Inverse Problems*, 3(4):711–728, 1987b.

Eliana M. Makhlouf, Wen H. Chen, Mel L. Wasserman, and John H. Seinfeld. A general history matching algorithm for three-phase, three-dimensional petroleum reservoirs. *SPE Advanced Technology Series*, 1(2):83–91, 1993.

Dean S. Oliver. Incorporation of transient pressure data into reservoir characterization. *In Situ*, 18(3):243–275, 1994.

Dean S. Oliver, Luciane B. Cunha, and Albert C. Reynolds. Markov chain Monte Carlo methods for conditioning a permeability field to pressure data. *Mathematical Geology*, 29(1):61–91, 1997.

Dean S. Oliver, Nanqun He, and Albert C. Reynolds. Conditioning permeability fields to pressure data. In *European Conference for the Mathematics of Oil Recovery, V*, pages 1–11, 1996.

Henning Omre, Bjørn Kåre Hegstad, and Håkon Tjelmeland. Alternative history matching approaches. Technical report, Department of Mathematical Sciences, Norwegian University of Science & Technology, Trondheim, Norway, 1996.

Henning Omre, Håkon Tjelmeland, Yuanchang Qi, and Leif Hinderaker. Assessment of uncertainty in the production characteristics of a sand stone reservoir. In *Reservoir Characterization III*, pages 556–603. PennWell Books, Tulsa, OK, 1993.

D. W. Peaceman. Interpretation of well-block pressures in numerical reservoir simulation with non-square grid blocks and anisotropic permeability. *Soc. Pet. Eng. J.*, pages 531–543, 1983.

Albert C. Reynolds, Nanqun He, Lifu Chu, and Dean S. Oliver. Reparameterization techniques for generating reservoir descriptions conditioned to variograms and well-test pressure data. *Soc. Petrol. Eng. J.*, 1(4):413–426, 1996.

H. L. Stone. Estimation of three-phase relative permeability and residual oil data. *J. Can. Pet. Tech.*, 12(4):53–61, 1973.

Ne-Zheng Sun. *Inverse problems in Groundwater Modeling*. Kluwer Academic Publishers, Dordrecht, The Netherlands, 1994.

Thomas B. Tan and Nicolas Kalogerakis. A three-dimensional three-phase automatic history matching model: reliability of parameter estimates. *Journal of Canadian Petroleum Technology*, 31(3):34–41, 1992.

Albert Tarantola. *Inverse Problem Theory: Methods for Data Fitting and Model Parameter Estimation*. Elsevier, Amsterdam, The Netherlands, 1987.

M. L. Wasserman, A. S. Emanuel, and J. H. Seinfeld. Practical applications of optimal-control theory to history-matching multiphase simulator models. *Soc. Petrol. Eng. J.*, 15(4):347–355, 1975.

A. Ted Watson, G. R. Gavalas, and John H. Seinfeld. Identifiability of estimates of two-phase reservoir properties in history matching. *Soc. Petrol. Eng. J.*, 24(6): 697–706, 1984.

Zhan Wu. *Conditioning Geostatistical Models to Two-Phase Flow Production Data*. PhD thesis, University of Tulsa, 1999.

Zhan Wu, A. C. Reynolds, and D. S. Oliver. Conditioning geostatistical models to two-phase production data. *Soc. Petrol. Eng. J.*, 3(2):142–155, 1999.

W. Xu, T. T. Tran, R. M. Srivastava, and A. G. Journel. Integrating seismic data in

reservoir modeling: the collocated cokriging approach, (SPE-24742). In *1992 SPE Annual Technical Conference and Exhibition*, 1992.

P. Yang and A. T. Watson. Automatic history matching with variable-metric methods. *SPE Res. Eng. J.*, pages 995–1001, 1988.

Pin-Huel Yang and A. Ted Watson. A Bayesian methodology for estimating relative permeability curves. *SPE Reservoir Engineering*, 6(2):259–265, 1991.

Pin-Huel Yang, A. Ted Watson, and R. V. Armasu. Automatic history matching with variable-metric methods. *SPE Reservoir Engineering*, pages 995–1001, 1988.

William W-G Yeh. Review of parameter identification in groundwater hydrology: The inverse problem. *Water Resour. Res.*, 22(2):95–108, 1986.